UNCLASSIFIED

AD NUMBER

AD818330

LIMITATION CHANGES

TO:

Approved for public release; distribution is unlimited.

FROM:

Distribution authorized to U.S. Gov't. agencies and their contractors; Critical Technology; JUN 1967. Other requests shall be referred to U.S. Army Aviation Materiel Laboratories, Fort Eustis, VA 23604. This document contains export-controlled technical data.

AUTHORITY

USAAVLABS ltr, 4 May 1971

THIS PAGE IS UNCLASSIFIED

FOR OFFICIAL USE ONLY

AD

AD818330

USAAVLABS TECHNICAL REPORT 67-33

AIRCRAFT FUEL SYSTEMS DESIGN STUDY

By

N. B. Johnson
J. N. Rogers
R. L. Cook

June 1967

U. S. ARMY AVIATION MATERIEL LABORATORIES
FORT EUSTIS, VIRGINIA

CONTRACT DA 44-177-AMC-442(T)
GOODYEAR AEROSPACE CORPORATION
LITCHFIELD PARK, ARIZONA

Each transmittal of this document outside the Department of Defense must have prior approval of U.S. Army Aviation Materiel Laboratories, Fort Eustis, Virginia 23604.

Protective marking may be removed 1 June 1970.

FOR OFFICIAL USE ONLY

Disclaimers

When Government drawings, specifications, or other data are used for any purpose other than in connection with a definitely related Government procurement operation, the United States Government thereby incurs no responsibility nor any obligation whatsoever; and the fact that the Government may have formulated, furnished, or in any way supplied the said drawings, specifications, or other data is not to be regarded by implication or otherwise as in any manner licensing the holder or any other person or corporation, or conveying any rights or permission, to manufacture, use, or sell any patented invention that may in any way be related thereto.

Trade names cited in this report do not constitute an official endorsement or approval of the use of such commercial hardware or software.

Disposition Instructions

Destroy this report when no longer needed. Do not return it to originator.

DEPARTMENT OF THE ARMY
U. S. ARMY AVIATION MATERIEL LABORATORIES
FORT EUSTIS, VIRGINIA 23604

This report was prepared by Goodyear Aerospace Corporation, Arizona Division, under Contract DA 44-177-AMC-442(T) for the U. S. Army Aviation Materiel Laboratories. It covers a theoretical and experimental design program conducted to extend the crashworthiness of the improved fuel cells to the complete aircraft fuel system.

The results of this study disclose specific areas in an aircraft fuel system which are particularly vulnerable to failure during crash conditions. Recommendations for changes in future aircraft fuel systems designs are offered.

FOR OFFICIAL USE ONLY

Task 1F121401A52904
Contract DA-44-177-AMC-442 (T)
USAAVLABS Technical Report 67-33
June 1967

AIRCRAFT FUEL SYSTEMS DESIGN STUDY

Final Report
GERA-1264

by

N.B. Johnson
J.H. Rogers
R.L. Cook

Prepared by

Goodyear Aerospace Corporation
Litchfield Park, Arizona

for

U.S. ARMY AVIATION MATERIEL LABORATORIES
FORT EUSTIS, VIRGINIA

Each transmittal of this document outside the Department of Defense must have prior approval of U.S. Army Aviation Materiel Laboratories, Fort Eustis, Virginia 23604.

Protective marking may be removed 1 June 1970.

FOR OFFICIAL USE ONLY

SUMMARY

This report presents the results of crashworthiness evaluations of the fuel systems of the UH-1B, UH-1D, CH-47, and OH-6A aircraft, with effort also directed to the study of ballistic threat. Work was also conducted in testing and developing component modifications to eliminate weaknesses existing in the present systems, with special effort devoted to highly extensible, self-closing fuel lines. This research effort resulted in a series of recommendations for changes and established guidelines for future aircraft fuel-system designs.

FOREWORD

This final report documents the engineering effort conducted by Goodyear Aerospace Corporation under Contract DA-44-177-AMC-442(T) for the U.S. Army Aviation Materiel Laboratories from July 1966 to January 1967. Certain portions of this work were subcontracted to Aviation Safety Engineering and Research (AvSER), a division of Flight Safety Foundation, Inc., who provided considerable assistance, especially in those areas relating to crash vulnerability and dynamic testing. Acknowledgement is made to the following companies for their assistance: Hughes Tool Company (Aircraft Division), Bell Helicopter Company, and The Boeing Company (Vertol Division). Additional information was supplied by Sikorsky Aircraft, a division of United Aircraft Corporation.

CONTENTS

CONTENTS (CONT)

ILLUSTRATIONS

ILLUSTRATIONS (CONT)

ILLUSTRATIONS (CONT)

ILLUSTRATIONS (CONT)

ILLUSTRATIONS (CONT)

ILLUSTRATIONS (CONT)

ILLUSTRATIONS (CONT)

ILLUSTRATIONS (CONT)

TABLES

TABLES (CONT)

PART I

INTRODUCTION

Data from studies of accident statistics involving fixed-wing and rotary-wing aircraft reveal that the greatest number of fatalities continue to occur in accidents involving postcrash fires. These data have also indicated that the postcrash fire problem in helicopters is significantly more serious, with respect to the incidence of fire and fatalities, than in fixed-wing aircraft.

Previous investigations have been limited primarily to research and experimental testing of improved crash-resistant fuel cell materials. New fuel cell materials have been developed which offer a significant improvement over the materials used in existing fuel cells designed to meet current military specifications. Improved full-scale fuel cells dynamically crash tested in both fixed- and rotary-wing aircraft have demonstrated the ability to withstand dynamic crash loads of the magnitude experienced in survivable-type aircraft accidents. However, the actual crashworthiness of a fuel system is dependent upon the dynamic behavior of not only the fuel tank but also the aircraft structure surrounding the tank, tank location, fuel fittings, lines, boost pumps, and other components which make up the complete fuel system.

The purpose of this research effort was to conduct a theoretical and experimental design program to extend the crashworthiness of the improved fuel cells to the complete aircraft fuel system.

The program began with an evaluation of the fuel systems of four helicopters currently used by the U.S. Army: the UH-1B, UH-1D, CH-47, and the OH-6A aircraft. This evaluation was centered on a vulnerability analysis of the fuel systems (from the crash environment standpoint), with extensive effort also directed to the study of ballistic threat. The program then continued in the testing and development of component modifications to eliminate weaknesses existent in the present systems. Special effort was devoted to a highly extensible, self-closing fuel line concept. The program culminated in a series of recommendations for changes and established guidelines for future aircraft fuel system designs.

PART II

PRELIMINARY DESIGN STUDY

INTRODUCTION

An initial fuel system analysis was conducted to define the failure modes and design deficiencies of the fuel systems in four operational helicopters. The assumption was made that an electrical inerting system is used and functions properly if an aircraft crashes. The electrical system itself was investigated only to the extent of analyzing its ballistic vulnerability. The deficiencies noted in existing systems during this initial phase of the study, as well as general recommendations for their correction, formed the basis for the more detailed studies conducted later.

In this preliminary study, use was made of all available design schematics, handbooks, installation drawings, and component drawings for the following aircraft: (1) CH-47, (2) UH-1B, (3) UH-1D, and (4) OH-6A. Each of these aircraft was inspected at the Bell Helicopter Company, Fort Worth, Texas, and at Edwards Air Force Base, California. Data obtained from previous U.S. Army programs relating to the crashworthiness and vulnerability of U.S. Army aircraft were used in the failure mode analysis. The AvSER crash evaluation method was also used to determine theoretical modes of fuel systems failure in a crash environment. A detailed discussion of this method is presented in Appendix I.

The following components and accessories were analyzed during this initial phase:

Fuel Cells	Fuel Cell Components	Fuel-Transfer System
Location	Fuel drains	Fuel cell interconnects
Spatial form	Fuel vents	Fuel-transfer lines
Installation	Filler necks	Transfer line fittings and couplings
	Quantity indicators	Fuel filters
	Fuel boost pumps	In-line valves
	Fuel line connections to cells	

CRASH VULNERABILITY ANALYSIS

Design Deficiencies of the CH-47 Fuel Cell Location

There are two internal, crash-resistant bladder-type fuel cells in the CH-47 helicopter, each with a capacity of 308 gallons; the lower 50 percent of these cells is

self-sealing. The cells are installed in drag pods, one on each lower side of the fuselage (Figure 1).

There is considerable physical separation between the fuel tanks and the engines, a desirable arrangement in that fuel spillage occurring at impact is kept from the engine ignition-source area. Locating the tanks outside the occupiable area is also a sound concept as it minimizes the chances of spilled fuel entering the cockpit or cabin areas. However, the pods themselves lack satisfactory strength. The pod structure has failed in moderate crashes, allowing the fuel tank to drop from the helicopter, thus causing bladder failure and total fuel spillage (Figure 2).

When fuel tanks are installed in the lower portions of a fuselage (the tank bottom being nearly level with the bottom of the aircraft), they are particularly susceptible to penetrations from stumps, rocks, and other ground objects. When such penetration occurs, the structure surrounding the tank is torn, punctured, and deformed. The interaction of the jagged structure with the fuel tanks constitutes one of the greatest threats to fuel containment during aircraft accidents.

Design Deficiencies of the UH-1B Fuel Cell Location

There are several slightly different fuel tank configurations in the UH-1B. Since the general design and installation techniques are the same for each configuration, they will be discussed together.

The fuel is carried in two flexible, self-sealing fuel cells that are interconnected to form a single 168-gallon tank. Although the lower portions of the cells are self-sealing, the upper bladder portion is made of fairly thin (0.051-inch) material that could easily be punctured and torn by jagged metal. The fuel cells are located directly behind the occupiable area, one on each side of the fuselage, as shown in Figure 3. Any rupture of these cells would almost certainly result in fuel spillage into the occupiable area, presenting a considerable personnel danger should ignition occur. However, the fuel cells are not located directly under the transmission or other heavy components. Survival-limit accident results with this aircraft indicate that the transmission rarely deflects enough to cause fuel cell damage. The bottoms of the fuel cells are slightly above the level of the fuselage bottom. This location allows for some crushing of the aircraft structure, thereby protecting the fuel cells somewhat from penetration by ground obstructions and lessening the impact forces upon the cells themselves.

Design Deficiencies of the UH-1D Fuel Cell Location

The UH-1D helicopter contains one fuel tank that is composed of five interconnected fuel cells having a total capacity of 200 gallons. Figure 4 shows the arrangement

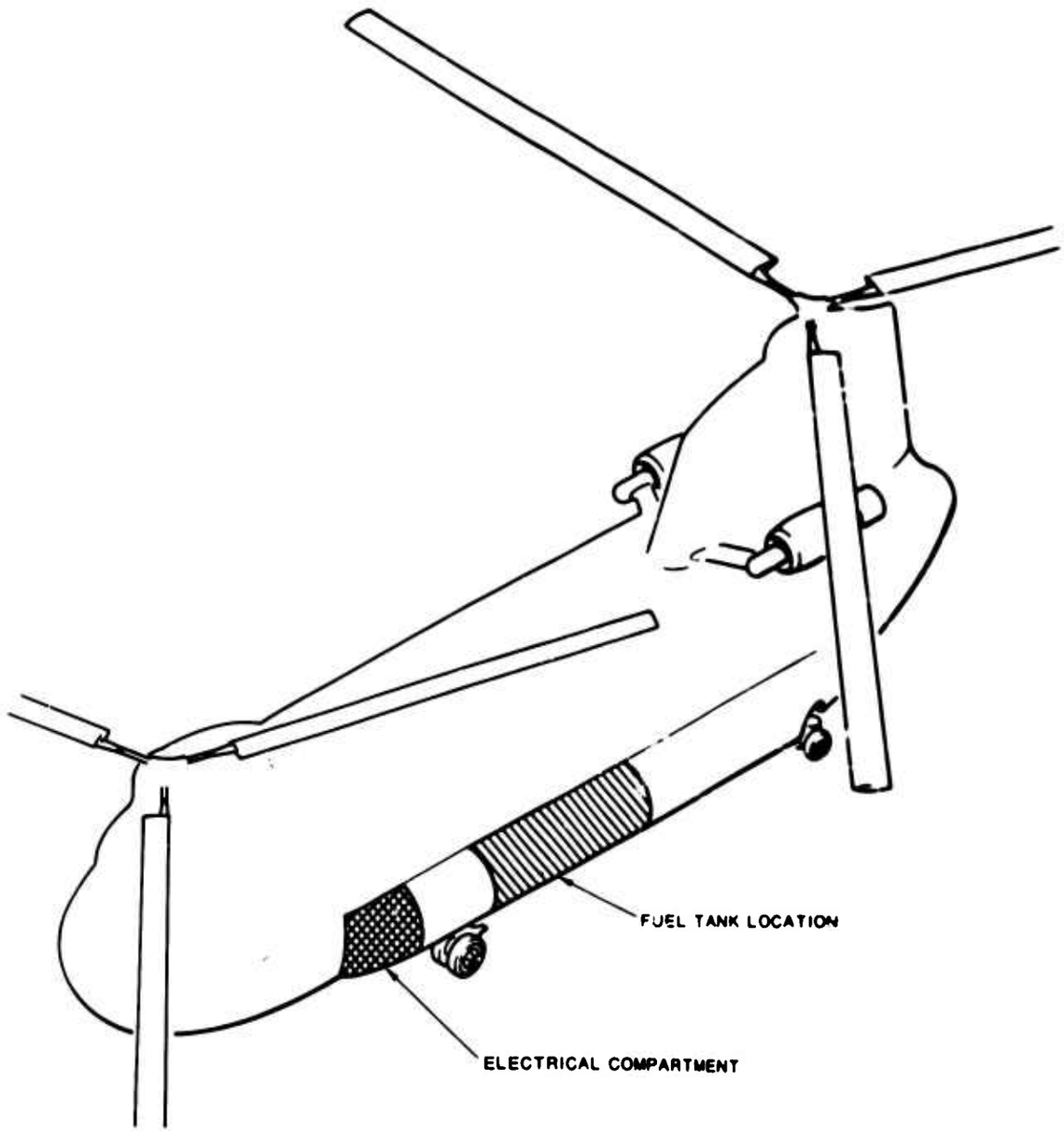

Figure 1. CH-47 Fuel Cell Location.

Figure 2. Pod Failure after CH-47 Crash.

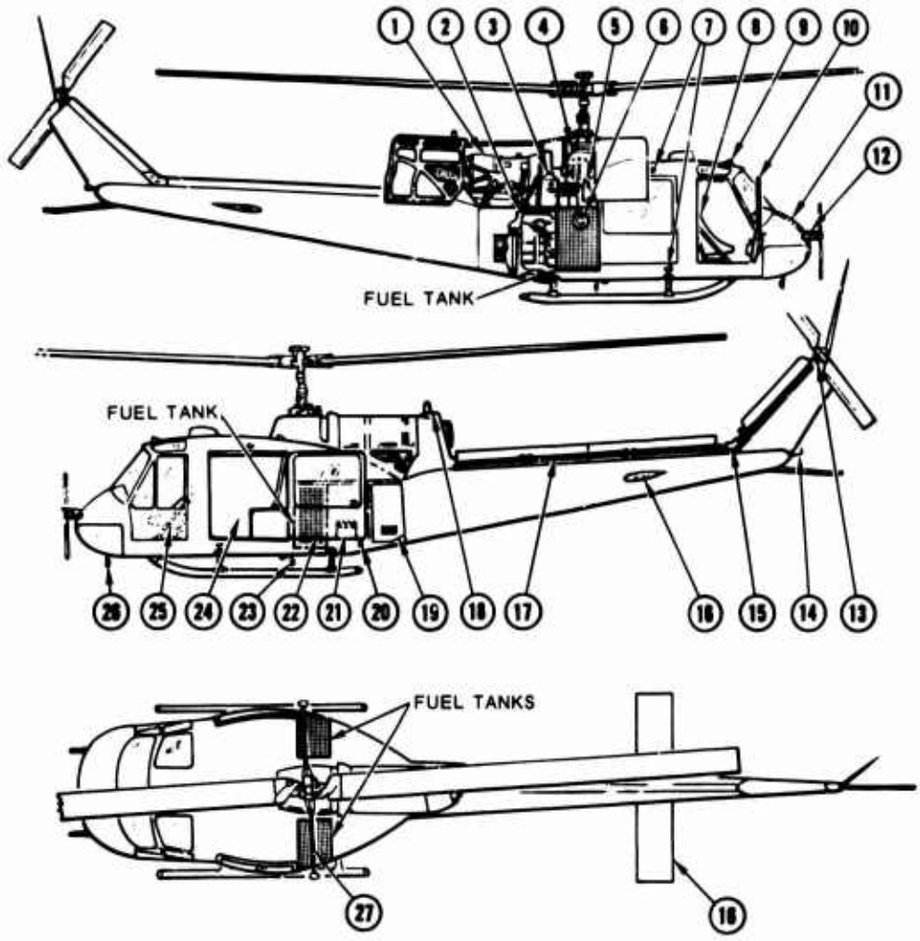

1. ENGINE
2. HEATING UNIT
3. OIL RESERVOIR
4. TRANSMISSION
5. HYDRAULIC OIL RESERVOIR
6. FUEL TANK FILLER
7. NAVIGATION LIGHTS
8. PILOT'S STATION
9. CABIN VENTILATOR
10. PILOT'S DOOR
11. ELECTRONIC EQUIPMENT COMPARTMENT
12. PITOT TUBE
13. TAIL ROTOR (90°) GEARBOX
14. AFT NAVIGATION LIGHT
15. TAIL ROTOR INTERMEDIATE (42°) GEAR BOX
16. SYNCHRONIZED ELEVATOR
17. TAIL ROTOR DRIVE SHAFT
18. ANTICOLLISION LIGHT
19. ELECTRICAL EQUIPMENT COMPARTMENT
20. EXTERNAL POWER RECEPTACLE
21. BATTERY
22. CARGO DOOR
23. LANDING LIGHT
24. CARGO COMPARTMENT
25. COPILOT'S STATION
26. SEARCH LIGHT
27. STABILIZER BAR

Figure 3. General Arrangement Diagram Showing Tank Location, UH-1B.

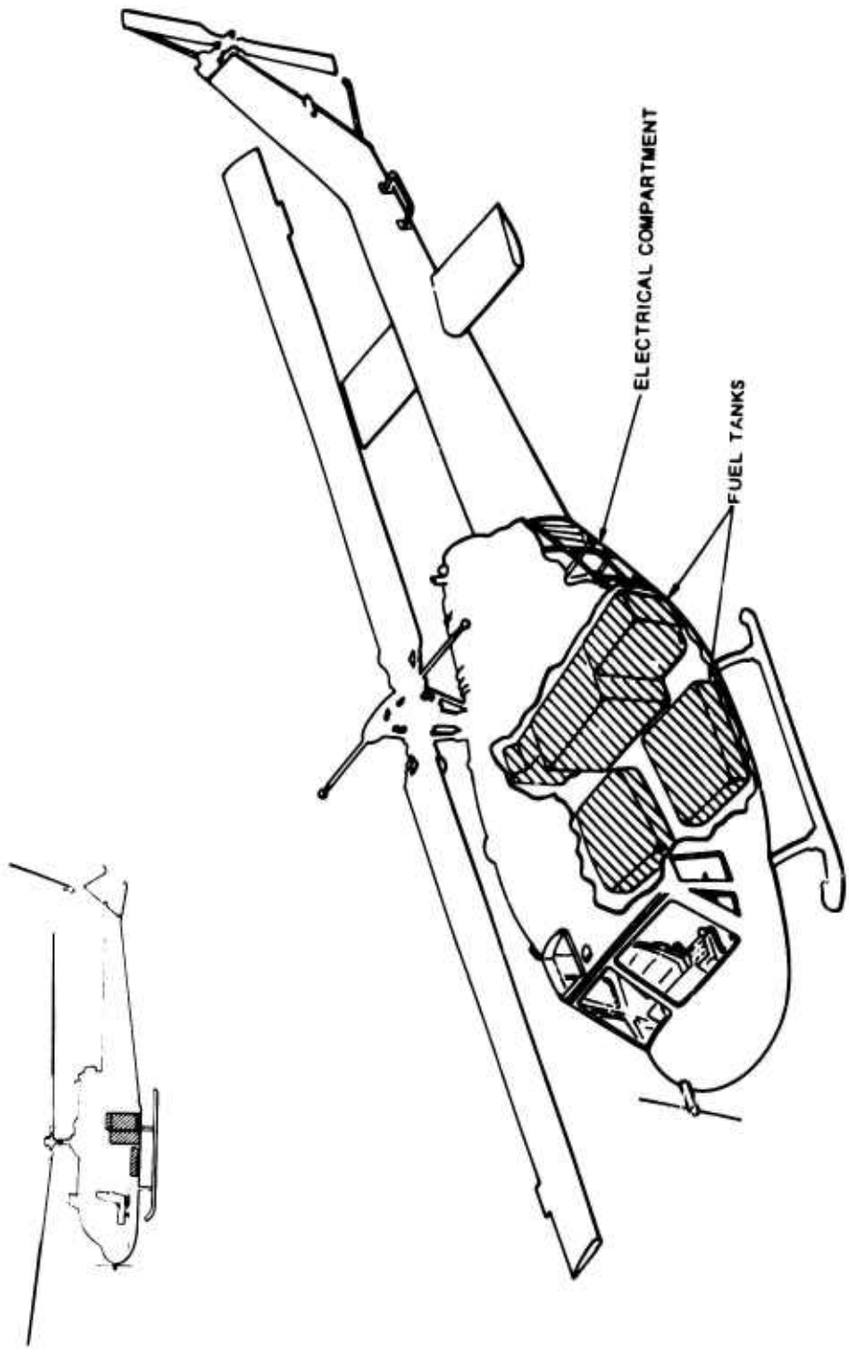

Figure 4. UH-1D General Arrangement Diagram.

of these cells. Two cells are located beneath the occupiable area, one on each side of the fuselage; two are directly aft of these, above the floor and behind the occupiable area; and the fifth cell is in the middle of the fuselage, between the two aft tanks. With this arrangement it is very likely that any cell rupture would send fuel into the occupiable area, endangering personnel. The two bottom cells are the .30-caliber, self-sealing type, while the three upper cells are made of thin-walled bladder-type material having no self-sealing capability. These low-strength upper cells could be easily punctured or torn during crash impact. The two forward tanks, located under the floor, are particularly prone to extensive crash damage resulting from contact with rocks, stumps, or other ground objects. In this case, the hazard is amplified by the probability of compressing the tanks between the ground and cargo during impact.

Design Deficiencies of the OH-6A Fuel Cell Location

The OH-6A helicopter contains two interconnected, self-sealing fuel cells that form one tank having a capacity of 66 gallons. These two cells are located very low in the fuselage and underneath the occupiable area, as shown in Figure 5. As discussed previously, the proximity of the cells to the occupiable area and the very low location are undesirable. There is also the problem of cell compression between the ground and payload during impact.

General Recommendations

In an ideal crashworthy fuel system, the tanks should be located moderately high in the aircraft structure, above the floor level. The airframe structure beneath the tanks would then afford maximum protection against tank puncture by ground objects. The buckling aircraft structure would also absorb some impact energy, thereby reducing structural damage in the vicinity of the tank itself. In addition, the tank should be located so that it minimizes exposure to impact damage from any heavy masses such as the transmission, engine, cargo, or rotor blades. Hot ignition sources such as the engine should be as far away as possible from the tank. The tank should also be located away from the occupiable area.

The above criteria must undoubtedly be compromised by other aircraft design criteria such as flight dynamics and the limited available space within the structure. Therefore, fuel containment must be primarily a function of the tank resistance to impact or penetration and tearing by jagged metal. The fuel tanks should be made from a material that will resist impact and puncture to a much greater degree than any now in common use. Several new fuel-tank materials have been developed and tested. These materials have demonstrated significantly better crash-resistant properties than any now in use (Reference 8).

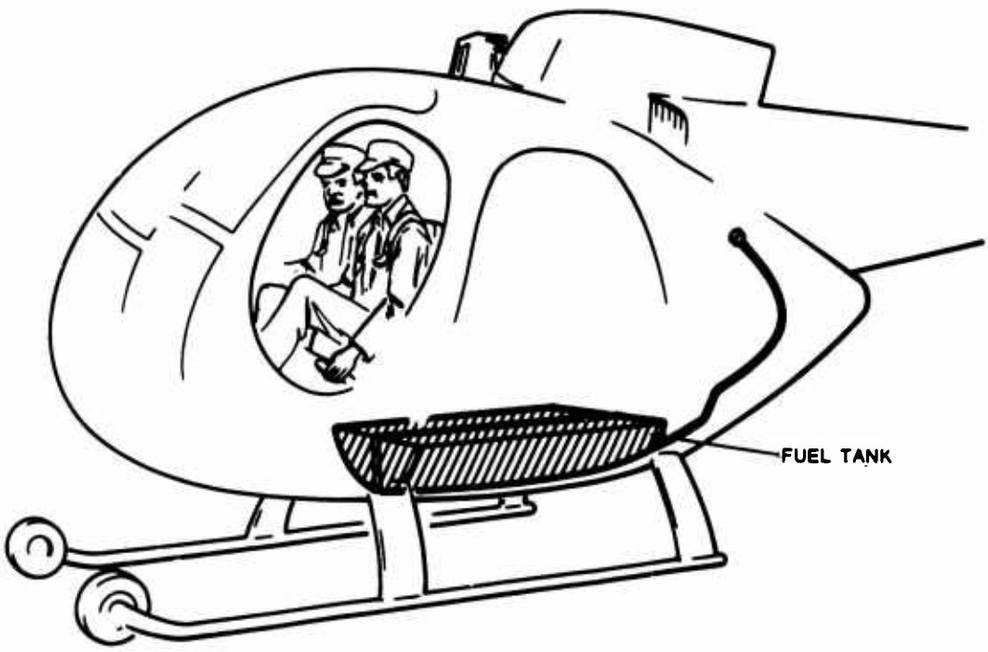

Figure 5. General Arrangement Diagram, OH-6A.

Fire curtains or protective shields should be located between fuel tanks and probable ignition sources and between the tanks and the occupiable area. The curtains should be fabricated from a flexible, fire-resistant material and should be 30 to 40 percent larger than the minimum size required to protect a given area. The curtains could then be installed in a pleated manner, thus allowing them to accommodate large structural displacements without tearing. The primary value of fire curtains is their ability to prevent spilled fuel from reaching ignition sources. An added benefit could be gained in that the protective curtain would tend to isolate a fire from the occupants, thereby increasing their escape time.

Spatial Form Design Deficiencies

The contours of the two lower forward cells and the middle aft cell in the UH-1D helicopter are generally satisfactory (refer to the fuel system diagrams in Appendix II). These cells are smooth and regularly shaped with no protrusions that could snag on surrounding structures as the structure and the cells move relative to each other during crash impact. (Attached components and lines will be discussed separately later in the design evaluation.) The smooth shapes of the two fuel cells in the CH-47 are also satisfactory in this regard.

The two aft outer cells of the UH-1D helicopter are generally smoothly shaped. However, the filler neck protrusion could be caught on or pinched in nearby collapsing structure. The bottoms of the fuel cells in the UH-1B and OH-6A aircraft all have pronounced protrusions in the sump area. A sump cup, approximately 3 inches in diameter and 2 inches deep, is located at the bottom of each fuel cell in the UH-1B. This cup is quite susceptible to snagging during crash impact. The sump area in the OH-6A helicopter is approximately one inch deep and is at the bottom of the aircraft fuselage; the sump plate is bolted through the aircraft skin. Even a moderate crash involving a sliding contact of the fuselage with the ground would almost certainly result in failure of the fuel tank in this area.

General Recommendations

Two factors which govern the ability of a tank to displace easily and without snagging are its contour and smoothness. Fuel cells should be designed without irregular shapes and protrusions. Sump areas should be contoured smoothly and gradually into the bottom of the tank, instead of projecting abruptly as they do in the UH-1B and OH-6A helicopters, and all corners should be rounded to minimize snagging.

Fuel Cell Installation Design Deficiencies

The fuel cells in all four of the aircraft analyzed are supported within the structure by nylon cord laced between the structure and the cell. The cord is fastened to the cell with triangular or circular metal hoops, approximately one-half inch across, which are mounted to the cell wall. Available crash information has never shown this hoop method of support to contribute to fuel cell failure during impact, as the metal hoops easily separate from the tank without rupturing the cell wall.

Aluminum honeycomb structural panels surround the flexible fuel cells in all of the aircraft except the OH-6A. A fiber glass backing on the honeycomb, between the cell and the structural panel, provides a smooth surface adjacent to the cell wall. These honeycomb panels provide a degree of protection to the fuel cells during crash conditions by absorbing some energy before the impact forces are transmitted to the tank. However, the honeycomb structure itself is inadequate in preventing fuel cell rupture during survivable crash impact, as witnessed in the crash of the CH-47 helicopter mentioned earlier (Figure 2).

One design factor that repeatedly causes fuel tank failure is the rigid attachment of fuel cell components to both the cell and the aircraft structure. In many cases the component is attached to the fuel cell and the aircraft with common fasteners. This technique does not allow structural displacement to occur without placing stress concentrations on the fuel tank at these attachment points. Boost pumps, filler necks, and drain valves are a few of the components which are rigidly attached to both the tank and the structure. Actual accident history has shown the prevalence of fuel cell tearing at these locations. The photographs in Figures 6 and 7, which illustrate this type of failure, were taken after a 1965 accident involving a CH-47 helicopter.

The capability of a cell to contain fuel during crash conditions depends to a large extent upon its ability to shift and reorient its volume as structural deformation occurs. Rigid attachments preclude this shifting, thus resulting in tank failure by actually tearing the tank away from the attachment. Rigid cell wall connections between fuel cells, as in the UH-1D and OH-6A helicopters (Figure 8), also restrict any shifting or reorientation of the tanks. It is practically impossible for any of the three aft tanks in the UH-1D to move relative to each other because of the rigid intercell attachments, and it is highly probable that failure will occur between the tanks at these points. This situation is discussed more fully in the sections devoted to fuel cell interconnects.

General Recommendations

Tank failures caused by rigid attachments between the cells and the aircraft structure or between the cells themselves can be prevented in several ways, depending

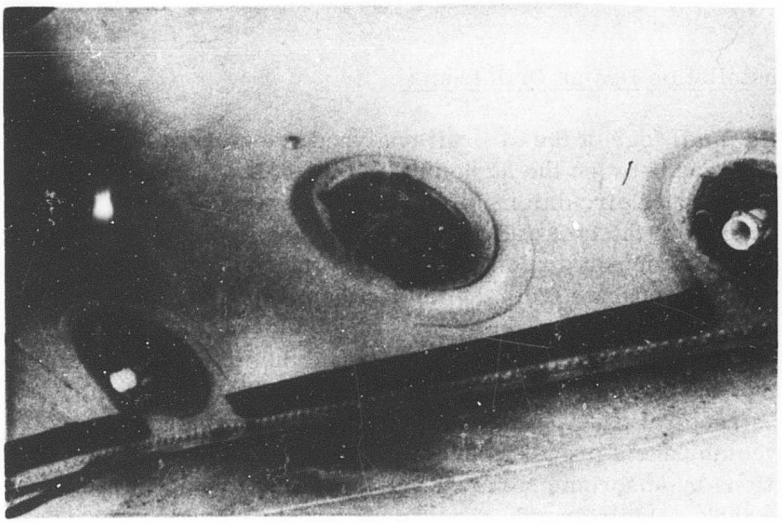

Figure 6. Fuel Tank Attachments to Basic Structure.

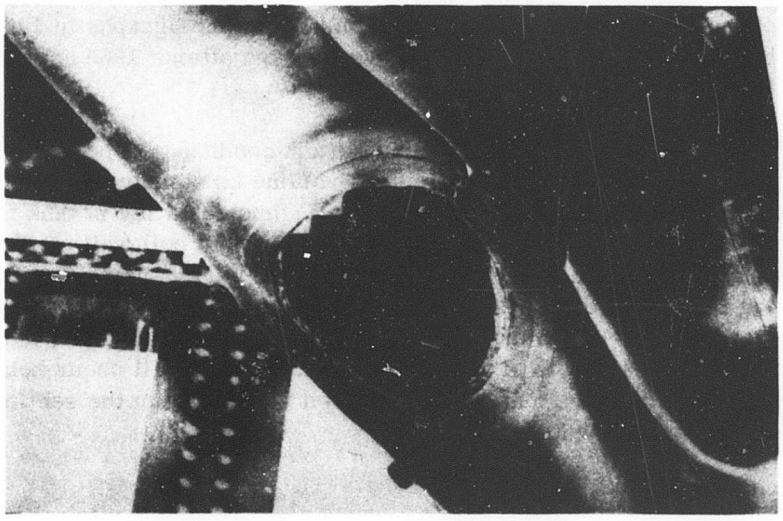

Figure 7. Fuel Bladder Failure After Structural Attachments Pulled Free.

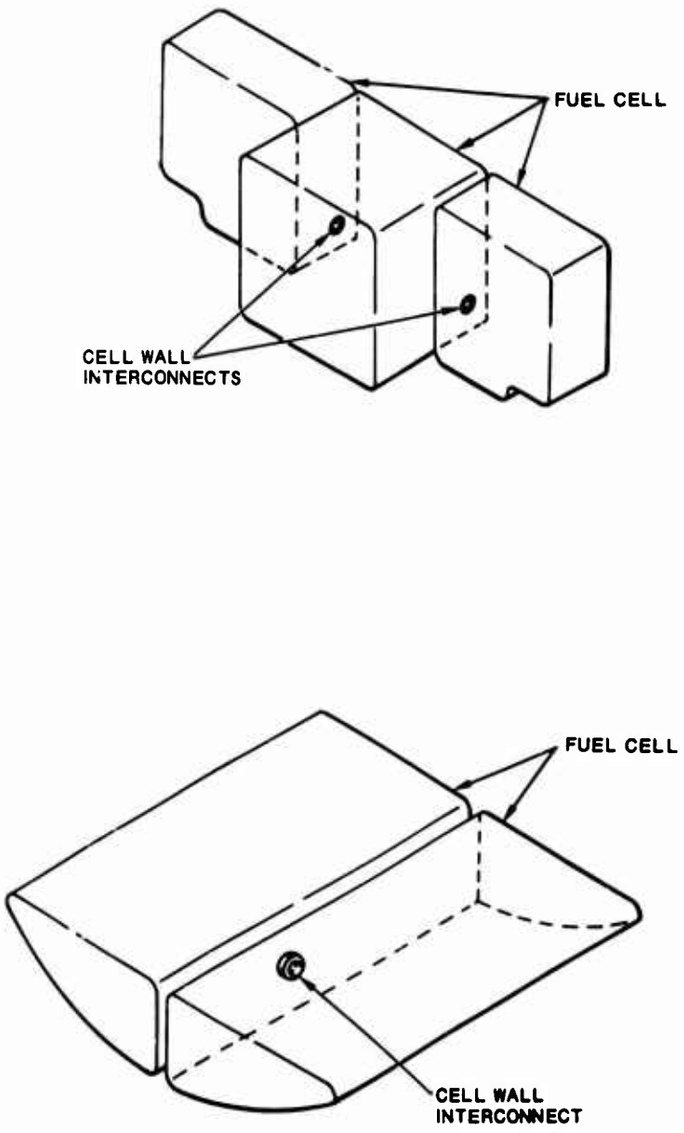

Figure 8. Cell Wall Interconnects, UH-1D (Top) and OH-6A (Bottom).

on the location and function of the attachment. In some instances, self-sealing breakaway fittings should replace the connections now in use. In other cases, the redesign or relocation of the component is desirable.

Another possibility is the centralization, insofar as possible, of all lines and connections to the tank at its least vulnerable area. This centralization would permit the greatest amount of displacement before a forcible separation of any connections could occur. The generally preferred location is at the top of the tank in an area where the probability of impact damage from crumbling aircraft structure and ground obstructions is low. The tank inlets and outlets might also be located on a protected side of the fuel cell, near the top of the tank. However, the structure of each aircraft would have to be analyzed carefully to determine which (if any) of the tank sides would be suitable from a crash vulnerability standpoint.

Design Deficiencies of Fuel Drains

The fuel drain valve is connected to a large crossfeed line in the UH-1B helicopter (Appendix II) and is exposed to impact damage from the surrounding structure during crash conditions. However, because the valve is located outside the fuel cell, it cannot cause fuel tank failure per se. The fuel drains and valves in the other three aircraft are all located in the bottoms of the fuel cells. There are common, rigid attachments between the cells and aircraft structures at these points. The fitting protrudes past the outside surface of the tank in every case; Figure 9 illustrates this typical type of installation. The fuel tank bottom in a helicopter is quite vulnerable to crash damage since many accidents occur in a near-level flight attitude and at high sinking speeds. The probability of these protruding drains in the bottoms of the fuel cells being torn from the tank during crash impact is therefore quite high.

General Recommendations

Several feasible methods are available for eliminating the hazards caused by drains in the bottom of the fuel cell. All attachments of the fitting to the structure should be eliminated and the entire valve and fitting recessed within the tank as shown in Figure 10. The drain line should be made of a low-strength material that can tear away from the tank without pulling the fitting out of the tank wall. Instead of recessing the valve and fitting, a self-sealing breakaway attachment could be placed between the cell and the valve, thus allowing separation of the two with no fuel spillage during crash impact. The use of a strong tank material, as well as reinforcing the tank around the fitting, would lessen the probability of the fitting tearing the tank wall under high-stress loads.

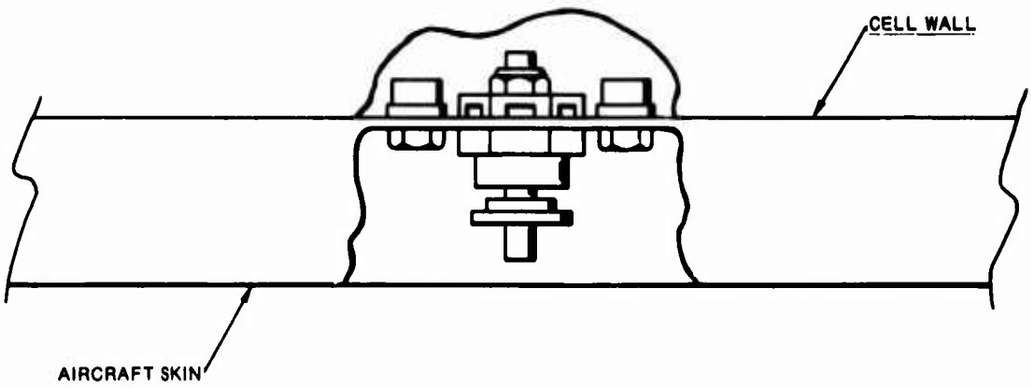

Figure 9. Drain Valve, UH-1D.

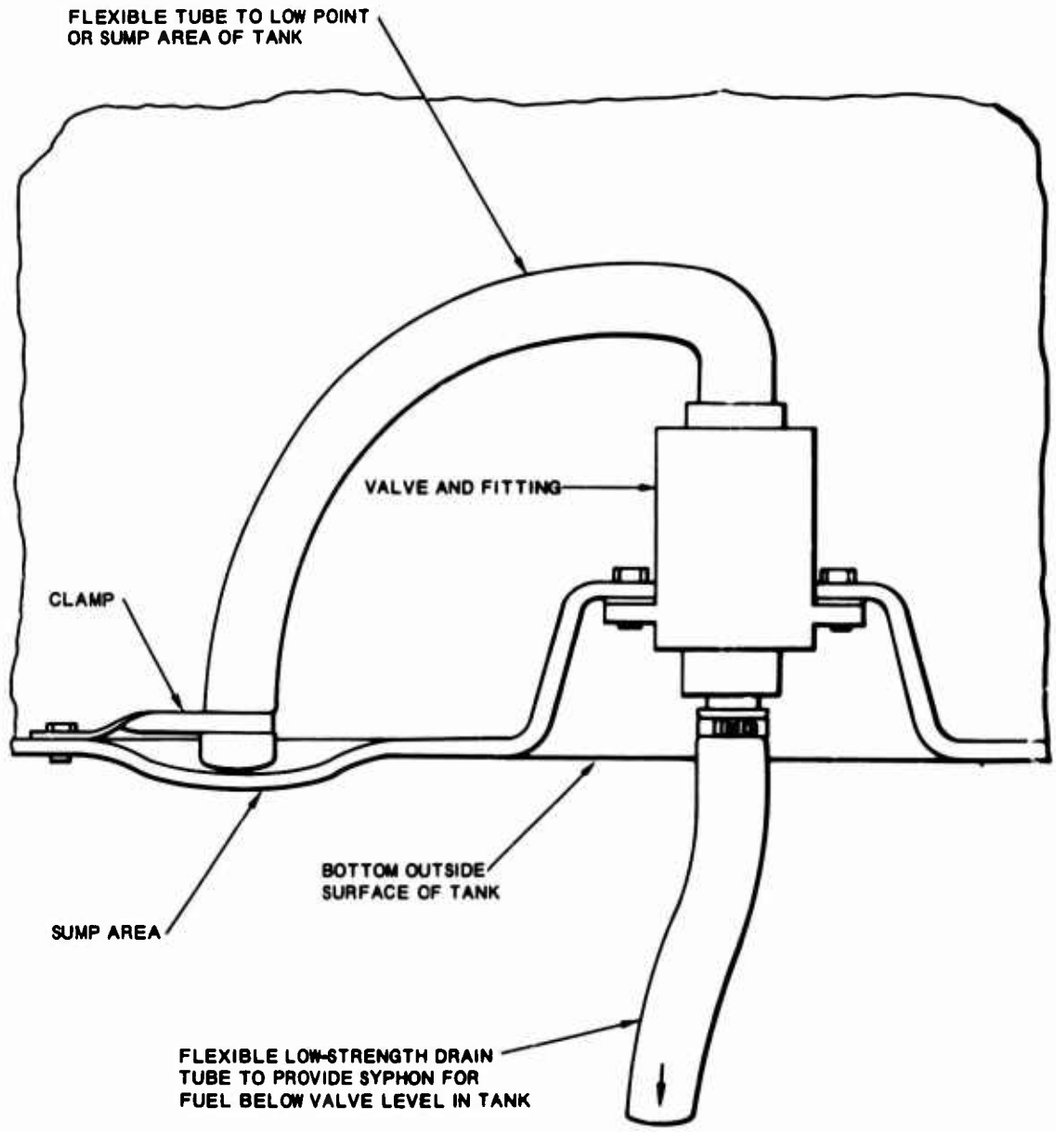

Figure 10. Suggested Drain Valve Installation in Tank.

Design Deficiencies of Fuel Vents

The fuel vent fittings protrude past the outside surface of the fuel cells in all four aircraft. In addition, these metal fittings are all rigidly attached to the tank and to the aircraft structure, with the exception of the UH-1B helicopter. Typical vent fitting installations are shown in Figure 11. When either the tank or the structure moves relative to the other under crash impact, the failure probability at this point is quite high. The valve fitting can be torn directly from the tank wall when tensile or shear loads are applied to the vent lines, or the fitting can snag (as the tank moves) on parts of the deformed structure, also tearing the tank wall. In either case, tank failure may occur with resulting fuel spillage.

Fuel spillage will occur through the vent whenever the tank comes to rest in other than a normal attitude, whether the vent is damaged or not. Additionally, the high hydraulic pressure within the tank at crash impact can also force fuel through the vent. Calculations show that, during a 100 G acceleration level, approximately two-tenths gallon of fuel could be forced through a 2-inch diameter opening. (Refer to Appendix III for the method of calculation.)

An emergency shutoff valve is incorporated in the vent line in the OH-6A helicopter. This valve is designed to close when tilted to any position exceeding 30 degrees from vertical, and also during survivable crash impacts. The incorporation of such a valve in the vent system is a sound concept. However, its installation negates its effectiveness during crash conditions. The vent line between the tank and the valve is generally composed of thin-walled, metal tubing which is rigidly clamped to the airframe structure immediately above and below the valve itself. This rigid attachment, together with the rigid attachment of the vent fitting at the fuel tank, is almost certain to cause line failure between the tank and the valve as a result of structural deformation during crash impact.

General Recommendations

Eliminating the attachment to the structure and recessing the fitting, as recommended in the case of the fuel drains, would help prevent tank failure at this point. Reinforcing the tank in this area and using a self-sealing breakaway fitting are also recommended. An internal trap system or check valve should be used to eliminate spillage from an inverted or inclined tank. The check valve should be located inside the tank to minimize the possibility of valve damage caused by shifting structure or moving objects during crash impact. A dual-purpose fitting, incorporating a check valve and self-sealing breakaway capabilities, might be designed to eliminate the necessity of two separate fittings. The incorporation of a check valve and self-sealing breakaway fitting should contain the fuel within the

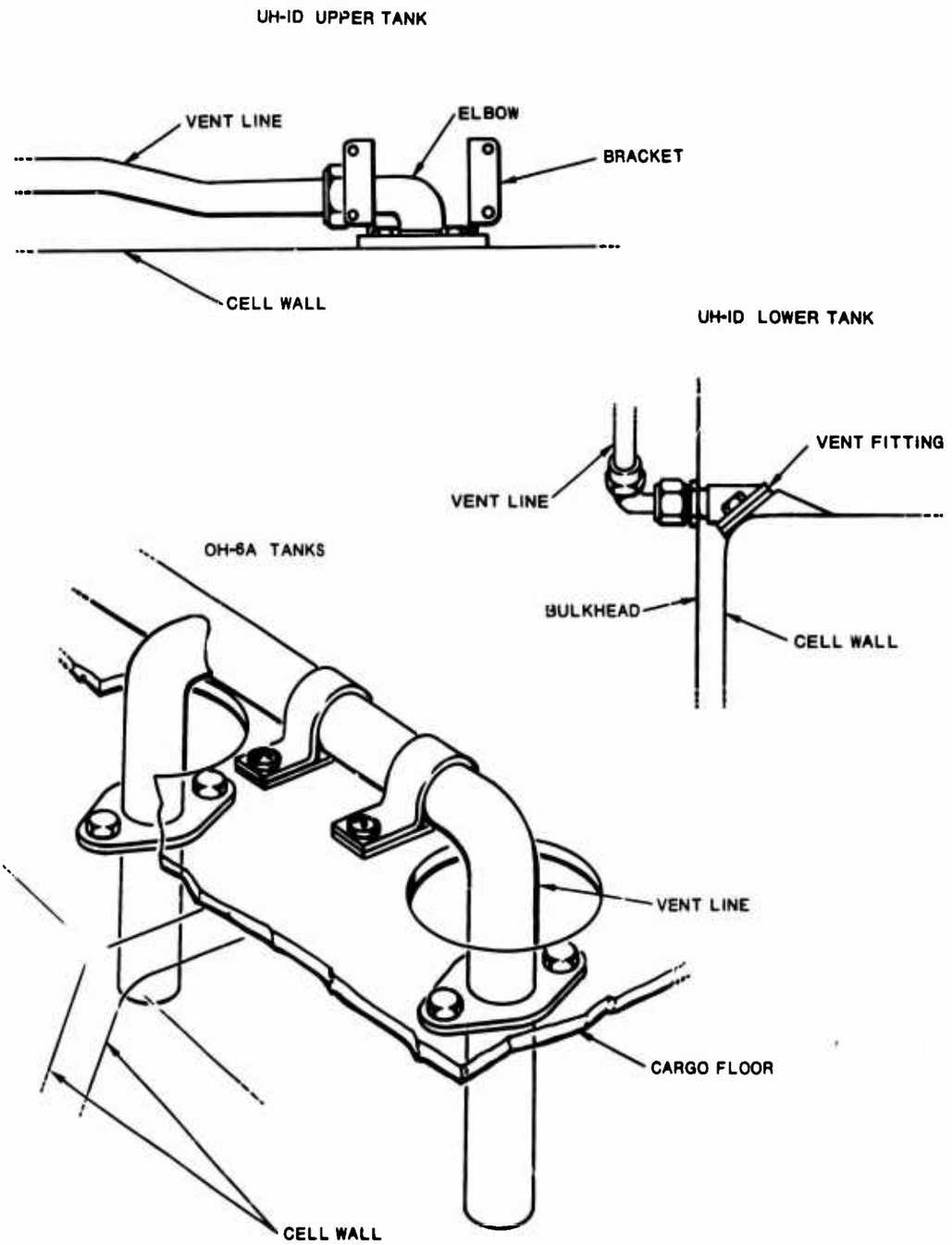

Figure 11. Fuel Vent Fittings.

tank during crash impact, thus preventing any fuel from entering the vent lines. The lines should be made of a low-strength material that will fail before transmitting to the fitting tensile or shear loads great enough to pull it from the cell wall. If there is a possibility of fuel being forced into the vent lines, however, the lines should be made flexible and longer so they can move during structural deformation without placing a high-stress load on the valve and fitting.

Design Deficiencies of Filler Necks

The CH-47 has two filler necks, one for each fuel tank. Each of the other three aircraft has only one filler neck for its entire tank system. The filler neck in the OH-6A helicopter is considerably longer than those in the other aircraft, as shown in Figure 12. The lower approximately 5 inches of the filler neck is fabricated from the fuel cell material and is bonded to the cell. This lower portion is joined to a rigid section by a clamp. The filler cap is part of the outside structure of the aircraft. The complete assembly is enclosed in a rigid shield between the aircraft skin and the tank wall.

The filler necks in the other three aircraft are attached to the aircraft structure and the fuel tanks with common bolts, with the filler cap ring a part of the aircraft structure. This type of attachment is illustrated in Figure 13. When structural deformation occurs during crash impact, the filler neck attachment pulls loose from the tank wall, leaving a large hole in the tank. Figures 6 and 7 demonstrate this failure mode.

General Recommendations

To prevent fuel spillage during crash impact, it is essential that the filler cap stay with the fuel tank when the structure and tank move relative to each other. The cap should be countersunk into the tank and the tank attached to the structure around the cap area with a frangible ring or coupling, as shown in Figure 14. The tank wall should be sufficiently reinforced in this area to prevent failure prior to separation of the frangible interconnect.

Long filler necks should be avoided if possible. If a long filler neck must be used, it should be made of flexible material having a breakaway capability to avoid excessive cell-filler neck restraint as the cell moves relative to the structure. Again, the cap should be countersunk into the fuel tank to ensure that the tank remains sealed in this area if a filler neck or attachment fails. This type of installation is shown in Figure 15.

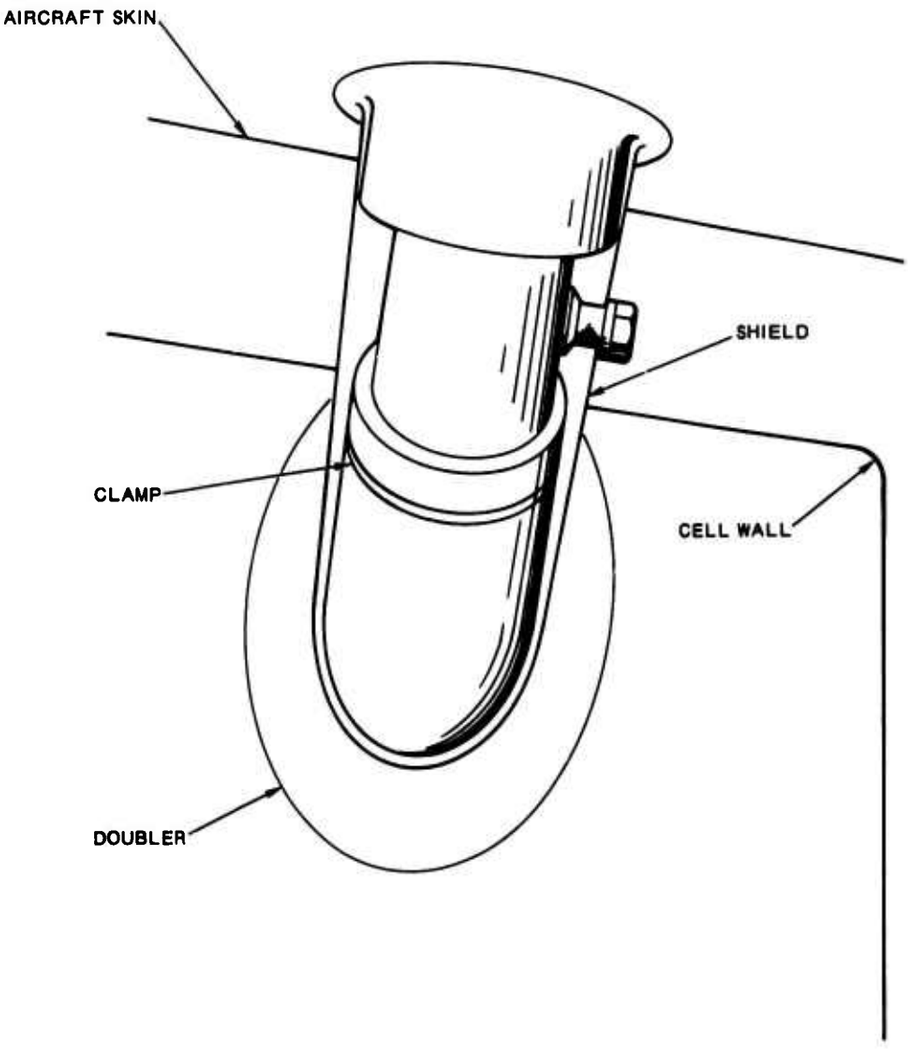

Figure 12. Filler Neck, OH-6A.

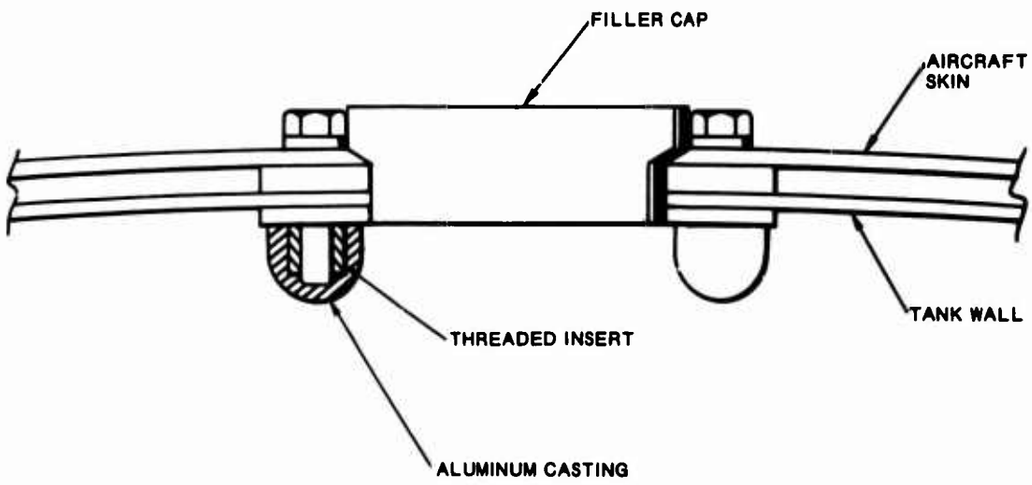

Figure 13. Typical Filler Neck Attachment.

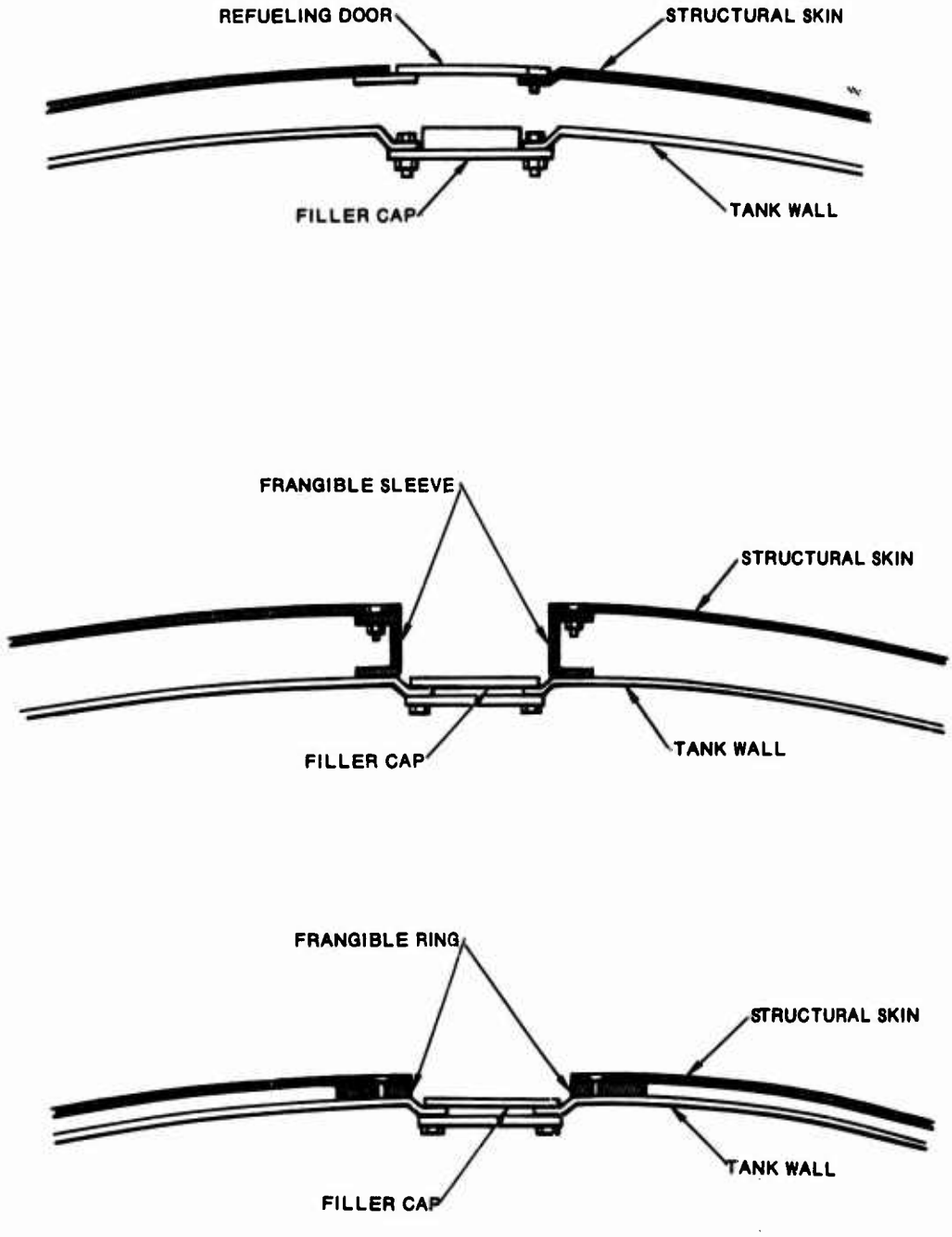

Figure 14. Various Filler Neck Attachments.

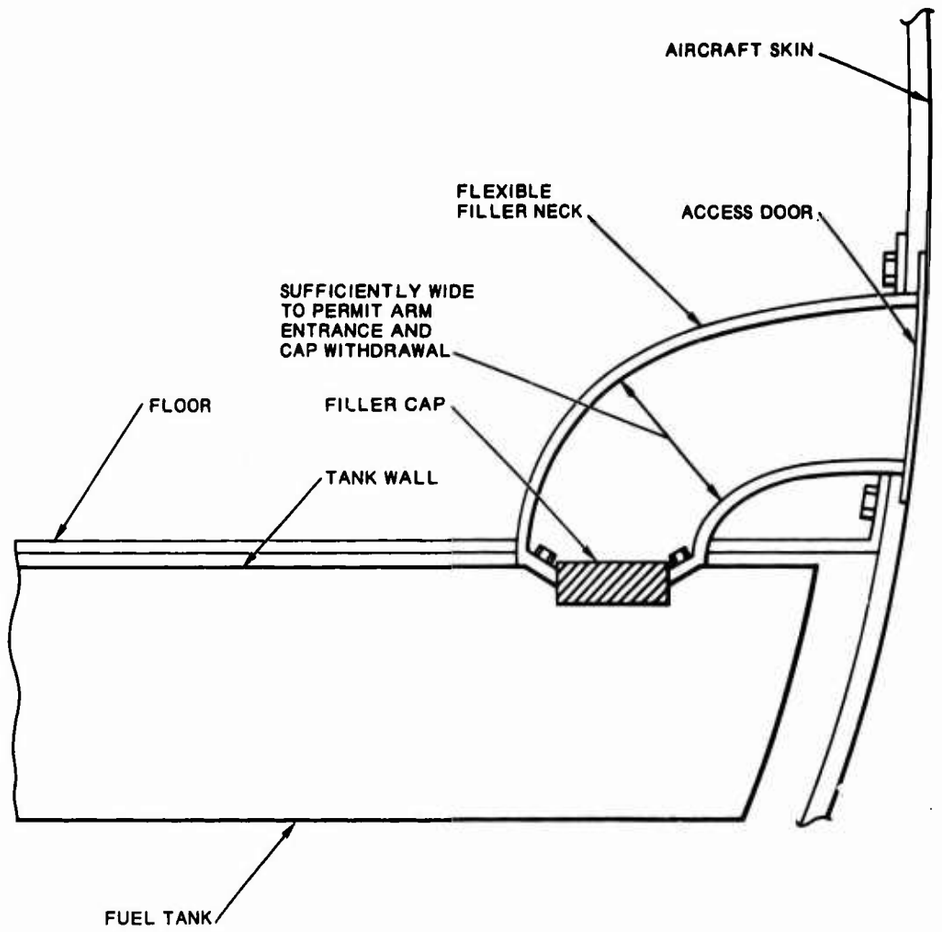

Figure 15. Flexible Filler Neck Installation.

Design Deficiencies of Quantity Indicators

The quantity indicator in the OH-6A helicopter is a float-type indicator that is rigidly mounted to a recessed cover in the top of the fuel tank. This cover is rigidly mounted to the aircraft structure. The other three aircraft all have capacitance indicator probes similar to those shown in Figure 16. The CH-47 helicopter has common rigid attachments between the tank wall, probe flange, and aircraft structure. The fuel quantity probes in the UH-1 helicopters are attached by clamps to metal fittings which are rigidly attached to the aircraft structure (Appendix II).

The common rigid attachment between the tank and the structure in the CH-47 is, as previously mentioned, quite prone to cause tank failure at this point. Although the quantity indicators in the other three aircraft are not attached to the aircraft structure and the tank wall with common fasteners, they are still rigidly bound to the structure and will move as the structure moves. This condition is particularly hazardous in the case of the capacitance indicator probes, which consist of rigid tubes mounted vertically within the fuel tank. The clearance between the ends of the probes and the cell walls varies from approximately one-half to one inch. During crash impact, it is highly probable that these probes will punch holes in the cell wall as the fuel tank and the structure move relative to each other.

General Recommendations

Serious consideration should be given to the use of other methods to measure fuel quantity, thus eliminating the rigid capacitance indicator probe within the tank. One such method would be the use of a fuel counter, as is currently used in the T-33 jet trainer, coupled with a warning float switch or thermistor sensor to indicate low fuel level. Although desirable from a crash vulnerability viewpoint, the use of a fuel counter is not satisfactory when ballistic vulnerability is considered. (See page 48)

If a quantity indicator is used within the tank, the float-type indicator is less dangerous to the tank than the probe. In those cases where a float indicator is not advantageous (as in a relatively deep tank), a flexible or frangible capacitance probe could be used. Thus, during crash impact the probe itself would deflect or break before damaging the cell wall. A smooth, rounded shoe at the probe base, as seen on the center fuel probe in Figure 16, should be used to prevent cell wall puncture before column failure of the probe occurs. The tank wall must be reinforced around the probe mounting to ensure that this area will not tear under loads which are less than those required to cause probe failure. No matter what type probe is actually used, there should be no high-strength rigid attachment between the probe and the aircraft structure. If a structural attachment is necessary, a frangible attachment should be used, as shown in Figure 17.

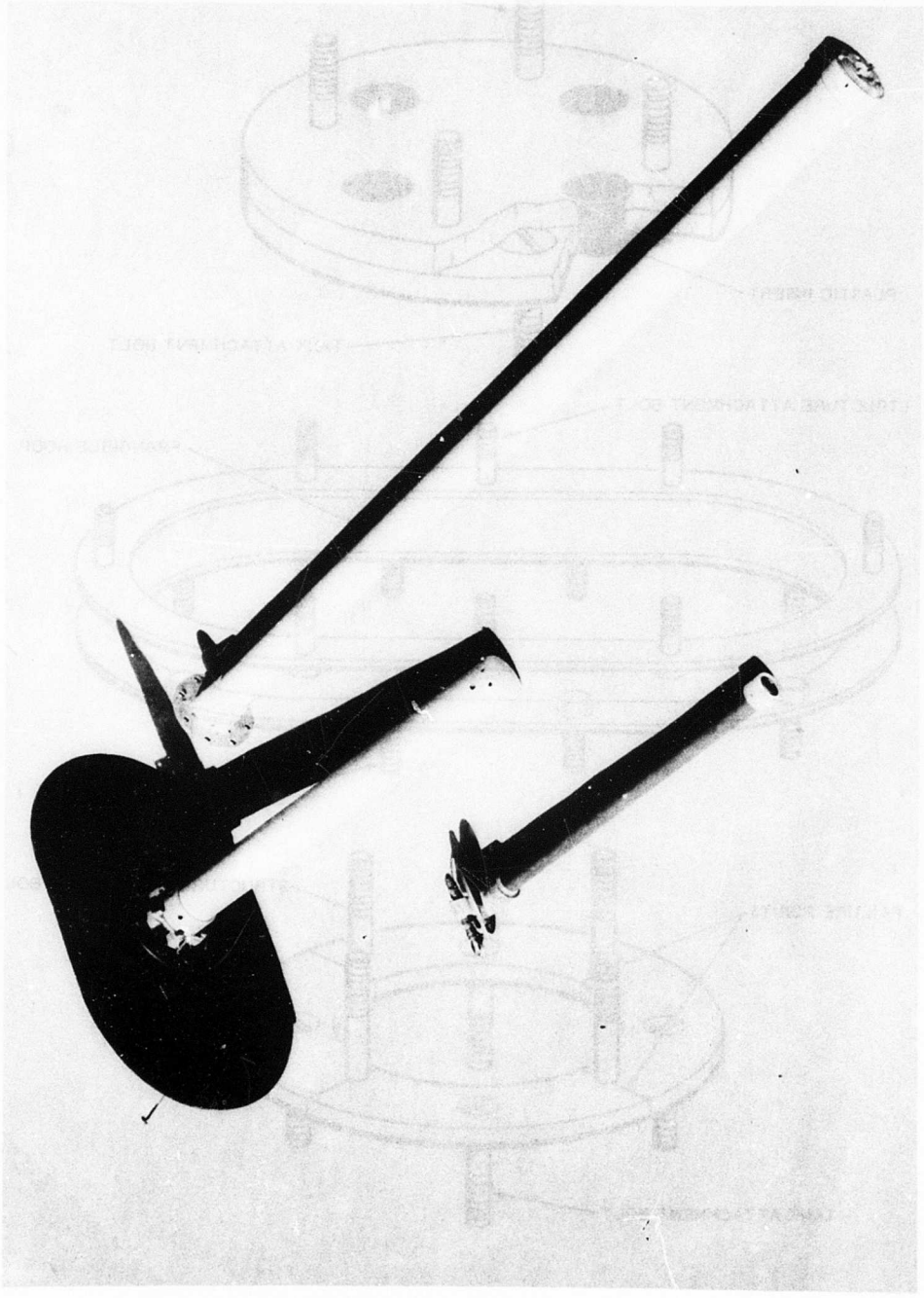

Figure 16. Typical Capacitance Indicator Probes.

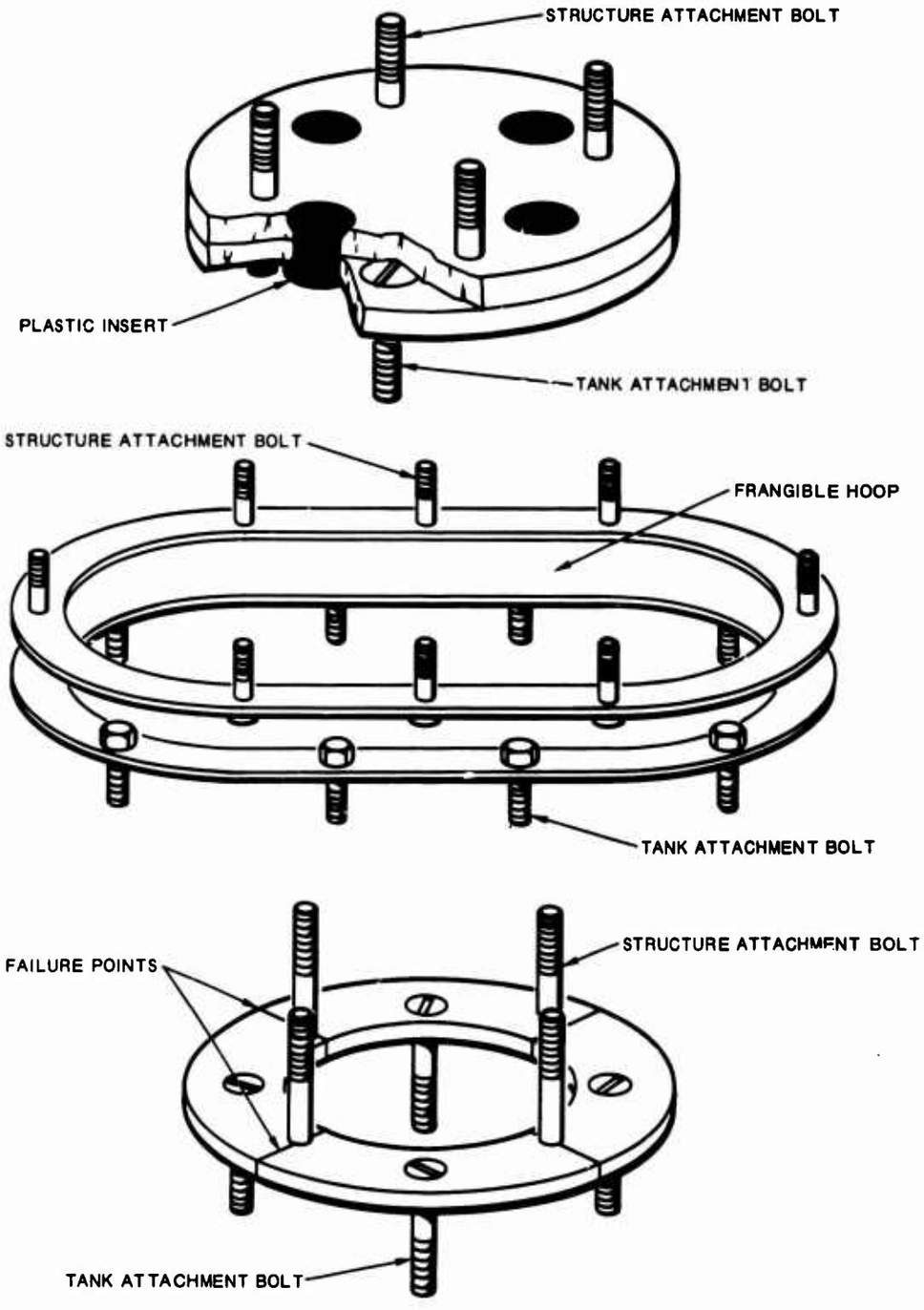

Figure 17. Frangible Attachment Concepts.

Design Deficiencies of Fuel Boost Pumps

All four of the aircraft use electrically driven boost pumps located within the fuel tank. The UH-1D helicopter has one electrically driven and one air-driven pump. However, the air-driven pump is equipped with an electrical low-level switch so that electrical wires are still close to the fuel tank.

The boost pumps in the CH-47 helicopter are mounted to the cell access doors at each end of the fuel tanks. These metal doors are mounted to the tank and the aircraft structure with common bolts. The pumps in the UH-1 helicopters are mounted to large (approximately 12 inches long and 8 inches wide) metal sump plates located in the bottoms of the cells. The sump plates are rigidly attached to both the fuel tank and the aircraft structure. Figure 18 illustrates this type of attachment. The rigid attachment of the pump to both the tank and the structure results in a high probability of tank tearing at this point during crash impact. In addition, the large size of the rigid access doors and sump plates severely limits flexure of the tank walls in these areas when structural deformation occurs. This rigidity makes the probability of the tanks tearing at these points even higher.

The boost pump in the OH-6A is mounted to a metal sump plate approximately 4 inches square. The position of this plate is particularly hazardous, as it rests on the bottom of the aircraft structure. The plate is attached by common bolts through it, the cell wall, and the bottom skin of the aircraft. This installation provides no protection for the fuel cell during crash impact, and the probability of fuel tank failure in this area is extremely high. Crash damage to the fuel pump results not only in fuel spillage but in the release of electrical sparks from damaged wires into the fuel area. The possibility of fuel spillage and electrical sparking makes the fuel pump a major threat in the initiation of crash fires.

General Recommendations

Several methods may be used to eliminate the fire hazards created by fuel boost pumps. The most desirable method would be to eliminate the pump completely and utilize an engine-driven, positive-displacement, suction-type system similar to that already in use in the CH-53 helicopter. A detailed description of this system may be found in Appendix VI.

If the boost pump is placed inside the fuel tank, the pump should not be rigidly mounted to the aircraft structure. If the fuel tank and pump must be attached to the structure to support the pump, the attachment should be frangible so that the attachment will separate before there is any possibility of tearing the tank wall.

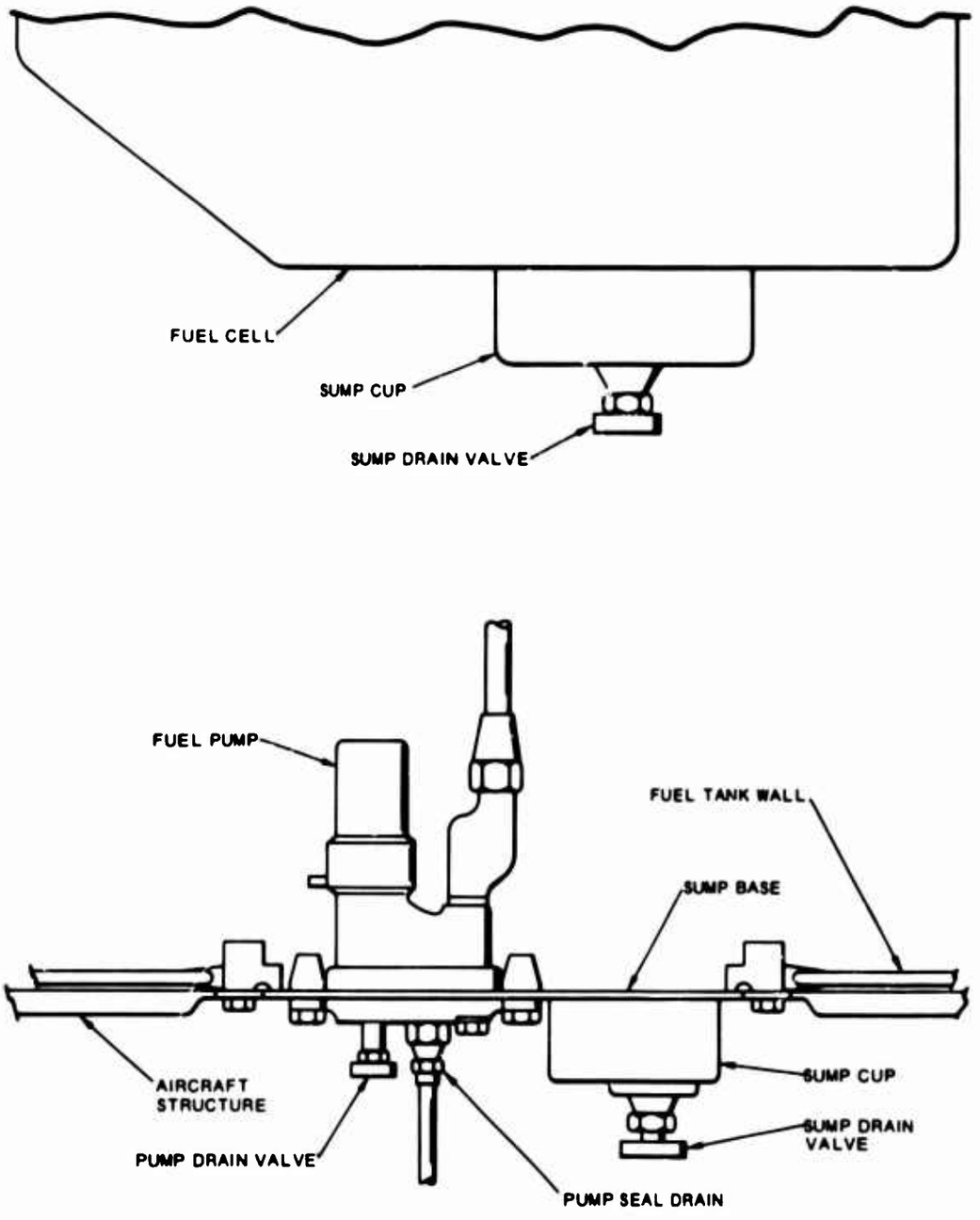

Figure 18. UH-1B Sump Assembly.

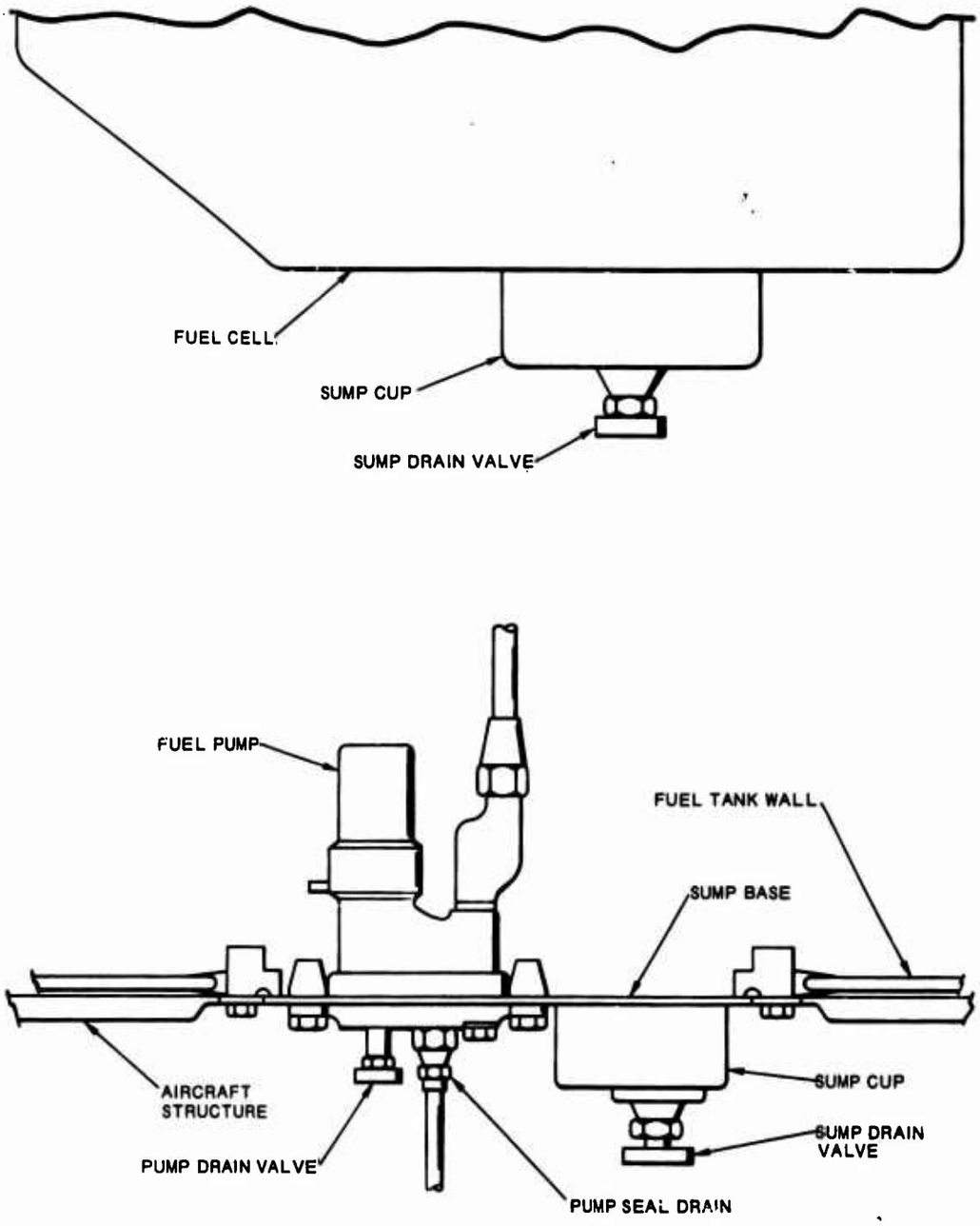

Figure 18. UH-1B Sump Assembly.

Design Deficiencies of Cell-Fuel Line Connections

The method of fuel line attachment to the fuel tanks in the CH-47, UH-1B, and UH-1D helicopters is identical in principle and typical of the present state of the art. The lines are connected to the tank by means of standard AN and MS fittings that are rigidly attached to the surrounding structure. This method of attachment is illustrated in Figure 19. As mentioned previously, rigid attachments are likely to cause cell failure at these points during crash impact.

The fuel line exits from the OH-6A tank directly from the fuel shutoff valve. This valve is mounted to the top cover plate which is in turn mounted to brackets rigidly attached to the aircraft structure (Figure 20). This arrangement is considerably safer than that found in the other aircraft, in that only one fuel line exits from the tank, and this from the tank's least vulnerable area. However, the rigid attachment between the tank and the structure still increases the probability of tank failure in this area.

General Recommendations

All fuel line connections to the tank should be made with self-sealing breakaway fittings which will separate and seal with no fluid loss if subjected to axial tensions or shear loads. Grouping all fittings in the least vulnerable area of the tank, insofar as possible, would allow maximum displacement of the tank before high-stress loads could be applied to the fittings. The fittings should be designed for actuation in all conceivable modes of separation, including shear. If they protrude beyond the mounting face, they should be recessed to prevent their snagging on the structure after breaking away, as shown in Figure 21. Reinforcement of the tank in the area of the fittings would also be necessary to ensure fitting separation before tank failure occurs.

Design Deficiencies of Fuel Cell Interconnects

There are no interconnecting lines between the two fuel tanks in the CH-47 helicopter. The small crossfeed line located near the engines permits fuel from the cells to be directed to either engine but does not allow fuel to pass from one tank to the other. (Refer to the fuel system diagrams in Appendix II for the arrangement of lines and interconnects.)

The crossover lines in the UH-1D helicopter are located directly above the landing gear crossover tubes and are therefore subject to extensive damage in case of landing gear failure. Since the results of accident studies of rotary-wing aircraft have shown repeated failures of landing-gear structures under moderate impact, the position of these lines constitutes a serious fire hazard.

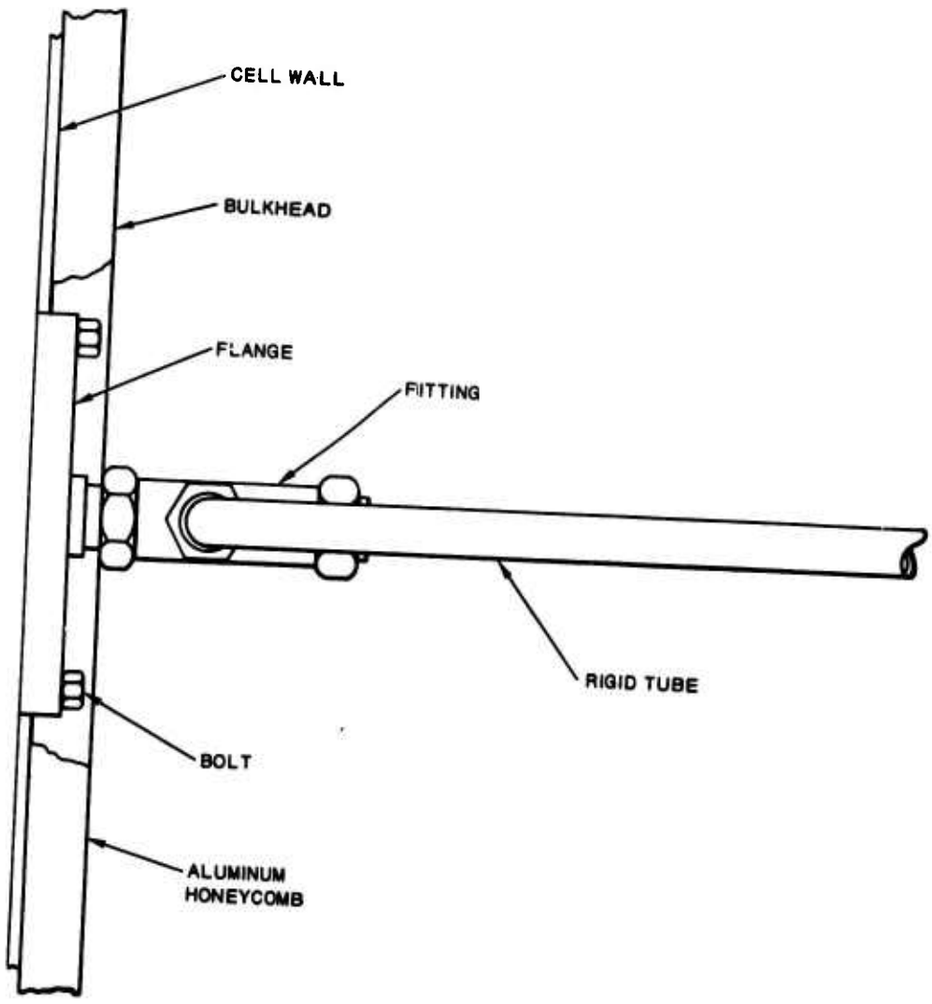

Figure 19. Typical Fuel Line Connection to Fuel Cell.

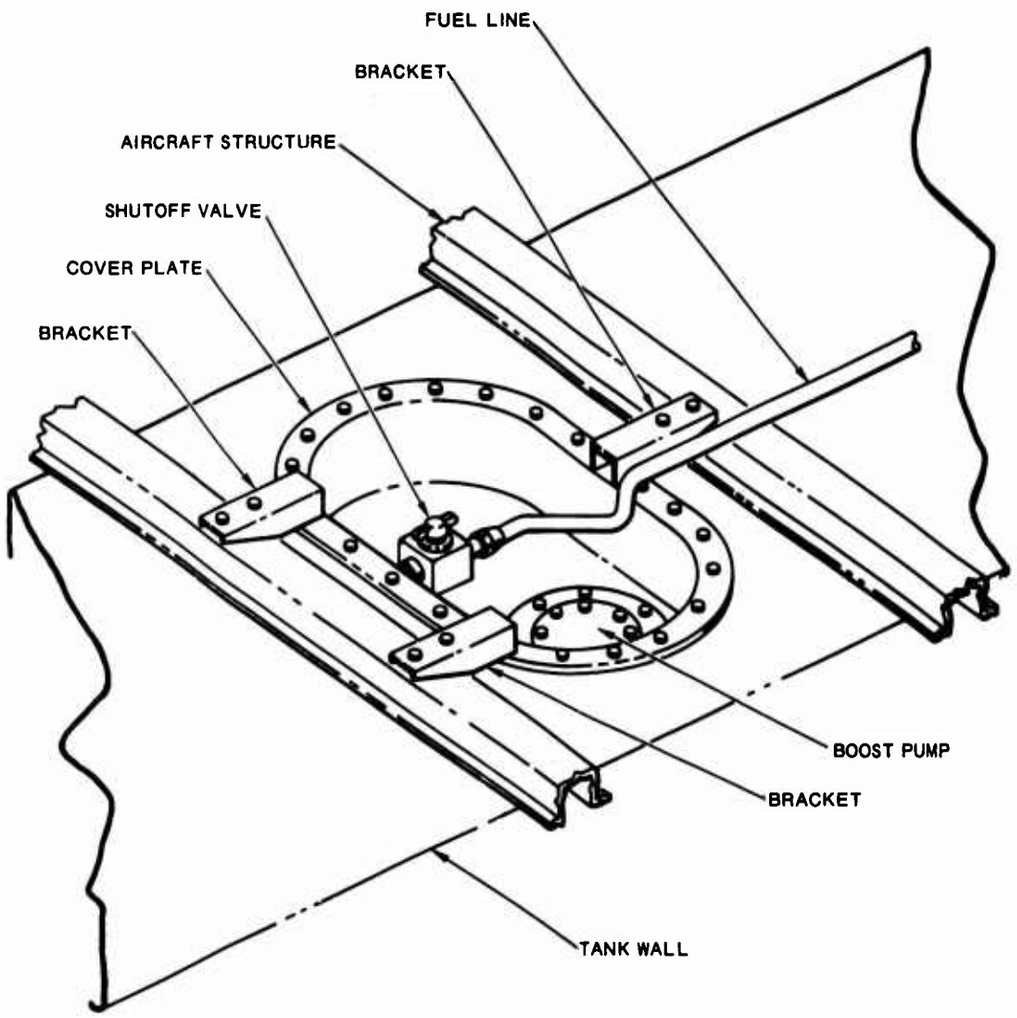

Figure 20. Cover Plate Installation, OH-6A.

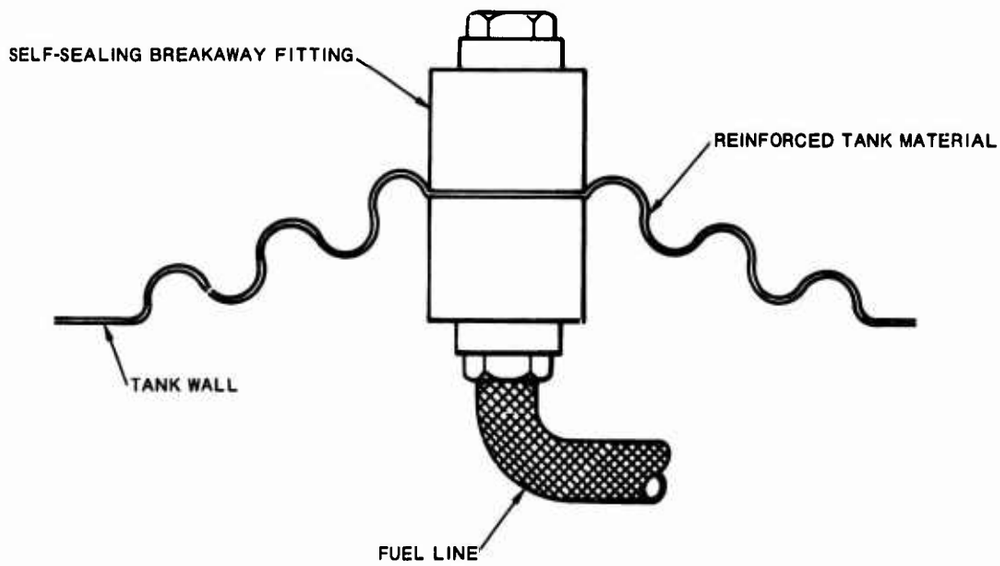

Figure 21. Recessed Cell Fitting.

In addition to the crossover lines, the UH-1D contains rigid interconnects, of the type shown in Figure 22, between the three aft cells themselves. The two fuel cells in the OH-6A helicopter are also joined by a rigid interconnect similar to those used in the UH-1D. These rigid interconnects prohibit the movement of the fuel cells relative to each other. When structural deformation occurs during a crash sequence, interconnects will very probably cause fuel cell failure, resulting in extensive fuel spillage.

General Recommendations

All interconnect lines should be completely flexible and approximately 20 percent longer than necessary for normal connection. These modifications would allow the lines to elongate or bend under tensile or shear loading without breaking. A frangible, gall-proof baffle around the line should be incorporated into the aircraft structure wherever the line goes through the structure (Figures 23 and 24). The baffle should be designed so that it will fail under crash impact without snagging and damaging the fuel line. This design would allow the line itself to move during structural deformation instead of being severed at this point.

Self-sealing breakaway fittings (Figure 21) should be used at all crossover line-tank connections. The rigid interconnects between the cells should be replaced with self-sealing breakaway valves capable of sealing with no loss of fuel under all conceivable modes of separation. Although quick-disconnect valves will seal with no fuel loss, it cannot make a direct tank-to-tank interconnect because of its displacement limitations. Conversely, the crash-resistant valves, some which have been tested for the Federal Aviation Agency (Reference 3), lack the ability to seal with no fluid loss in the interconnect portion of the device. The elimination of a direct tank-to-tank interconnect and the installation of a quick-disconnect valve represent one possible solution to this problem, although an entirely new valve with direct tank-to-tank contact would be most satisfactory.

Special consideration must be given to the location of crossover lines. These lines should be routed along heavier structural members of the aircraft which are less likely to deform during crash impact. Extra consideration must be taken to avoid areas where structural displacement is likely to occur, such as the wheel well and landing-gear crossover tubes.

Design Deficiencies of Fuel-Transfer Lines

Most of the fuel-transfer lines in all four aircraft are made of rigid aluminum tubing which is routed directly between connections. As previously noted, these rigid lines readily fail when deformed during crash-induced structural displacement. Figures 25 and 26 show typical failures of rigid tubing that occurred under

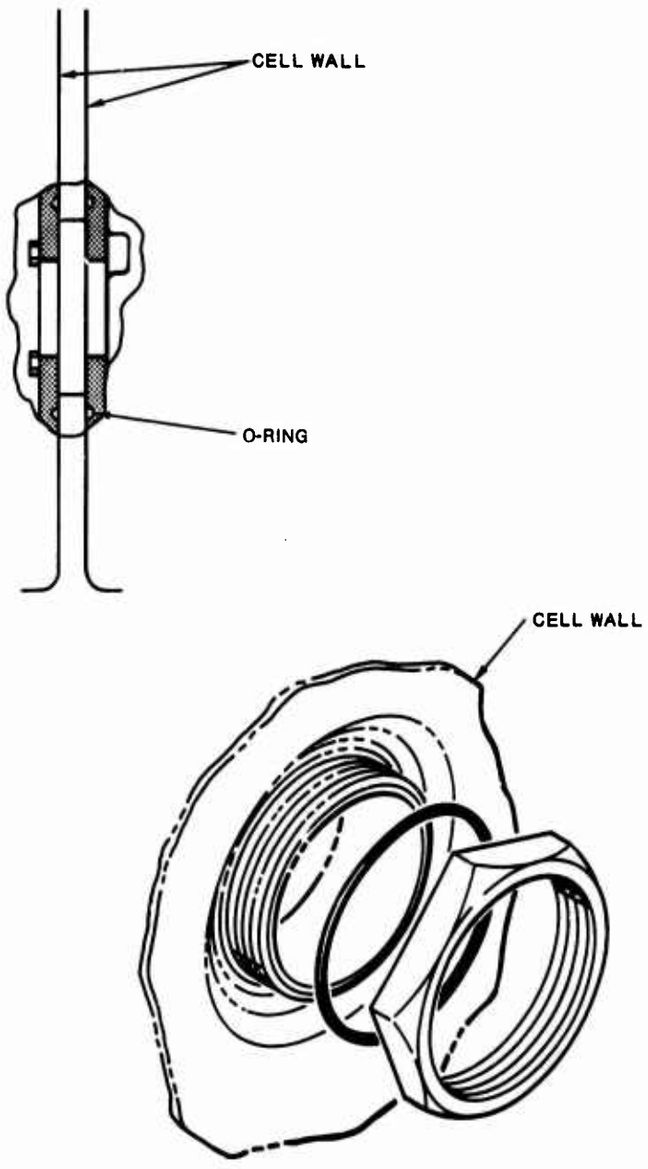

Figure 22. Fuel Cell Interconnects, UH-1D (Left) and OH-6A (Right).

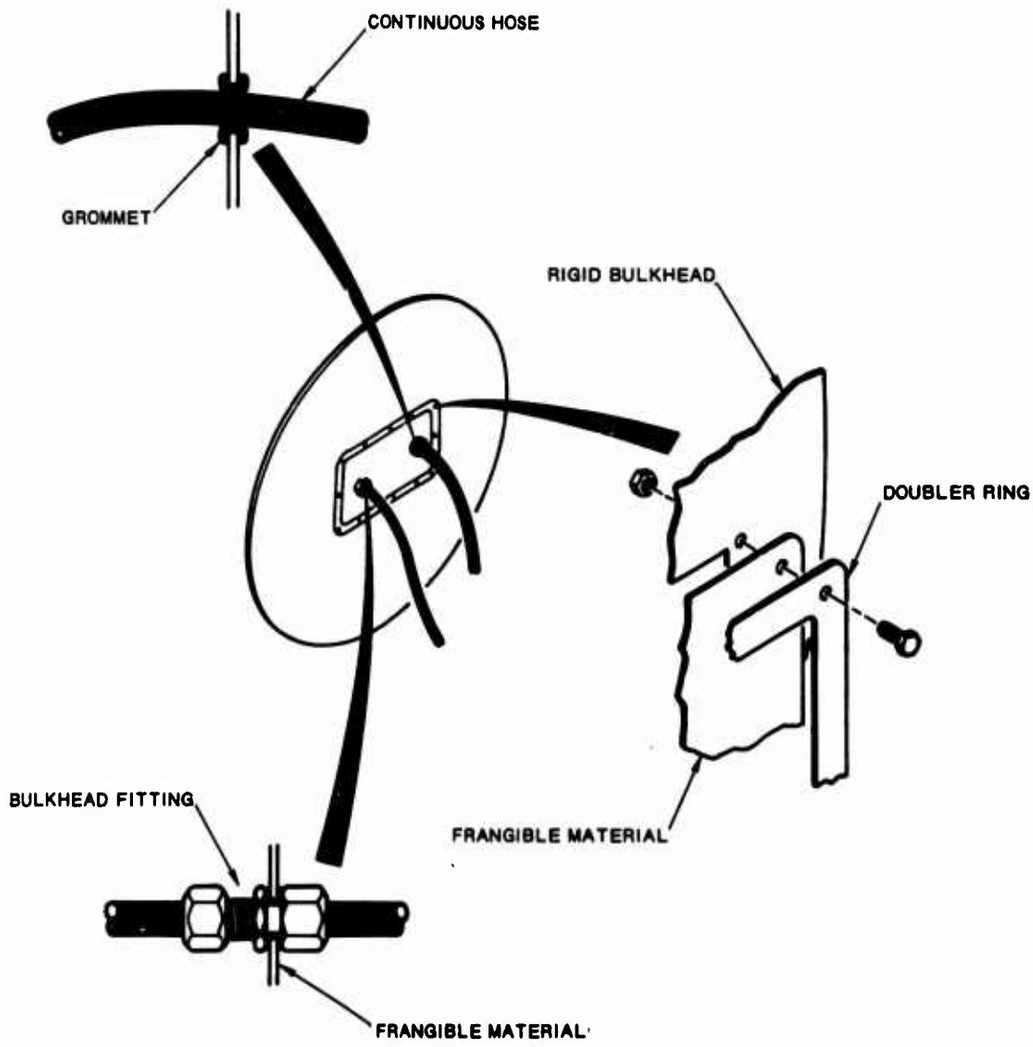

Figure 23. Tube Stabilizing With Frangible Structure.

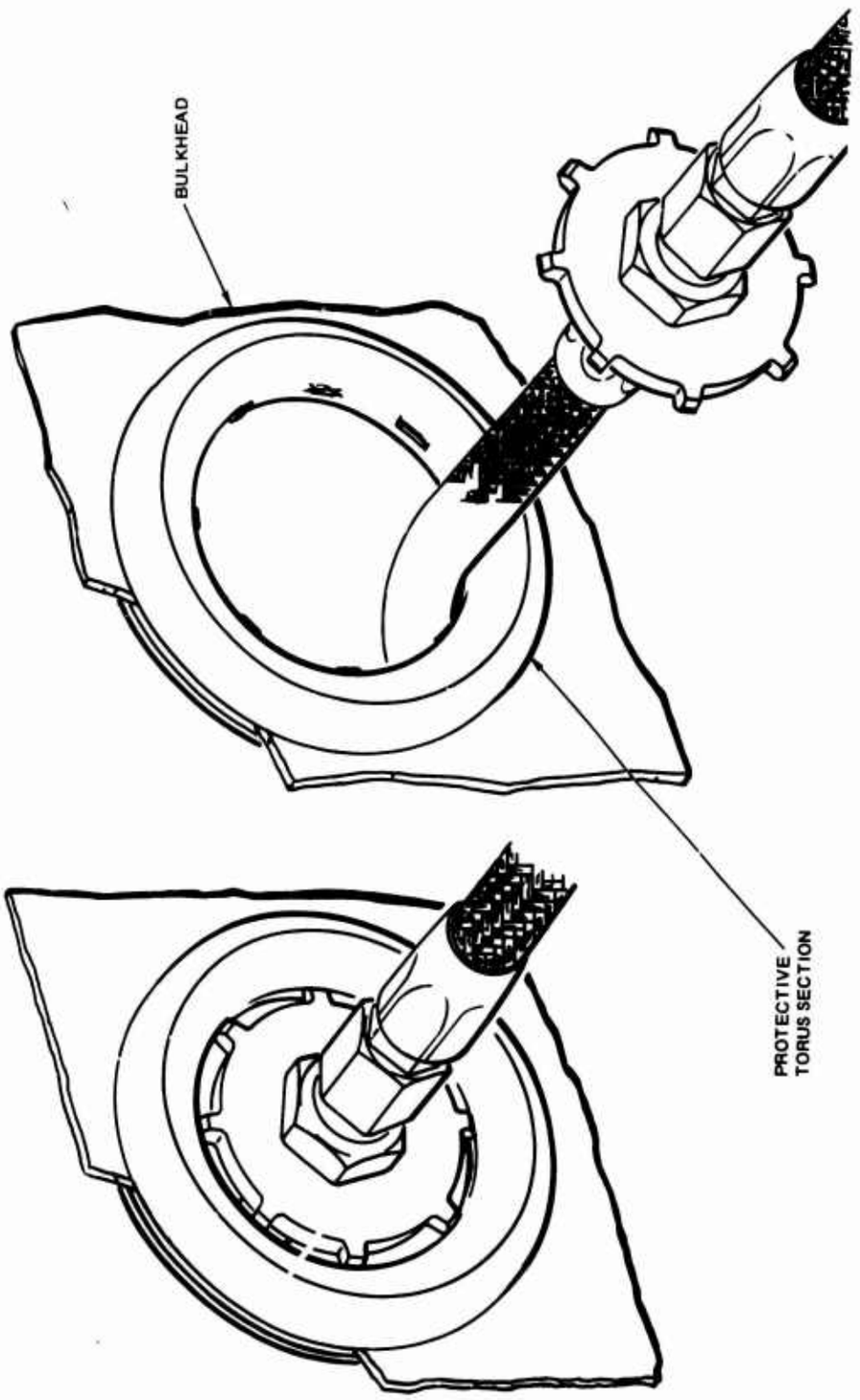

Figure 24. Tube Stabilizing With Frangible Toroidal Structure.

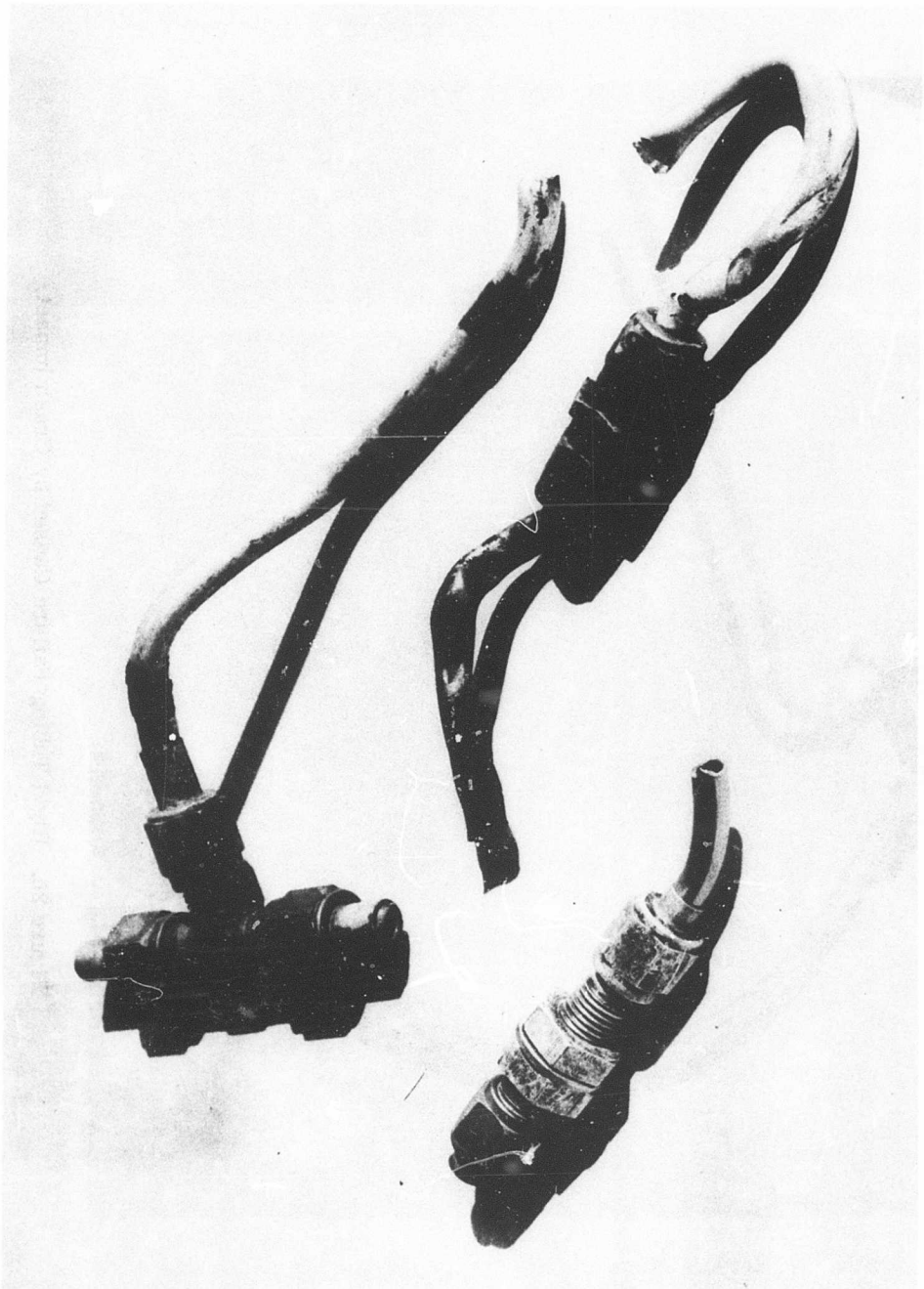

Figure 25. Rigid Tubing Failures Caused by Crash Impact.

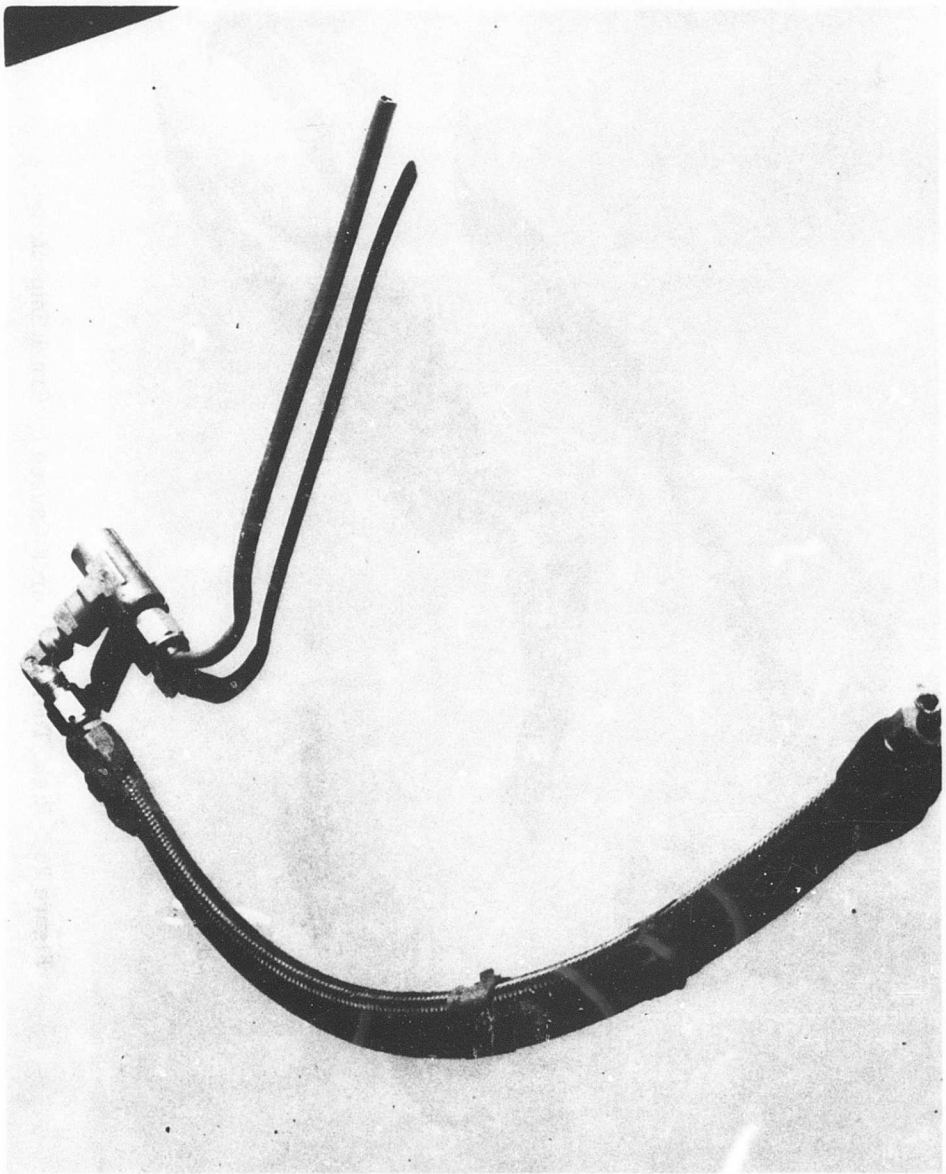

Figure 26. Rigid Tubing Failure Caused by Crash Impact.

controlled crash conditions in studies conducted by AvSER. As shown in Figure 26, the flexible hose was undamaged, although both the rigid tubing and the fittings failed.

Fuel-transfer-line routings in some of the aircraft studied constitute definite crash fire hazards because of their vulnerable positions. Flammable fluid lines in the upper fuselage area of a CH-47 helicopter were severed when the rotor blade struck that area during a survivable crash (Reference 7). The small crossfeed lines between the two forward tanks in the UH-1D are quite vulnerable to impact damage from stumps and rocks because of their location low in the fuselage.

General Recommendations

All fuel lines should be flexible and of extra length to enable them to accommodate structural displacement. These lines should be supported along their route by low-load breakaway clamps. Careful selection of support points is important to ensure that the lines will not rupture. Frangible, nongalling fittings should be used wherever the lines must pass through flat plate areas such as bulkheads and firewalls.

Expandable, self-closing fuel lines now under development also offer a method of coping with structural displacements that would ordinarily rupture a rigid line. These self-closing lines are discussed in detail later in this report.

The fuel-transfer lines should be routed away from areas of anticipated impact or structural collapse, such as the aircraft bottom, landing-gear area, and rotor blade impact area. The lines should never be routed near high-current electrical wiring. Routing the fuel lines along heavier structural members of the airframe, which are less likely to deform under crash impact, is also desirable.*

Design Deficiencies of Transfer Line Fittings and Couplings

There are numerous aluminum fittings and connections in the transfer systems of all four aircraft. Many of these are rigidly attached to the structure at firewalls and bulkheads. Data obtained from crash histories and studies conducted by AvSER have shown that failure of these rigid fittings on impact is fairly common. In many instances, these fittings have failed well before the failure of flexible lines attached

* As mentioned previously, all lines should be grouped together and exit the fuel tank, insofar as possible, from the least vulnerable area of the tank.

to them, as seen in Figures 27 and 28. Again, this failure is caused by structural deformation with resultant high-tension or shear loads applied to the fitting.

General Recommendations

All lines to the fittings should be flexible and of extra length to prevent transmitted high-stress loads from affecting the fittings. An absolute minimum number of fittings should be used, and self-sealing breakaway fittings used wherever possible. Frangible, nongalling baffles should be placed around bulkhead and firewall connections. These baffles should be designed to fail before the connection fails.

Those connections and fittings not of the breakaway type should be strengthened by redesigning or using different materials, or both. Various failure modes of the connections and fittings should be evaluated and the results of this evaluation used as criteria for redesign. The substitution of standard steel fittings in place of the aluminum fittings might be in order, depending on the failure modes involved.

Design Deficiencies of Fuel Filters

The CH-47 helicopter has either a fuel purifier or barrier fuel filter, depending on the engine model used. In both cases, these units are rigidly mounted to the engine itself, as shown in Figures 29 and 30. When the fuel purifier is used, the rigid fuel supply line from the tanks connects directly to the purifier. When the barrier fuel filter is employed, the rigid fuel supply line first enters a fuel boost pump mounted on the engine. The filter is connected to this pump by a flexible hose. Flexible hose is also used to carry the fuel from the filters in both cases.

Although the use of rigid tubing constitutes a definite crash fire hazard, especially in such close proximity to a hot ignition source, the installation of the filters per se is satisfactory from a crash vulnerability standpoint. The rigid attachment to the large mass of the engine tends to preclude the filters being torn loose during crash impact, and the mass and shape of the engines afford good protection from flying objects or deforming structure. However, the juxtaposition of the filter and engine is undesirable from a ballistic standpoint. Penetration of the filter by a projectile would send fuel and spray directly into contact with the hot engine surface, resulting in ignition and subsequent fire. This hazard is discussed more fully in the section devoted to ballistic vulnerability.

The cylindrical fuel filter in the UH-1B helicopter consists of a detachable sump bowl connected to the head by means of a "V" band clamp. The filter is mounted on a bracket above the service deck, at the left of the engine (Appendix II). The rigid aluminum fuel line from the tanks enters directly into the filter. A flexible hose connects the filter to the engine.

Figure 27. Fitting Failure Caused by Crash Impact.

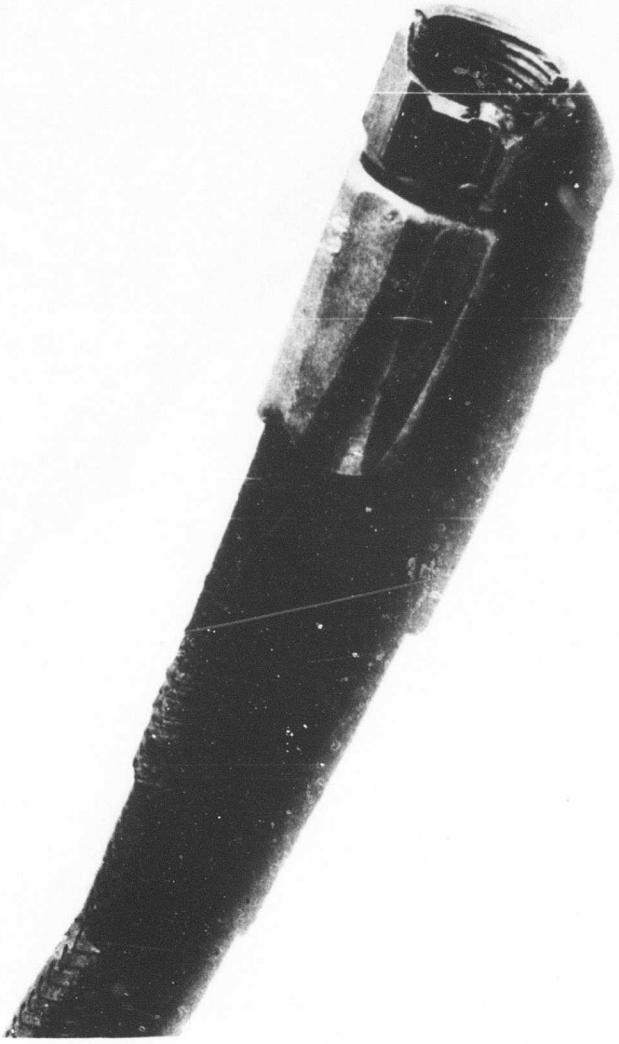

Figure 28. Fitting Failure.

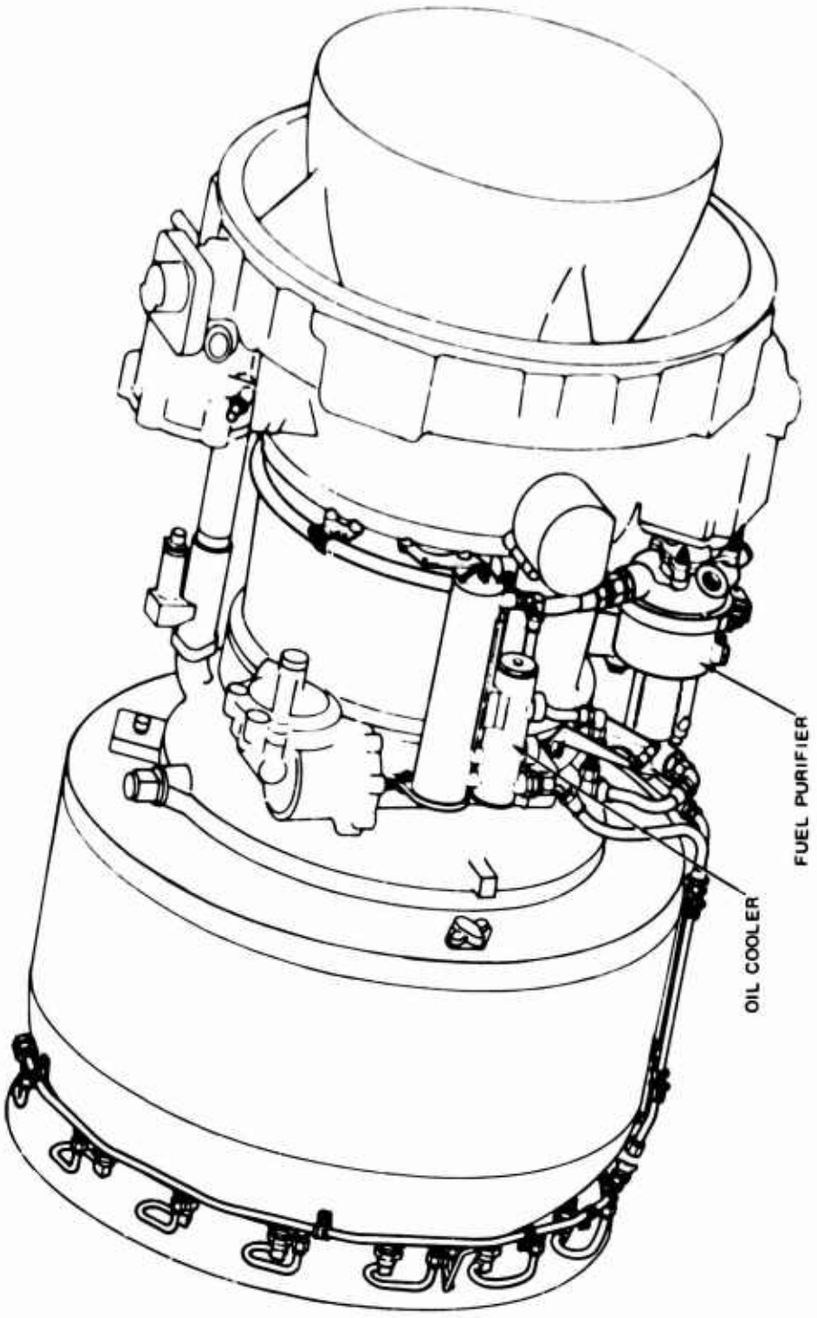

Figure 29. CH-47 Engine Fuel Purifier, Right-Hand Side.

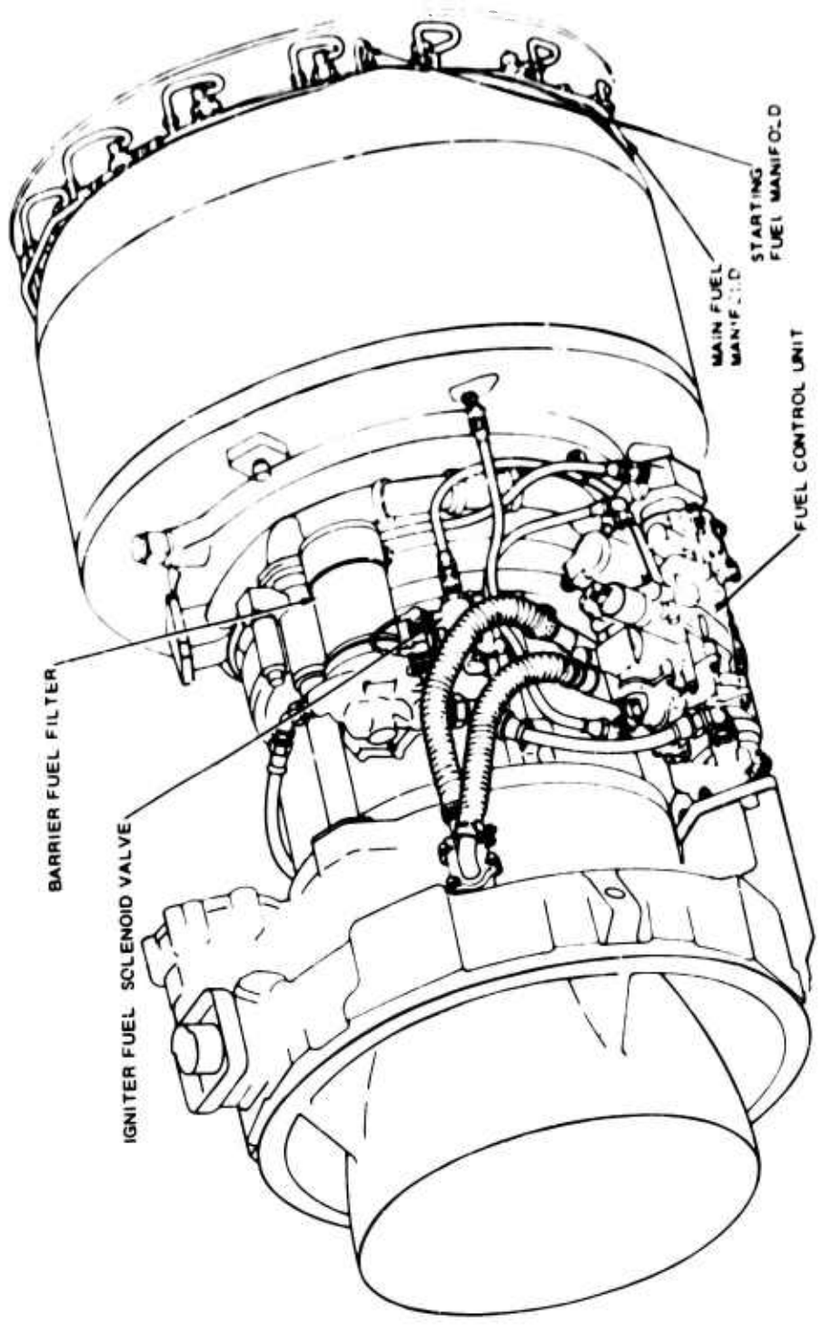

Figure 30. CH-47 Engine Barrier Fuel Filter, Left-hand Side.

The UH-1D helicopter employs the same type fuel filter as the UH-1B. In all but one model of the UH-1D, the filter is mounted to a bracket on the firewall in the left side of the engine compartment. In the other model, the filter is mounted to the front of the firewall in the pylon support compartment. The filter is connected through the firewall by rigid fittings to the fuel shutoff valve and check valve manifold. The rigid fuel supply lines enter the manifold from below. The filter is connected to the engine by a flexible hose.

Again, the use of rigid tubing to connect the fuel cell to the filter is very undesirable. The tubing is rigidly connected to the filter and to the structure a short distance away. Any structural deformation would certainly result in tubing failures at these points, with considerable resulting fuel loss. The size of the filter assemblies in the UH-1D makes them quite vulnerable to damage or displacement by flying objects or deforming structure, or both. Additionally, the proximity of the filters to the hot engines makes fuel loss a great crash fire hazard.

No separate fuel filter is provided in the OH-6A helicopter. An engine fuel filter of the paper element type (10-micron) is employed, thus eliminating the crash fire hazard of a separate filter.

General Recommendations

The elimination of a separate fuel filter by incorporating an engine fuel filter, as in the OH-6A, is an effective way of eliminating attendent fire hazards. If a separate fuel filter must be used, it should be mounted outside the engine compartment. From a crash vulnerability analysis only, the filter could be mounted securely on or near the firewall, with extra-length flexible hose used to and from the filter. When considering ballistic vulnerability, placing the filter within the fuel tank is the most satisfactory arrangement. (See page 49.) Locating the filter within the tank would not increase the crash vulnerability so long as the filter attachment to the structure were frangible, as discussed on page 24.

If the filter is located outside of the tanks it should be as small as practicable to decrease the danger of being hit by flying objects or snagging on deformed structure. Compartmentalizing the filter would also decrease its vulnerability to crash damage caused by foreign objects.

Design Deficiencies of In-Line Valves

The OH-6A helicopter contains only two in-line valves: a fuel shutoff valve and a drain valve. The mechanically operated shutoff valve is mounted to the recessed cover plate on top of the left-hand fuel cell (Appendix II). The drain valve is located on the tee that joins the rigid fuel line to the flexible line leading to the engine. Both valves are well protected and present little crash fire hazard.

The other three aircraft contain numerous in-line valves, including fuel shutoff, check, thermal relief, and drain valves. In addition, the CH-47 has two selector valves located just outside the tank areas. The shutoff valves in the UH-1 helicopters are motor-operated and therefore are fairly large (approximately 6 inches × ⅞ inches × 3 inches). The selector valves and shutoff valves in the CH-47 are electrically operated and are approximately the same size as those in the UH-1 aircraft. These valves are all rigidly mounted to the aircraft structure. In addition, many of the smaller (approximately 1 inch in diameter and 2 inches long) check valves and drain valves are rigidly attached to the structure. All lines leading to and from the valves are composed of rigid aluminum tubing.

As in the case of the fuel filters, the large size of the shutoff and selector valves makes them vulnerable to impact damage from projectiles or deforming structure. The use of rigid tubing to and from the valves, together with the attachment of the valves to the aircraft structure, will almost certainly cause line failure in these areas when structural deformation occurs.

General Recommendations

The valves should be as small as possible to decrease the possibility of impact damage. If large valves must be used, they should be located in a protected area and fastened securely to the structure so that they will not tear loose under crash conditions. All lines entering and exiting the valves should be flexible and of extra length so that they can move with the valve.

Flexible, extra-length hose should also be used with the smaller check and drain valves. These valves should be supported in protected areas with low-load breakaway clamps, thus allowing the valve and hose to move, free of the structure, during crash impact.

Decreasing the number of large valves in the fuel line system would correspondingly lower the vulnerability of the system.

BALLISTIC VULNERABILITY ANALYSIS

The ballistic vulnerability study was based on the assumption that the fuel system components would be struck by small arms projectiles; therefore, no hit-probability study was included. Hit-probability is discussed only in general terms and only in those instances where wide variations in probability would be likely. The objective of this analysis was to determine the extent of ballistic damage on and the post-hit functioning capability of the component, as well as to determine the possibility of fuel system fires induced by ballistic impact.

The primary effect of ballistic penetration of any part of the fuel system can be placed in one of the following categories:

1. Loss of fuel only
2. Loss of fuel followed by fuel ignition by an outside source (either hot surfaces or electrical sparks)
3. Ignition of the fuel vapor by ballistic impact flash resulting from projectile penetration of metal.
4. Complete loss of the functioning capability of the component.

Although these categories will be discussed separately, any combination of the categories may be in operation during a ballistic hit on the fuel system.

Loss of Fuel Only

Total loss of fuel pressure will occur if the main fuel line is severed by ballistic impact. This complete loss will immediately cause engine stoppage. The probability of the line being severed by a direct ballistic hit increases as the diameter of the line decreases. However, increasing the diameter to minimize the possibility of line severance also increases the probability of the line being hit. Regardless of whether the line is completely severed or not, a ballistic hit on the fuel line will cause fuel loss with a resultant fuel pressure drop to the engine, limiting engine performance.

A redundant fuel line system incorporating an automatic switching valve should be used in all aircraft that might be subjected to ballistic hits. In case of ballistic damage to one fuel line, the valve would automatically shut off this line and switch the fuel into the other line. The valve could be actuated by pressure transducers which act as hit sensors. The CH-47 helicopter is the only aircraft studied during this analysis that incorporates any degree of fuel line redundancy. Both engines can be supplied by one fuel tank under emergency conditions. However, no provision is made for automatically switching to a single tank in the event of line failure. Rapid, automatic switching from one line system to the other must occur if engine failure is to be avoided. Redundant lines must also be used if an engine-driven, suction type, fuel system is used instead of a boost pump. In this case, a cavitation sensor could also actuate the switching valve.

Fuel loss caused by a ballistic hit on the fuel tank or the large crossover lines would not immediately affect engine operation. The main consequence of such fuel loss, providing a fire did not follow, would be a reduction in flight time. Quantity

indicators within the fuel tank would register a greater-than-normal fuel capacity drop, thus alerting the pilot to the fuel loss and enabling him to reach safety before complete fuel depletion.

Use of a fuel counter coupled with a low-level warning switch, which would be desirable from a crash vulnerability viewpoint, would not be satisfactory in terms of ballistic vulnerability. Any fuel loss occurring in that part of the system from the fuel tank to the counter would not be registered, and the fuel loss would be undetected until the low-level warning light illuminated. At this point it is quite possible that the pilot would not have enough fuel left to reach safety. For example, only 20 minutes of flight time is available in the UH-1 helicopter after the light illuminates, and the time remaining would be even less with fuel leakage.

Although shielding the fuel tanks by armor would certainly protect the tanks from ballistic impact, the weight penalty is almost prohibitive. It has been estimated that, even using newly developed lightweight armor, small-arms protection for the UH-1B fuel tanks would represent a weight penalty of almost 50 percent of the useful load (Reference 4). The self-sealing fuel tanks currently in use are only partially effective against all types of ballistic penetration (Reference 4). More effective sealing of fuel cell ballistic damage is imperative. Research is being conducted in several areas to improve the self-sealing capabilities of fuel tanks, including effort in the development of a coagulant system to be used in conjunction with the ARM-021 material.

The metal access doors and sump plates in these aircraft leave a large area of the fuel tanks with no self-sealing capabilities whatever. Access plates on the top of the tank, as in the UH-1B and OH-6A, do not pose as great a threat as the access doors in the CH-47 and UH-1D helicopters, which are located on the sides of the tanks (Appendix II). The sump plates on the bottoms of the tanks constitute a considerable threat from a ballistic vulnerability standpoint. Their location not only exposes them to a high probability of ballistic hits from ground fire, but also makes complete loss of fuel from the tank probable in the event of ballistic penetration. The sump plates and access doors should be made from reinforced, self-sealing tank material, both from a ballistic and a crash vulnerability standpoint.

The large crossover lines between the fuel cells in the UH-1 helicopters should also have self-sealing capabilities, as a ballistic hit on these lines will result in as much fuel loss as if the tanks themselves were hit. Self-sealing could be obtained by shrouding the lines with the ARM-024 coagulant system or one of several polymer materials now under investigation.

Ballistic hits on any in-line components, such as shutoff valves and filters, could also result in fuel loss, depending on the area of penetration. The immediate

threat of a hit on these components, considering fuel loss only, would depend on the rate of loss. If the fuel pressure loss is great enough, engine failure will occur. These components could be armor shielded without too great a weight penalty. However, the self-sealing shrouding discussed previously would offer the advantages of less weight and less volume than the armor.

Any component within the fuel tank presents no threat of fuel loss from ballistic hits as long as the damage in the cell wall seals. Therefore, from a ballistic vulnerability standpoint, components should be placed within the tank wherever possible. Quantity indicators and fuel boost pumps are ordinarily located inside the tank; this practice should continue, although some materials substitutions are necessary to eliminate the threat of ballistic impact flash. Consideration should also be given to placing the fuel filter inside the tank, slightly before the fuel line outlet. An engine fuel filter, as used in the OH-6A, could then be used to provide additional fuel filtration before it enters the combustion chamber. The installation of all components within the tank should also follow the recommendations set forth in the crash vulnerability analysis to ensure that these components will not damage the fuel cell during crash impact.

Other components that may be hit by projectiles without fuel loss include the vent lines and filler neck, as long as the attitude of the aircraft remains fairly level. If the vent outlet at the tank incorporates a check valve, as recommended in the crash vulnerability analysis, the attitude of the aircraft would be inconsequential and no fuel loss would occur upon ballistic penetration of the vent lines. Similarly, if the filler cap were attached directly to the fuel tank wall, ballistic hits on the filler neck would result in no fuel loss regardless of the attitude of the aircraft.

Loss of Fuel Followed by Ignition

Although complete containment of the fuel after ballistic impact would remove the threat of fuel ignition by hot surfaces or electrical sparks, no such system is now in existence. Even a few milliliters of fuel, once ignited, pose a serious threat to the entire fuel system and the aircraft. Ballistic penetration of components containing fuel invariably results in fuel mists erupting as the projectile exits, as well as liquid fuel being lost from the damaged area. These fuel-air mixtures will seldom be close to equilibrium and will thus present a combustible mixture in some regions around the spraying fuel jet (Reference 4).

The filters mounted in the engine compartments of the UH-1 helicopters, as well as the filters mounted directly to the engines in the CH-47, constitute a definite fire hazard from the standpoint of ballistic vulnerability. Projectile penetration of

these filters would almost certainly spray fuel onto the hot engines, resulting in ignition. The filters should be located outside the engine compartment and precautions taken to prevent fuel loss, as mentioned in the preceding section.

The fuel lines around the engine also present the same fire threat as the filters. Since these lines cannot be moved away from the engine, they must be shielded to prevent fuel or fuel mist from punctured lines coming in contact with the hot engine surface. Surrounding the engine compartment with armor presents a large weight penalty. If armor is not used, the lines should be shrouded with a material, such as nylon felt, which would reduce fuel spraying and loss from a ballistic hit on the lines. However, shrouding lines installed next to the hot engine would be ineffective unless complete closure of the ballistic damage was quickly effected.

The heating unit in the UH-1B helicopter is located in a compartment directly behind the fuel tanks (Figure 3). Leaking fuel from a ballistic hit on the fuel system could easily flow into this compartment and be ignited if the heater were operating. Flow diverters or drip fences should be placed around this compartment, and drainage holes should be located to drain internal spillage.

Ballistic hits can sever electrical lines as well as cause fuel loss. The combination of released fuel vapor and electrical sparking creates a definite ignition or explosion hazard, or both. Therefore, all electrical sources should be as far away from the fuel system as possible. Components within the fuel system itself which comprise electrical hazards are the fuel boost pumps and motor-operated selector and shutoff valves. Elimination of the boost pumps by using an engine-driven, suction type system, as recommended in the crash vulnerability analysis, would effectively eliminate this hazard. Consideration should also be given to replacing the motor-operated valves by mechanically operated valves.

Electrical ignition sources present outside of the fuel system include the battery, inverter, generator or alternator, and electrical wiring. The generator or alternator, which is mounted on the engine, is close to the fuel lines feeding the engine; sparking from this source might ignite surrounding fuel vapor. Shrouding the lines to prevent fuel loss, as discussed previously, would help reduce this danger.

The electrical compartments carrying the battery and inverter in the CH-47 are located in the front of the pods, some distance away from the fuel tanks (Figure 1). This location is fairly safe, but there is a possibility that leaking fuel might run down the pod and enter the electrical compartment. Flow diverters around the compartment and drainage holes in the bottom of the pod could reduce this hazard.

The electrical compartments in the UH-1 helicopter are located directly behind the fuel tanks (Figures 3 and 4). It is likely that any leaking fuel would drain into these compartments, with the attendant danger of ignition or explosion, or both, should sparking occur. Although flow diverters and drainage holes could eliminate this hazard, there is also the possibility of a projectile striking at such an angle that it would penetrate both the fuel tank and the compartment wall behind the tank, thus sending a jet of fuel vapor into the electrical compartment. Therefore, these electrical components should be moved as far away from the fuel system as possible.

Fuel Ignition by Ballistic Impact Flash

Results from previous studies have shown that an impact flash occurs when fragments penetrate metal plates and that under certain conditions these flashes can start fuel fires in aircraft (Reference 6). The properties of the flash depend upon the size, shape, material, velocity, and orientation of the fragment and upon the kind of material, thickness, and obliquity of the plate. The duration of the flashes ranges from a fraction of a millisecond to several milliseconds.

Fuel fires have been started by fragments penetrating an aluminum plate in front of the fuel cell, causing a flash on both the entry and exit sides of the plate. The fragment then penetrates the cell wall, allowing the fuel to spurt from the cell and be ignited by the flash. It is thought that the aluminum, upon fragment impact, is broken into many fine particles with clean surfaces. These particles then oxidize rapidly and burning proceeds as an aluminum vapor fire.

A sizable impact flash is produced when an aluminum sheet is penetrated by a small-arms projectile, as shown in Figure 31. (Experimental details in connection with this photograph may be found in the section devoted to ballistic sparking.) Although test data (Figure 32; see Reference 2) indicate that small-arms projectiles cannot cause a fuel fire by penetrating a plate in front of the fuel cell, no data have been collected on the penetration of aluminum components surrounded by a flammable fuel-air mixture.

It should be recognized that combustible mixtures can exist in all aircraft fuel tanks at one time or another during flight. The flammability limits of fuels, which are calculated under equilibrium conditions, cannot be relied on to provide a margin of safety under flight conditions. The Ad Hoc Group on Aviation Fuel Safety (Reference 1) states, "Under the dynamic conditions of actual flight, an almost unlimited series of localized conditions can be generated within the tank which invalidate the predictions made by assuming that equilibrium existed." Therefore,

Figure 31. Ballistic Flash Impact From Projectile Penetration of an 0.125-Inch Thick Aluminum Sheet.

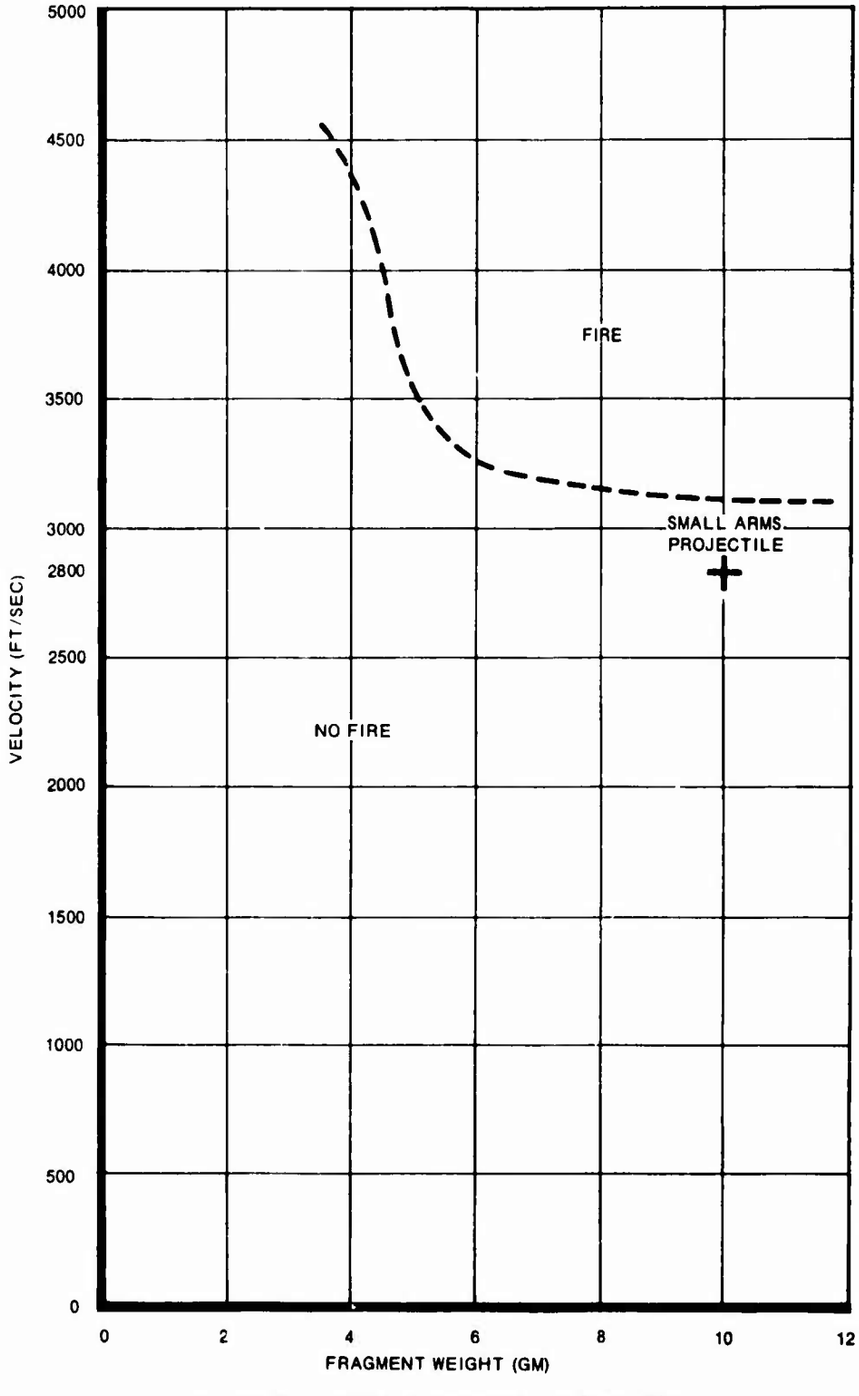

Figure 32. Ability of Fragments to Cause Fire.

the assumption must be made that a flammable fuel-air mixture exists within the system at the time of ballistic penetration and that this mixture can be ignited by the ballistic impact flash. The results of subsequent work under this contract have shown that fuel vapors can be ignited in this manner. Refer to the section concerning ballistic impact flash for further details.

Fuel system components commonly made from cast aluminum alloys include: boost pump housings, filter sumps and heads, valve housings float indicator bodies, capacitance indicator heads, and fuel line fittings and connections. These are all potential ballistic impact flash hazards. Internal fuel tank components pose the greatest threat to fuel ignition because of the amount of vapor surrounding them. Since fuel must be in the vapor state to be ignited, a ballistic hit on a component beneath the fuel level should not be an ignition source. As fuel is emptied from the tank, however, more of these components are exposed in the vapor area, thus increasing the hit ignition probability. The possibility also exists that ballistic flash from components in the line, such as filters and valves, could ignite fuel vapor released upon ballistic penetration of the component.

The fuel cell access doors and sump plates in all four of these aircraft are made of wrought aluminum alloys. Ballistic impact flash from these metals might ignite either the fuel vapor within the tank or the fuel sprayed from the tank through the projectile opening. The substitution of nonflashing materials for metal parts would eliminate the hazard of ballistic impact flashes. Any synthetic material possessing the desired physical properties could be used. The sump plates and access doors could also be fabricated from reinforced cell wall material, as mentioned earlier. If metal in-line components must be used, shrouding them with a material such as nylon felt would reduce the amount of vapor spray from ballistic hits and reduce ignition probability if flashing occurs.

Loss of Component Function

The functioning capabilities of the following items could be lost because of ballistic impact: the fuel boost pumps, quantity indicators, filters, and valves. The consequences of losing these capabilities depend entirely on which component is damaged. All the aircraft analyzed in this study, with the exception of the OH-6A, have more than one fuel boost pump. If one pump is disabled by a ballistic hit, the other pump can provide enough fuel pressure to continue normal engine operation. This redundancy provides fairly good protection against ballistic vulnerability, as the probability of two identical components being damaged at any one time is small. If necessary, most aircraft can maintain normal flight operations without using a boost pump; the boost pump can be destroyed with no serious consequences, so long as it is located within the tank. If the boost pump must be used during flight, more than one pump should be provided.

Loss of fuel quantity readings caused by impairment of the quantity indicators poses no serious threat to the aircraft. All four helicopters incorporate low-level warning switches to alert the pilot when the fuel quantity declines to a certain percentage.

The main consequence of a ballistic hit on the filters would be fuel loss, not impairment of functioning capabilities. The only way in which ballistic impact could impair the functioning of the filter, disregarding fuel loss, would be by plugging the filter; this possibility is highly unlikely.

Ballistic damage to the valves, again disregarding fuel loss, could either cause the valves to freeze in position or to cycle to the reverse position. There would be no additional threat to the aircraft if the valves froze in their original positions. The only consequence of one of the selector valves in the CH-47 closing would be the inability to use the fuel contained in the tank connected to that valve. However, if one of the check valves in the main fuel lines were closed upon ballistic impact, fuel flow to the engine would cease. Similarly, if a shutoff valve closed upon being hit, fuel flow would be stopped. In the case of the motor-operated shutoff valves, a ballistic hit on the valve motor might produce stray signals which would close the valve.

As in the case of the fuel filter, the greatest hazard from a ballistic hit on any of the valves is fuel loss, with the exception of actuation of a shutoff valve from damage to the valve motor. Shielding the filter and valves either by armor or self-sealing shrouding, as discussed previously, would prevent such fuel loss. The motor-operated shutoff valves should be designed so that stray signals cannot inadvertently close the valve.

PART III

ANALYSIS OF EXISTING COMPONENTS

FUEL SYSTEM COMPONENT ATTACHMENTS

The most common and hazardous design deficiency of fuel cell components noted in the crash vulnerability analysis is the rigid attachment of the component to both the cell wall and the aircraft structure. These attachments pull out of the fuel cell as the cell and structure move relative to each other during crash impact. This predominant failure mode is illustrated in Figures 6 and 7. Those components attached to both the cell wall and the structure include the fuel drains, fuel vents, filler necks, quantity indicators, boost pumps, and the sump and access plates. Typical attachments found in the four aircraft studied are shown in Figures 9, 11, 13, 18, and 20.

A frangible attachment that would fail before the cell wall failed would reduce fuel loss by allowing the component to stay with the tank instead of the structure during crash impact. Several frangible attachments which could be used are shown in Figures 14, 15, and 17. A feasibility study of one of these suggested attachments was conducted during this program. (See the section devoted to preliminary design modifications.)

Fuel line connections to the tank and fuel cell interconnects are also commonly attached to both the cell wall and the structure, as shown in Figures 19 and 22. These attachments may also cause fuel cell failure during crash impact. Self-sealing breakaway fittings, as illustrated in Figure 21, would allow the line or interconnect to pull free from the tank with no fuel loss. The results of a feasibility study of this attachment may also be found in the section relative to design modifications.

Fuel-transfer lines and fittings have a high incidence of failure during crash impact. The rigid aluminum tubing and the many bulkhead fittings preclude any flexibility of the lines. The lines and fittings are broken as the structure deforms. Typical line and fitting failures are shown in Figures 25, 26, 27, and 28.

The use of extra-length flexible hose would help reduce the number of line and fitting failures. However, this modification would not be completely effective in eliminating failures during crash impact. Routing the transfer lines through the airframe necessitates the use of some bulkhead fittings. Structural deformation may be so great in some areas that even extra-length hose would not provide enough flexibility to prevent line failure.

Frangible, nongalling bulkhead baffles, as illustrated in Figures 23 and 24, would allow a bulkhead fitting and the attached hose to move, as the structure deforms, without causing either hose or fitting failure. A self-sealing breakaway fitting incorporated into the lines at strategic locations would prevent line rupture or fitting failures in areas of high structural deformation. The feasibility of both these concepts has been investigated and is discussed in the section devoted to design modifications.

FUEL LINES AND FITTINGS

Introduction

The high incidence of both rigid fuel line and fuel line fitting failures during crash impact was noted in the crash vulnerability analysis. These failures are caused, in most instances, by tensile or shear loads applied to the tubing and fittings as the aircraft structure deforms. The use of extra-length flexible hose, the elimination of as many fittings as possible, and the strengthening of the remaining fittings were all recommended as methods of improving the fuel transfer systems. In addition, a test program was conducted to acquire data on the behavior of fuel lines and fittings under tension and shear loads.

Any changes incorporated in the fuel-transfer system to improve its crashworthiness must also be compatible with improved ballistic protection. Recommending the substitution of flexible hose for rigid tubing necessitated ballistic tests on both lines to assess their vulnerability to small-arms projectiles.

Tensile and Shear Tests

Tensile and shear loads were applied to various combinations of flexible hose, rigid aluminum tubing, and fuel line fittings to determine: (1) their mode of failure, (2) the load at which failure occurs, and (3) the maximum elongation at failure. All test combinations were composed of fuel line components frequently used in current aircraft. Complete test descriptions and data may be found in Appendix IV.

The mode of failure under tensile loads was the same for both flexible hose and rigid tubing regardless of which fittings were used. In all cases, the hose or tubing pulled out of the fitting. As might be expected, the failure loads increased with specimen size. Generally, there was no significant difference in the failure loads of comparable size hose and tubing. (Average failure loads and extensions are listed in Table I.) Tensile tests of the hoses alone showed that the hoses pulled out of the fittings at a load equal to only one-half the ultimate strength of the hose. Thus, the method of attaching the hose to the fitting must be improved to take full advantage of the hose properties.

TABLE I

AVERAGE FAILURE LOADS AND ELONGATIONS, LINE AND FITTING TESTS

	Tensile Tests		Shear Tests	
Test Specimen	Failure Load (lb)	Elongation (%)	Failure Load (lb)	Elongation (%)
3/8-in. hose and fitting	735	51	511*	57*
3/8-in. tubing and fitting	558	1	755	13
5/8-in. hose and fitting	1662	55	927*	64*
5/8-in. tubing and fitting	1671	7	1224	15
1-in. hose and fitting	2471	47	1770*	53*
1-in. tubing and fitting	2361	5	2055	19
3/8-in. hose plus hose elbow fitting	-	-	171	58
5/8-in. hose plus hose elbow fitting	-	-	503	56
1-in. hose plus hose elbow fitting	-	-	1150	54
3/8-in. hose only	1525	-	-	-
5/8-in. hose only	2860	-	-	-

*Excludes results obtained with hose elbow fitting.

Although the tensile failure loads of the flexible hose and rigid tubing were approximately equal, the elongation of the hose before failure was considerably greater. As may be seen in Table I, the elongation of the 3/8-inch hose was 50 times greater than that of the 3/8-inch tube, while the 5/8- and 1-inch hoses exhibited approximately a 9 to 1 advantage in extensibility over the comparable sized tubing. Test data showed that an extension of only 1/8 inch pulled the smaller tubing from the fitting, while an extension of 6-1/4 inches was necessary to pull out the smaller hose. The flexible hose, even without extra length, thus affords a much greater degree of protection from structural deformation during crash impact than does the rigid tubing.

Combinations of fittings with flexible hose or with rigid tubing exhibited different modes of failure under shear loads. The hose fittings failed in all tests with the 5/8- and 1- inch size hoses, and in approximately half of the tests with the 3/8-inch size. The remaining 3/8-inch hose failures occurred in the AN fitting which was coupled to the hose fitting. Failure of the rigid tubing combinations were all accompanied by failure of the tubing itself. (See Appendix IV.)

The failure loads in a shear direction were less than in a tensile mode in all cases except the 3/8-inch tubing. The tubing assemblies failed at somewhat higher loads than those of the hose assemblies. As was the case in the tensile tests, the failure loads in a shear direction were much less than would be required to fail the hose itself and considerably less than the loads required to pull the hose out of the fitting. Therefore, the fittings must be considered the weakest link in the hose assemblies. The nonstandard hose elbow fittings are grossly inferior to the standard AN elbows, and should not be used in fuel-transfer systems.

The ultimate elongation of the hose assemblies was three to four times greater than that of the comparable sized tubing assemblies. The flexible hose, therefore, can accommodate more structural deformation during crash impact before rupture occurs.

Ballistic Tests

Ballistic tests were run on the 1-inch rigid tubing and flexible hose used in the preceding tests. Both test specimens were filled with water and capped on the ends to simulate full fuel lines at the time of ballistic impact. Both specimens were hit with small arms projectiles. One hit was made through the center of each specimen.

The damage to the 1-inch aluminum tube consisted of a normal size entrance hole and a slightly enlarged exit hole with some outward petalling (Figure 33). The entrance hole of the 1-inch flexible hose had a number of cut strands of the

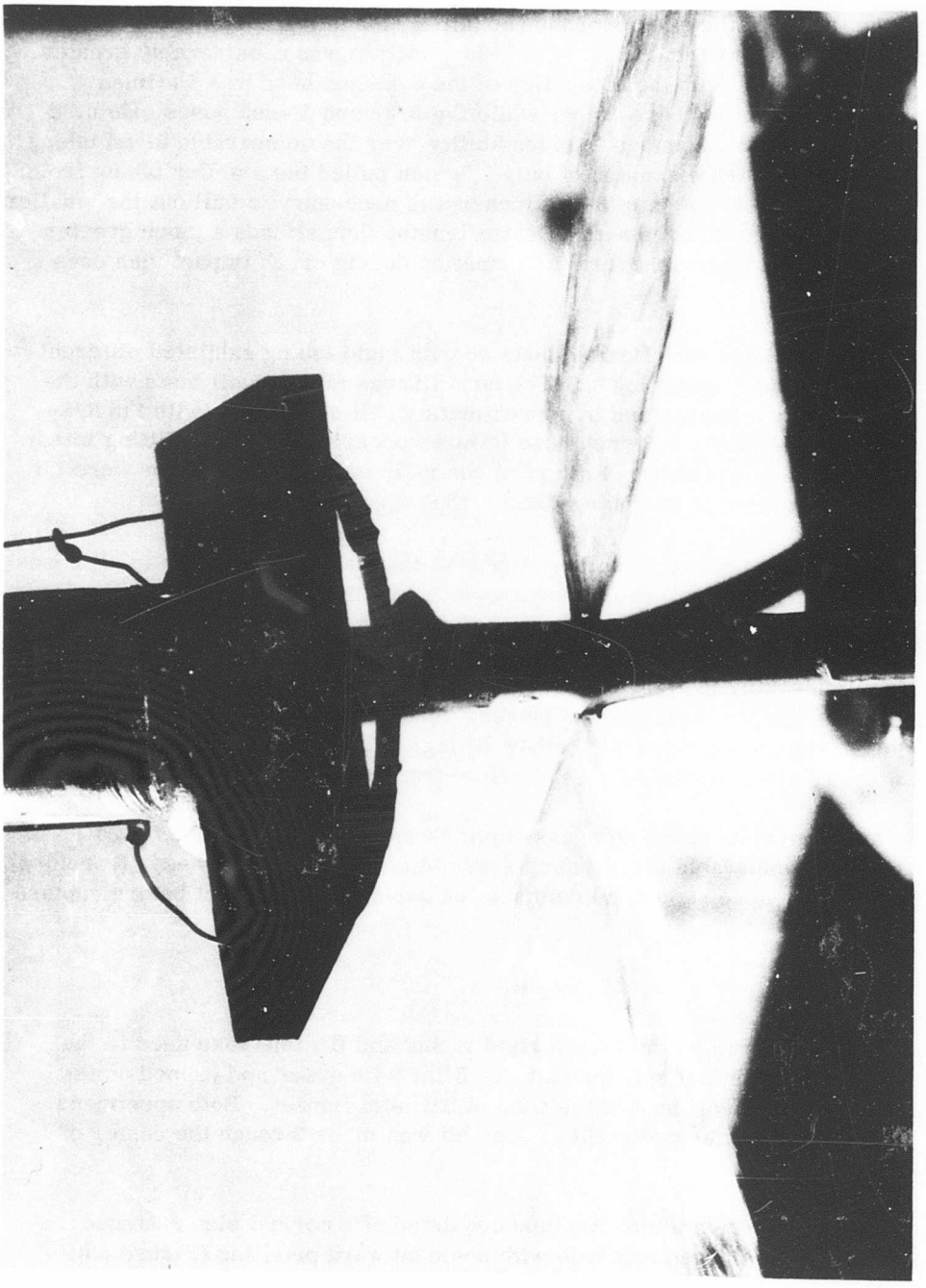

Figure 33. Rigid Aluminum Tubing Ballistic Damage and Resulting Fuel Leakage.

braided wire sheath; a large number of strands were cut as the bullet exited (Figure 34). These strands did not progressively loosen beyond the impact area. The synthetic inner lining allowed some closure of both the entry and exit holes.

A test was performed to determine the leakage rate from the entrance and exit holes of both the tube and the hose. One end cap was removed and the test piece was supported vertically by a test fixture. A fluid head yielding 1.3 pounds per square inch was maintained above the holes and the leakage rate was determined.

The difference in fluid leakage of the two specimens may be seen by comparing Figures 33 and 34; leakage rates are recorded in Table II.

TABLE II

WATER LEAKAGE FROM BALLISTICALLY PERFORATED HOSE AND TUBING

(Pressure = 1.3 psi)

Specimen	Time (sec)	Leakage (ml) Entry Hole	Exit Hole	Total
1-in. flexible hose	10	125	125	250
1-in. rigid tube	10	1850	2100	3950

The leakage rate of the rigid aluminum tubing was over 10 times that of the flexible hose, indicating that the vulnerability of the tubing to ballistic damage is much greater than that of the hose.

Conclusions

The use of presently available flexible hose instead of rigid aluminum tubing in aircraft fuel lines would provide significant improvements to both the crashworthiness and ballistic protection of aircraft fuel systems. Strengthening the hose-to-fitting attachments and using stronger fittings would further improve the crashworthiness of fuel-transfer systems.

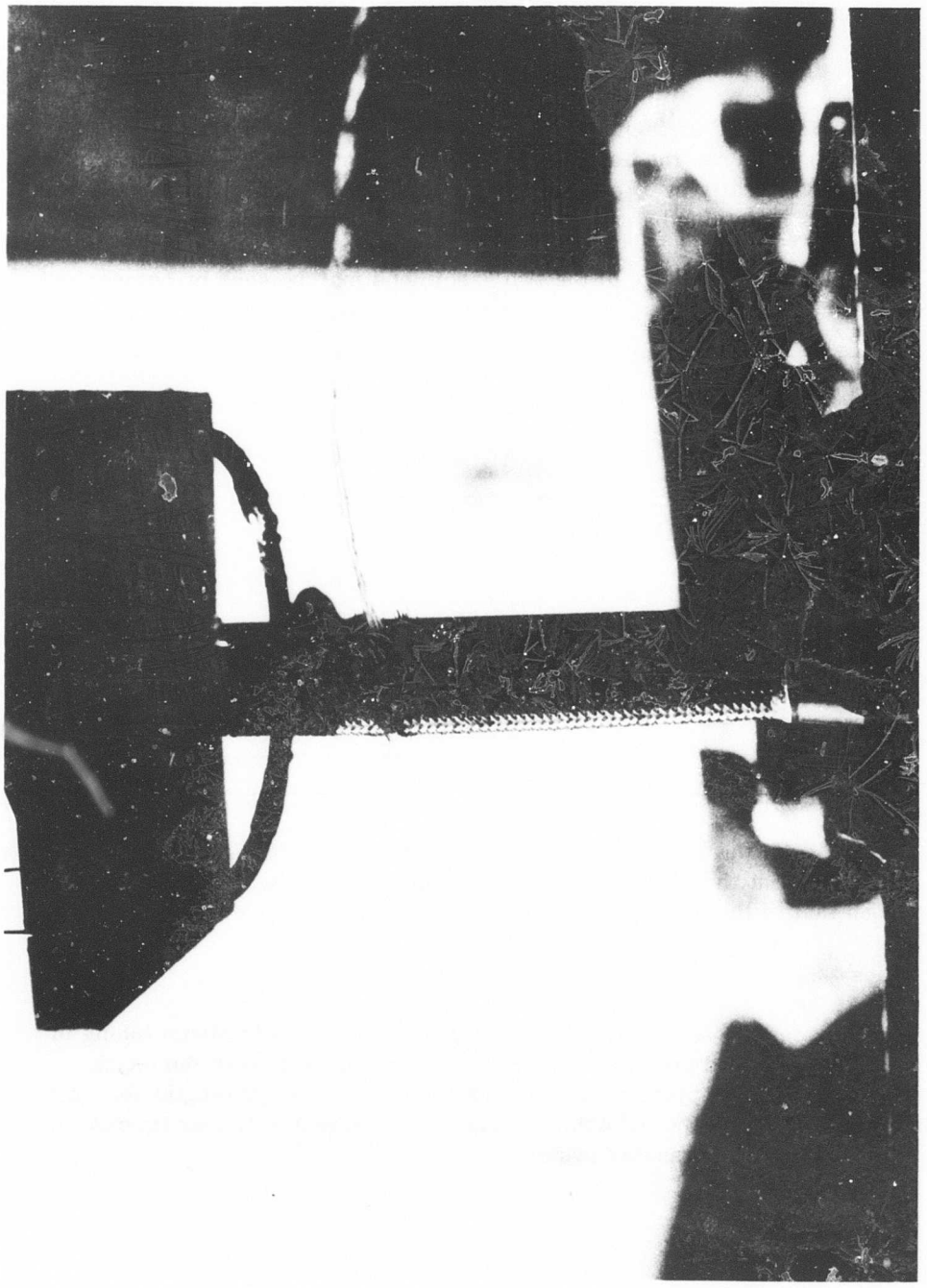

Figure 34. Flexible Hose Ballistic Damage and Resulting Fuel Leakage.

BALLISTIC IMPACT FLASH

General

In the ballistic vulnerability analysis conducted as part of the preliminary design study, ignition of fuel vapors by ballistic impact flash was assumed to be a definite threat to aircraft fuel systems. This assumption was based on the following observations:

1. The impact flash of fragments penetrating aluminum plates can cause aircraft fuel fires (Reference 6).

2. Flammable fuel-air mixtures exist within all aircraft tanks at one time or another under typical flight conditions (Reference 1).

It was also noted that, although small arms projectiles would not start fuel fires under the test conditions imposed during fragment studies conducted by the New Mexico Institute of Mining and Technology, no data were available concerning impact flashes generated by small arms ballistic hits on aluminum fuel system components. The fact that these components, especially those mounted within the fuel tanks, might be in contact with flammable fuel-air mixtures at the time of ballistic impact makes the acquisition of such data highly desirable. Therefore, the primary objective of this study was to determine the ballistic impact flash hazards of presently used fuel system materials and to suggest methods of eliminating these hazards.

An impact flash occurs whenever high-velocity fragments penetrate metal plates. Previous studies (Reference 6) have shown that the size, shape, intensity, and duration of an impact flash vary widely, depending upon the fragment size, shape, material, velocity, and orientation, and on the target material, thickness, and obliquity. The durations of the flashes range from a fraction of a millisecond to several milliseconds.

It was also determined in these previous studies that a very thin aluminum plate produced comparatively little flash on either side when penetrated by a fragment. A comparatively large flash (entry side only) was produced when the plate thickness approached the penetration threshold, and sizable flashes were produced on both sides with plates of intermediate thicknesses. High-speed motion pictures, taken in conjunction with ballistic tests on ARM-018 tank material, also showed a sizable impact flash when a 0.062-inch-thick aluminum facing plate (6061-T3 material) was struck by a small arms projectile.

The mechanism of impact flash has not been definitely established. It is thought that aluminum, upon fragment impact, breaks into many fine particles with very clean surfaces. These particles, energized by the impact, oxidize rapidly, and burning then proceeds as an aluminum vapor fire (Reference 2). Results from tests conducted by the New Mexico Institute of Mining and Technology indicate that aluminum flash temperatures are above 5000° F and may sometimes be above 9000° F.

Test Program

The scope of this study was limited to determining the relative maximum energies of ballistic impact flashes generated by small arms projectiles striking fuel system components. Several polymer materials were also tested to assess their suitability as nonflashing substitute materials for aluminum.

The size and intensity of the flashes were recorded on high-speed infrared film. The film exposure densities of the flashes were then determined and compared with densities obtained from photographing several heat standards. This comparison provided a rough estimate of maximum flash temperatures and durations. Finally, ballistic tests were conducted on aluminum components surrounded by fuel-air mixtures to determine if the ballistic impact flash could ignite a flammable mixture.

Experimental Procedure

Photographic

Photographic time exposures were taken of impact flashes in total darkness using an open shutter. Kodak High-Speed Infrared Film was used to record the flashes and a Wratten F filter, number 29 (red), was used on the camera to screen out as much visible light as possible. The camera was located 12 feet from the target (Figure 35). The aperture on the camera was set at f/2.9.

The infrared film was standardized by photographing a 4.5-inch long Nichrome heating element. Four thermocouples were evenly spaced along the element to record exact temperatures, which ranged from 500 to 1165° F. These photographs were also taken from a distance of 12 feet using an aperture of f/2.9 and a shutter speed of 1/150 second. Thus, except for the exposure time, identical conditions existed for both the heat standard and the impact flash photography. Film-developing conditions were also held constant; each roll was developed in fresh solutions and at the same temperatures for 11 minutes.

The densities of the exposed infrared films were read on a Macbeth TD-102 diffusion densitometer, which has a density accuracy of 0.02. At the fast shutter

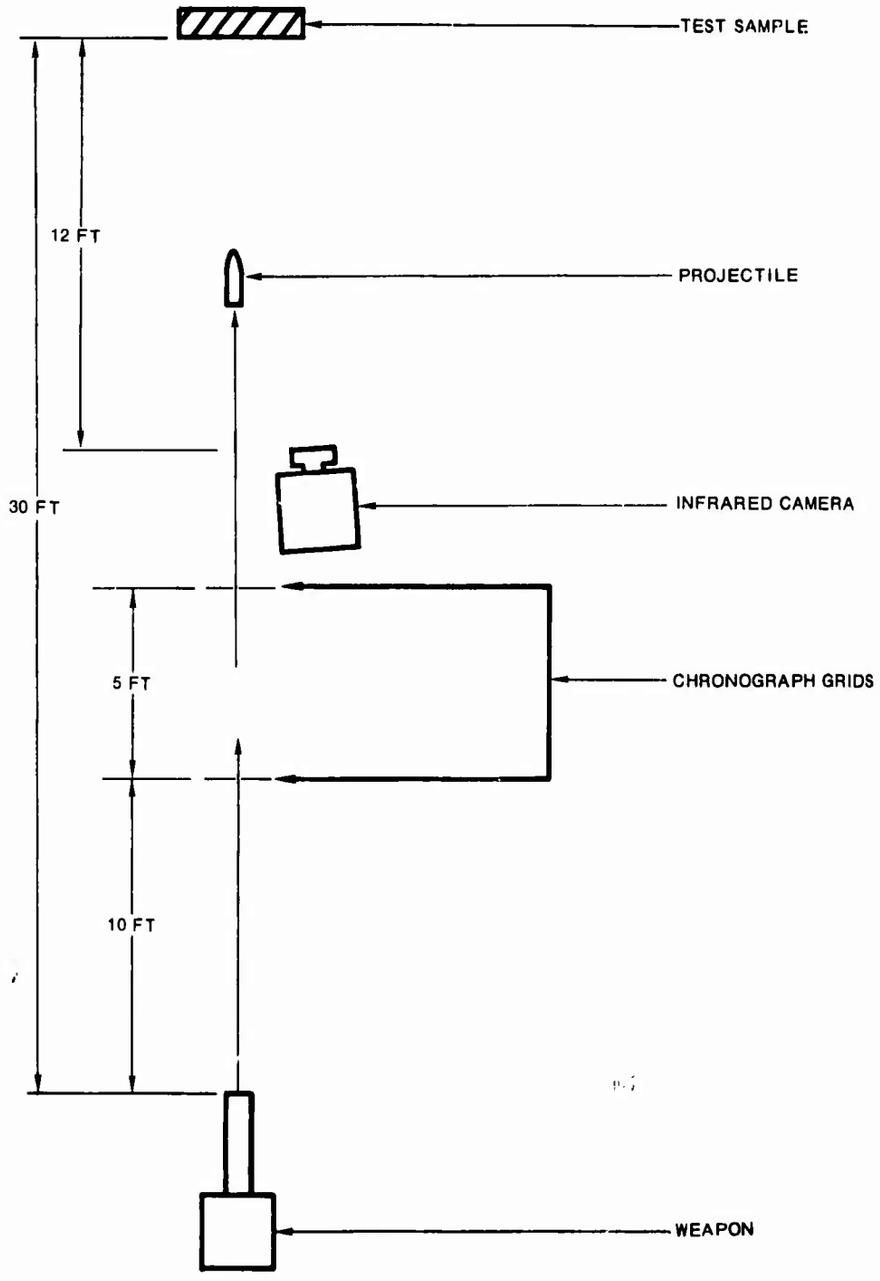

Figure 35. Ballistic Test Arrangement.

speeds used, the lowest temperature that could be read on the heat standard negatives was 872° F. Data obtained from the standards are presented in Figure 36. The correlation between temperature and density is readily apparent. The width of the envelope containing all the data points is an indication of the error to be expected in this correlation. At higher temperatures and densities this error is approximately 70° F, or about 6 percent.

Ballistic

The ballistic tests were conducted using small arms ammunition. Velocities were measured using a counter chronograph with a 5-foot spacing between the chronograph grids. Test samples were mounted at an obliquity angle of zero degrees to the path of the bullet. The distance between the sample and the gun muzzle was 30 feet (see Figure 35).

Test Specimens

The test specimens and their thicknesses are listed in Table III. All specimens were in sheet form except the cast aluminum (Figure 37), which consisted of a valve housing such as commonly found in aircraft. Care was exercised to be sure that the bullet passed only through the flat flange of the cast housing. The steel and magnesium samples were tested for comparative purposes only.

Results and Conclusions

No impact flashes were recorded with any of the polymer materials. However, several of these materials are not considered satisfactory substitutes for metals because of their brittleness. Figure 38 shows the physical appearance of these specimens after ballistic penetration, along with the 6061-T6 specimen for comparison. The nylon and polyvinyl chloride (PVC) samples exhibited severe spalling and cracking around the exit side of the bullet hole. This condition is particularly noticeable with the nylon, where a hit 1 inch from the edge of the sample knocked out a triangular piece of nylon approximately 2 inches long. It should be noted that the hole in the urethane is almost completely closed.

Infrared photographs of the ballistic impact flashes obtained from the metal specimens are shown in Figures 39 and 42. The impact flash of the steel sample is very small compared to that of the magnesium. Very hot fragments of steel are responsible for the streaks of light shown in Figure 39 but no streaks are visible in the magnesium flash (Figure 40), indicating that the entire flash is caused by vapor fire; the aluminum flashes exhibit both characteristics. The photograph of the 6061-T6 aluminum (Figure 41) shows the presence of more hot metal fragments than does that of the cast aluminum (Figure 42). The most significant aspect of

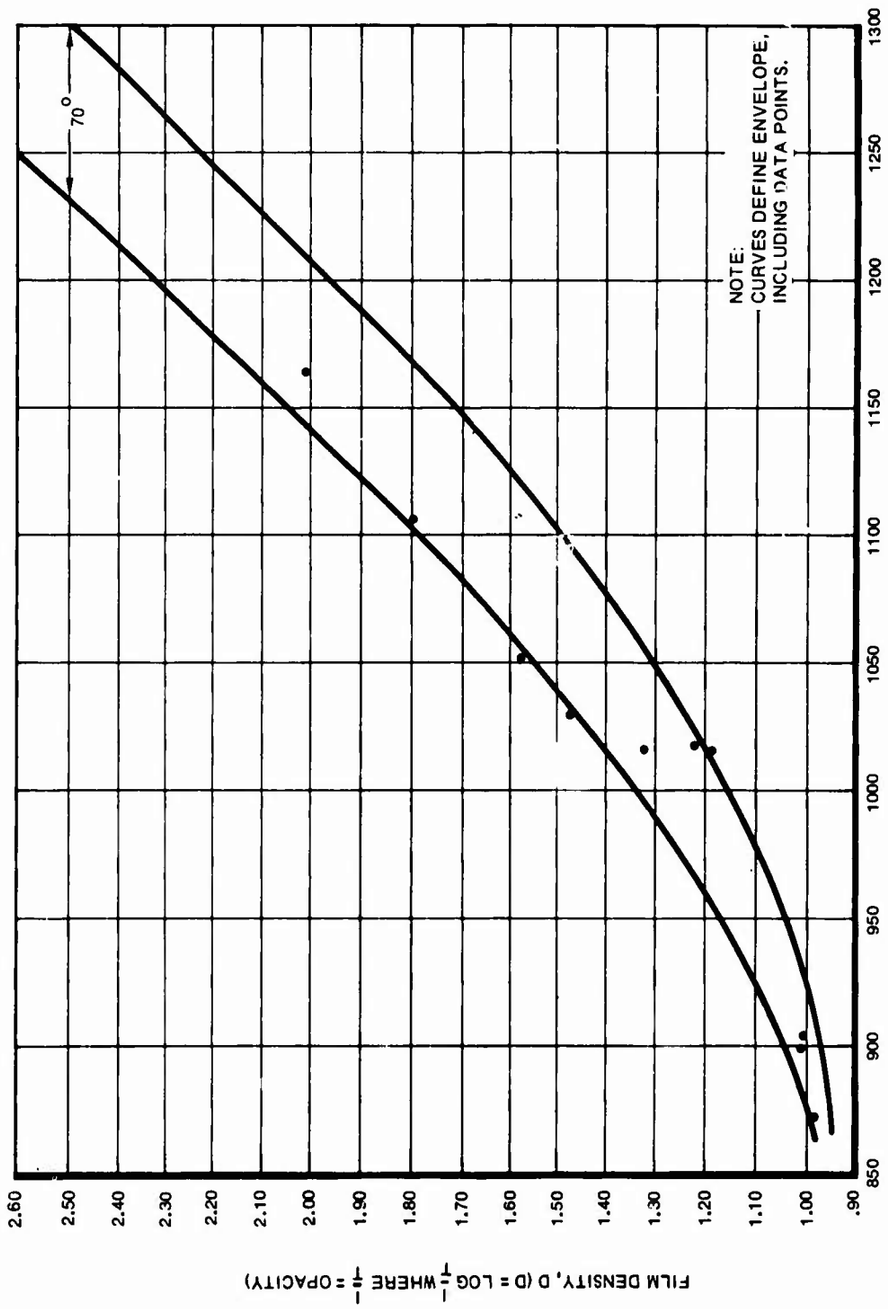

Figure 36. Temperature Versus Density, High-Speed Infrared Film.

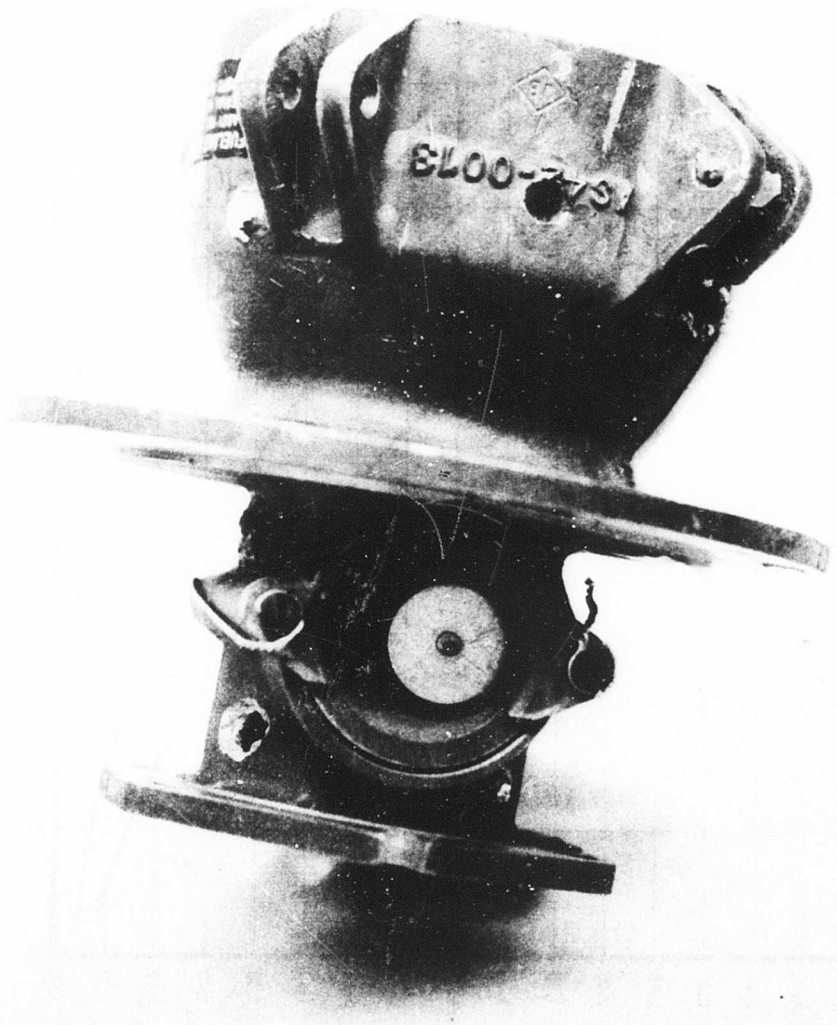

Figure 37. Cast Aluminum Valve Housing Used in Ballistic Tests.

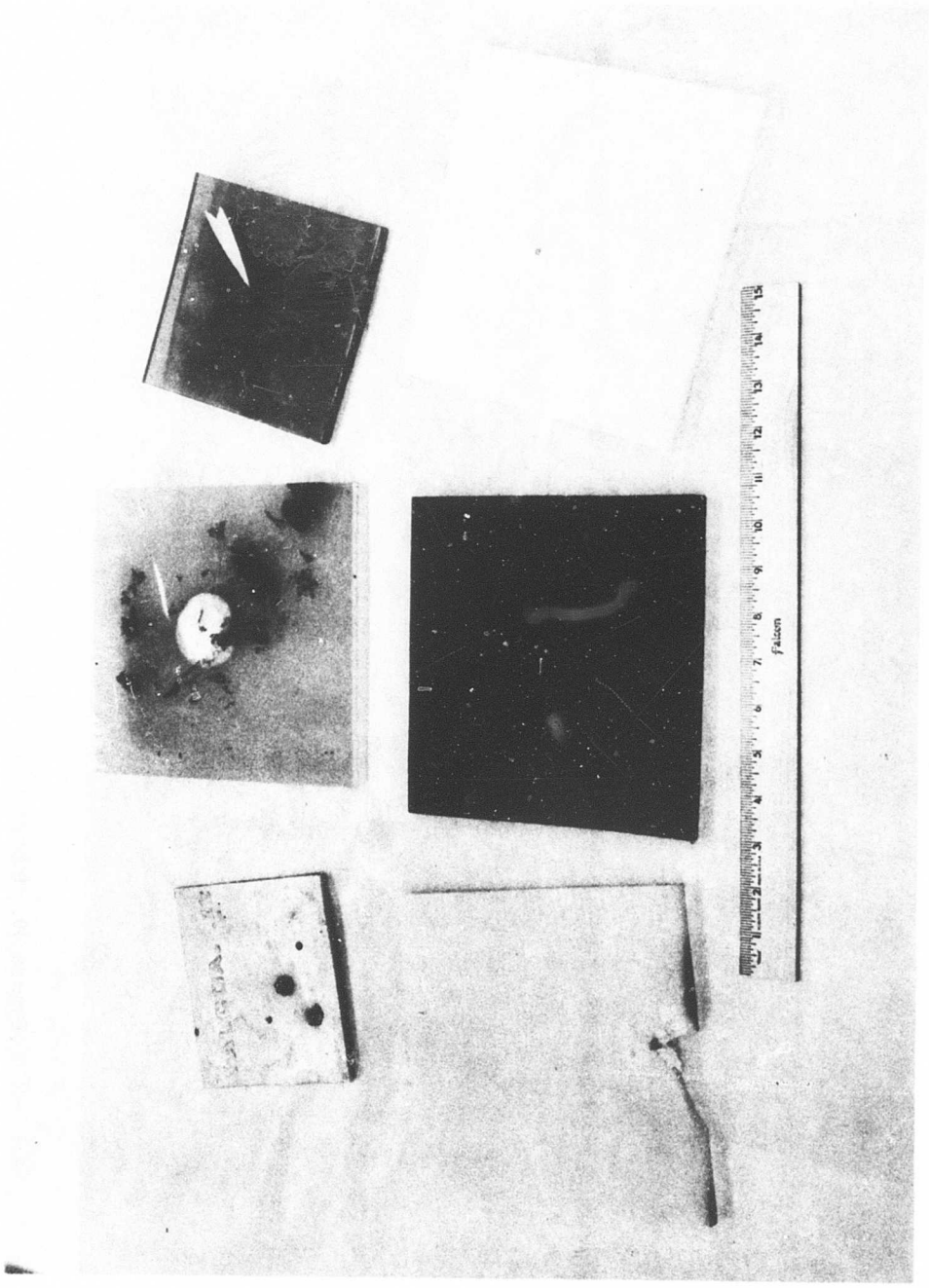

Figure 38. Test Specimens after Small Arms Ballistic Tests (Upper Row, Left to Right: 6061-T6, Glass-Filled Polyester Urethane).

Figure 39. Infrared Photograph, Ballistic Impact Flash of Steel.

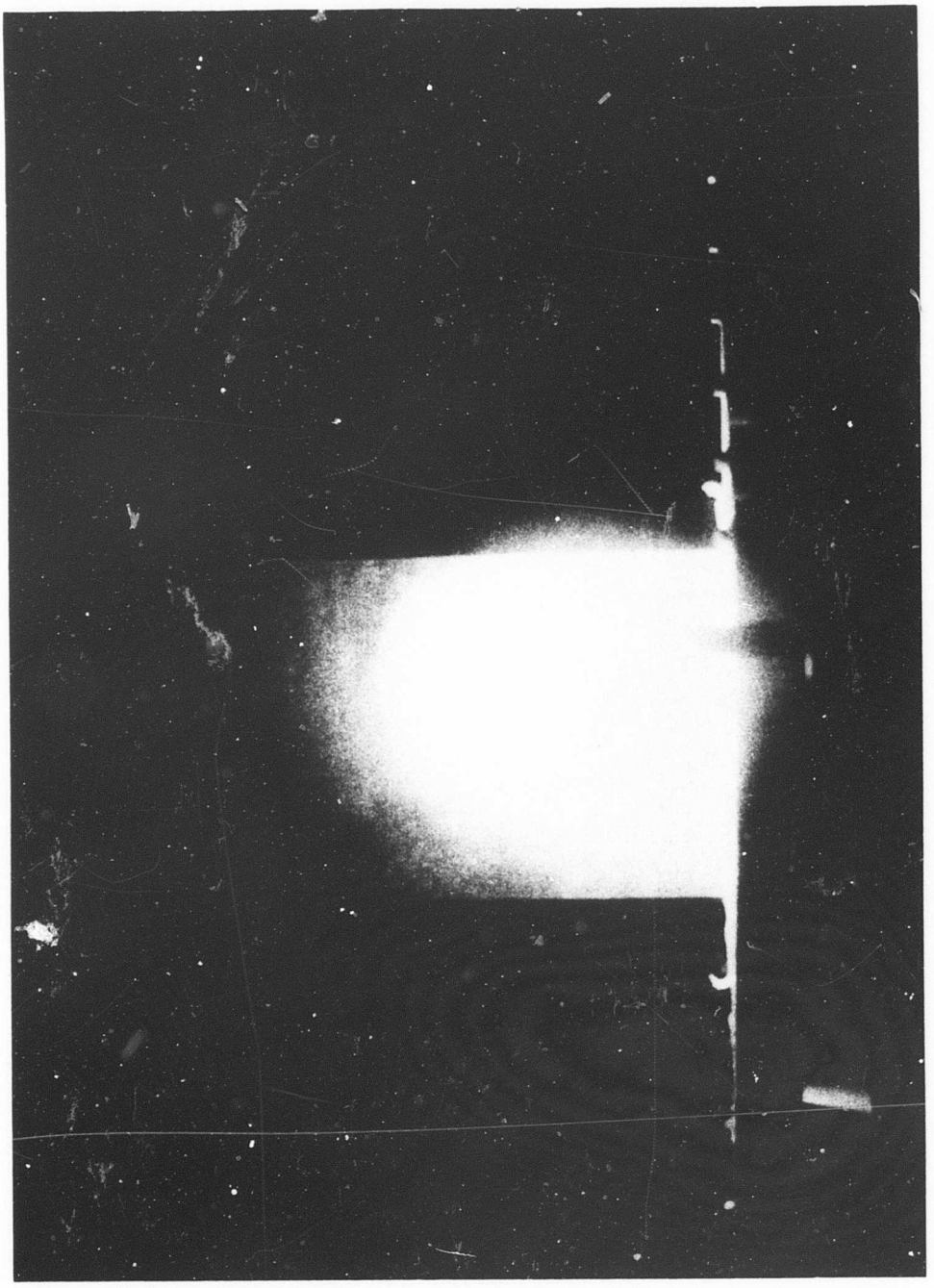

Figure 40. Ballistic Impact Flash of Magnesium, Infrared Photograph.

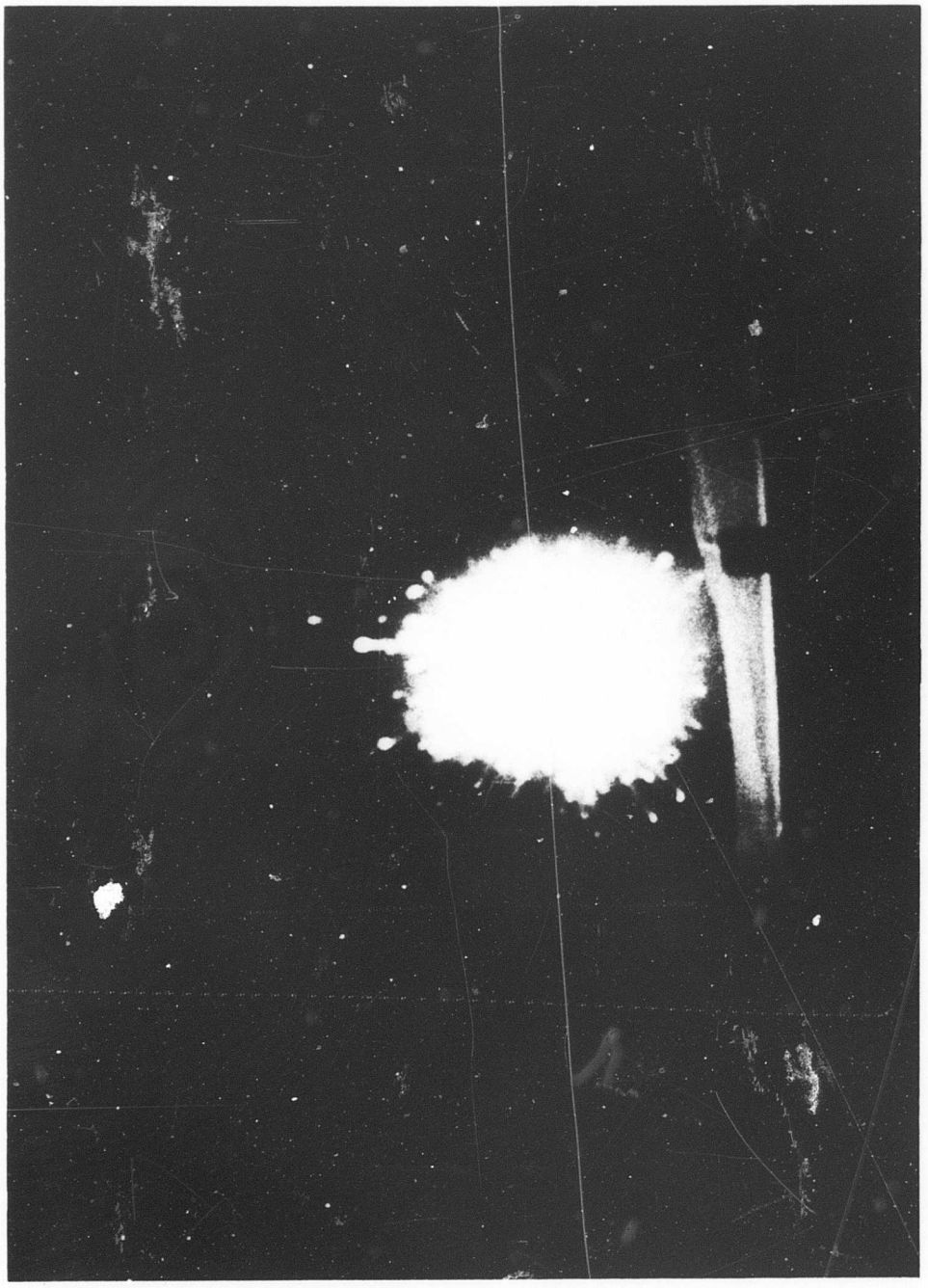

Figure 41. Ballistic Impact Flash of 6061-T6 Sheet, Infrared Photograph.

Figure 42. Ballistic Impact Flash of Cast Aluminum Valve Housing, Infrared Photograph.

TABLE III

TEST SPECIMENS USED FOR BALLISTIC FLASH TESTS

Material	Thickness (inches)
Magnesium	0.390
Steel	0.100
Wrought aluminum (6061-T6)	0.125
Cast aluminum	0.250
P-910 urethane elastomer	0.280
Linear polyethylene	0.375
Type 1 polyvinyl chloride	0.375
Nylon 6	0.375
Glass-filled polyester (40% glass)	0.375

the aluminum flashes is the large vapor fire present in both samples. These fires are high-energy sources and are a much greater threat to fuel ignition than the small hot fragments thrown off at impact.

The relative sizes and intensities of the impact flashes are given in Table IV. The shapes of the flashes from magnesium and 6061-T6 aluminum are nearly circular. For comparative purposes, the circumference of the flash was defined so that the area enclosed within the circle had a minimum density of 2.00. Unfortunately, much of the impact flash from the cast aluminum was obscured by the shape of the casting. However, the assumption was not made that the basic shape of the flash would be different from the others and, therefore, a minimum diameter was determined that intentionally excluded some of the high-energy flash extending beyond both sides of the casting.

The density of the photographic negative is directly related to the logarithm of the film exposure. The exposure is a function of both the time and intensity radiation, and thus a measure of the energy reaching the film per unit area. Combining the

TABLE IV

RELATIVE SIZES AND INTENSITIES OF BALLISTIC IMPACT FLASHES

Sample	Diameter of Flash* (inches)	Maximum Density
Magnesium	8	2.55
6061-T6	4	2.45
Cast Aluminum	4.5	2.49

*Minimum density of 2.00 defines diameter.

density with the exposed area gives a measure of the total energy released during the flash. The diameters of the flashes listed in Table IV yield relative energy ratios for magnesium, 6061-T6, and cast aluminum of 1.00 to 0.25 to 0.32, respectively. These ratios are actually somewhat high because the differences in maximum density were not considered. The energy released by the ballistic impact flash from the cast aluminum is approximately 25 percent higher than that from the 6061-T6.

Due to the limited scope of this study, no measurements were obtained of the flash durations. Using an estimated spark duration of 0.3 millisecond (obtained from high-speed motion pictures of ballistic tests), the temperatures of the flashes were calculated from the maximum flash density. The temperature corresponding to the flash density was obtained from the heat standard graph shown in Figure 36. This temperature was then multiplied by six to equate the exposure times of the standard and the flashes. The temperature thus calculated for the magnesium flash is 7710° F, compared to a theoretical flame temperature of pure magnesium of 8760° F (Reference 5). Therefore, though there is some discrepancy in the temperature, the flash duration can safely be estimated at between 0.2 and 0.4 millisecond. The temperatures of the aluminum flashes, again using an estimated flash time of 0.3 millisecond, were calculated at 7560° F for the cast aluminum and 7500° F for the 6061-T6. These temperatures are only approximate because the flash duration is unknown and might not be the same for both samples. However, even if the flash duration were twice that estimated, the calculated temperature would be approximately 4100° F, which is hot enough to ignite combustible fuel-air mixtures.

The ignition of fuel vapors depends on the total amount of energy available from the ignition source and the rate at which this energy is supplied. Although the calculated temperatures of the aluminum impact flashes are hot enough to ignite flammable vapors (the autoignition temperature of JP-4 aircraft fuel is about 475° F; see Reference 1), the flash duration is also of critical importance. Therefore, ballistic tests were conducted on both wrought (6061-T6) and cast (356) aluminum alloys surrounded by fuel-air mixtures to determine if fuel vapor ignition could occur from the ballistic impact flashes of these metals.

Sheet 6061-T6 (0.125-inch thick) and two cast aluminum components (0.250-inch thick) were suspended in separate 5-gallon cans containing 1 pint of JP-4 fuel. The lids were replaced on the cans but they were not tightly sealed. The cans were then allowed to stand at a temperature of approximately 80° F for various time intervals before small arms projectiles were fired into them. The distance between the gun muzzle and the targets was approximately 40 yards.

Ballistic hits on the 6061-T6 sheet after standing times of 4, 9, 13, 17, 25, and 33 minutes failed to ignite the fuel vapors. A hit on a cast aluminum tank interconnect (after a standing time of 16 minutes) knocked the can over and produced smoke, but no flames were seen. This component shattered when struck, as seen in Figure 43. A hit on a cast aluminum filler neck after a standing time of 10 minutes produced fuel vapor ignition. Flames, seen issuing from the fragment holes in the back of the can, extended a distance of approximately 10 to 12 inches. The component and the 5-gallon can in which it was suspended are shown in Figure 44.

The reasons for the difference in behavior of the wrought and cast aluminum alloys are unknown. Considerable fragmentation occurred from the ballistic hit on the cast aluminum (Figure 44), although the casting did not shatter. The fragmentation from the 6061-T6 alloy was negligible in comparison, and no fragment penetration of the can occurred. The difference in the ballistic damage to the two alloys may be seen in Figure 45, which shows the bullet exit holes. The 6061-T6 alloy had peeled back from the exit, and a large portion of the metal in the path of the projectile remained attached to the sheet. In contrast, the exit hole in the casting was sharp and none of the metal in the bullet path remained. It is possible that the more brittle casting breaks into many small fragments that can oxidize readily because of their increased surface area, thus creating a more energetic impact flash than can be obtained from the 6061-T6 alloy.

Much more information is needed in this area. Whether the greater energy of the casting flash is caused by the size of the flash or by its duration is unanswerable from the small amount of data available from this study. Another question is whether this energy difference is a universal difference between all cast and wrought aluminum alloys, or if the difference depends on the type of alloys and their

Figure 43. Cast Aluminum Fuel Cell Interconnect After Being Struck by a Small Arms Projectile.

Figure 44. Cast Aluminum Component and Container After a Small Arms Ballistic Hit.

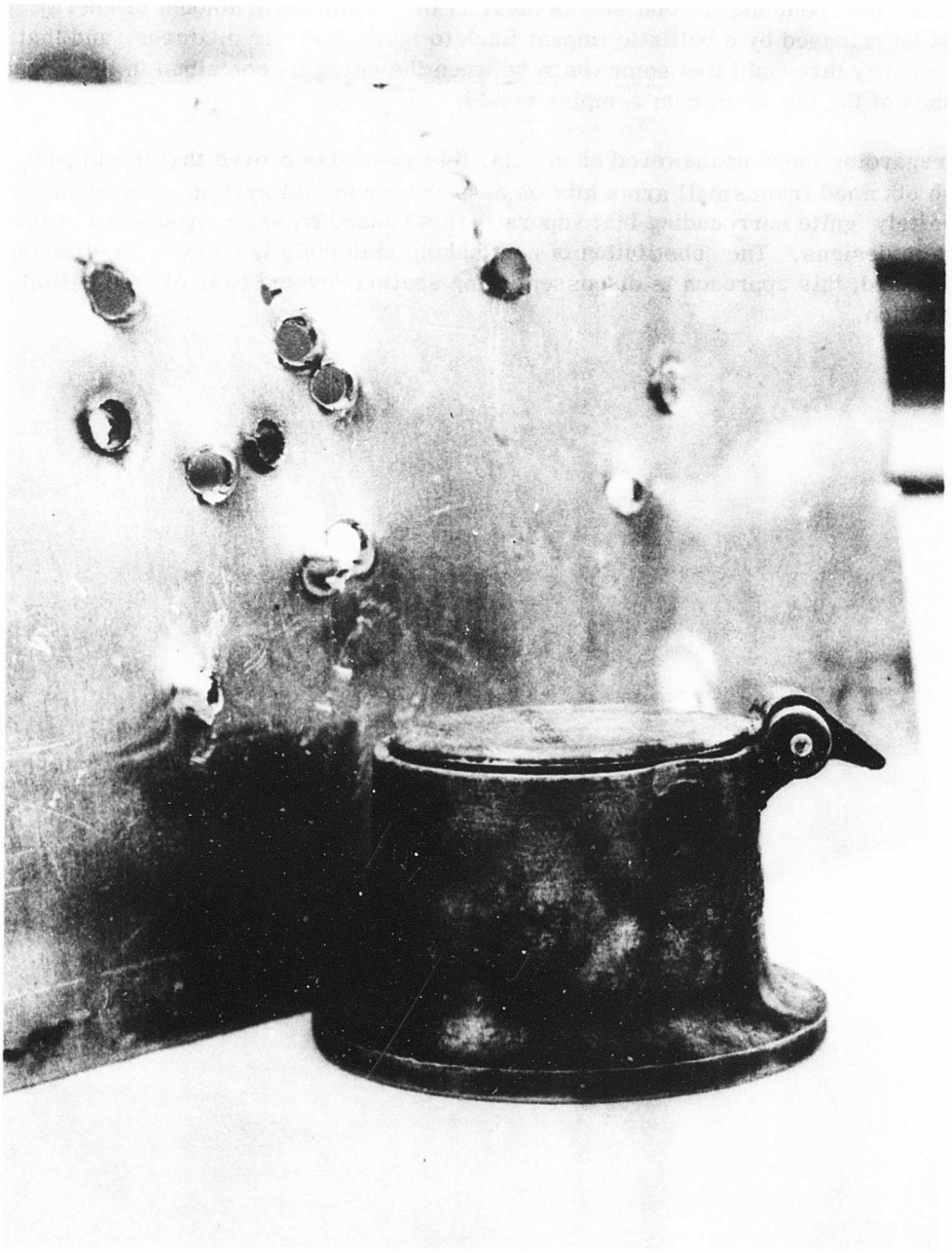

Figure 45. Cast Aluminum Component and 6061-T6 Aluminum Sheet After Ballistic Penetration by Small Arms Projectiles.

thicknesses. One aspect that seems clear is that a minimum amount of energy must be released by a ballistic impact flash to ignite fuel-air mixtures, and that this energy threshold lies somewhere between the energies contained in the impact flashes of the two aluminum samples tested.

Disregarding these unanswered questions, this study has proved that the impact flash obtained from small arms hits on cast aluminum fuel system components can definitely ignite surrounding fuel vapors. This hazard must be considered in fuel system designs. The substitution of nonflashing materials is one way to eliminate the hazard; this approach is discussed in the section devoted to improved ballistic protection.

PART IV

PRELIMINARY DESIG MODIFICATIONS

FUEL CELL ATTACHMENTS

The use of improved fuel cell materials permits large volumetric rearrangement of the fuel cell during crash-induced displacements with little probability of leakage but, to take full advantage of this feature, certain considerations must be taken into account. The general shape of the cell must be free from all protrusions that might snag on adjacent structure as the cell deforms. This subject is covered in detail in the crash vulnerability section. The attachments to the structure used to support the fuel cell and the internal cell components (fuel pump, quantity indicators, etc.) should only be strong enough to provide the support needed for normal flight loads and service condition, but not strong enough to contribute to fuel cell failure caused by crash-induced displacement loads. No passageways of fluid to the cell (transfer and supply line connections, filler ports, drains, vents, or return lines) should be connected to the adjacent structure in any manner that would result in tearing the fitting from the cell. Filler ports and drain valves must not protrude past the outside surface of the cell wall and must stay with the cell and remain sealed as the cell moves relative to the structure. Connections normally open to flow, such as supply lines and transfer lines, should consist of self-sealing breakaway fittings that are recessed below the cell wall so they will not protrude past the outside surface after disconnecting.

Two devices were investigated: (1) frangible attachments between the fuel cell and adjacent structure; and (2) self-sealing breakaway fittings that provide for fitting disconnections from the cell without fuel loss.

Frangible Fuel Cell Attachments

Strength requirements for attachments between fuel cells and the surrounding structure vary widely, depending on their installation design. The limiting factors for all such attachments should be the strength of the cell material and the normal flight and service loads to be encountered. Severe crash-induced displacement loads can result in rupture at the cell-to-structure attachments unless the restraint is released before failure loads are transmitted to the cell material. Several suggestions for frangible attachments are illustrated in Figure 17.

A nominal strength in direct tension or direct shear that would result in separation of the attachment was established before preliminary studies were initiated. For a circular bolt pattern, 150 pounds per inch of bolt-circle circumference was used. Results from previous tests indicated that the use of this value would result in loads of only 10 to 15 percent of that required to fail improved fuel cell materials such as ARM-018. (Refer to final report, Contract DA 44-177-AMC-347(T).) This nominal strength would be adequate for attachment purposes for normal flight loads and service conditions. It should be understood that specific attachment installations might require higher or lower restraint-release strengths, but in all cases the limiting factors stated previously must be observed.

The feasibility of using plastic inserts as frangible fasteners was investigated, including the fabrication and testing of attachment assemblies for evaluation. Figures 46 and 47 show an assembly before and after separation. The assemblies consisted of two aluminum discs fastened together with potted plastic inserts. One disc remains with the cell and one remains attached to the structure after separation. A 4-inch diameter bolt circle was used for the bolts and the four plastic inserts. The assemblies were mounted to suitable adapter plates and a series of static tests was conducted using an Instron Model TTC testing machine; Figures 48 and 49 show the test setup. The desired restraint-release strength (both in tension and shear) of approximately 1880 pounds (±15 percent) was achieved by the proper combination of insert diameter and plastic material.

The plastic inserts used were fabricated from a polyester toluene diisocyanate-terminated prepolymer (equivalent weight: approximately 1000) plus Epon 828 epoxy resin (equivalent weight: approximately 188). The curing agent used was 4, 4'-methylene-bis-(2-chloroaniline). The formulation adopted for final testing was a mixture of 46 percent by weight of the diisocyanate-terminated prepolymer, 31 percent by weight of the Epon 828 resin, and 23 percent by weight of the 4, 4'-methylene-bis-(2-chloroaniline). The materials were preheated to 250° F before mixing. The prepolymer and the resin were mixed together before the curing agent was added. This mix was then evacuated and poured into the prepared test specimens which had also been preheated to 250° F. The cure cycle was 16 hours at 285° F.

A series of dynamic tests was conducted to simulate the various loading modes encountered during a survivable crash. Eight number 10 screws and an aluminum doubler ring were used to secure the attachment assembly to a 2-foot square specimen of ARM-018 fuel cell material which was bolted to the test fixture. An adapter plate, used to simulate the aircraft structure, was fastened to the opposite side of the attachment assembly with four 1/4-inch diameter bolts. A dynamic

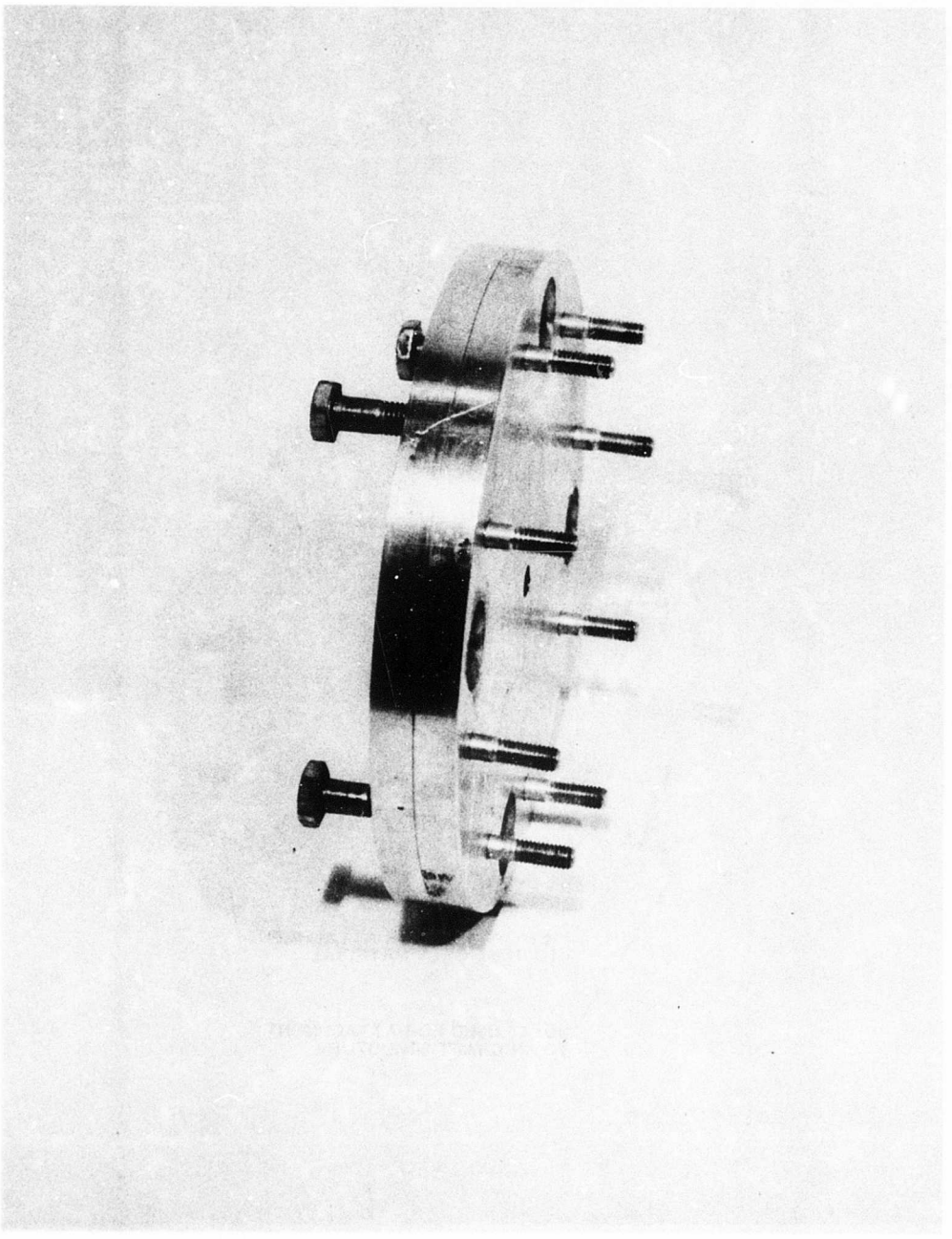

Figure 46. Frangible Fuel Cell Attachment.

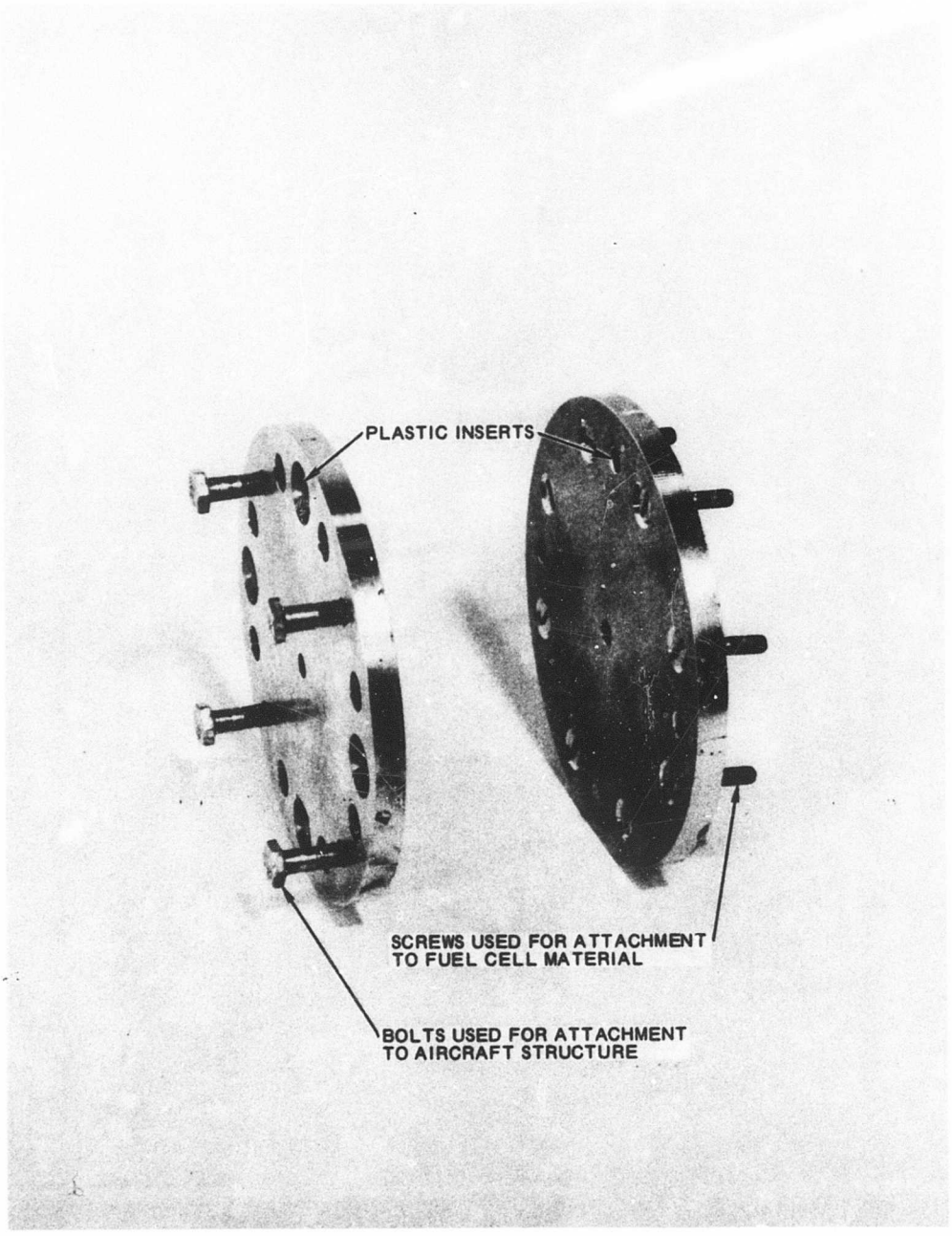

Figure 47. Frangible Fuel Cell Attachment After Release.

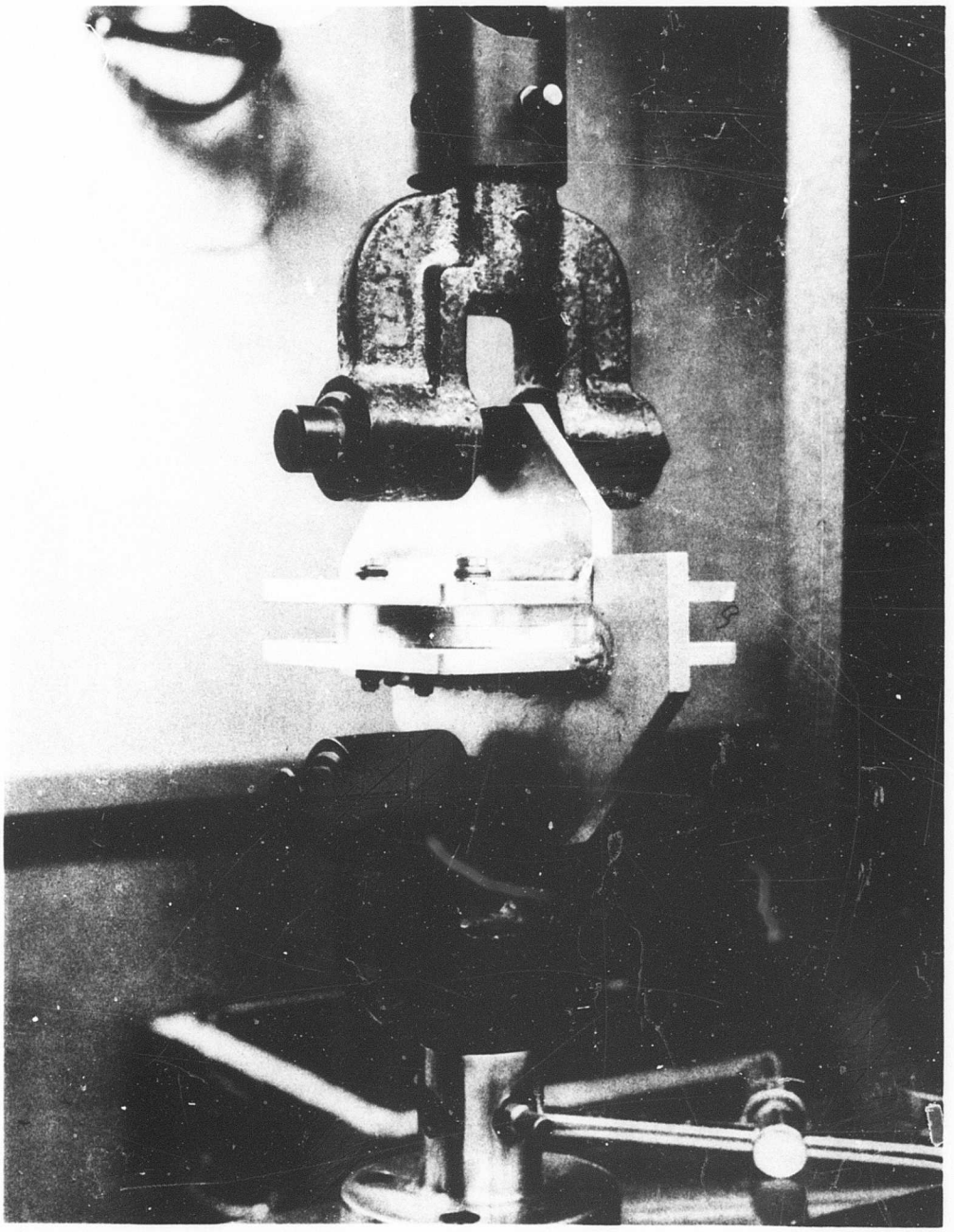

Figure 48. Frangible Attachment Static Tension Test.

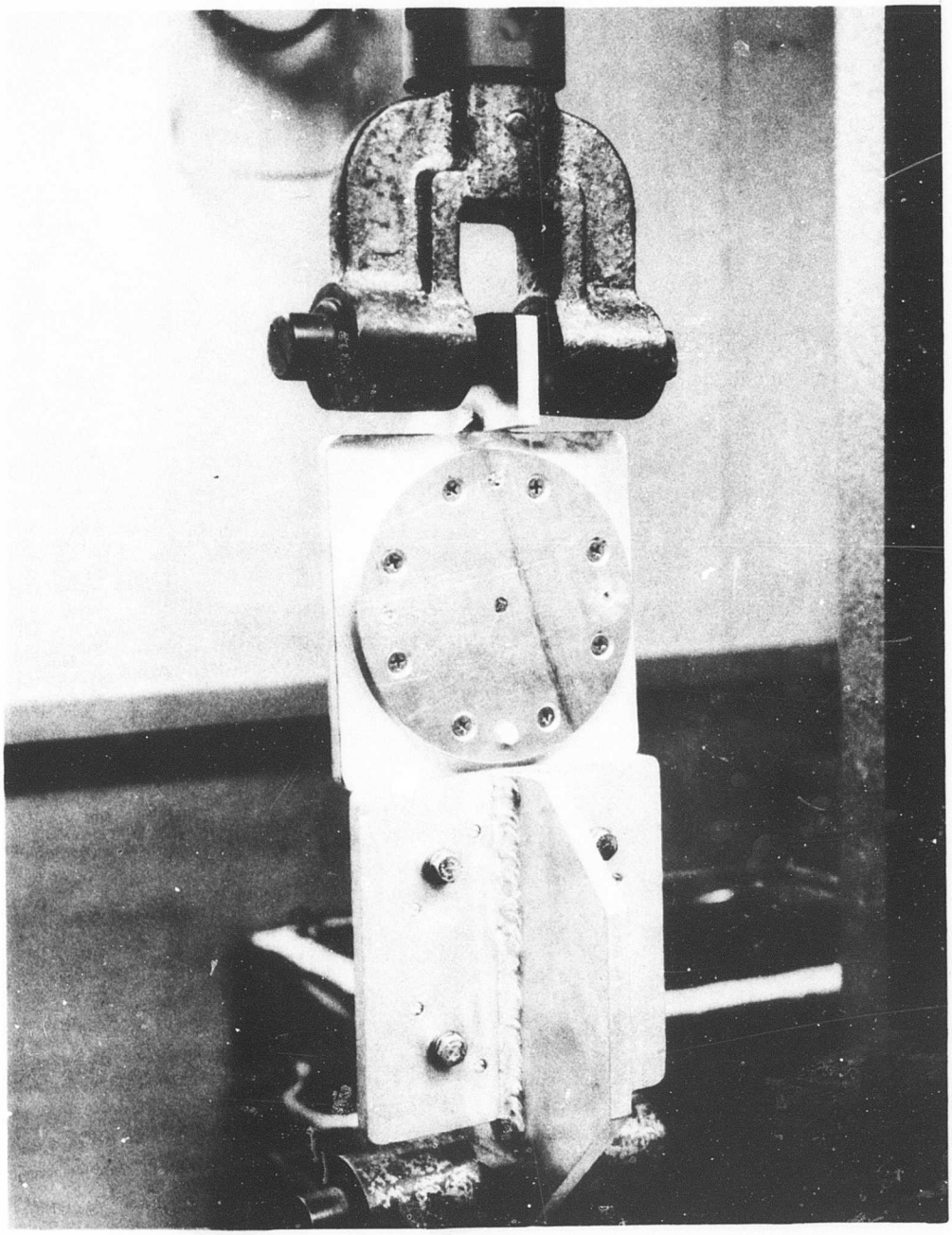

Figure 49. Frangible Attachment After Static Shear Test.

load was then applied to the adapter plate. A full description of these tests and the test data are included in Appendix V.

Design considerations for this application required a plastic material having closely matched tensile, shear and torsional properties. The prepolymer and epoxy resin formulation was considered adequate, but, further work in this area will undoubtedly provide superior materials, and the polyurethanes, various formulations of epoxies, and acetal and nylon polymers should be investigated. The attachment assemblies used for evaluation were intended for repeated use in the test series; their size, weight, and other properties necessary for a final design were not fully considered.

Plastic inserts for frangible fuel cell attachments could readily be developed for an attachment system that would greatly reduce the threat of fuel cell rupture in survivable crashes.

Self-Sealing Breakaway Fuel Cell Fittings

The need for self-sealing breakaway fuel cell fittings has long been recognized. Development of such a fitting was begun as early as 1957 (refer to Federal Aviation Agency Task No. 59-203.8). Numerous private and government-sponsored endeavors since that time have failed to fulfill this need, and there are no such fittings readily available for use at this time.

Two types of self-sealing breakaway fuel cell fittings are required: (1) Fuel cell-to-fuel cell -- a short coupling used to interconnect two closely spaced fuel cells. This type of connection is commonly found in multicell fuel systems that function as a single tank unit. The coupling frequently passes through a compartment wall or bulkhead. (2) Fuel cell-to-fuel line -- intended for use on all installations that result in a line connection to the fuel cell, including vent lines and fuel return lines.

All connection halves that remain with the fuel cell must be self-sealing. The particular installation and line function determine whether the fitting that remains with the line must possess self-sealing capabilities. The function of all self-sealing breakaway fittings is basically the same in that they must separate with no fuel loss before crash displacement loads can rupture the fuel cell or line. The optimum force required to separate the fitting is dependent on such factors as the probable mode of loading, fitting size, and the location of the fitting on the fuel cell. In all cases, this force must be greater than that encountered during flight and service conditions and less than that which would cause cell rupture.

Mil Spec MIL-V-27393A, originally released in 1960 and revised in 1964, defines the requirements for self-sealing breakaway fittings. These specification

requirements have restrictions that might not be necessary in a satisfactory fitting. The sequence of operations, movement distances, loads required to operate the valves, and the envelope dimensions appear to be suitable for one particular design concept only, whereas the actual functional requirement of preventing fuel loss should be of primary importance. The restrictive requirements established in MIL-V-27393A have hindered the development of other design concepts (see Appendix VII). No fittings have ever been operationally certified to this specification.

The development, design, and limited testing of a series of self-sealing breakaway fittings were undertaken in 1963 and 1964 as part of the work accomplished under Contract FA-WA-4580 issued by the Federal Aviation Agency (FAA). The technical report prepared for the FAA indicated that a feasible approach had been taken in the development of the cell-to-cell type interconnect fittings. An attempt to obtain complete information concerning these fittings was unsuccessful because the manufacturer would not divulge these data. A conclusive evaluation of the fittings and their present state of development could not be made with the limited information available. The fact that these fittings are still in the developmental stage, plus their high cost, made it impractical to obtain any quantity for testing during this program. Limited design evaluation, however, indicated satisfactory fuel containment in every respect except for the fuel occupying the bellows area at time of separation. This would be susceptible to dispersion in the form of a mist and would constitute a hazard. A continuation of the FAA development effort is expected in the near future under Contract FA67-WA-1652. To avoid duplication of effort, this study was limited to fuel cell-to-fuel line breakaway fittings.

Numerous low-cost, quick-disconnect couplings per MIL-C-7413C are available. The feasibility of adapting these designs to the requirements for a self-sealing breakaway fitting was investigated; the modified Wiggins POLS1D20L and POLN1D20 socket and nipple assemblies described on page 102 were used. Socket mounting was accomplished by bonding the outer actuating sleeve to a 2-foot square specimen of 3-ply, ARM-018 fuel cell material. Suitable fabric reinforcement was used to strengthen the attachment, resulting in the recessing of the socket slightly below the surface of the cell material (Figures 50, 51, and 52). Any movement of the nipple away from the mounted socked released the locking mechanism and allowed the coupling to separate with subsequent sealing of both halves. A frangible restraining collar (also described on page 102) was used to provide approximately 500 pounds of release restraint under static loading.

A series of dynamic tests was conducted to simulate the various loading modes imposed on a fuel cell-to-line disconnect during survivable crash conditions. A full description of these tests and the test data are included in Appendix V.

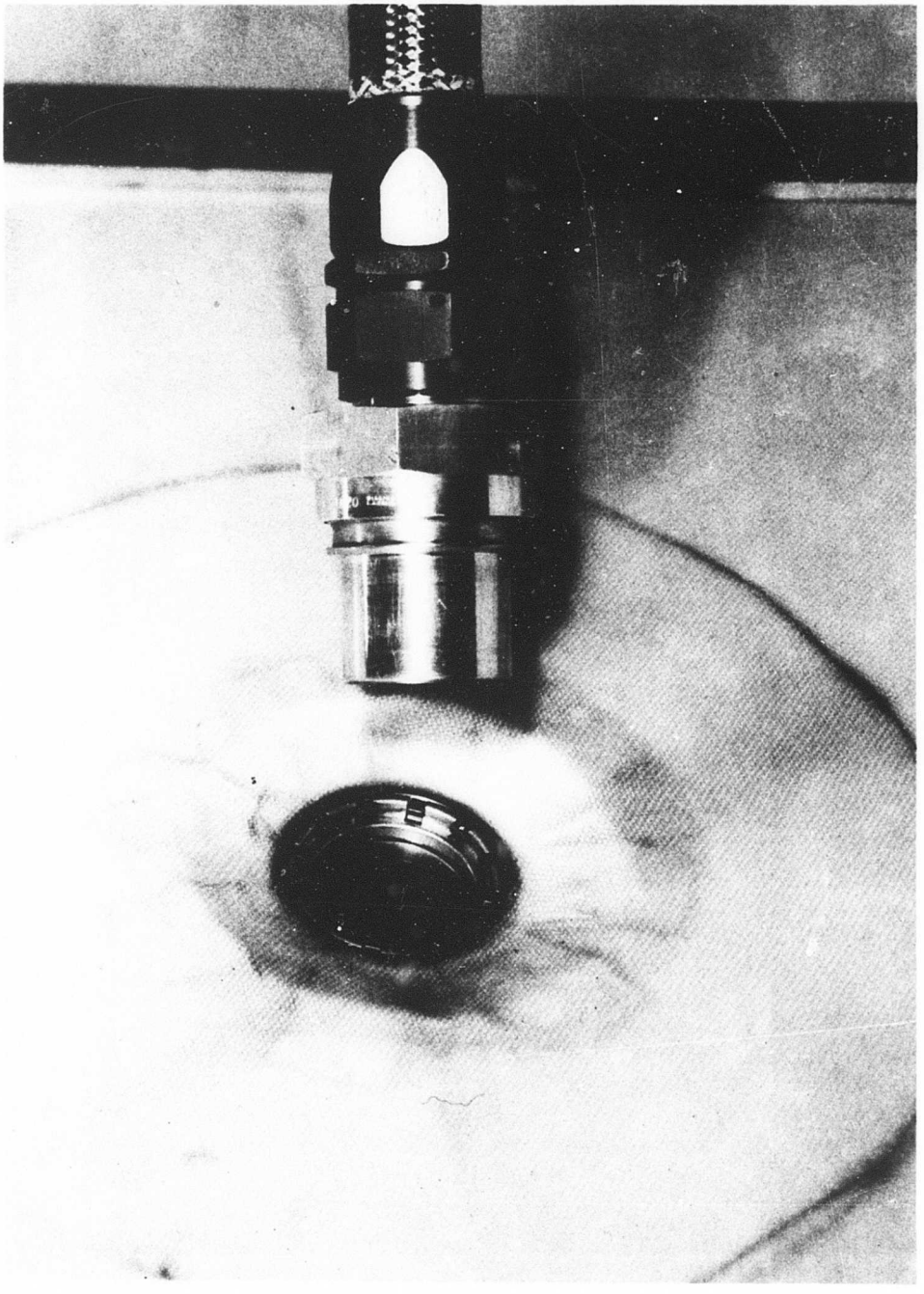

Figure 50. Self-Sealing Breakaway Fuel Cell Fitting After Separation.

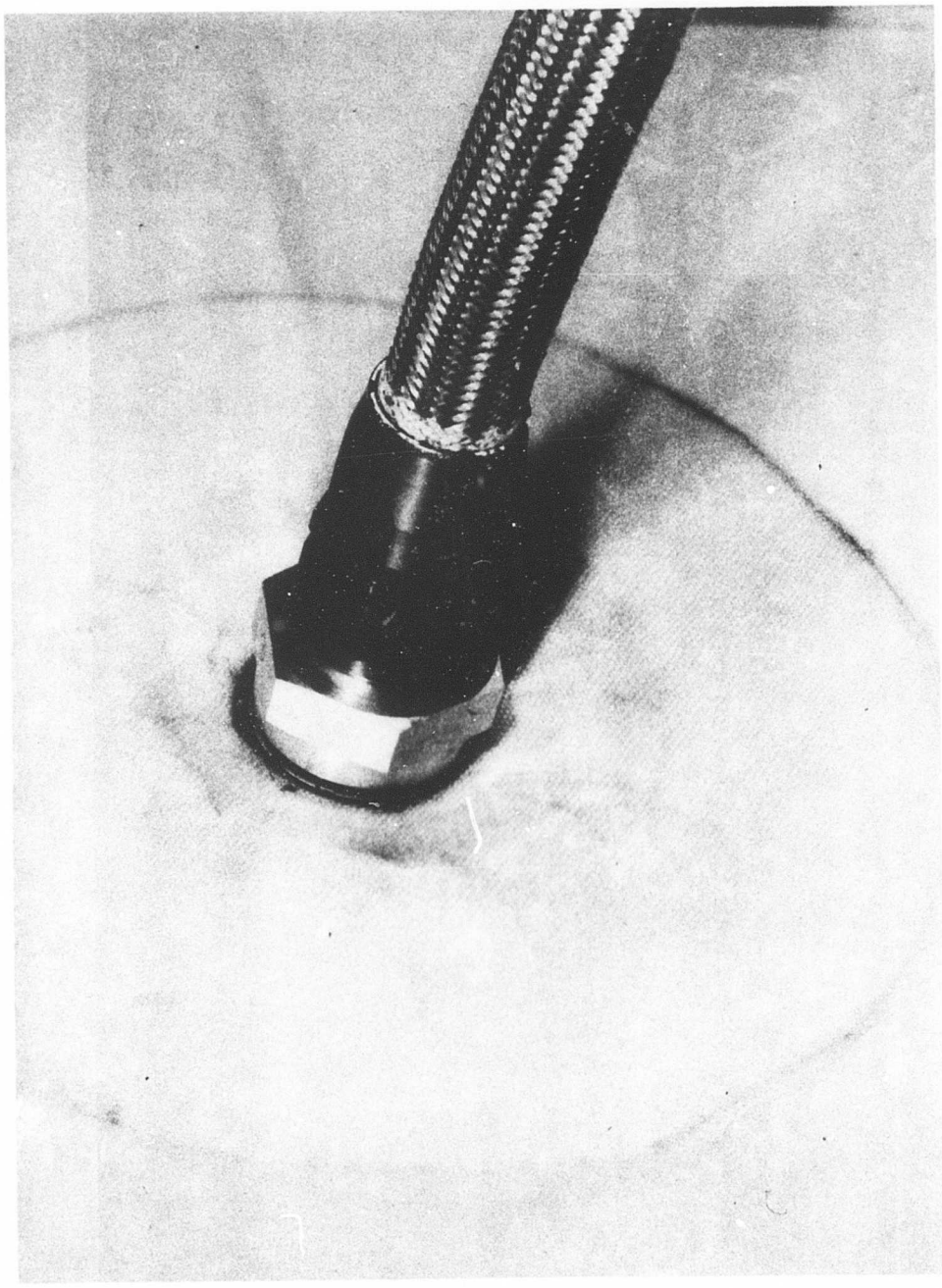

Figure 51. Self-Sealing Breakaway Fuel Cell Fitting Shown Connected.

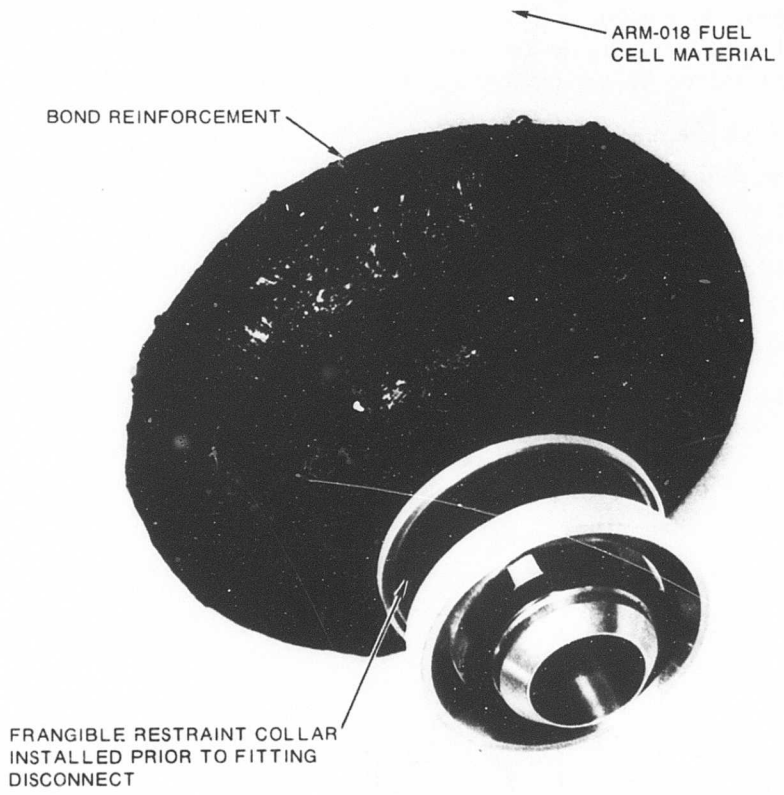

Figure 52. Self-Sealing Breakaway Fuel Cell Fitting Inside Fuel Cell.

Tests indicate good performance of the modified coupling under a wide range of conditions. Redesign of the coupling or mounting could result in a fitting adequate in many installations. The chief advantage of this type of closure is that fuel containment is complete with no fuel loss during separation.

Improved separation of the fitting, when subjected to loads with a high lateral component (shear load), might be obtained by providing swiveling capabilities in the mounting of the coupling socket to the cell material (see Figure 53). The standard coupling does not provide a fluid seal between the socket body and the outer actuating sleeve. An O-ring or seal would correct this. The frangible collar could be eliminated by redesigning the coupling socket spring arrangement. A general redesign might reduce weight and make more suitable mounting.

COMPONENT ATTACHMENT METHODS

As pointed out, fuel system failures commonly occur because of the method of attaching fuel system components to the aircraft structure. Large structural displacements that occur during survivable crashes often cause failure of both fuel cells and fuel lines. Certain design and installation criteria which would reduce the incidence of these failures are presented in this section.

Fuel Line Attachments

Fuel lines must be capable of reorienting with the structure during deformation. All fuel lines should be made from extra-length flexible hose with an outer protective sheath to reduce the possibility of cutting. The hose should be attached to the structure with clamps that provide adequate support during

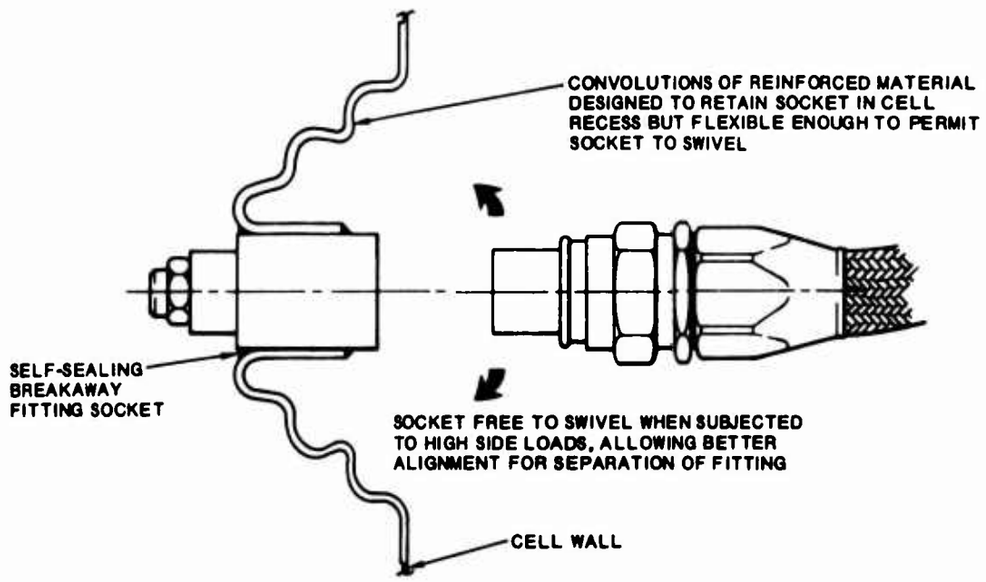

Figure 53. Recessed Swivel Mounting for Breakaway Fitting.

normal flight conditions and that allow the hose to separate from the structure before crash-induced loads can cause the hose or attached fittings to rupture.

Standard bulkhead fitting installations, because of the rigidity and strength of the attachment, frequently contribute to fuel line failure and can continue to do so even with the use of flexible hose. Two methods of reducing this hazard were investigated:

1. The use of a frangible, protective bulkhead adapter to provide the release of standard bulkhead fittings prior to failure of the fuel line. (After release, the adapter should provide a protective passage through the bulkhead for line-to-structure displacement.)

2. The use of self-sealing breakaway fittings to provide fluid shutoff and fitting disconnect prior to line failure.

Frangible, Protective Bulkhead Adapter

Two suggestions for frangible bulkhead adapters are illustrated in Figures 23 and 24. To investigate the feasibility of a frangible, protective adapter and to establish design concepts for future development, the configuration illustrated in Figures 54 and 55 was chosen for fabrication and testing. This design allows the use of standard MS fluid line fittings and requires a standard punched hole in the bulkhead material. As illustrated in Figure 56, the reduced cross section provides a predictable fracture path that results in a protective torus covering the opening through the bulkhead for passage of hose and fittings. Type I PVC (polyvinyl chloride) was chosen for this feasibility study because of its physical properties, machinability, availability, and cost. The material is rigid enough to support structural loads but has enough elongation (about 10 percent at low-onset load rates) to have some degree of elasticity. It can be readily solvent bonded and is not affected by hydrocarbon fuels.

An adapter sized to accommodate 5/8-inch-diameter hose and fittings was used in this effort. Aeroquip Corporation Type 601 flexible hose and hose end fittings were chosen as representative of the type normally used in aircraft installations and were used in all tests. It was determined that a predictable fracture path for the frangible adapter could be obtained under static test conditions. A strength of 500 pounds in axial tension was chosen because it was adequate for all service and flight load conditions, yet low enough to allow the adapter to perform its protective function for 5/8-inch hose under all anticipated crash loading modes. By reducing the cross sections (Figure 56) to 0.200-inch wide by 0.058-inch thick, the desired strength in axial tension was obtained. Three adapter specimens were

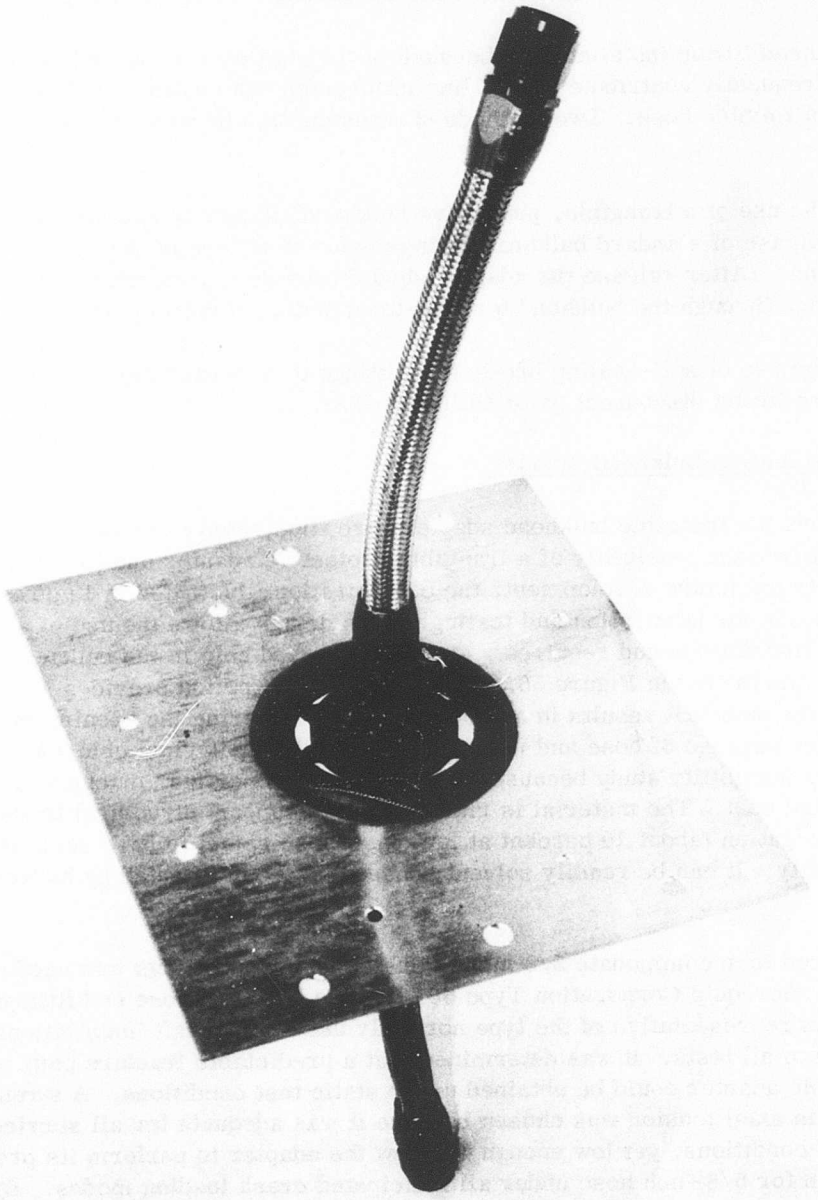

Figure 54. Frangible Protective Bulkhead Adapter.

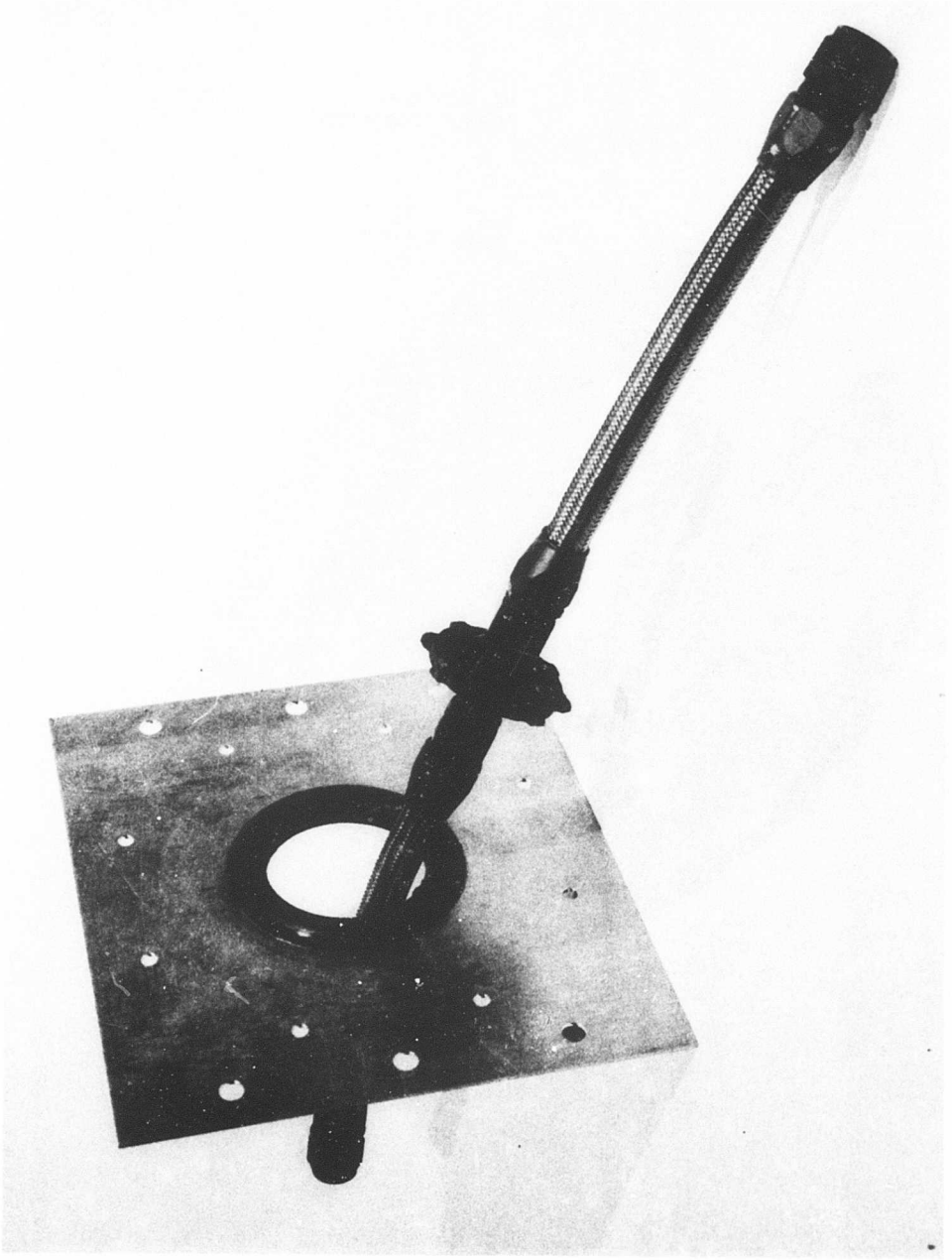

Figure 55. Frangible Protective Bulkhead Adapter After Release

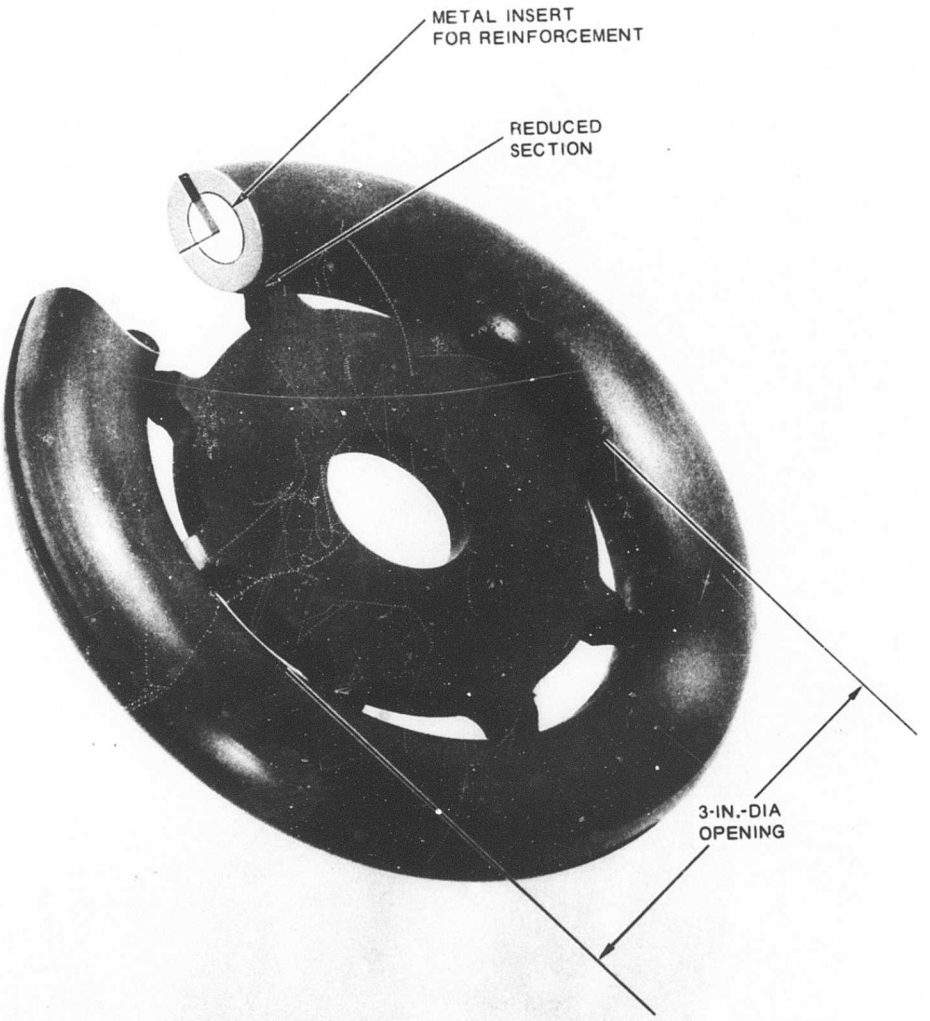

Figure 56. Cross Section of Frangible Protective Bulkhead Adapter

statically tested on an Instron machine (see Figures 57 and 58) at a load rate of 1 inch per minute. Separation occurred at the predicted fracture path at the desired load level. One test was conducted at a load rate of 2 inches per minute to determine the effect of fitting release with a load applied 90 degrees to the axis of the fitting. The amount of protection offered to the hose as it bore against the torus following release was also evaluated. The fitting released properly and then passed through the opening, allowing the hose to bear on the rounded torus section of the adapter. Continued extension resulted in an eventual load of 2150 pounds, at which time the steel cable that was used to attach the slack end of the hose failed. No serious degradation of the hose was evident in the area that contacted the adapter torus, but the hose did rupture at the adjacent fitting.

A series of dynamic tests was also conducted to simulate the various loading modes encountered during survivable crash conditions. A full description of these tests and the resultant data are included in Appendix V.

Data indicate that a high degree of protection could be afforded to fuel line passage through bulkheads by the use of appropriately designed frangible bulkhead adapters. The use of plastic materials in these adapters shows excellent promise. The apparent brittleness of the plastic adapter under high-velocity impact (the failure of the torus section when impacted by the hose fittings) might be corrected by changes in the formulation of the polyvinyl chloride or by substituting other material, such as acrylonitrile butadiene styrene (ABS), nylon, or acetal polymers.

The high stress concentrations at the edges of the bulkhead that tend to reduce the impact strength of the torus section could be relieved by increasing the inside radius of the torus or by using a metal ring embedded in the adapter, as shown in the section view of Figure 56. Test data indicate that the inside diameter of the torus section should be dictated by the type of bulkhead fitting that might be required to pass through the adapter. The two most common fittings used are standard bulkhead unions and bulkhead elbows. On the basis of the diameter needed to circumscribe the attaching nut (usually AN924), the following minimum diameter openings should be used: 1.25 × nut diameter for AN815 bulkhead unions, and 3.0 × nut diameter for AN833 bulkhead elbows.

Self-Sealing Breakaway Fuel Line Fittings

Investigation disclosed that no self-sealing breakaway fuel line fittings specifically designed for postcrash fire prevention are available. A study of the requirements indicated that the design criteria for such a fitting should include the following considerations:

statically tested on an Instron machine (see Figures 57 and 58) at a load rate of 1 inch per minute. Separation occurred at the predicted fracture path at the desired load level. One test was conducted at a load rate of 2 inches per minute to determine the effect of fitting release with a load applied 90 degrees to the axis of the fitting. The amount of protection offered to the hose as it bore against the torus following release was also evaluated. The fitting released properly and then passed through the opening, allowing the hose to bear on the rounded torus section of the adapter. Continued extension resulted in an eventual load of 2150 pounds, at which time the steel cable that was used to attach the slack end of the hose failed. No serious degradation of the hose was evident in the area that contacted the adapter torus, but the hose did rupture at the adjacent fitting.

A series of dynamic tests was also conducted to simulate the various loading modes encountered during survivable crash conditions. A full description of these tests and the resultant data are included in Appendix V.

Data indicate that a high degree of protection could be afforded to fuel line passage through bulkheads by the use of appropriately designed frangible bulkhead adapters. The use of plastic materials in these adapters shows excellent promise. The apparent brittleness of the plastic adapter under high-velocity impact (the failure of the torus section when impacted by the hose fittings) might be corrected by changes in the formulation of the polyvinyl chloride or by substituting other material, such as acrylonitrile butadiene styrene (ABS), nylon, or acetal polymers.

The high stress concentrations at the edges of the bulkhead that tend to reduce the impact strength of the torus section could be relieved by increasing the inside radius of the torus or by using a metal ring embedded in the adapter, as shown in the section view of Figure 56. Test data indicate that the inside diameter of the torus section should be dictated by the type of bulkhead fitting that might be required to pass through the adapter. The two most common fittings used are standard bulkhead unions and bulkhead elbows. On the basis of the diameter needed to circumscribe the attaching nut (usually AN924), the following minimum diameter openings should be used: 1.25 × nut diameter for AN815 bulkhead unions, and 3.0 × nut diameter for AN833 bulkhead elbows.

Self-Sealing Breakaway Fuel Line Fittings

Investigation disclosed that no self-sealing breakaway fuel line fittings specifically designed for postcrash fire prevention are available. A study of the requirements indicated that the design criteria for such a fitting should include the following considerations:

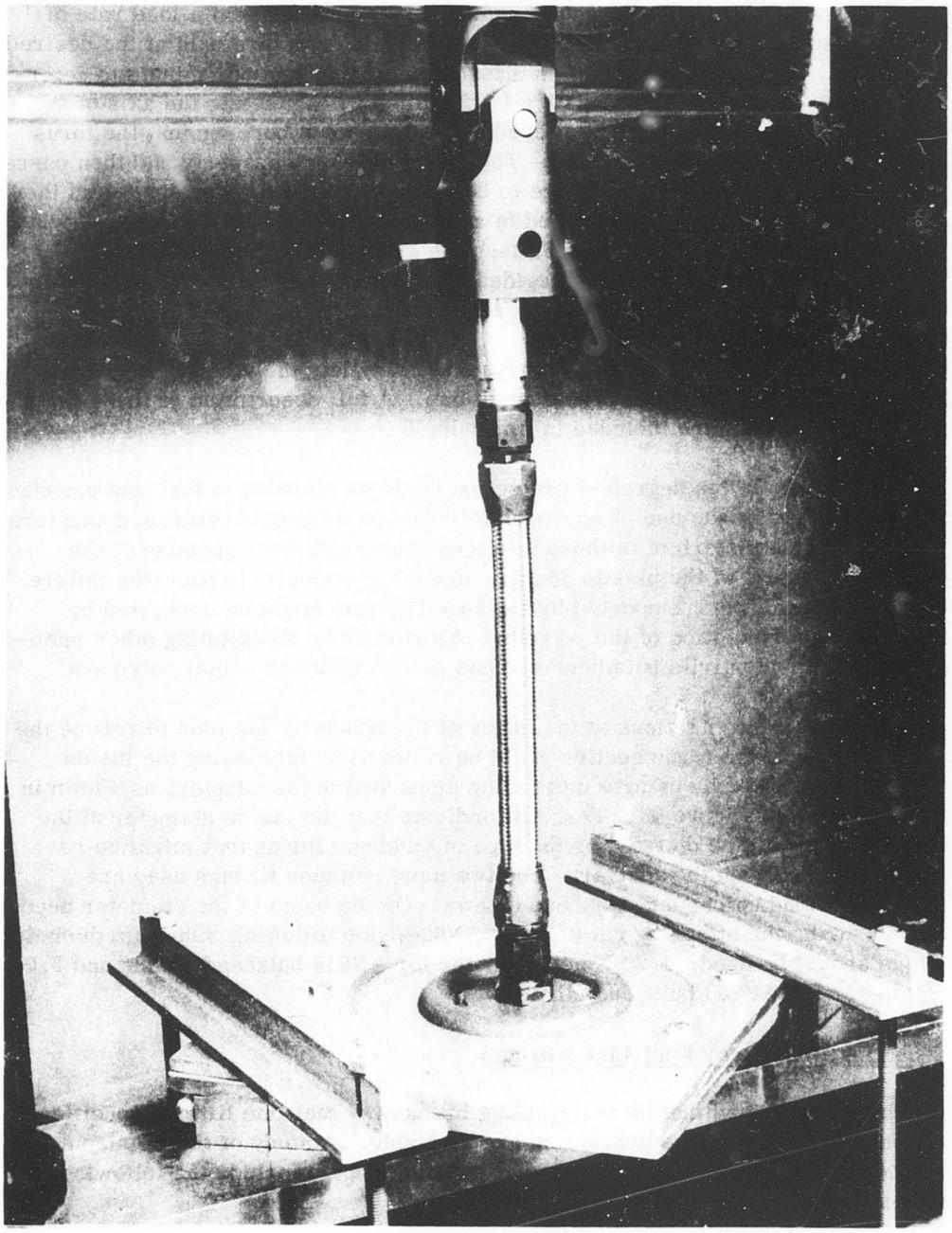

Figure 57. Static Test of Bulkhead Adapter (1 of 3).

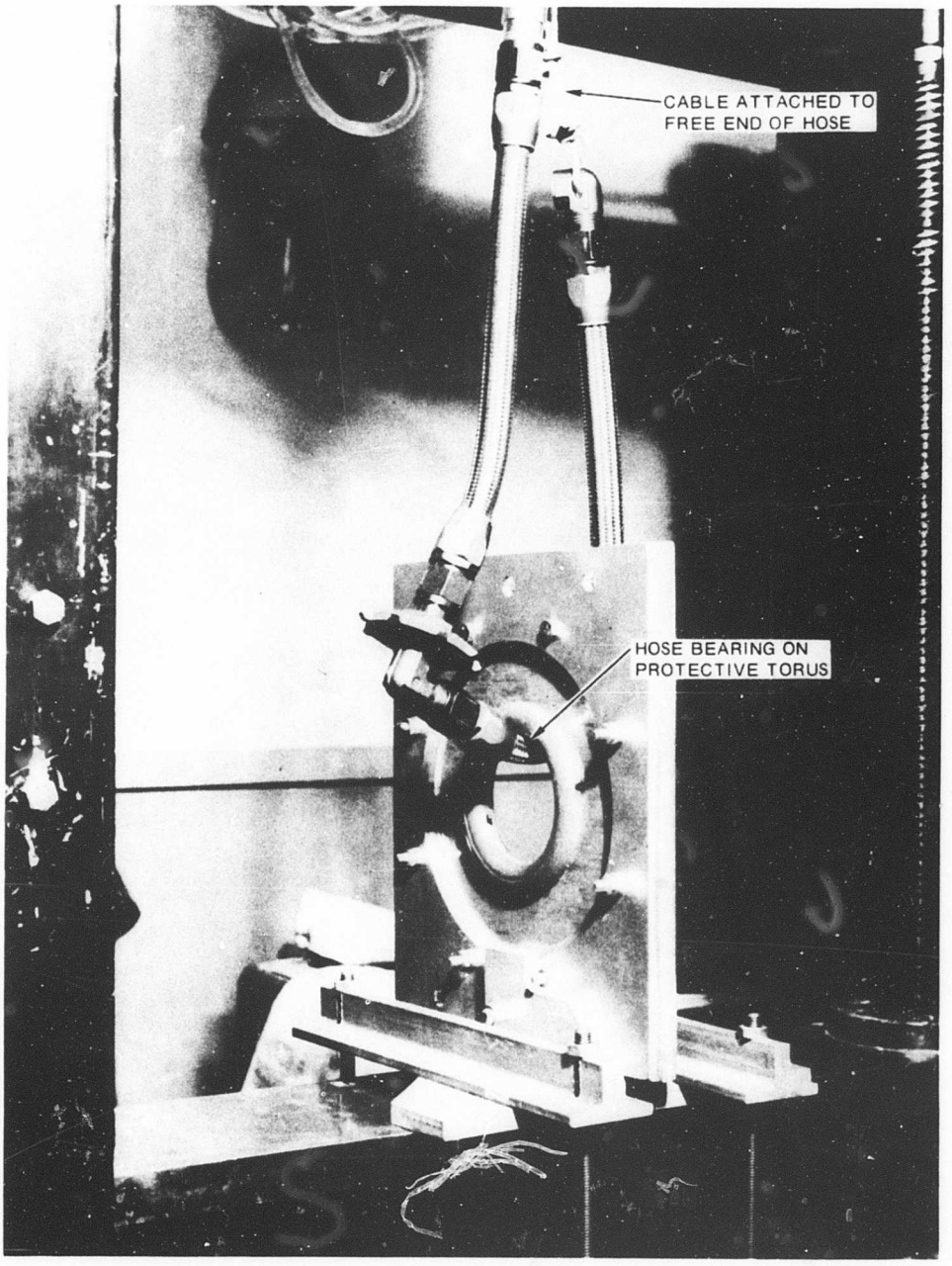

Figure 57. Static Test of Bulkhead Adapter (2 of 3).

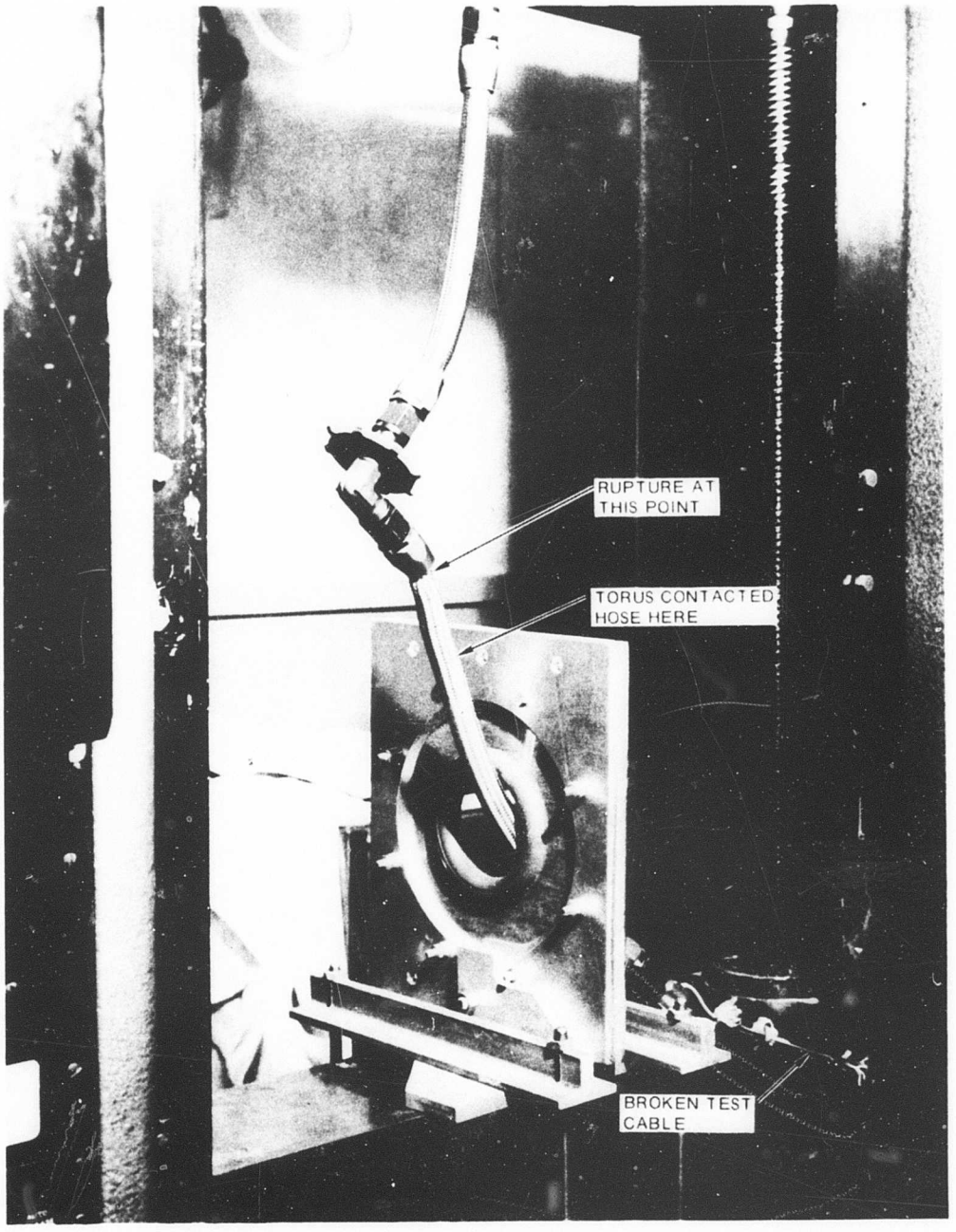

Figure 57. Static Test of Bulkhead Adapter (3 of 3)

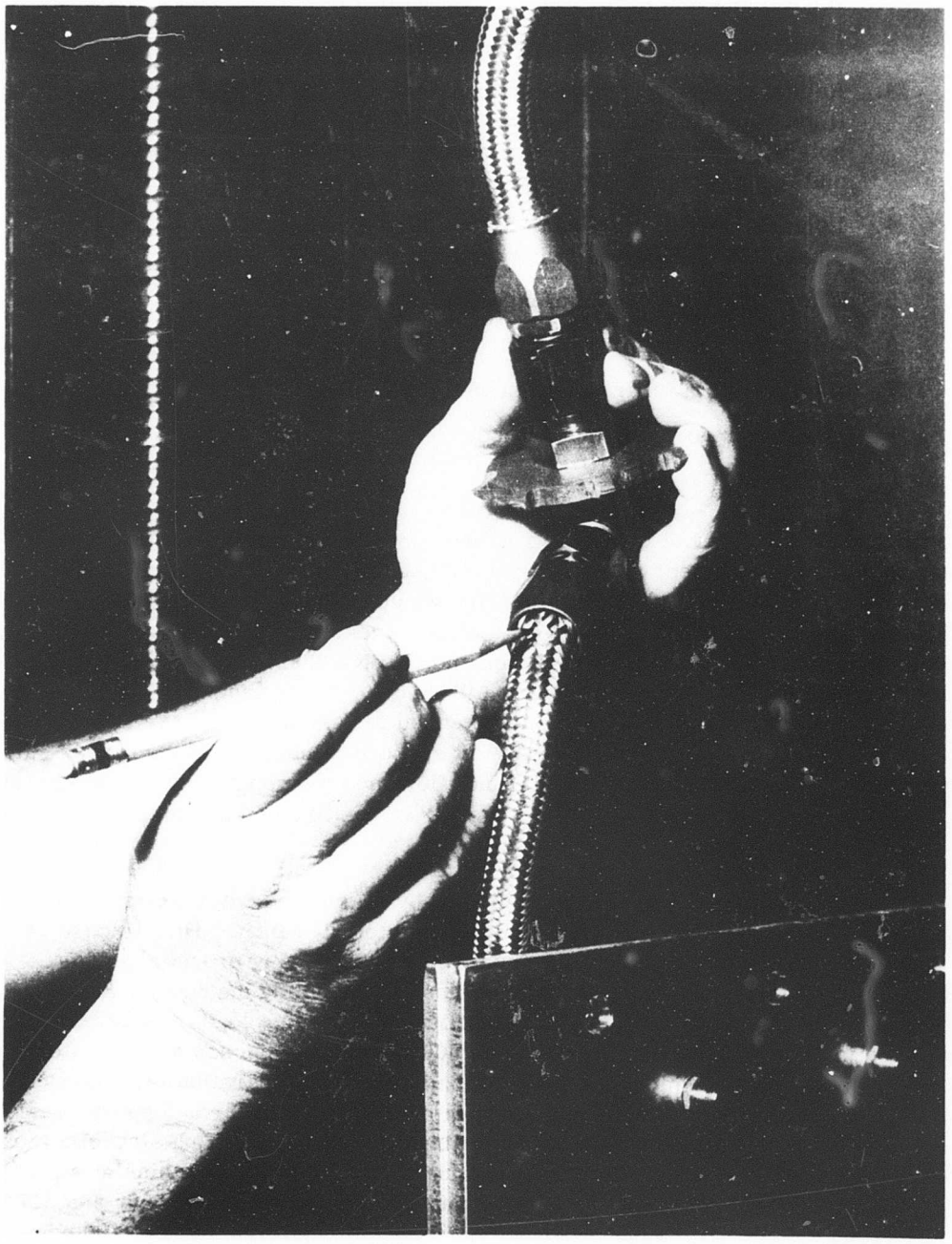

Figure 58. Location of Hose Rupture During Static Test of Bulkhead Adapter.

1. Lightweight and of minimum size.
2. Cause little or no flow restriction when installed.
3. Reliable, with a positive means of withstanding service and flight loads without inadvertent shutoff of fuel flow, and preferably with a visual means of ensuring that fuel flow is not obstructed and that the connection is locked in place.
4. Release and sealing of both halves should result from fuel line extension that would otherwise cause failure and fuel loss.
5. Allow little or no fuel spillage due to separation.
6. Adaptable for use with standard fuel line fittings and hose ends.
7. Available in a full range of sizes (3/8-inch to 2-1/2-inch diameter).
8. Easily serviced and maintained.
9. Low cost.

To implement the study of the above requirements, a number of commercially available quick-disconnect couplings (per MIL-C-7413A) were obtained, modified, and tested. A 1-1/4-inch diameter fuel line was chosen because this size is representative of intercell transfer (crossfeed) lines. The couplings used were modified POLS1D20-L socket assemblies and POLN1D20 nipple assemblies manufactured by E.B. Wiggins, Inc. (Figures 59 and 60). These couplings are designed for use in aircraft refueling. They are intended for use under severe service conditions and separate with very little fuel spillage. Internal valves in both halves are designed to prevent interruption of fuel flow prior to separation. The mechanical connection that locks both halves together is positive and strong enough to meet all flight and service conditions.

In normal operation, the coupling is released by sliding the outer sleeve of the socket assembly away from the nipple approximately 1/4 inch. This release requires a 3- to 5-pound force to overcome the internal spring pressure. It is necessary, therefore, to provide some means of preventing inadvertent release and closure of the coupling during normal flight and service loads. A release force required in axial tension of approximately 500 pounds was chosen as adequate for normal conditions and which would still permit coupling separation prior to line failure. A frangible restraining collar of laminated kraft paper and epoxy resin was installed on the socket half of the coupling to hold the actuating sleeve in the locked position. Three release tests, conducted on an Instron machine at a load rate of 10 inches per minute, resulted in coupling releases at 533, 500, and 517 pounds (see Figure 61). Figures 62 and 63 show the modified coupling and hose assembly.

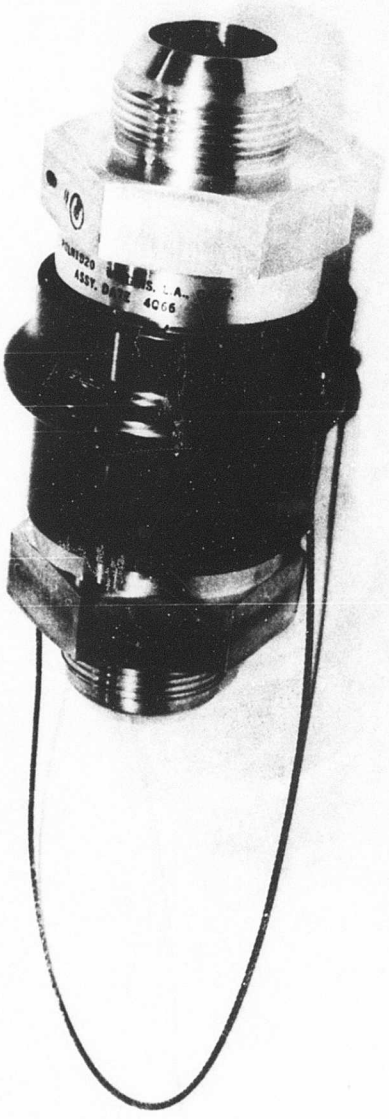

Figure 59. Connected Standard Coupling.

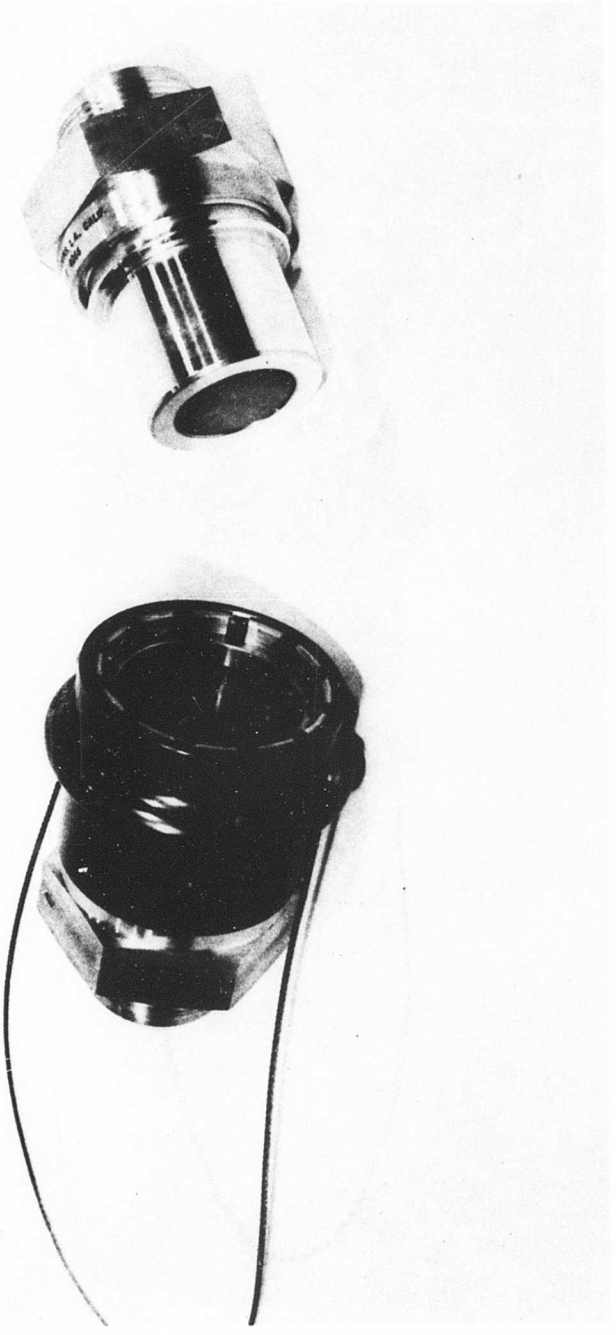

Figure 60. Unconnected Standard Coupling.

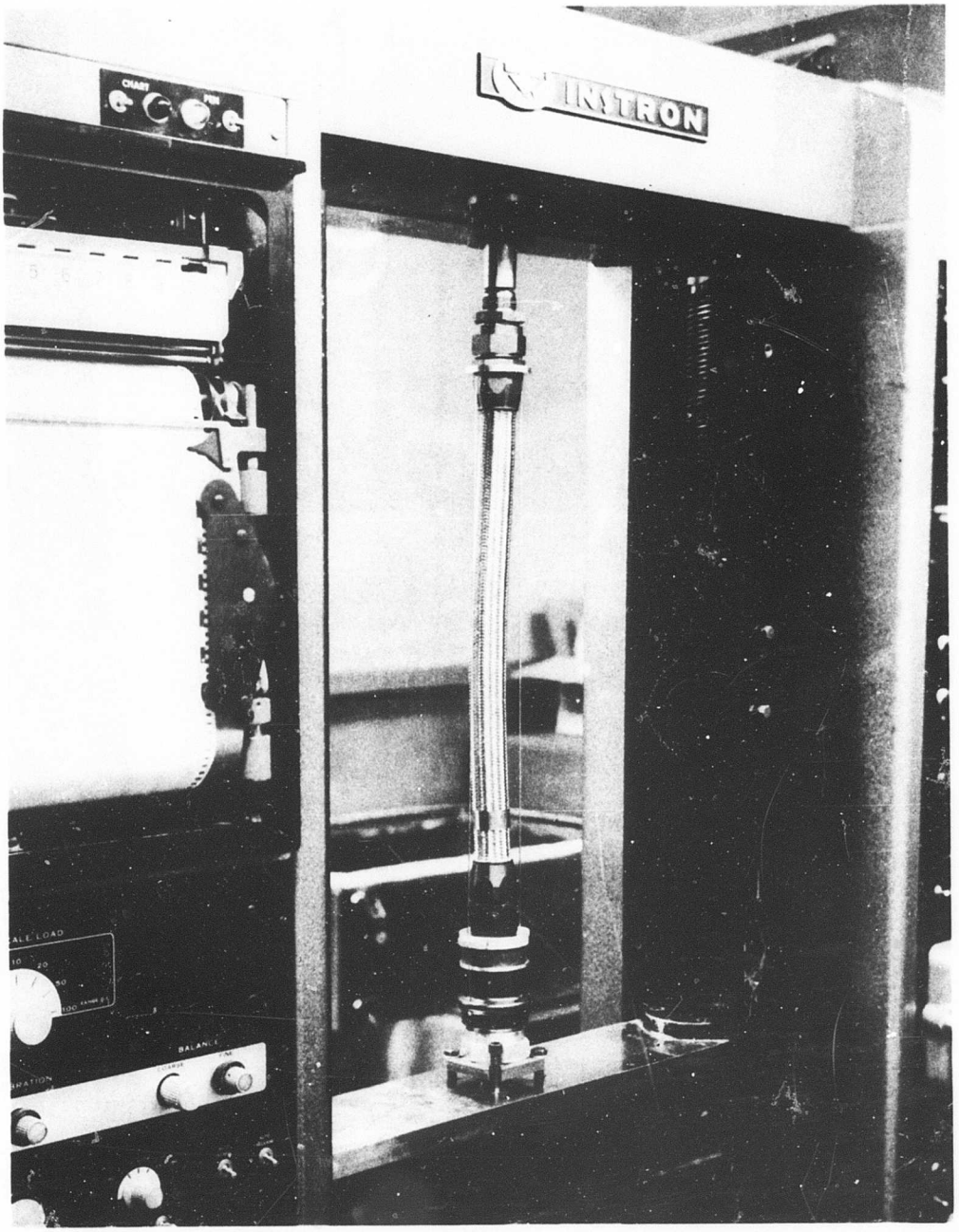

Figure 61. Static Test of Breakaway Line Fitting (1 of 2).

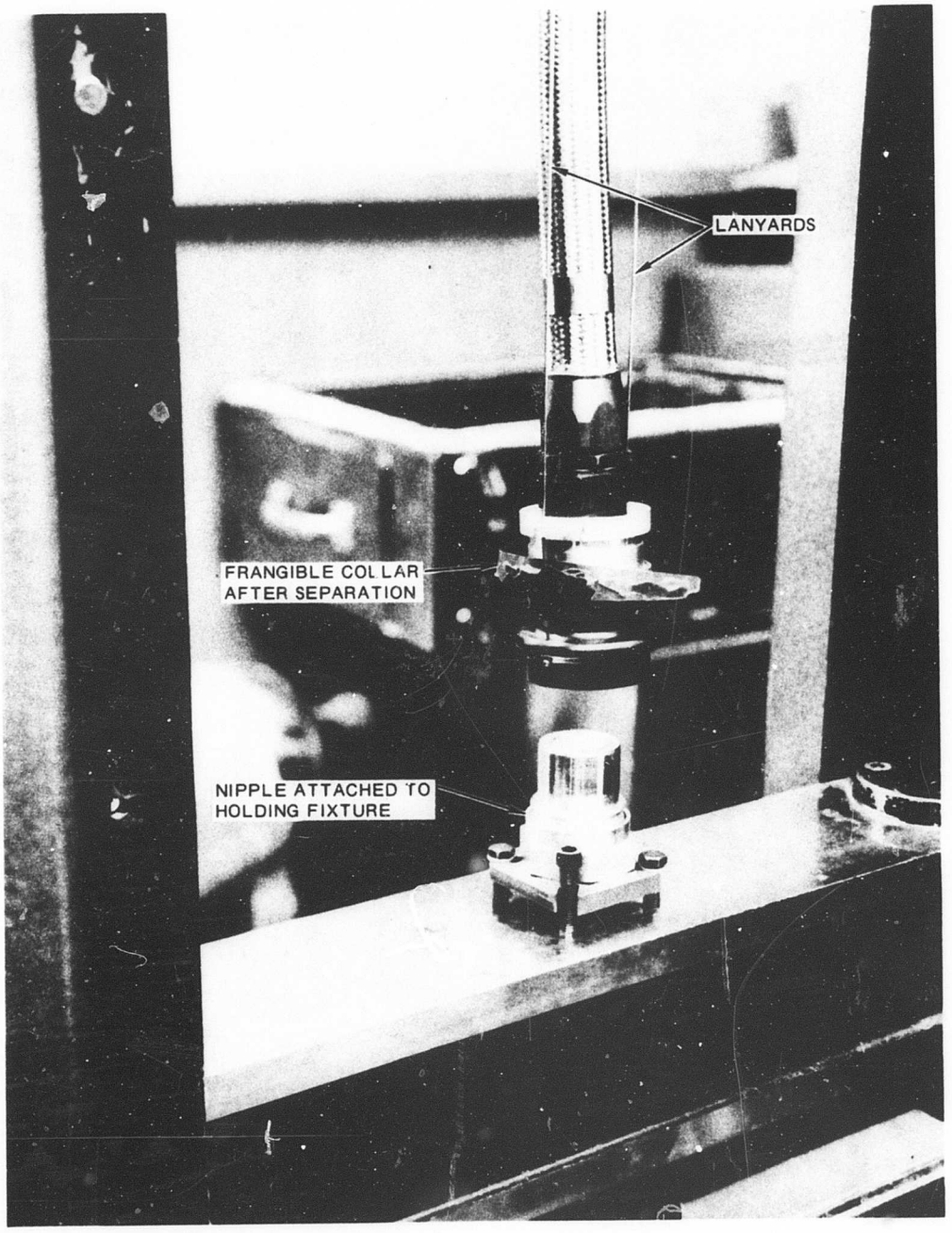

Figure 61. Static Test of Breakaway Line Fitting(2 of 2).

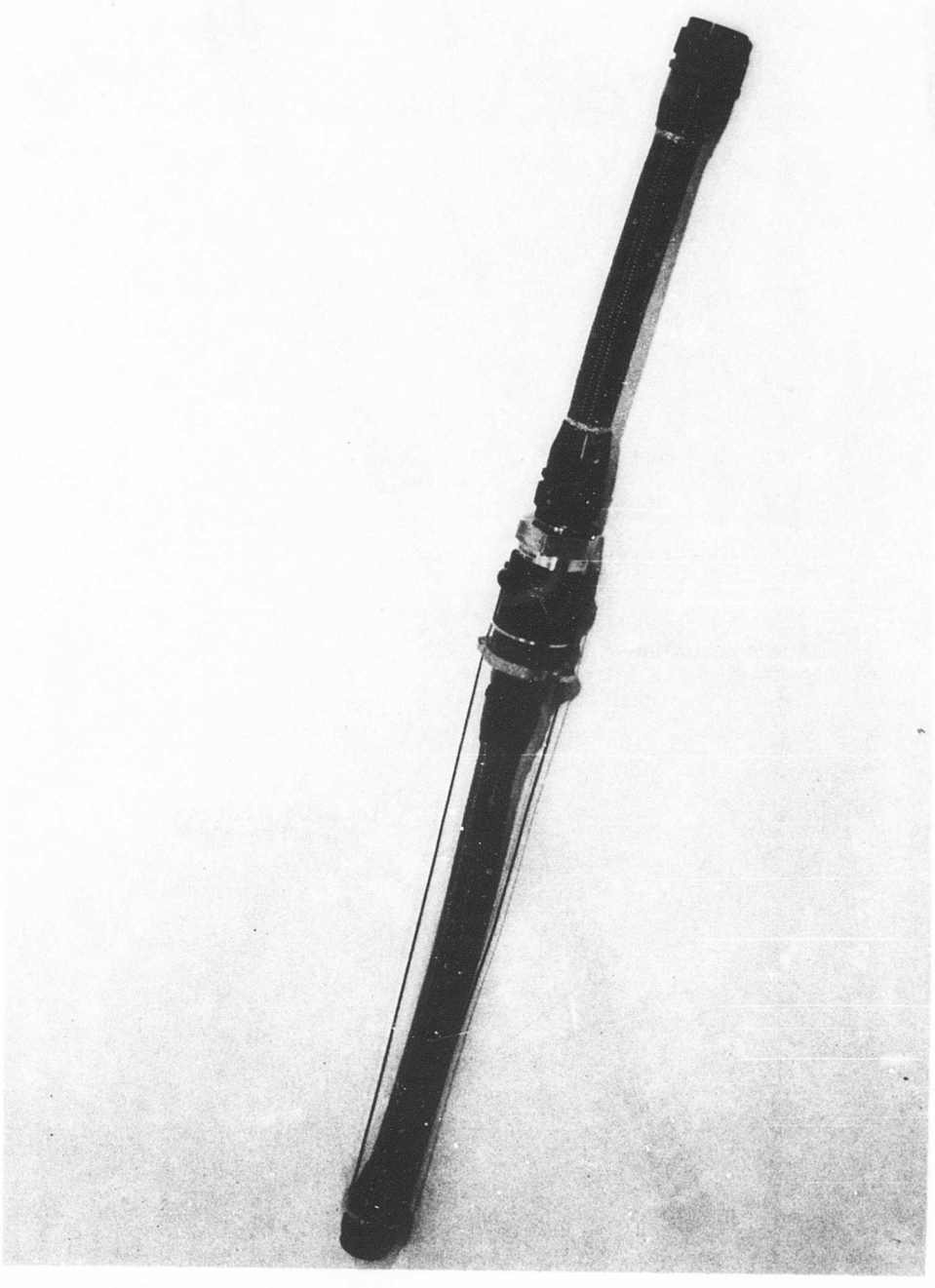

Figure 62. Self-Sealing Breakaway Fuel Line Assembly.

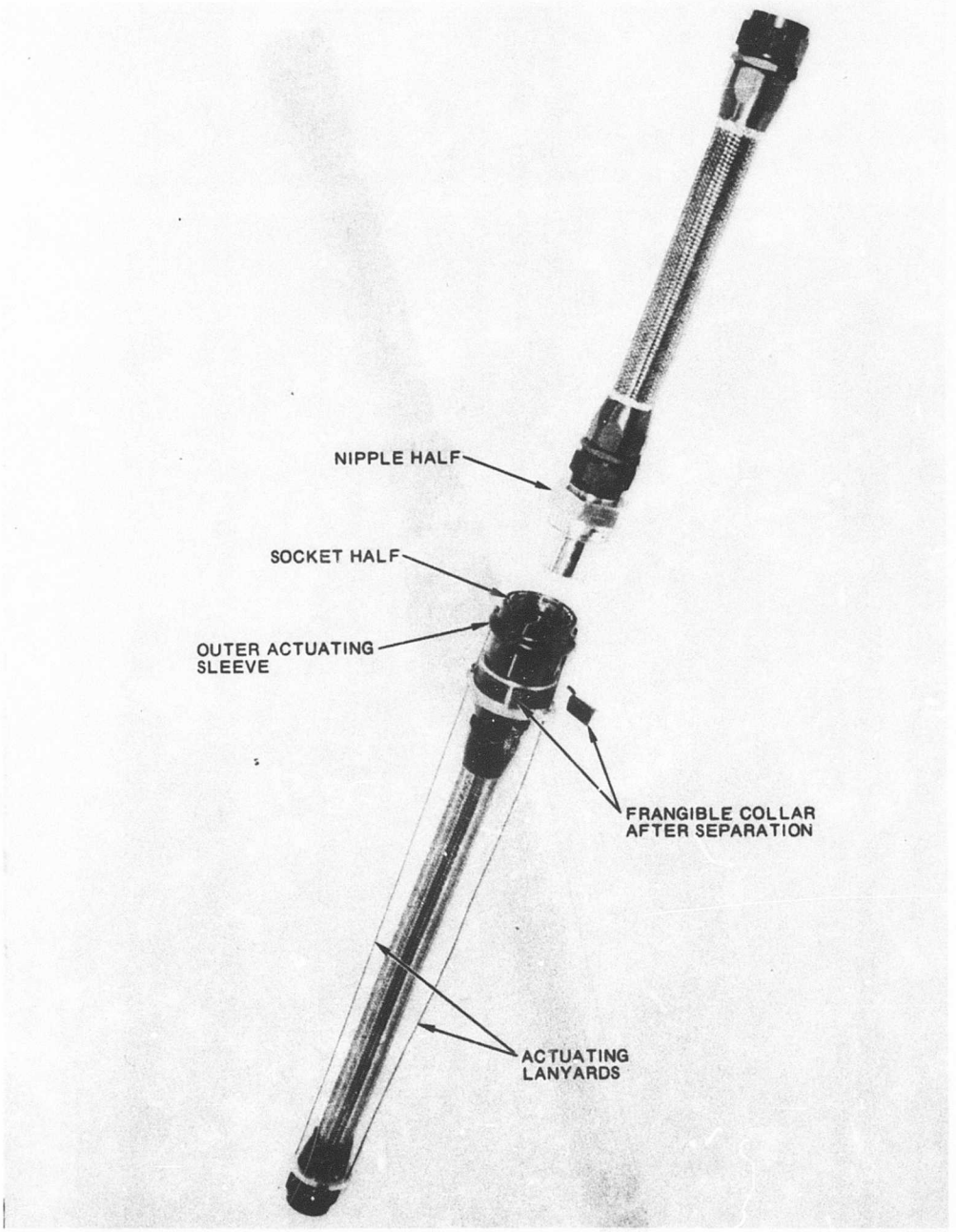

Figure 63. Self-Sealing Breakaway Fuel Line Assembly After Separation.

The two lanyards (1/16-inch steel cables) used on the test sample assembly were attached to the hose fitting for convenience, resulting in a longer cable length than would normally be required. The test results indicate an extensibility for Aeroquip 601 hose of approximately 50 percent of the original hose length. A 7- to 8-inch cable extending from the fitting and cable attachment to a suitable clamp mounted to the hose should provide the extension required to effect fitting disconnect. This clamp would have to accommodate the hose diameter reduction as tension is applied. Hose deflections that result in combined tension and side loads result in a sharp bend in the hose adjacent to the hose end fitting. Additional development is needed to provide both a cable attachment clamp and cable guide system to ensure satisfactory breakaway and closure of the fitting disconnect device under these conditions. This clamp and cable guide should be suitable for installation on standard hose assemblies.

Dynamic tests were conducted on the coupling and hose assembly to simulate the various loading modes that would be imposed on a fuel line disconnect during crash conditions. A description of these tests and the test data are included in Appendix V.

Results of the dynamic tests indicate that a high degree of protection can be afforded by a properly designed and installed breakaway fuel line system. The development of a self-sealing breakaway fuel line fitting, specifically designed for crash fire resistance, is quite feasible. Modification of existing fitting designs could result in a moderately low-cost assembly that would meet the desired functional requirements for installation in present and future aircraft fuel systems.

IMPROVED BALLISTIC PROTECTION

Potential Material Substitutions

Review of Physical Properties of Various Materials

Numerous fuel-transfer system components and in-tank components are fabricated from aluminum castings, including valve and filter housings, fuel outlet fittings, filler necks, fuel quantity-indicator heads, and fuel pump bodies. These cast fittings have two basic weaknesses: they present an explosion hazard when struck by small-caliber projectiles (Part II), and resultant damage causes massive fuel loss when hits occur below the fuel level. Consequently, it is desirable to substitute materials that will not flash or cause large fuel losses under these conditions. Although plastics do not flash, to be satisfactory substitutes for metals they must possess high tensile and flexural strength and stiffness, creep resistance, and compatibility with aircraft fuels. Table V shows representative values of various plastics, both of the thermoplastic and thermosetting groups, which are at least partially suitable for these components. The fact that this table may not include a particular type of plastic is not necessarily an indication that the plastic is unsuitable for these applications. However, the suitable types are relatively few because of their mechanical limitations and the environmental conditions to which they must be subjected.

These materials may be used in many applications in which cast aluminum is currently used, but they will not approach the strength or stiffness of metals. Fortunately, the lower specific gravity of the plastics permits a considerable increase of volume with no weight penalty, thereby at least partially compensating for the

FOR OFFICIAL USE ONLY

TABLE V

REPRESENTATIVE PHYSICAL PROPERTIES OF VARIOUS PLASTICS

Property	Nylon	Acetal	Linear Polyethyl-ene	Type I PVC	Diallyl Phthalate Fiber Glass	Phenolic Fiber Glass
Tensile strength (1000 psi)	7.1 - 12.6	8.8 - 10	3.3	8	10	10 - 12
Impact strength ft-lb/in.notch	0.6 - 1	1.2 - 1.4	2	0.6	5 - 8	1.5
Flexural modulus (10^5 psi)	1.5 - 4	3.7 - 4.4	1.2	4 - 6	10 - 18	12 - 25
Heat distortion temp (F), 66 psi	>340	>300	>160	>200	>300	>350
Fuel and oil resistance	Excellent	Excellent	Good	Excellent	Excellent	Excellent
Permeability (fuel)	Very low	Very low	Low	Low	Low	-
Creep resistance	Fair	Good	Fair	Fair	Excellent	Excellent

FOR OFFICIAL USE ONLY

sacrifice of strength and stiffness. Figure 64 shows the relative properties of plastics versus metals.

Self-Sealing Materials

Because of the tendency of most rigid materials to remain open when penetrated by a bullet, measures must be taken for sealing rigid components for military aircraft fuel systems. The use of gum sealants has been the usual approach to this problem. These materials swell on contact with the fuel, thereby sealing the wound. Several non-fuel-reactive materials have also been provided at least partially satisfactory for this purpose: (1) polyurethane elastomers, and (2) ionomer resins. Table VI shows some representative physical properties of these materials.

Material Applications

To apply design data to specific hardware items such as filler necks, fuel pump housings, or fuel probes, it is necessary to evaluate each component individually. Many current components are conducive to direct materials substitution with very limited design modification. Others, for reasons of strength or stiffness requirements, will need extensive redesign. The selection of materials for direct substitution depends on the following conditions: (1) the dependence of the component's function on its stiffness or strength; (2) the postballistic hit function of the component and its dependence on full or partial closure of the wound.

The components currently used in the four aircraft under consideration may be broken down as shown in Table VII. This table should be used as a general guideline and not as a rigid standard for materials selection. Obviously, no universal solution to the numerous design problems can be derived from these data; even though additional information will be supplied for each specific component, it too will be general in nature.

Filler Neck

The filler neck shown in Figure 13 is typical of those currently used. The inner ring is of cast aluminum with stainless steel inserts, and represents a flash (and consequent explosion) hazard. A material substitute would probably be a glass-reinforced diallyl phthalate (DAP) resin with stainless steel inserts.

Fuel Pump Housing

In some installations a portion of the fuel pump housing is outside of the tank. In such cases the exposed portions of the pump should be encased in (or made of) a

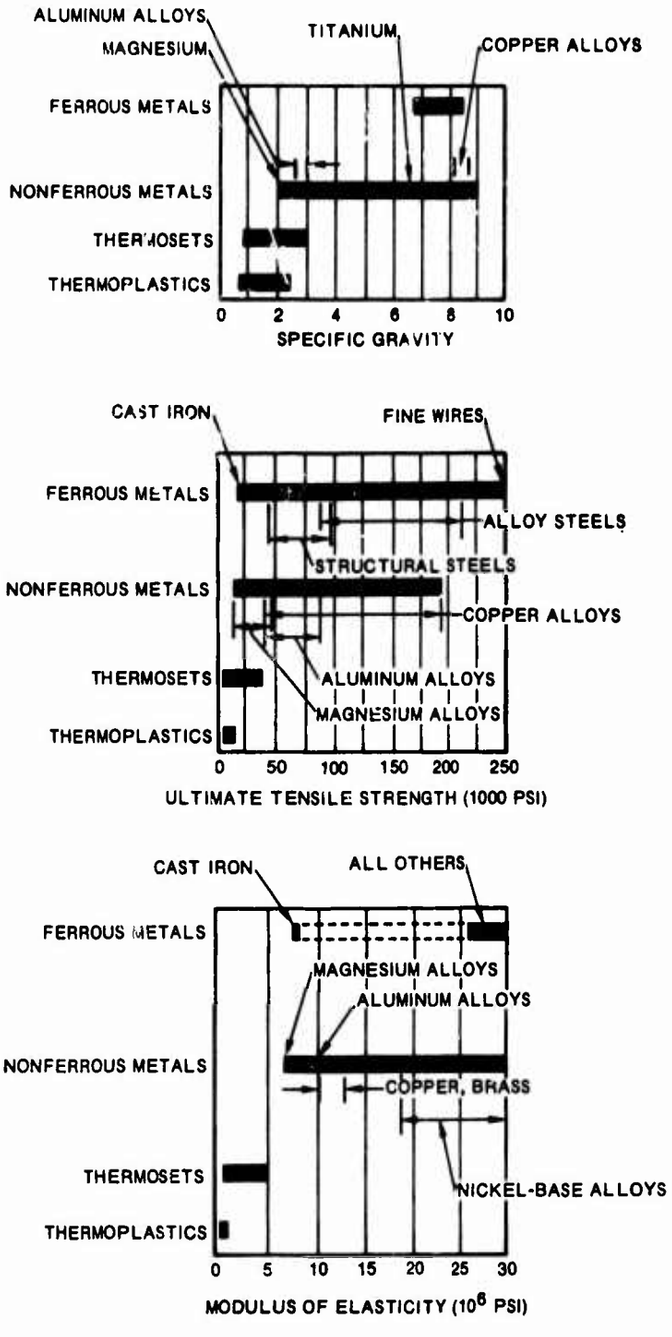

Figure 64. Properties of Plastics and Metals.

FOR OFFICIAL USE ONLY

TABLE VI

REPRESENTATIVE PHYSICAL PROPERTIES OF SELF-SEALING MATERIALS

Property	Ionomer Resin	Urethanes		
		Standard Isocyanate Content		High Isocyanate Content
		Formula A	Formula B	
Tensile, psi (20 in./min)	4000	7400	3000	5500
Elongation, %	450	450	800	200
Tear die C (20 in./min)	-	260	110	490
Stiffness, psi	22,000	~1000	<1000	5500
Hardness, shore	"D" 60	"A" 71	"A" 40	"D" 80
Bullet wound closure, small arms				
0° yaw	Very good	Very good	Very good	Fair - good
tumbled	Cored	Slightly cored	Slightly cored	Cored
Fuel resistance	Very good	Very good	Very good	Very good
Heat distortion temp (F), 66 psi	110	>200	>200	>250
Brittle temp (F)	-160	-20	-40	32

FOR OFFICIAL USE ONLY

TABLE VII

CRITICAL FACTORS OF AIRCRAFT COMPONENTS

Component	Critical Factors Stiffness	Strength	Self-Sealing
Filler neck	B	B	No
Fuel pump housing	A-B	A-B	Yes
Quantity indicator	A-C	A-C	Yes
Fuel drain	A	A-B	Yes
Filter pump	A	B	Yes
Fuel vent	A	A	No
Fuel cell interconnects	D	D	D
Fuel line connectors	A-C	B-C	Yes
Shutoff valves	A-B	A-B	Yes

Code: A = Noncritical; may be met by nylon, acetal, or PVC.
B = Semicritical; may be met with glass-reinforced plastics.
C = Highly critical; cannot be met with glass-reinforced plastics.
D = Present component not to be considered; new design mandatory.

self-sealing material. Because of the precision required in the construction of these pumps, a glass-reinforced DAP resin would appear to be a most satisfactory substitute for the aluminum housing, although metals have been used successfully for pump housings and should be investigated for aircraft use.

Quantity Indicator

The currently used quantity indicator probes create a severe crash vulnerability hazard. These rigid metal probes can puncture the fuel cell wall during crash impact, allowing extensive fuel spillage. Cast aluminum portions of the probes also pose the threat of ballistic impact flashing. The ideal way of eliminating these hazards is to dispense with the probes entirely; barring this, the reduction of their crash and ballistic vulnerability necessitates complete material substitutions and possibly extensive redesign.

To reduce ballistic flash vulnerability, the heavy metal components must be eliminated. The probe head falls into this category (Figure 65) and should be replaced by a nonflashing material. The glass-reinforced DAP would probably be best suited for this purpose because of its stiffness, impact strength, and fatigue resistance. However, because of its relatively low flexural modulus (compared to aluminum), a bulkier probe head would be necessary to cope with bending loads imposed by fuel slosh on the tube, especially if a cantilever mounting is used, as in the CH-47. For this reason, a cantilever mounting may prove to be impractical, necessitating the use of a two-point mount instead, as found in the UH-1 helicopters.

The fuel-probe body is of a relatively thin-wall construction in existing helicopters, and probably does not constitute a significant ballistic flash hazard. However, it has an excessively high resistance to column failure. Test results indicated that the compressive failure thresholds ranged from 12,000 to 20,000 pounds. Yet without thorough testing and analysis, it cannot be definitely suggested that more frangible materials be used. Although the probes should have a low threshold of column failure, they must be rigid enough to withstand fuel sloshing. Mounting the probe diagonally from a top-forward to bottom-aft position would allow the probe to reorient itself parallel to the ground during a crash with consequent hazard reduction. A more rigid material could be used if this mounting arrangement were used.

Miscellaneous External Components

Components such as fuel drains, filter sumps, valve bodies, and line connectors that are outside the tank envelope are highly vulnerable to ballistic damage. The shrouding of these components helps to reduce fuel loss from ballistic damage, but their post-hit functional capability is negligible. Many of these components consist of housing elements having no moving parts and could continue to function almost normally if materials substitutions were made. Even where moving parts and critical tolerances are involved, components could be redesigned to accommodate the use of the more rigid urethanes. Unfortunately, the ionomers cannot be considered for structural use because of their extremely limited service temperature.

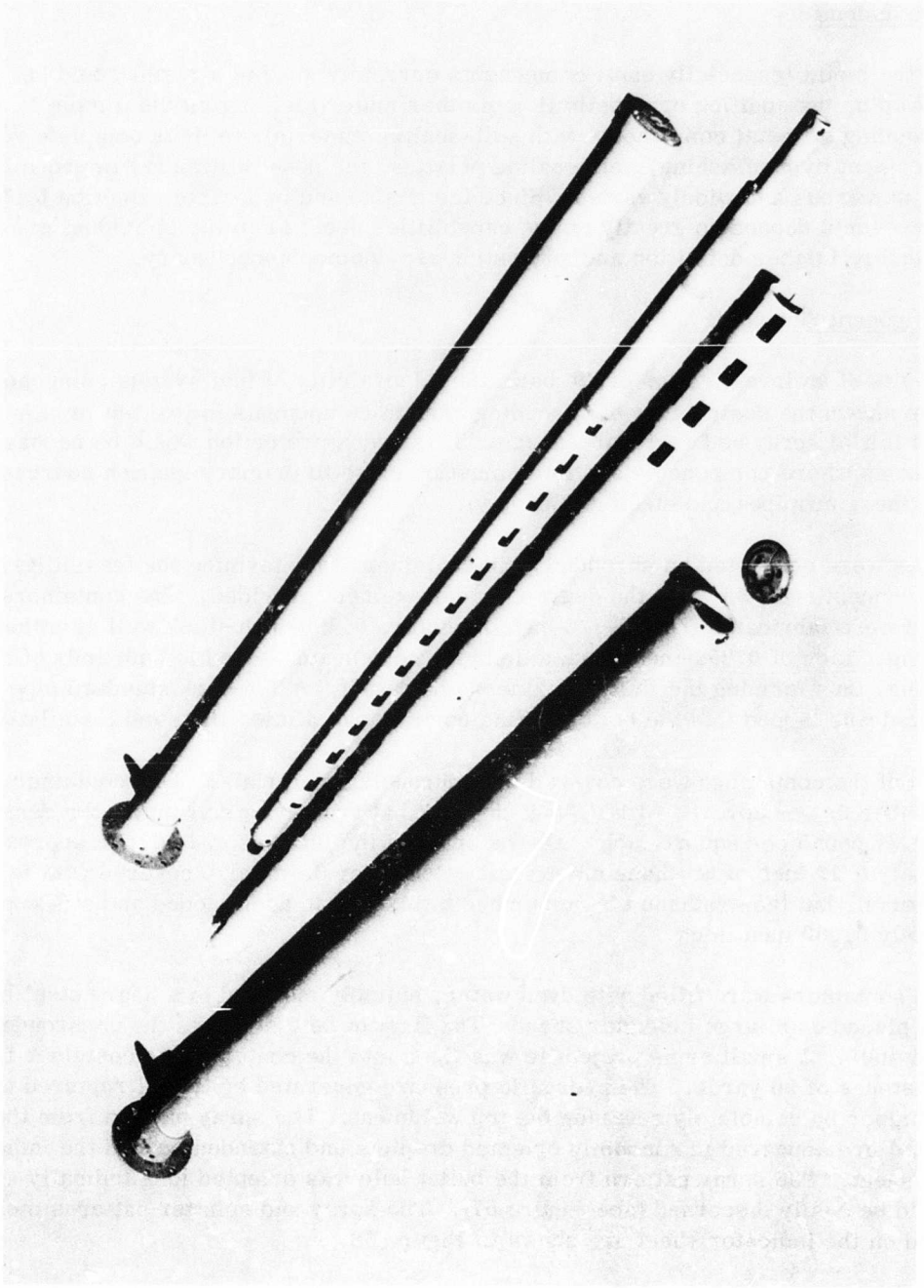

Figure 65. Quantity Indicator Probe Assembled (Right) and Disassembled (Left)

Conclusions

All the metal (especially cast) components currently used in aircraft could be improved by the addition or substitution of other materials. From the simple shrouding of metal components with self-sealing materials to their complete replacement by nonflashing, self-sealing plastics, the possibilities for improvement are numerous and widely varied. Since the design and materials selection for such components depend so greatly on the capabilities peculiar to the individual manufacturer, further definition and suggestion are deemed unnecessary.

Component Shrouding

Results of an investigation of the ballistic vulnerability of fuel system components have shown the desirability of shrouding certain components to prevent or minimize both initial spray and residual leakage. This added protection would be necessary in areas where components and lines must be close to primary ignition sources (engines, tailpipes, and electrical supply).

Tests were conducted on shrouded fluid containers to determine the feasibility of the concept and to assess the degree of improvement provided. The containers used were fabricated from 3-1/2-inch diameter, 0.190-inch-thick wall aluminum tubing. Lids of 0.250-inch-thick aluminum were seam welded to both ends of this tubing, thus forming the fluid container (Figure 66). A 1/4-inch standard pipe thread was tapped into the bottom of the container to allow filling and installation.

Two of the containers were covered with shrouding materials. One container (number 2) was covered with 0.35-inch-thick ballistic nylon felt that had a density of 0.37 pound per square inch. The exterior of the felt was coated with approximately 0.10 inch of urethane elastomer. Container 3 was also covered with felt material, but the urethane elastomer had a thixotropic agent added and was approximately 0.060 inch thick.

The containers were filled with dyed water, suitably mounted to a heavy steel base, and placed on a large indicator sheet. The first to be tested was the unshrouded container. A small arms projectile was fired into the center of the container from a distance of 30 yards. The hydraulic pressure generated by the hit ruptured the container by completely severing the top weldment. The spray pattern from the lid failure appeared in randomly oriented droplets and extended beyond the indicator sheet. The spray pattern from the bullet hole was oriented longitudinally and could be easily discerned (see Figure 67). The spray and splatter patterns measured on the indicator sheet are shown in Figure 68.

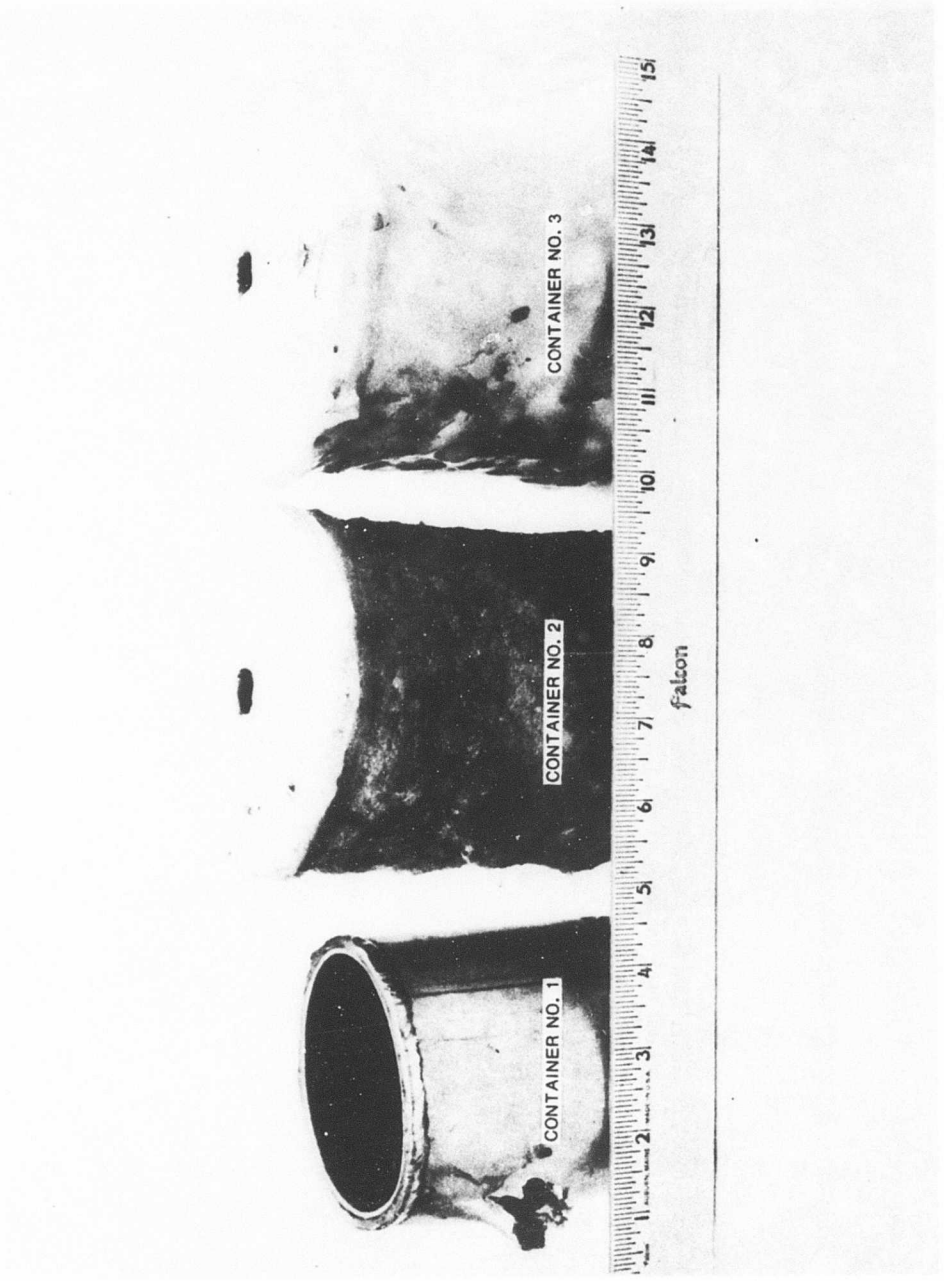

Figure 66. Containers Used in Component Shrouding Tests.

Figure 67. Spray Pattern From Unshrouded Fluid Container Number 1.

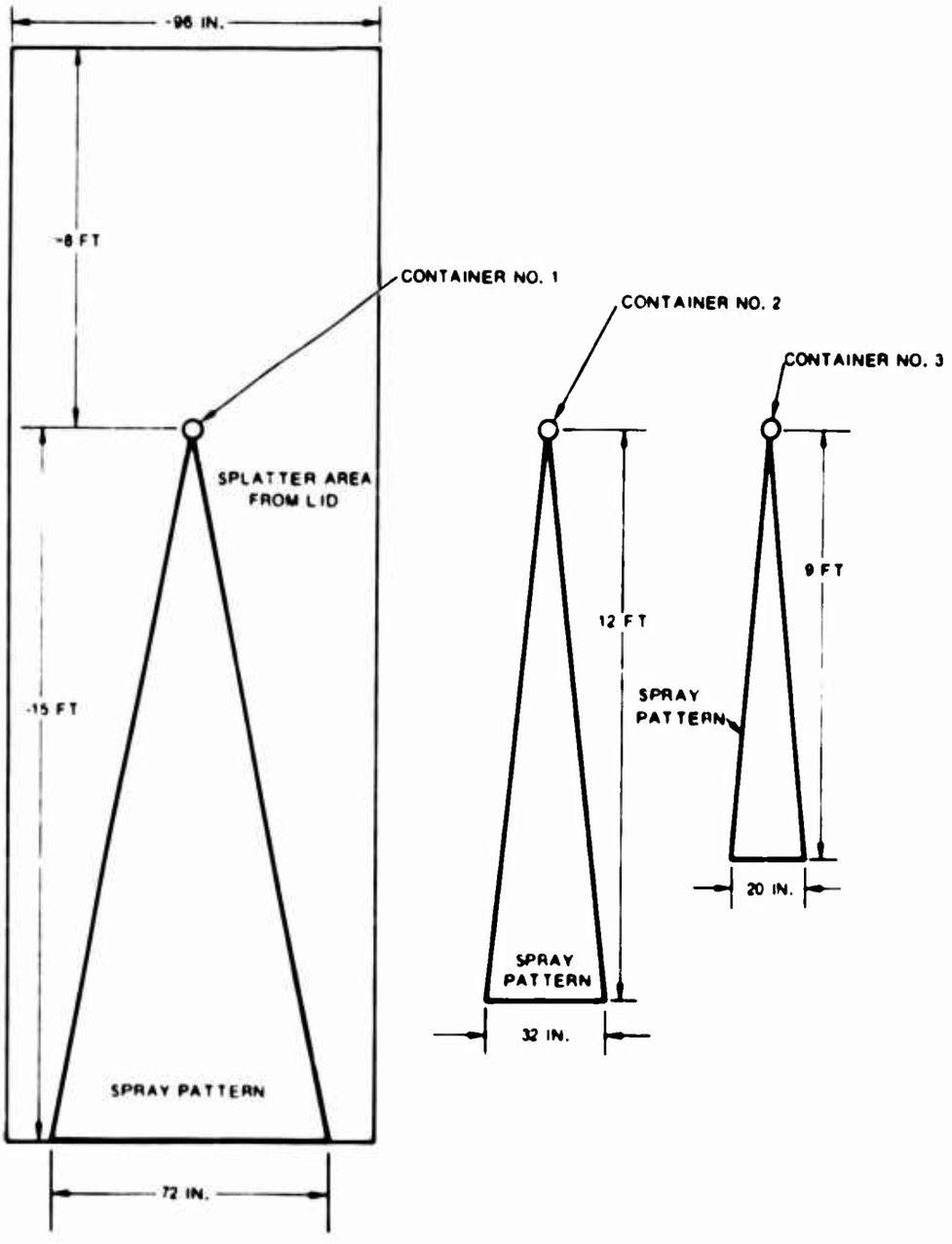

Figure 68. Spray Patterns From Ballistic Penetrations of Fluid Containers.

Container 2 was tested under the same conditions as container 1. It did not burst when struck, but the greater energy absorbed was sufficient to strip the pipe threads from the container base. The container tumbled forward, coming to rest midway down the indicator sheet (Figure 69). Again, the spray pattern erupting from the ballistic penetration was readily discernible from the leakage of the tumbling container. The measured spray pattern from this test is illustrated in Figure 68. Splatter would not have resulted in this test if the container had not tumbled; for this reason it is not included in this figure.

Container 3 was tested under the same conditions as the other two. This container also absorbed sufficient energy to strip the mounting threads and it also tumbled free following impact. As seen in Figure 70, the outer elastomer closed about the projectile, considerably reducing the spray pattern and quantity. The spray that escaped with the bullet was deflected by the shrouding approximately 30 degrees to the left of the projectile path.

These tests were necessarily limited and were devised to quickly assess the feasibility and potential of the shrouding concept. On the basis of the test results, the following conclusions were drawn: (1) shrouding of fuel system pumps, valves, lines, and other components will significantly reduce not only the resultant spray but also the fragmentation following ballistic penetration; (2) greater spacing between the component and its shroud would probably reduce the spray to a negligible quantity; and (3) though satisfactory as a spray reducer it is doubtful that a secondary shroud would greatly reduce continuous fuel loss from a perforated component. Such loss reduction would be dependent on primary component sealing or switching to a redundant system.

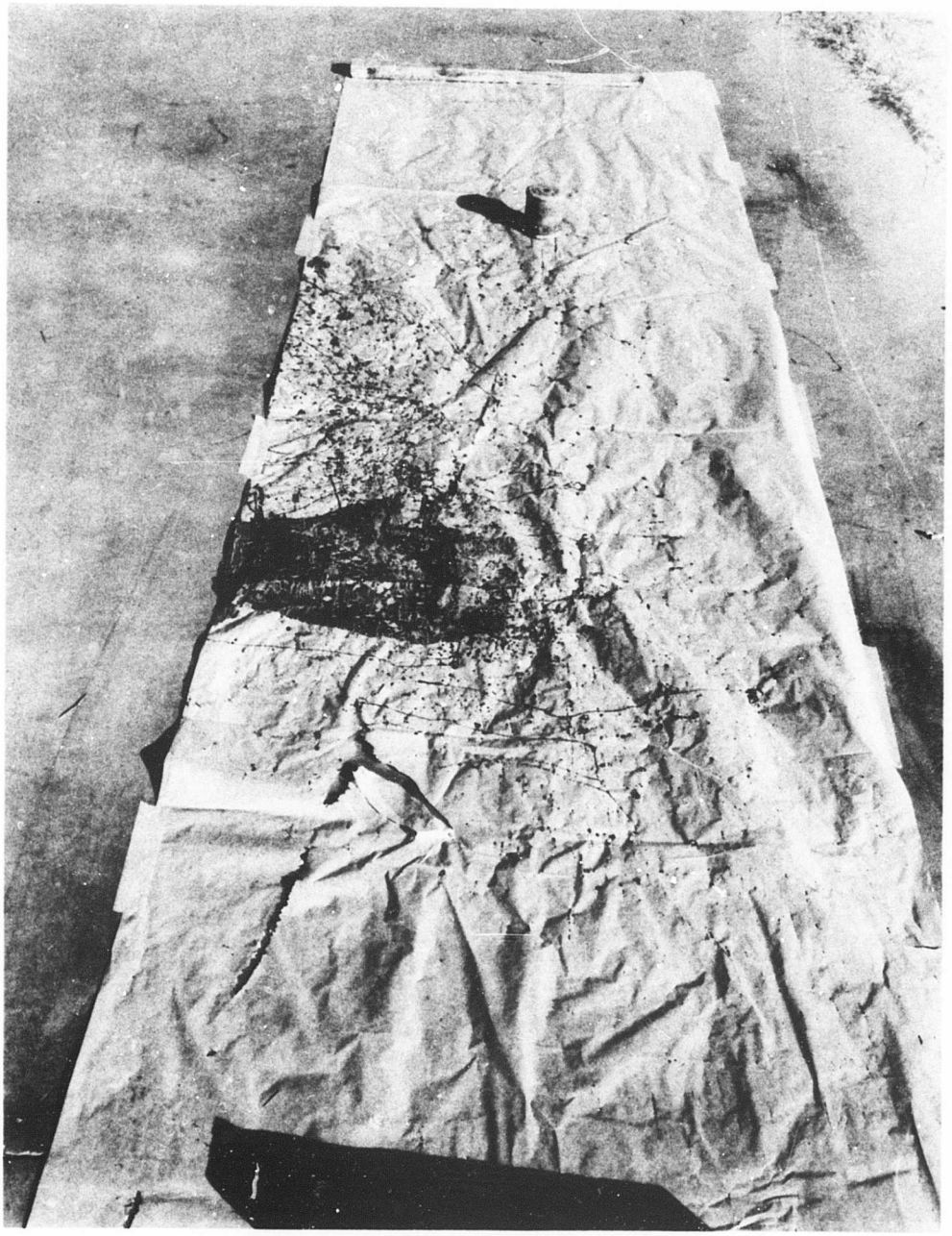

Figure 69. Spray Pattern from Shrouded Fluid Container Number 2.

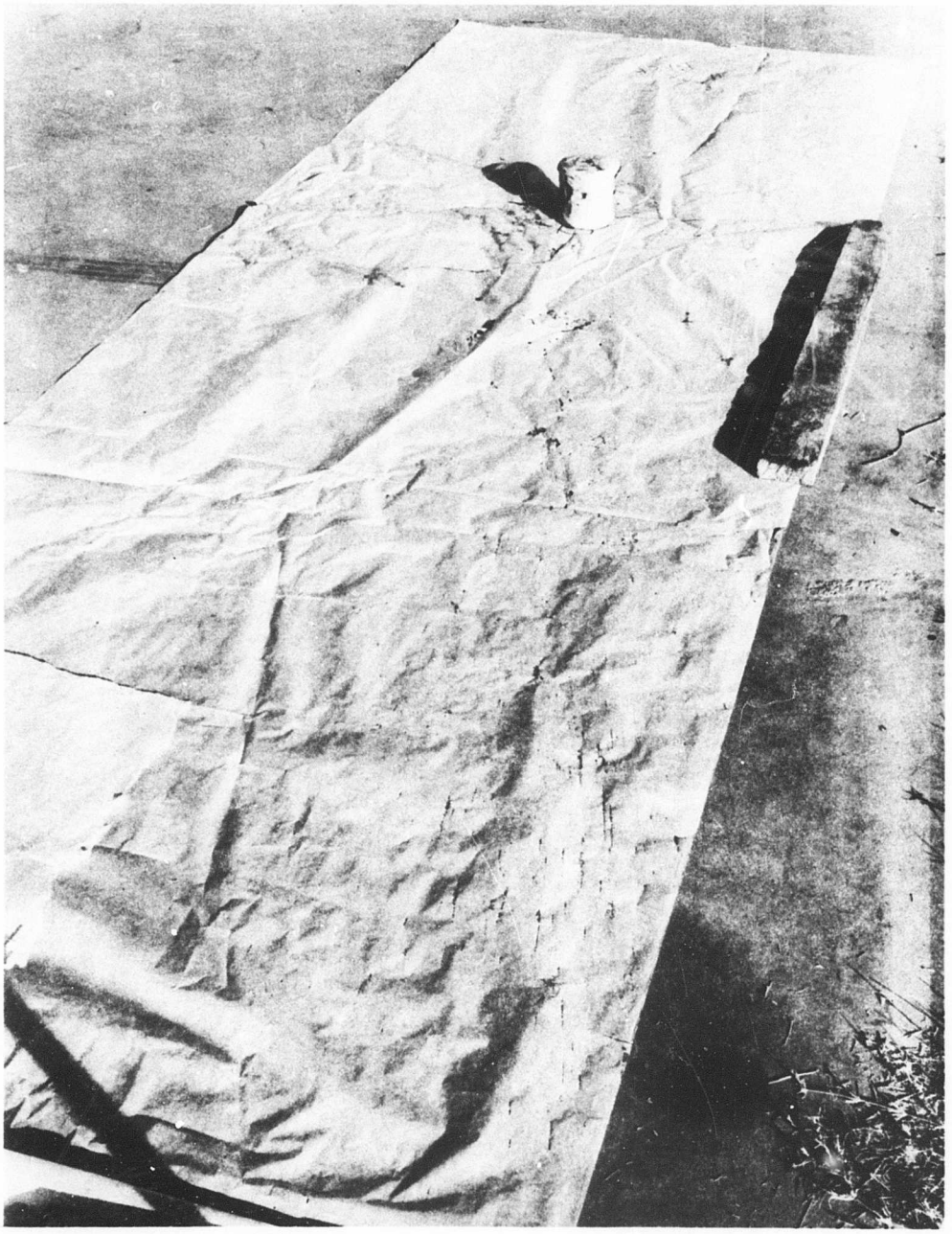

Figure 70. Spray Pattern from Shrouded Fluid Container Number 3.

PART V

STUDY OF SELF-CLOSING FUEL LINES

GENERAL

An important aspect of the work performed during this program was the design, development, and testing of a self-closing fuel line. This effort was conducted to reduce the crash vulnerability caused by the low extensibility of lines currently used in aircraft. The objective of this effort was to produce a design for a line that would elongate, close, and seal when subjected to the gross structural displacements which often occur in a crash.

DESIGN OBJECTIVES

The self-closing fuel line design objectives differ from those of conventional flexible fuel lines, as discussed in the following subsection.

Elongation

The self-closing fuel line must elongate to at least 5 times (preferably 10 times) its original length prior to failure. Rapidly applied tensile and flexural loads must elongate the fuel line until it reaches its maximum elongation, at which time it will be fully closed and locked so that no fuel loss can occur.

Point of Failure

The line must be designed to fail at a point other than at the fitting.

Operational Pressure

The line must withstand normal operational pressures of 30 pounds per square inch and a dynamic closure pressure of 100 pounds per square inch. After line severance, the line must remain closed at 30 pounds per square inch.

End Fittings

End fittings must be designed so that the line will not be cut by the fitting when subjected to maximum elongation. The fitting design must also ensure that the line will not pull loose from the fitting at maximum elongation. It must surpass

the ultimate strength of the line in all failure modes and must be adaptable to standard fuel fittings.

Fuel Compatibility

The fuel line and its components must be compatible with aircraft fuels and solvents, and degradation from environmental effects must not occur after long-term usage.

Mechanical Stability

The fuel line must be dimensionally stable, abrasion resistant, and kink proof, and must have adequate fatigue resistance when subjected to vibrations encountered during normal aircraft operations, as well as during fuel line installation.

Locking Devices

The fuel line must incorporate locking or constricting devices. They must be self-closing or have the capability of being closed by the elongating line. The locking devices must not fail because of fatigue when subjected to long-term vibrational environments.

DESIGN CONCEPTS

Commercially available materials were screened to determine the properties most suited to and compatible for use as the inner fuel-carrying liner; initial screening was performed to determine which of the materials were available in tube form. The compilation of data on the best materials found is shown in Table VIII. Several inner-liner concepts were tested during the program. As the design concepts evolved, the materials requirement for the inner liner also changed. The design concepts and the liner materials related to each are presented in the order in which they were developed.

Accordian Liner (Crinkled Tube, Configuration A)

The first inner-liner design concept tested was that of using a thin-wall, smooth inner tube compressed upon itself over a suitable mandrel (Figure 71). The resultant crinkled tube, when built into a complete prototype fuel line, would extend up to 10 times its length before rupturing. Materials most suitable for processing this configuration were determined from those in Table VIII.

Cellulose acetate tubing was selected as an expedient in constructing the prototype test samples. Because of the irregular inner surface resulting from the crinkling

FOR OFFICIAL USE ONLY

TABLE VIII

PROPERTIES OF MATERIALS FOR SELF-CLOSING LINES

Type of Plastic Base	Tensile Strength (psi)	Elongation (%)	Propagating Tearing Strength (gm)	Initial Tearing Strength (lb/in.)	Folding Endurance (cycles)	Resistance*							Resistance	
						Strong Acids	Alkalies	Grease, Oil	Organic Solvents	Water	Humidity	Sunlight	Heat (°F)	Cold (°F)
Fedfluorocarbon	2500 - 3000	300	125	600	4000	E	E	E	E	E	E	E	400 - 525	-425
Cellulose Propionate	4000 - 5000	60 - 80	100	900	20 - 80	P	P	G	P	G	G	G	150 - 200	-50
Polyethylene (LD)	1250 - 2500	200 - 700	100 - 300	65 - 575	Very high	E	E	P	G	E	E	G	180 - 200	-70
Polyethylene (HD)	2400 - 6100	10 - 650	15 - 30	-	Very high	E	E	G	G	E	E	G	250	-50
PE terephthalate	25,000 - 30,000	70 - 120	12 - 15	1000 - 1300	14000	G	G	E	E	E	E	F	300	-75
Polytetrafluoro-ethylene	1500 - 4000	100 - 350	10 - 100	-	-	E	E	E	E	E	E	E	500	-130
Vinyl-Chloride Acetate Copolymers Nonrigid	1400	150 - 500	30 - 1400	-	-	G	G	G	P	E	E	G	150 - 200	G
Ionomer	5000	250 - 450	30	-	Very high	G	E	G	G	E	E	G	140 - 160	-110
Vinyl Nitrile Rubber	2500 - 4000	250 - 500	200 - 960	-	Very high	G	G	E	G	E	E	F	200	32
Polyurethane	5500	575	-	350	-								170	-100
Polyurethane	6000	475	-	500	-								250	-100
Cellulose Acetate	11,000	15 - 70	4 - 10	55 - 415	500 - 2000	F	P	E	P	G	G	E	150 - 200	-15

* Legend: E - Excellent; G - Good; F - Fair; P - Poor.

FOR OFFICIAL USE ONLY

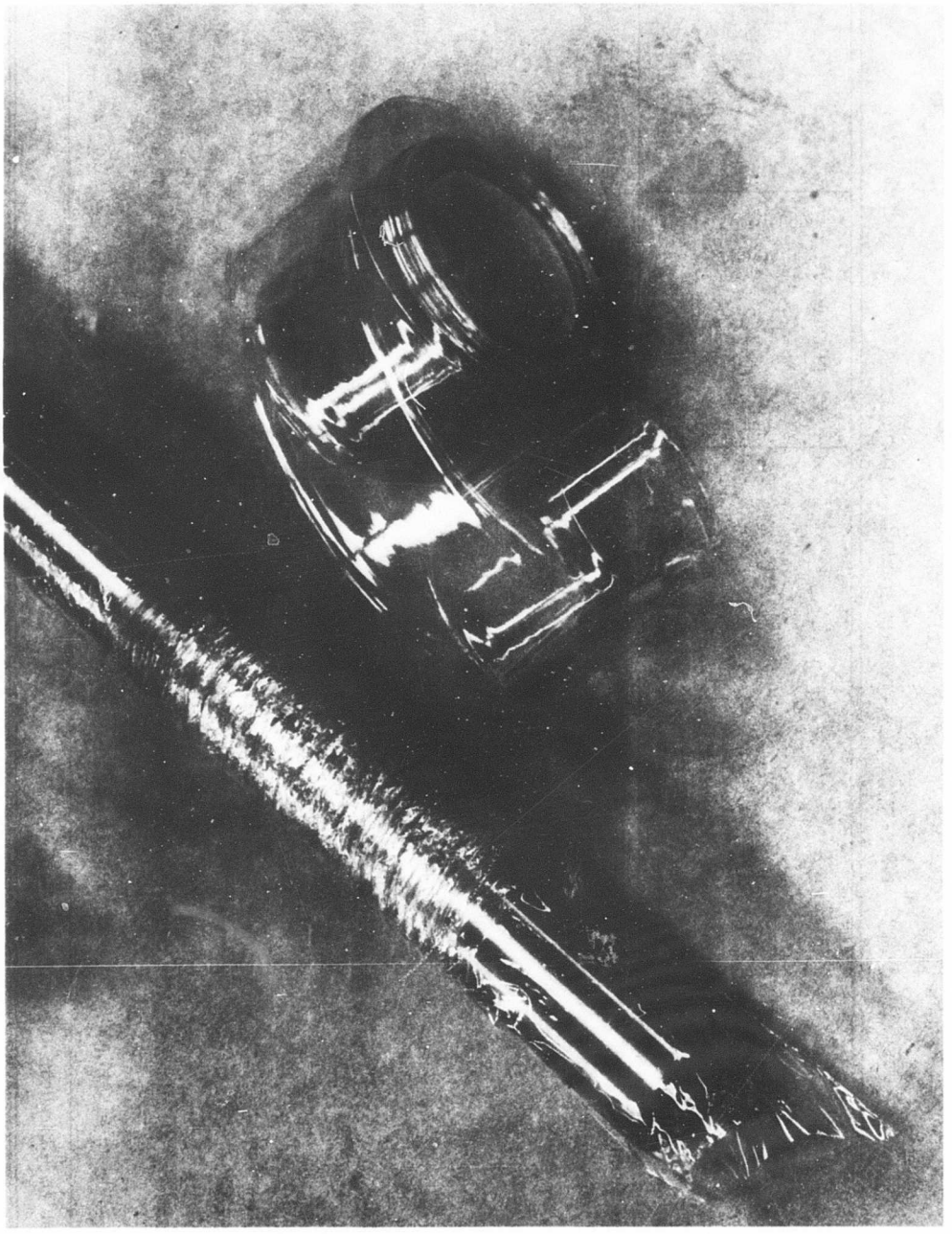

Figure 71. Self-Closing Fuel Line, Configuration A.

process, a smooth inner tube (also cellulose acetate) was applied over the mandrel. This smooth tube thus became the actual fuel-carrying medium with the crinkled expandable liner formed over it.

As permeability test results became available, it was apparent that a coating would be desirable over the smooth cellulose acetate tubing to reduce permeability (Table IX). The 0.001-inch-thick acetate tubing was coated by both dip and spray processes, adding from 0.001- to 0.0015-inch thickness of nylon. The crinkled acetate expandable liner was coated with approximately 0.005 inch of urethane to give the liner added strength.

Prototype Line Fabrication (Configuration B)

Several prototype fuel line test samples were fabricated using this coated tubing. The line was made with an outer-wire helix consisting of two independent layers wrapped contradirectionally. The helix was made by coiling 14 small-diameter ductile wires about the fuel line while maintaining a 5- to 10-degree helix angle. Seven wires were coiled left-handed and seven right-handed, forming a sheath over the fuel line. The wire ends passed through the end fitting and through small, radially oriented holes. The wire ends were swaged securely to the end connectors.

A sheath formed from urethane-impregnated woven glass yarns was placed between the crinkled expendable liner and the wire helix to provide longitudinal stability during normal line operation. The construction details of these lines are shown in Figure 72 The locking device had not been incorporated on these initial models.

Prototype Line Tests (Configuration B)

Tests performed on the prototype samples consisted of applying a tensile load to the line using a "snatch" method for dynamic closure and an Instron tensile-testing instrument for low-speed closure. The elongation of the lines showed some inherent weaknesses in the crinkled inner-liner design and in the helical sheath. Radial contraction of the helically wound constrictor sheath progressed as the line extended. During this extension,the helix separated randomly along its entire length, allowing the inner sheath to balloon through the openings (Figure 73). Failure of the crinkled sheath was caused by the combination of excessive internal pressure and the scissoring action of the constricting wire helix. The obvious weakness lay in the inability of the helix to maintain a uniform restraint around the crinkled sheath, although there was also strong evidence that the crinkled sheath itself was not entirely satisfactory. Consequently, efforts were diverted to effecting changes in the inner liner and the external helix.

TABLE IX

PERMEABILITY TESTS OF SELF-CLOSING FUEL LINE MATERIALS

Materials	MIL-J-5624 Jet Fuel, Grade JP-4	MIL-J-5624 Jet Fuel, Grade JP-5	MIL-G-5572 Aviation Gasoline	MIL-S-3136 Type III Test Fluid
Nylon film (0.002 in.)	0.008	0.008	0.008	0.008 - 0.010
Polyurethane elastomer	-	-	0.105	-
Polyurethane elastomer with film barrier before folding	0.008	0.007	0.007	0.007 - 0.009
Polyurethane elastomer with film barrier after folding	0.008	0.007	0.009	0.008- 0.009
Cellulose acetate tubing (0.001 in.)	0.060	-	-	0.016
Nylon tubing (0.007 in.)	0.010	-	-	0.016
High-density polyethylene (0.08 in.)	0.274	-	-	0.277
Elastomer SF-2	-	-	-	0.010

Note:
1. Average diffusion rates are in fluid ounces per square foot per 24 hours.
2. Accept permeability shall be less than 0.025 fluid ounce per square foot per 24 hours.

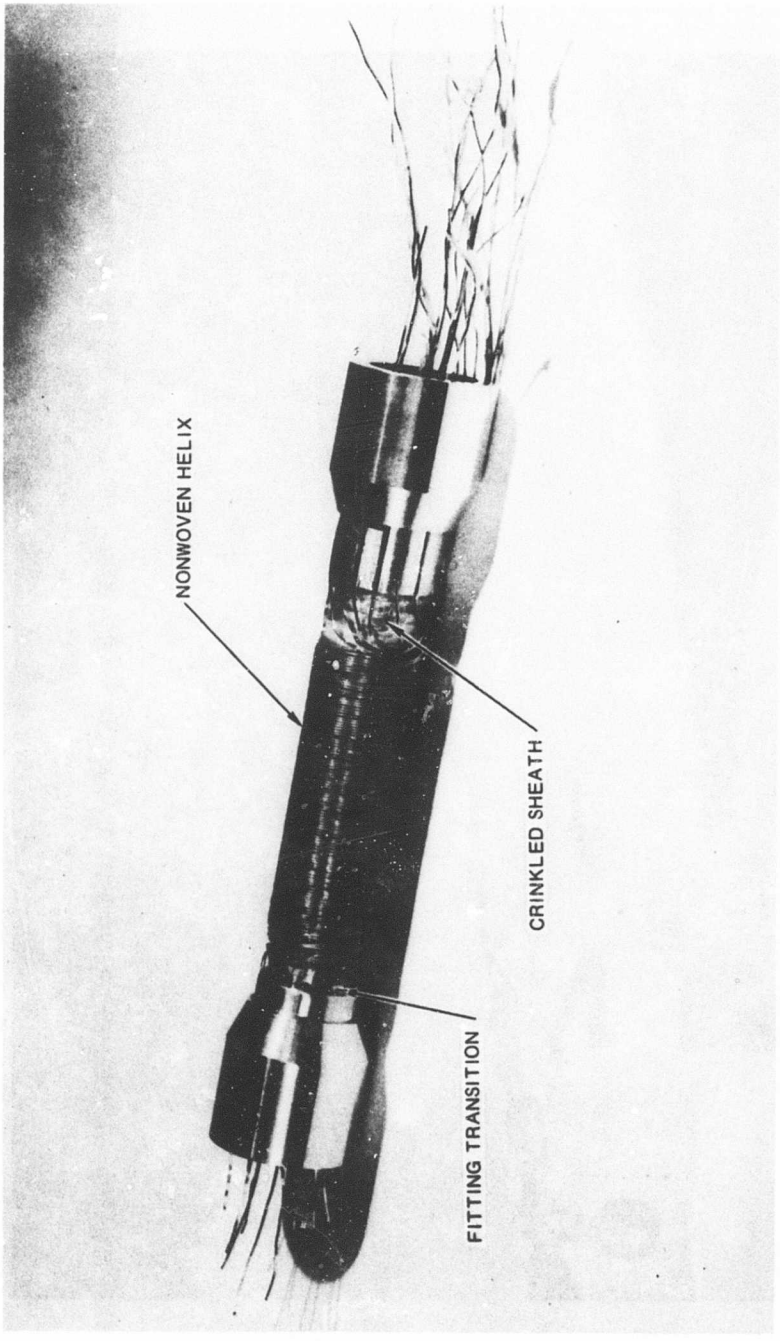

Figure 72. Self-Closing Fuel Line, Configuration B.

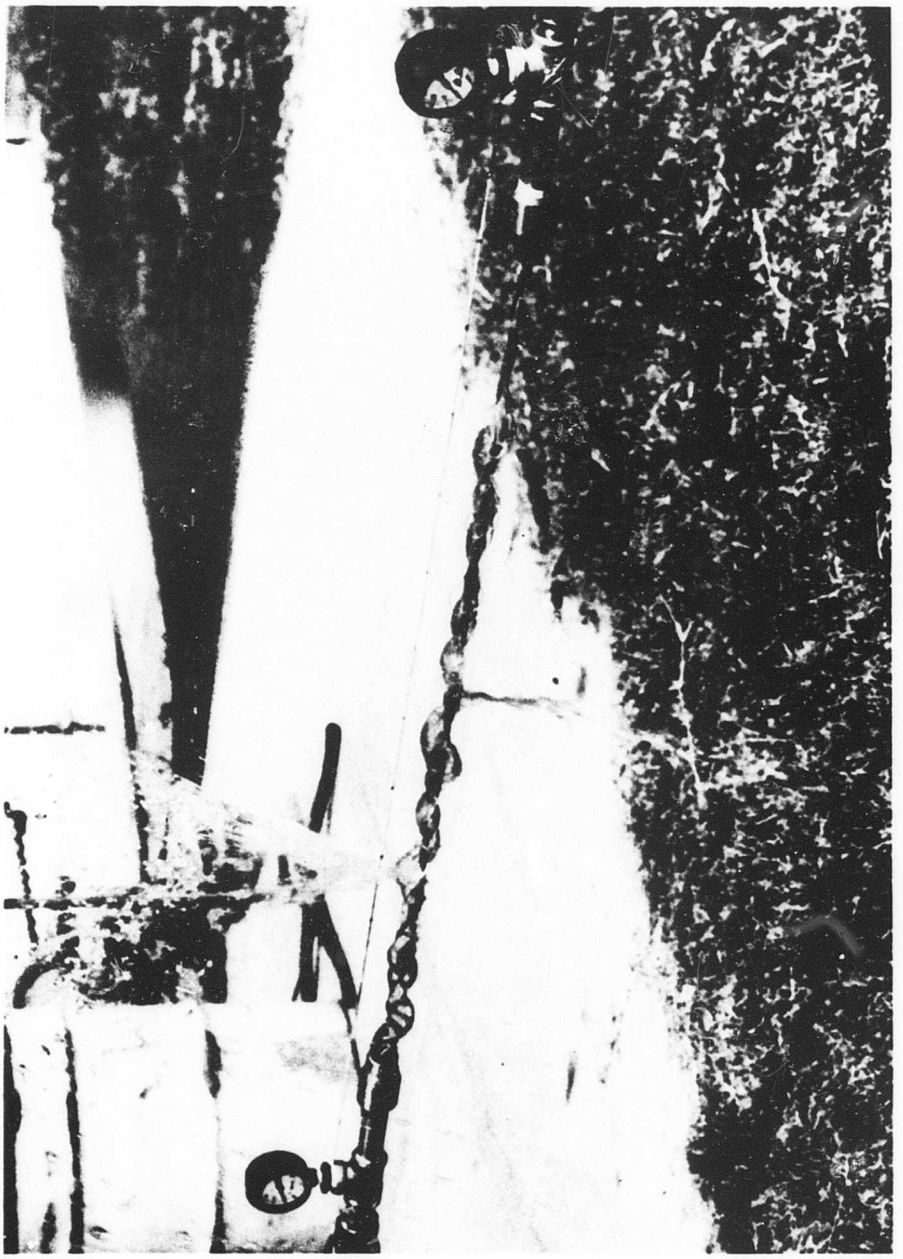

Figure 73. Failure of Configuration B Self-Closing Fuel Line.

Woven Helical Sheath (Configuration C)

This sheath (Figure 74) consisted of a helically interwoven wire mesh which envelopes the fuel line, providing both a longitudinal extension and a radial contraction capability. The woven sheath girdles the fuel line during all conditions of extension. The longitudinal elongation of the wire mesh is dependent on the closed sheath diameter, type of weave, number of strands per weave, and the wire diameter. The minimum helix angle at fully closed length is obtained by the following expression:

$$\tan \theta = \frac{d N_w N_s + 2d(N_s)}{\pi D} \qquad (1)$$

where d = Wire diameter (in.)

D = Closed diameter of sheath (in.)

N_w = No. of wires per strand

N_s = No. of strands per rev (in.), one direction

θ = Helix angle (deg.)

By varying the number of wires per strand, N_w, the elongation can be increased considerably with an accompanying reduction in cross-sectional area. See Table X for a representative example.

The tensile strength of the wire mesh sheath can be approximated by the following expression, which holds for large values of θ, the helix angle.

$$P = \frac{\sigma \pi d^2 N_w N_s}{4K} \text{ lb} \qquad (2)$$

where P = Ultimate load (lb)

σ = Ultimate tensile strength (psi)

K = End-fitting factor (dependent on end-fitting configuration; must be determined by testing).

Fabrication of Woven Helical Fuel Lines (Configuration C)

Prototype lines were fabricated with a 5 x 5 (filaments per strand), 0.9-inch diameter helix. This construction was chosen because of its reduced area of

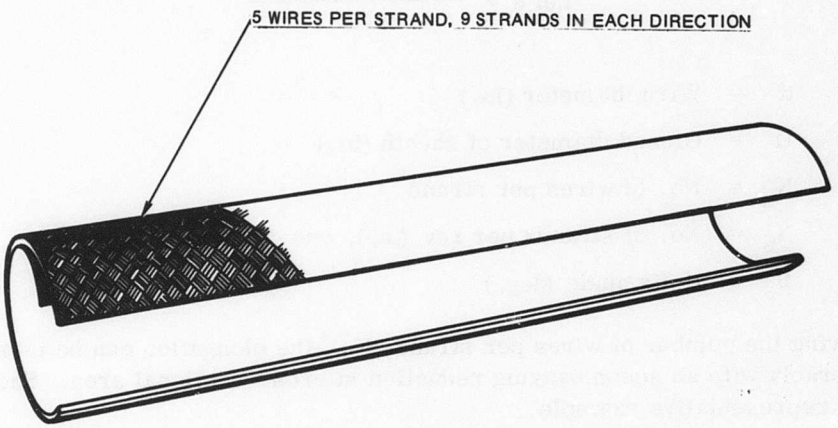

Figure 74. Wire Mesh Sheath Configuration.

TABLE X

WIRE MESH SHEATH DATA

Weave Type	Single Wire Dia (in.)	Elongation*	Dia Reduction*	Wire Hose Max Dia (in.)	Length of Square Opening** (in.)	Area of Opening (in.)
9 strands, 5 x 5*** single weave	0.008	5.09 to 1	4.25 to 1	0.90	0.12	0.0144
9 strands, 4 x 4 single weave	0.008	6.82 to 1	8.26 to 1	0.90	0.15	0.0225
9 strands, 3 x 3 single weave	0.008	9.5 to 1	9.03 to 1	0.90	0.16	0.0256

* 5- to 10-pound tensile load (estimated).

** Length of opening measured at 45-degree helix angle.

*** Filaments per strand.

maximum exposure and because of its availability. The disadvantage of using this helix was that its elongation was only 5.1 to 1, barely above the minimum specified as a design objective. This is not a severe penalty to the over-all design plan, however, since the substitution of a 3 x 3 strand helix could render an ultimate elongation ratio of almost 10 to 1. The first of the samples employing the woven helix was made with a crinkled sheath fuel barrier (Configuration CA) as described in the earlier tests. No locking device was used.

Test Procedures and Results

Because of the need to observe the deformation mode of the line, low-speed tests (2 inches per minute crosshead speed) were conducted on the Instron tester. The specimen was mounted in the pressure-controlled fixture shown in Figure 75. The line was pressurized to 20 psi and deformation was begun.

At approximately 200 percent elongation, the crinkled sheath began to bunch in some portions of the line and to overstress in others. The portions of the sheath which were bunched extruded through the woven helix during the phase of maximum helix opening and, as in the preceding tests, were cut by the scissoring action of the helix. Severe leakage ensued, and the test was terminated. Consequently, the crinkled inner sheath was discarded, and a smooth, high-elongation sheath was used in its place.

Elastomeric Inner Linings (Configuration D)

An investigation of elastomeric polymers was initiated as a result of the unsatisfactory experiences with the crinkled linings. Several promising formulations were considered usable as highly extensible inner linings which could be incorporated into the woven helix outer sheath. The elongation of these polymers ranged from 500 to 800 percent. Although of limited extensibility, they would be satisfactory for the 5.1 to 1 expansion helix. The physical values of the formulation selected for this application are given in Table XI.

TABLE XI

PHYSICAL PROPERTY VALUES OF ELASTOMERIC INNER-SHEATH MATERIAL

Tensile (psi)*	5000
Tear (psi)*	450
Elongation (%)*	800
Shore "A"	60

*Tests run at 20 in./min at standard conditions.

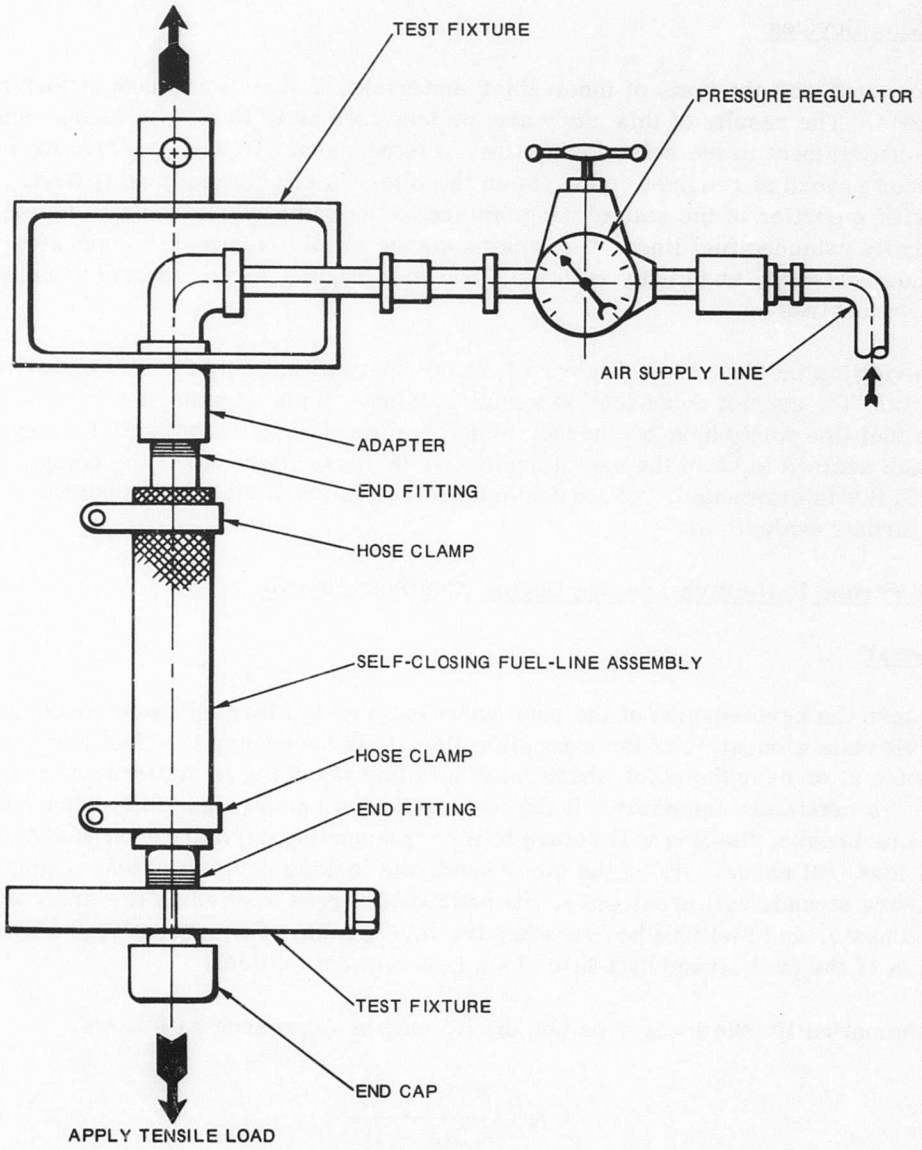

Figure 75. Self-Closing Line Test Setup.

In addition to the low-speed tensile values, high-velocity tests were conducted at onset rates up to 80,000 inches per minute. The results of these tests showed no apparent reduction of elasticity as the rate of onset increased.

Locking Devices

Concurrent with the tests of inner-liner materials, a study was made of locking devices. The results of this study are summarized as follows: to ensure complete fuel containment in the self-closing line, it is necessary to have positive locking devices spaced at required intervals on the line. In effect, the locking devices provide a portion of the self-closing feature to the radially contracted and longitudinally extended fuel line. The locking device should be simple to operate, fatigue resistant, and highly reliable. Shown in Figure 76 are several simple locking devices.

In reviewing the devices in Figure 76, it is apparent that only two of the devices, "e" and "f", are not dependent on spring loading. Since a spring-loaded device on a fuel line would have a tendency to deform the line, the most satisfactory approach seemed to be in the use of nonloaded devices. Because of the complexity of "f", it was eliminated; "e", a dual-strand half-hitch device, was chosen for further evaluation.

Dual-Strand Half-Hitch Locking Device (Configuration E)

General

Because the performance of the continuous longitudinal locking device depends on the ultimate elongation of the extensible line, it is necessary to effect complete closure at or near the point where minimum line diameter is attained; that is, near its maximum extension. If the locking device remains partially open when the line breaks, the line will return to a corresponding partially open position and fuel loss will ensue. If, on the other hand, the locking device tightens prematurely, the wire strands will break under the additional stress applied as the line continues to elongate, and fuel will be lost when the line breaks. Consequently, the node length of the dual-strand half-hitch lock is somewhat critical.

Mathematically, the ideal node length, N, may be expressed as follows:

$$N = \frac{\pi(d_1 - d_2)}{2(e - 1)} \qquad (3)$$

(a) THREE LEAF SPRINGS ARRANGED TO PROVIDE A SINGLE LOCK.

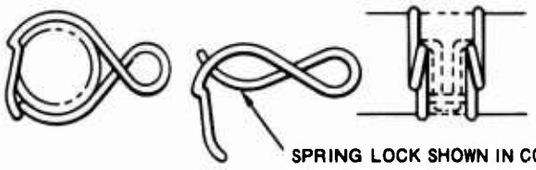

(b) SELF-LOCKING, SELF-STABILIZING LOCKING DEVICE.

SPRING LOCK SHOWN IN COMPRESSED POSITION.

(c) TWO FLAT SPRINGS CONNECTED TOGETHER BENDING TO CLOSE WITH A REDUCTION IN FUEL-LINE DIAMETER.

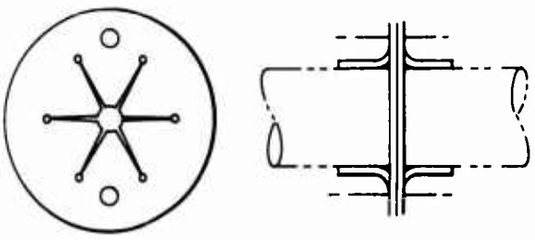

(d) SPRING-LOADED LOCK WHICH CONSTRICTS THE OPENING AS THE FUEL LINE EXTENDS AND CONTRACTS. RATCHETED EDGE PREVENTS LOCK FROM OPENING ONCE IT HAS CLOSED.

(e) CONTINUOUS WIRE FORMED INTO LOOPS WHICH CONTRACT AS THE LINE EXTENDS LONGITUDINALLY. THE WIRE SHOULD BE DUCTILE TO REMAIN LOCKED ONCE FULLY STRETCHED OUT.

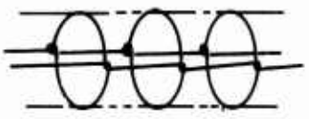

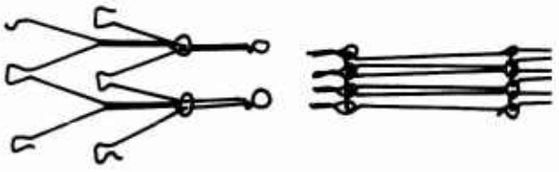

(f) CONSTRICTOR IN OPEN CONDITION
CONSTRICTOR IN CLOSED CONDITION

Figure 76. Self-Closing Line-Locking Devices.

where: d_1 = Line diameter before elongation

d_2 = Line diameter at closure (determined experimentally)

e = Elongation of helix sheath.

For a 0.93-inch-diameter sheath with an elongation of 5.121, the above equation provides a node length of 0.26 inch. However, because of the variables introduced by the slackness and looping of the half-hitch lock, a mathematical approach proved unsatisfactory and an experimental method was used. Locks were formed over the 0.90-inch-diameter helix and tested by the simple expedient of hand pulling. Samples having node lengths of 7/16 inch performed best, while the 3/8-inch-diameter sample was too loose and the 1/2-inch-diameter sample closed prematurely.

Fabrication of Prototypes (Configuration CDE)

Prototype lines were designed and fabricated to include the elastomeric inner lining (D), the woven 5 x 5 helix (C), and a stabilizer sheath and the dual strand half-hitch locking sheath (E).

Configuration CDE-1

This prototype line is shown in Figure 77. The lines were 6 inches long and were mounted on fittings inserted 2 inches into each end of the test line. The fitting ends were tapered to reduce the radial loading of the line, thus permitting better reorientation of the helix and avoiding any cutting of the elastomeric lining.

Test Procedure (Configuration CDE-1)

Specimens were tested under the same conditions as those in the earlier static test. The line was pressurized to 20 pounds per square inch; rate of onset was 2 inches per minute.

The line extended normally and the outer-sheer-nylon longitudinal stabilizer failed under an applied load of 260 pounds. The load decreased to 100 pounds as the fuel line began extending in an expected manner, contracting radially in the process. At an approximate tensile load of 250 pounds, the constrictor loops worked their way off the end fitting in a uniform manner while contracting radially. No air leaks were observed at this point. The line continued its longitudinal extension and radial contraction with the tensile load oscillating between 200 and 250 pounds. The line failed to contain the pressurized air at about 200 percent extension.

This failure of the inner lining was caused by the cutting action of the helix and the end fitting as the helix extended. Further extension caused the wire mesh

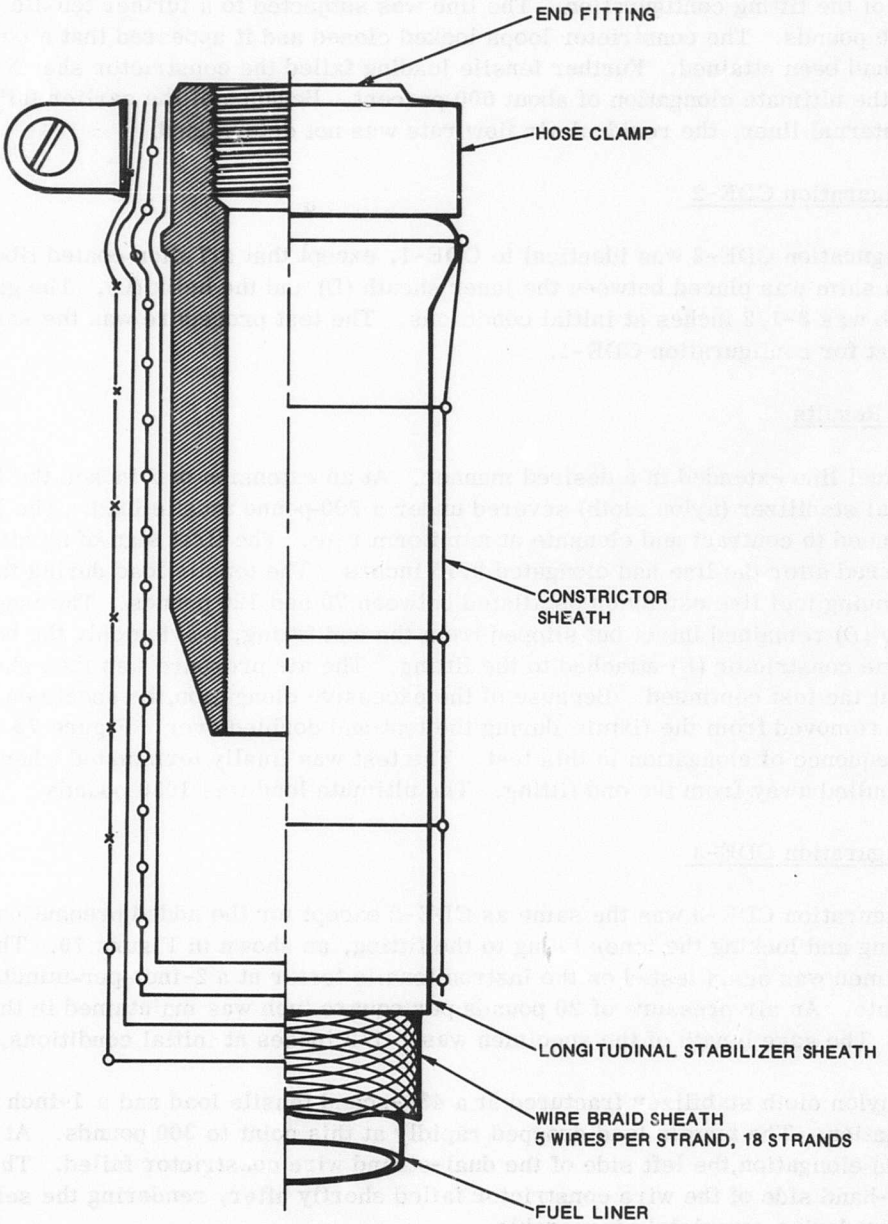

Figure 77. Self-Closing Line Configuration CDE-1.

sheath to pinch and then shear the elastomeric liner, revealing the inherent weakness of the fitting configuration. The line was subjected to a further tensile load of 670 pounds. The constrictor loops locked closed and it appeared that a complete seal had been attained. Further tensile loading failed the constrictor sheath before the ultimate elongation of about 500 percent. Because of the earlier failure of the internal liner, the residual air flow rate was not determined.

Configuration CDE-2

Configuration CDE-2 was identical to CDE-1, except that a Teflon-coated fiber glass shim was placed between the inner sheath (D) and the helix (C). The gage length was 3-1/2 inches at initial conditions. The test procedure was the same as that for configuration CDE-1.

Test Results

The fuel line extended in a desired manner. At an extension of 2 inches the longitudinal stabilizer (nylon cloth) severed under a 200-pound tensile load. The line continued to contract and elongate at a uniform rate. The first sign of an air leak occurred after the line had elongated 9.15 inches. The tensile load during the continuing fuel line extension oscillated between 70 and 120 pounds. The inner lining (D) remained intact but slipped from the end fitting, leaving only the helix (C) and constrictor (E) attached to the fitting. The air pressure was then shut off but the test continued. Because of the excessive elongation, the specimen had to be removed from the fixture during the test and doubled over. Figure 78 shows the sequence of elongation in this test. The test was finally terminated when the line pulled away from the end fitting. The ultimate load was 1050 pounds.

Configuration CDE-3

Configuration CDE-3 was the same as CDE-2 except for the added precaution of bonding and locking the inner lining to the fitting, as shown in Figure 79. The test specimen was again tested on the Instron tensile tester at a 2-inch-per-minute onset rate. An air pressure of 20 pounds per square inch was maintained in the line. The gage length of the specimen was 1-1/2 inches at initial conditions.

The nylon cloth stabilizer fractured at a 430-pound tensile load and a 1-inch line elongation. The tensile load dropped rapidly at this point to 300 pounds. At 2 inches elongation, the left side of the dual-strand wire constrictor failed. The right-hand side of the wire constrictor failed shortly after, rendering the self-locking device completely inoperable.

sheath to pinch and then shear the elastomeric liner, revealing the inherent weakness of the fitting configuration. The line was subjected to a further tensile load of 670 pounds. The constrictor loops locked closed and it appeared that a complete seal had been attained. Further tensile loading failed the constrictor sheath before the ultimate elongation of about 500 percent. Because of the earlier failure of the internal liner, the residual air flow rate was not determined.

Configuration CDE-2

Configuration CDE-2 was identical to CDE-1, except that a Teflon-coated fiber glass shim was placed between the inner sheath (D) and the helix (C). The gage length was 3-1/2 inches at initial conditions. The test procedure was the same as that for configuration CDE-1.

Test Results

The fuel line extended in a desired manner. At an extension of 2 inches the longitudinal stabilizer (nylon cloth) severed under a 200-pound tensile load. The line continued to contract and elongate at a uniform rate. The first sign of an air leak occurred after the line had elongated 9.15 inches. The tensile load during the continuing fuel line extension oscillated between 70 and 120 pounds. The inner lining (D) remained intact but slipped from the end fitting, leaving only the helix (C) and constrictor (E) attached to the fitting. The air pressure was then shut off but the test continued. Because of the excessive elongation,the specimen had to be removed from the fixture during the test and doubled over. Figure 78 shows the sequence of elongation in this test. The test was finally terminated when the line pulled away from the end fitting. The ultimate load was 1050 pounds.

Configuration CDE-3

Configuration CDE-3 was the same as CDE-2 except for the added precaution of bonding and locking the inner lining to the fitting, as shown in Figure 79. The test specimen was again tested on the Instron tensile tester at a 2-inch-per-minute onset rate. An air pressure of 20 pounds per square inch was maintained in the line. The gage length of the specimen was 1-1/2 inches at initial conditions.

The nylon cloth stabilizer fractured at a 430-pound tensile load and a 1-inch line elongation. The tensile load dropped rapidly at this point to 300 pounds. At 2 inches elongation,the left side of the dual-strand wire constrictor failed. The right-hand side of the wire constrictor failed shortly after, rendering the self-locking device completely inoperable.

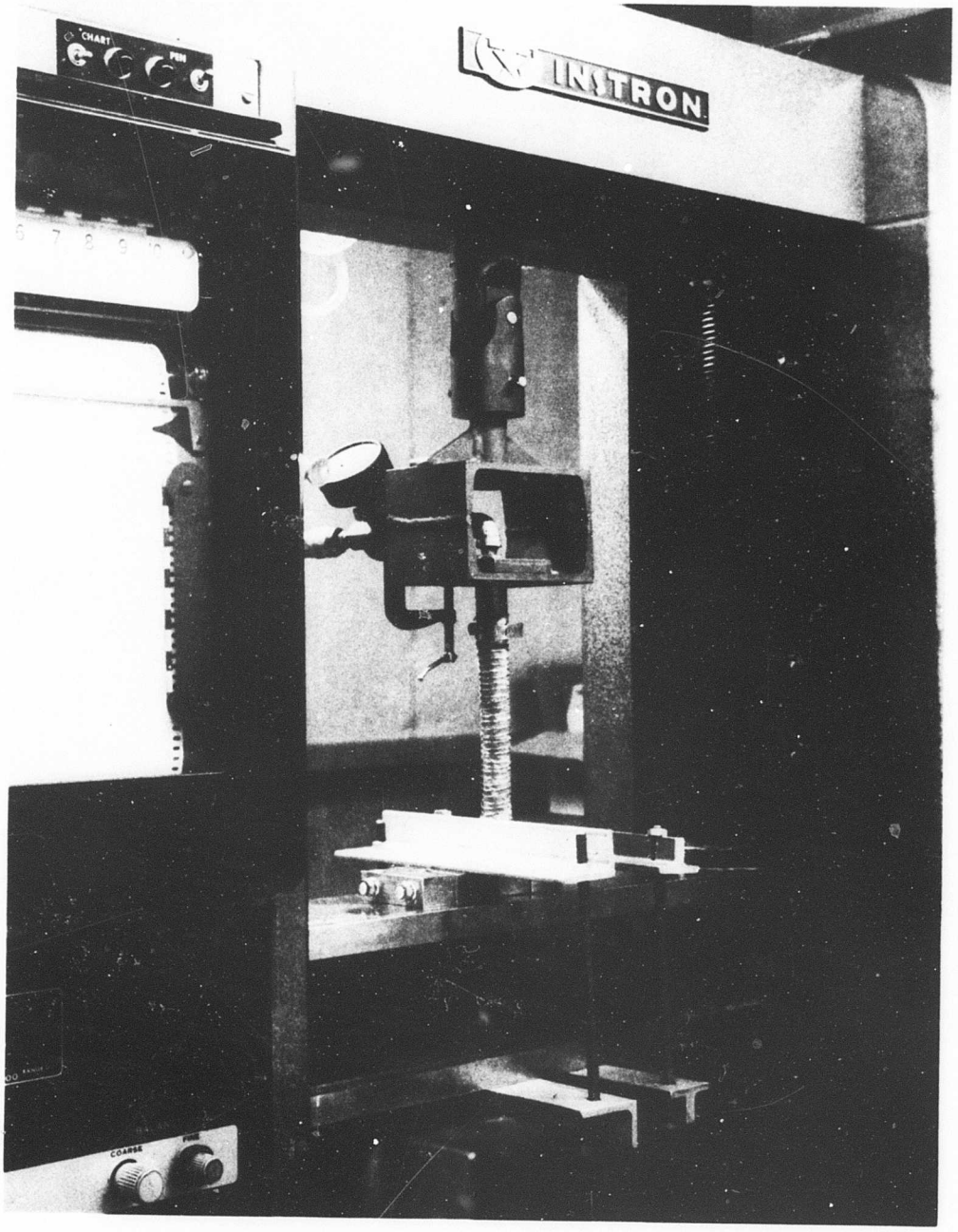

Figure 78. Testing of Self-Closing Line, Configuration CDE-2 (1 of 6).

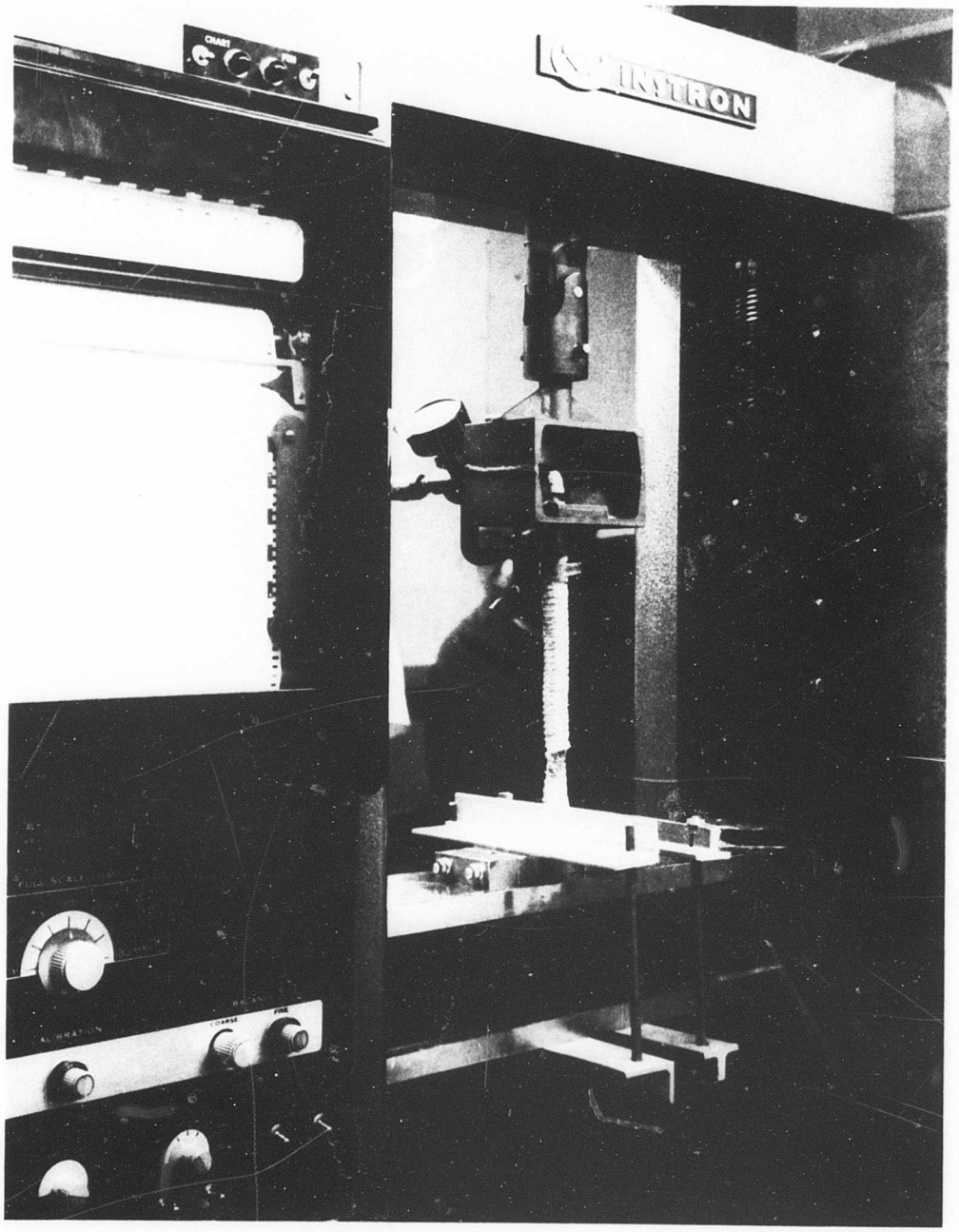

Figure 78. Testing of Self-Closing Line, Configuration CDE-2 (2 of 6).

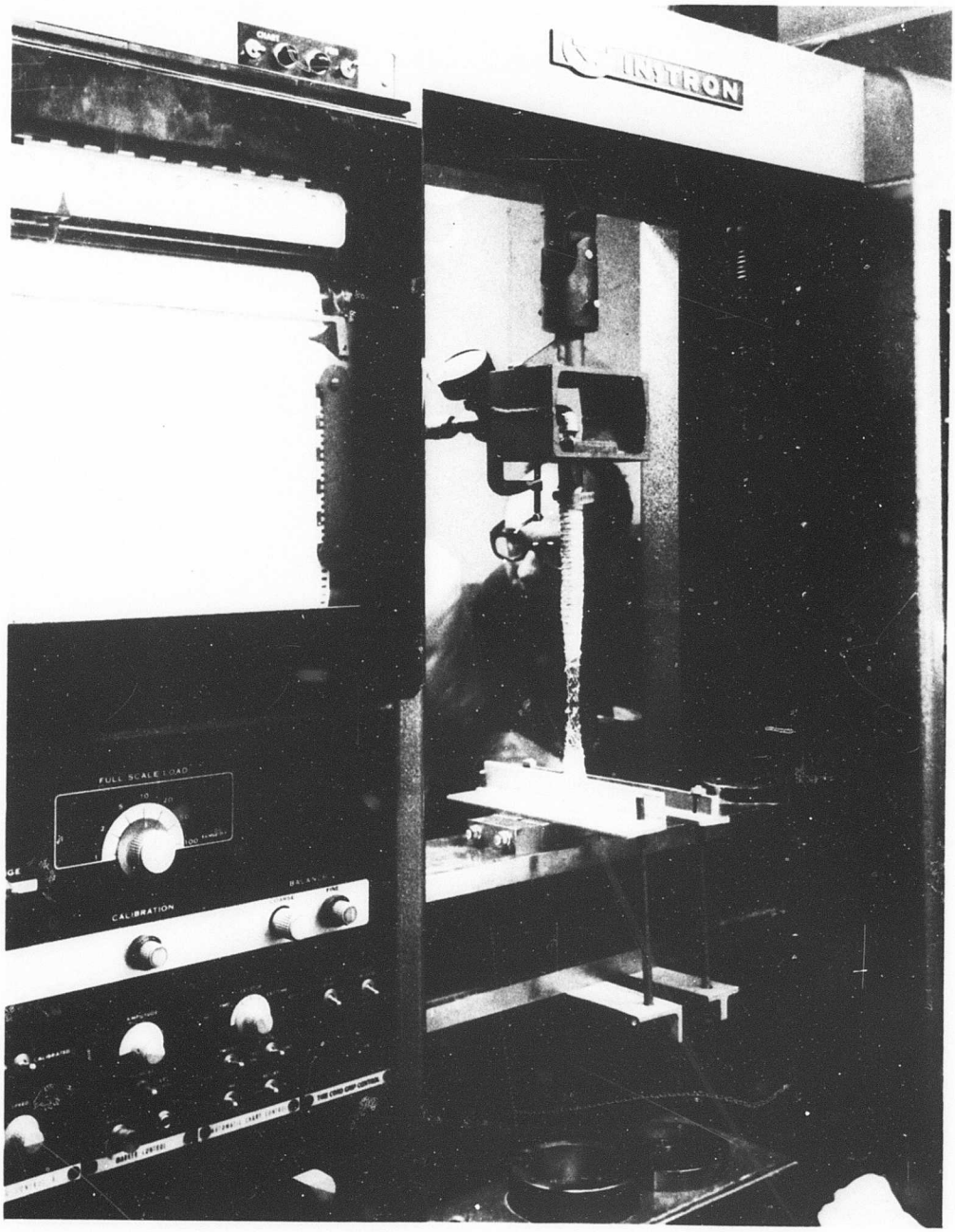

Figure 78. Testing of Self-Closing Line, Configuration CDE-2 (3 of 6).

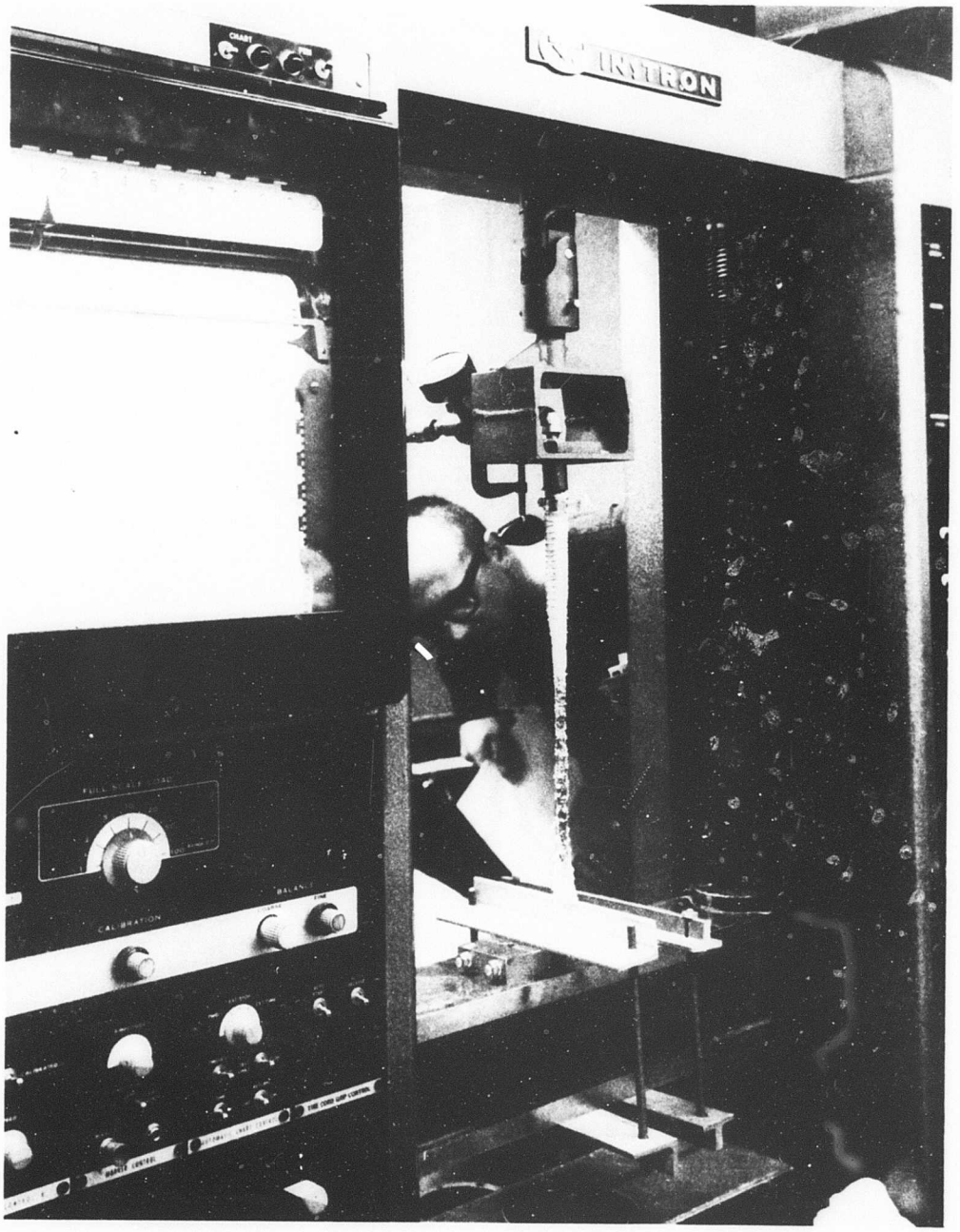

Figure 78. Testing of Self-Closing Line, Configuration CDE-2 (4 of 6).

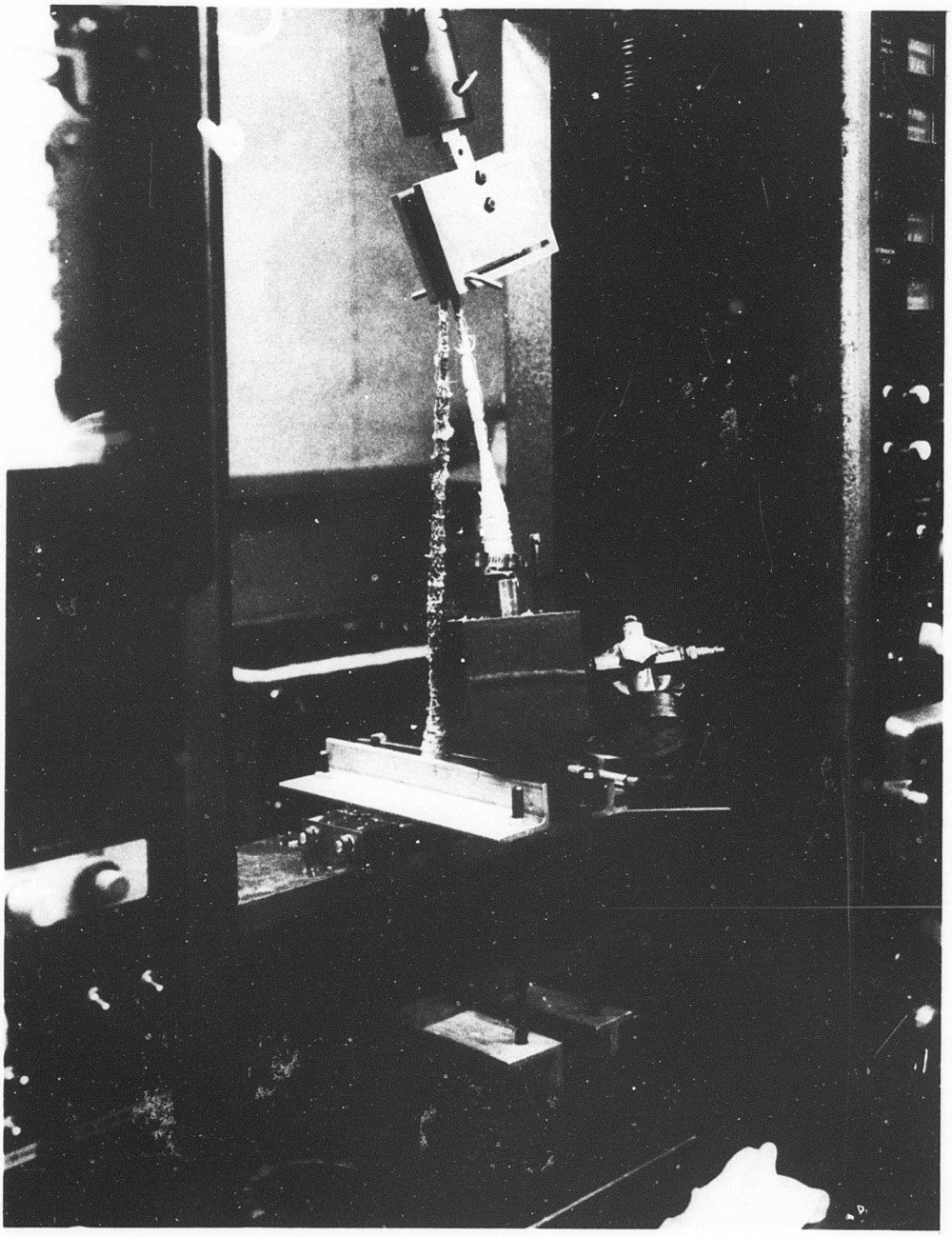

Figure 78. Testing of Self-Closing Line, Configuration CDE-2 (5 of 6).

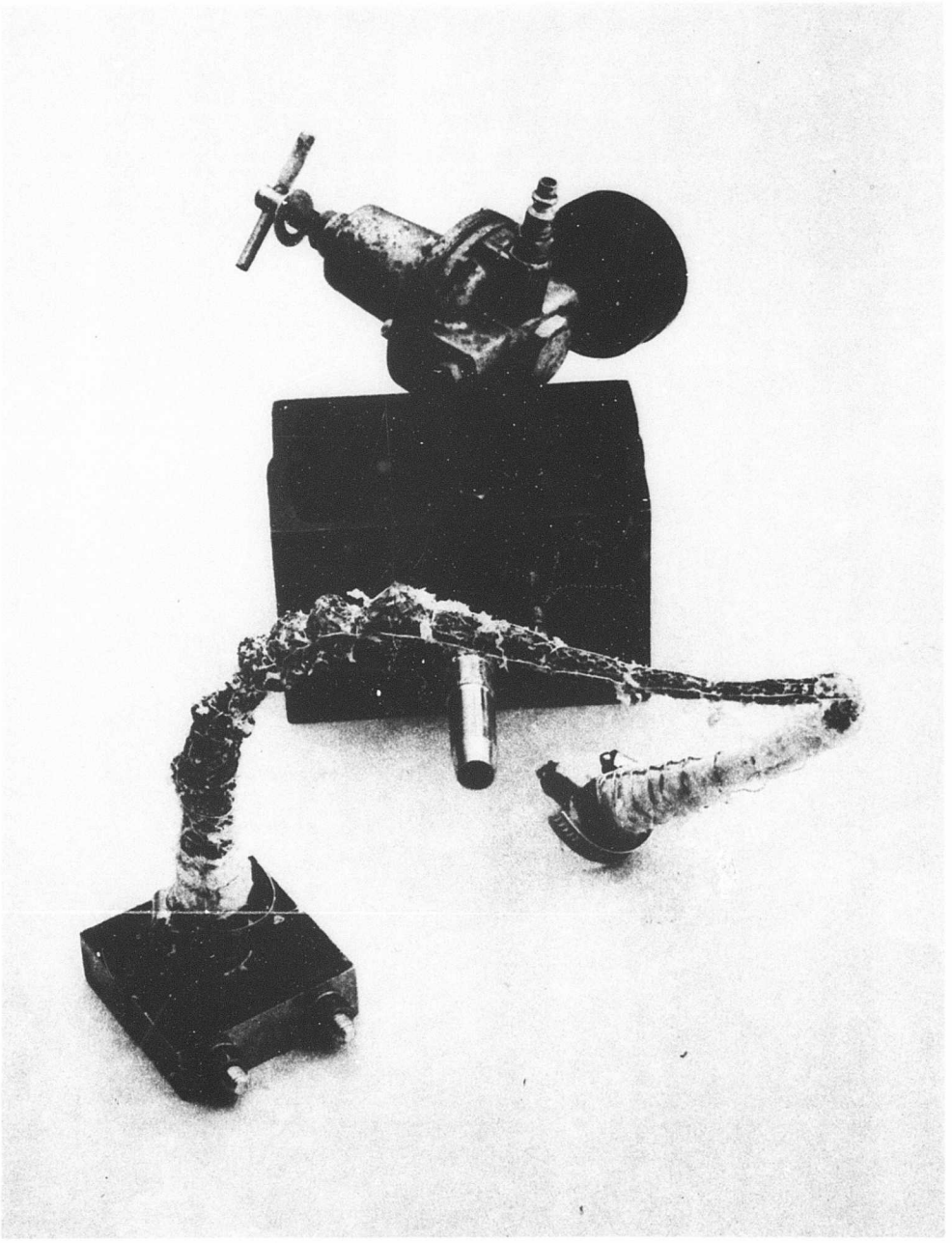

Figure 78. Testing of Self-Closing Line, Configuration CDE-2 (6 of 6).

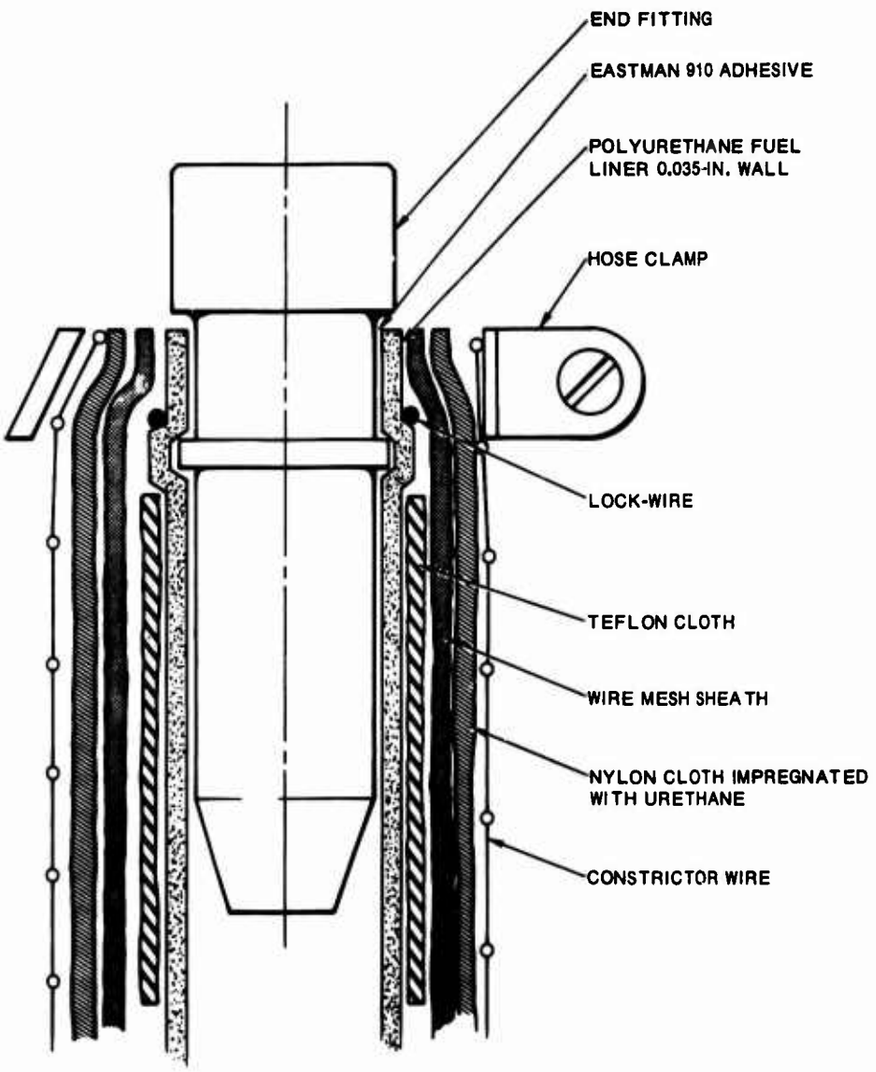

Figure 79. Self-Closing Fuel Line, Configuration CDE-3.

The test was continued, however, and measurements were taken. At an extension of 12 inches, the cross-sectional diameter of the wire mesh sheath was 0.287 inch. The inner lining (D) failed at a 12.7-inch elongation and a small air leak was observed at this point. Figure 80 shows the sequence of elongation in this test.

The tensile loading was continued until the failure of the helical sheath. The rupture load was 570 pounds at an ultimate length of 18 inches. Separation was caused by the helix peeling from the end fitting.

Analysis of CDE Configuration

The characteristics of the CDE configuration can be summarized as follows: (1) the inner lining (D) and the stabilizer sheath and helix (C) performed satisfactorily in all cases where the adverse influence of the fittings was absent; (2) the locking sheath (E) performed satisfactorily except in the case of CDE-3, in which a processing flaw is blamed for the premature failure; and (3) in every case the fitting failed to satisfactorily transfer the load from the line and impeded line extension.

The greatest flaw in the locking sheath is that its performance depends on its total continuity until after constriction has been made. One break or flaw, as demonstrated in test CDE-3, renders it completely ineffective. This problem could be eliminated by the spaced attachment of the locking sheath to the helix. Unfortunately, with this configuration it is impractical to do so. To change the location of the lock to a position inside the stabilizer sheath would make it less vulnerable to abuse, but might also obstruct its proper function. An alternative would be to substitute one of the other locking devices described previously.

In all tests, the fittings performed unsatisfactorily because the helix was forced to constrict and elongate throughout its entire length, including the portion enclosing the rigid end fitting. The elastomeric inner lining was caught between the sheath and the rigid fitting, and as the compressive load of the constricting helix increased, failure was imminent. The basis of the problem lay in the fact that the bearing surface was on the wrong side of the helix.

To cope with the fitting problem, an entirely new approach is being taken: locating the bearing surface outside the helix. One embodiment of this concept is shown in Figure 81. It is anticipated that this design will eliminate line restriction and the need for a long rigid fitting, that it will make a positive locking surface, and that it will permit greater uniformity of stresses during line deformation. Unfortunately, the time limit of the program prohibited the inclusion of this test series; this phase should be concluded on the basis of work done beyond the scope of this contract.

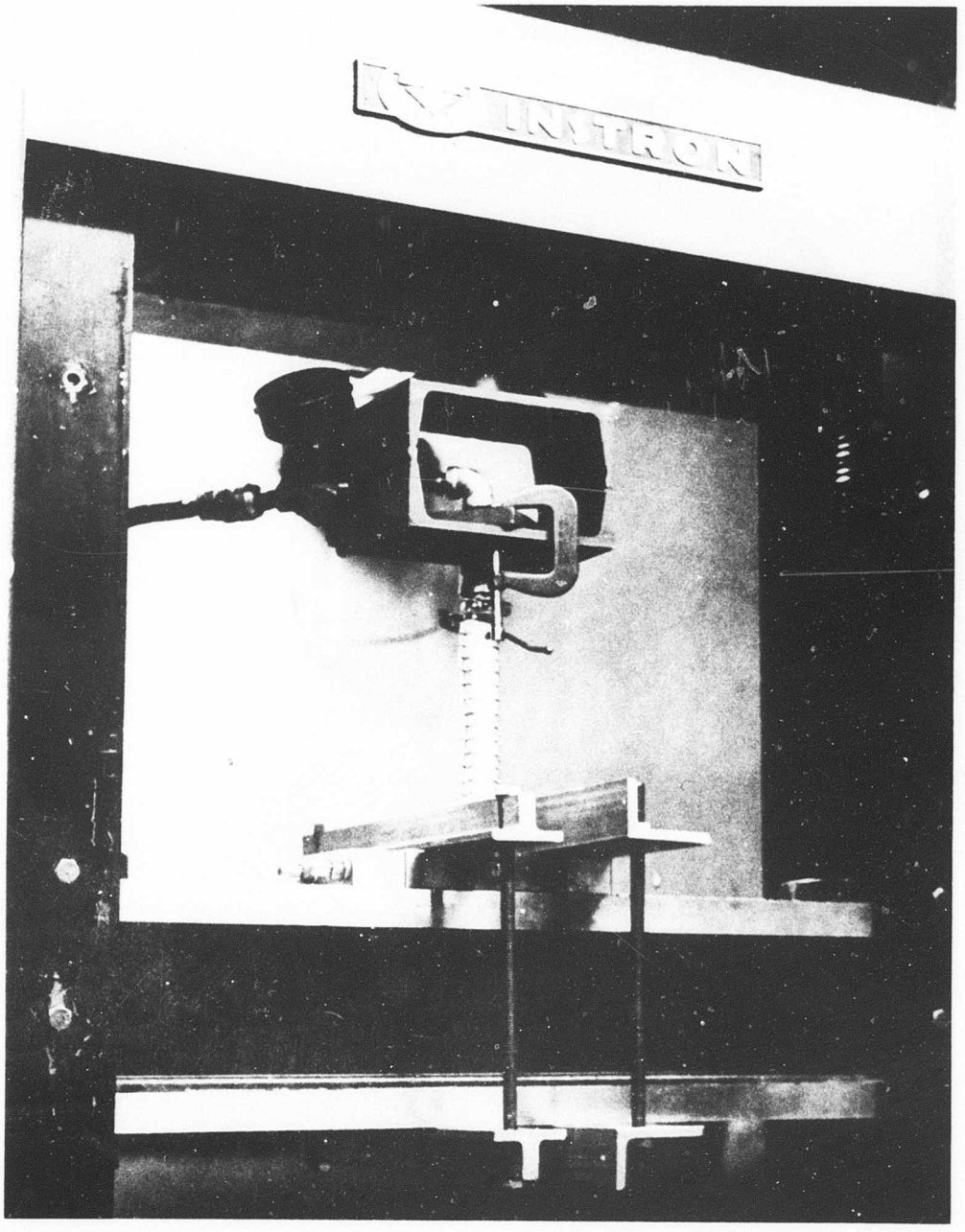

Figure 80. Testing of Self-Closing Line, Configuration CDE-3 (1 of 3).

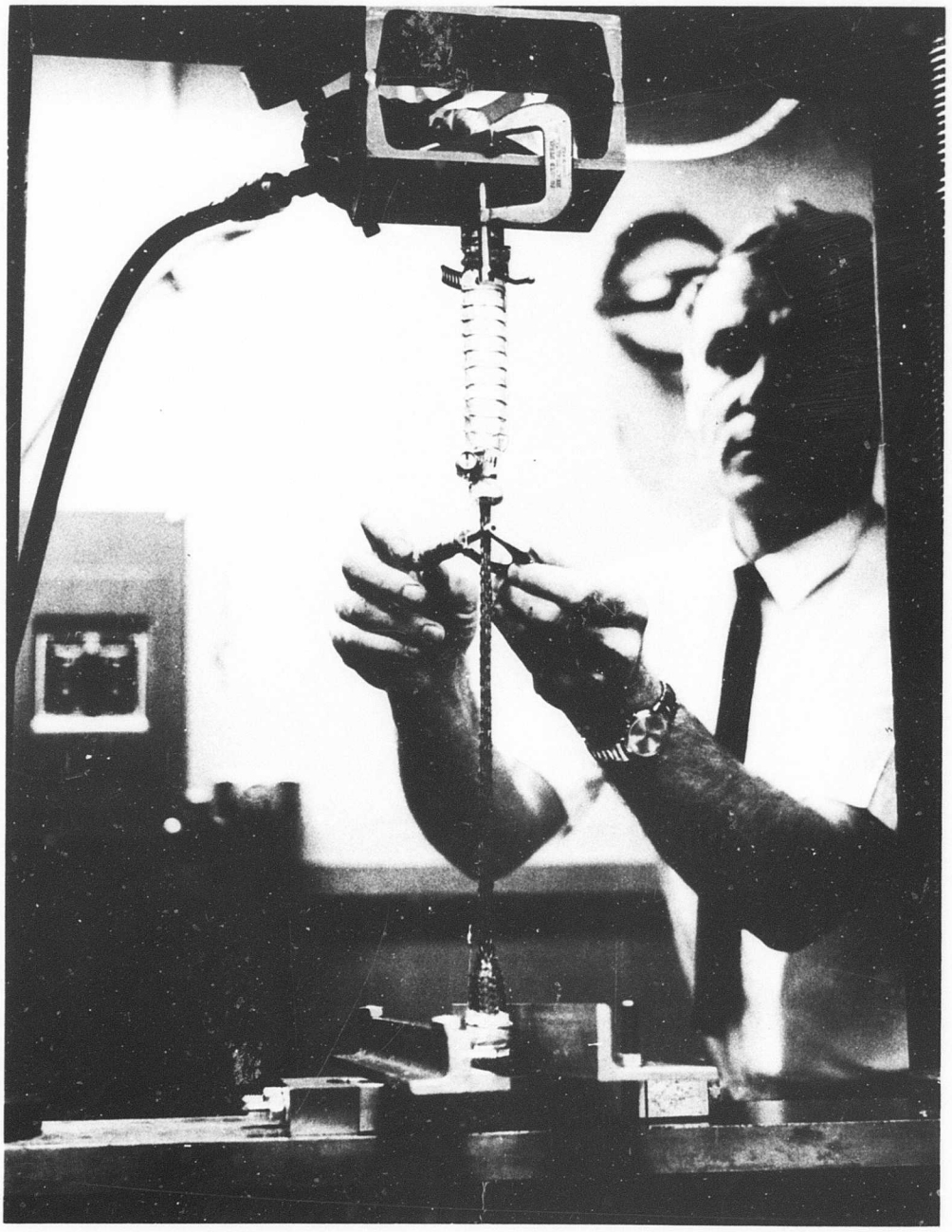

Figure 80. Testing of Self-Closing Line, Configuration CDE-3 (2 of 3).

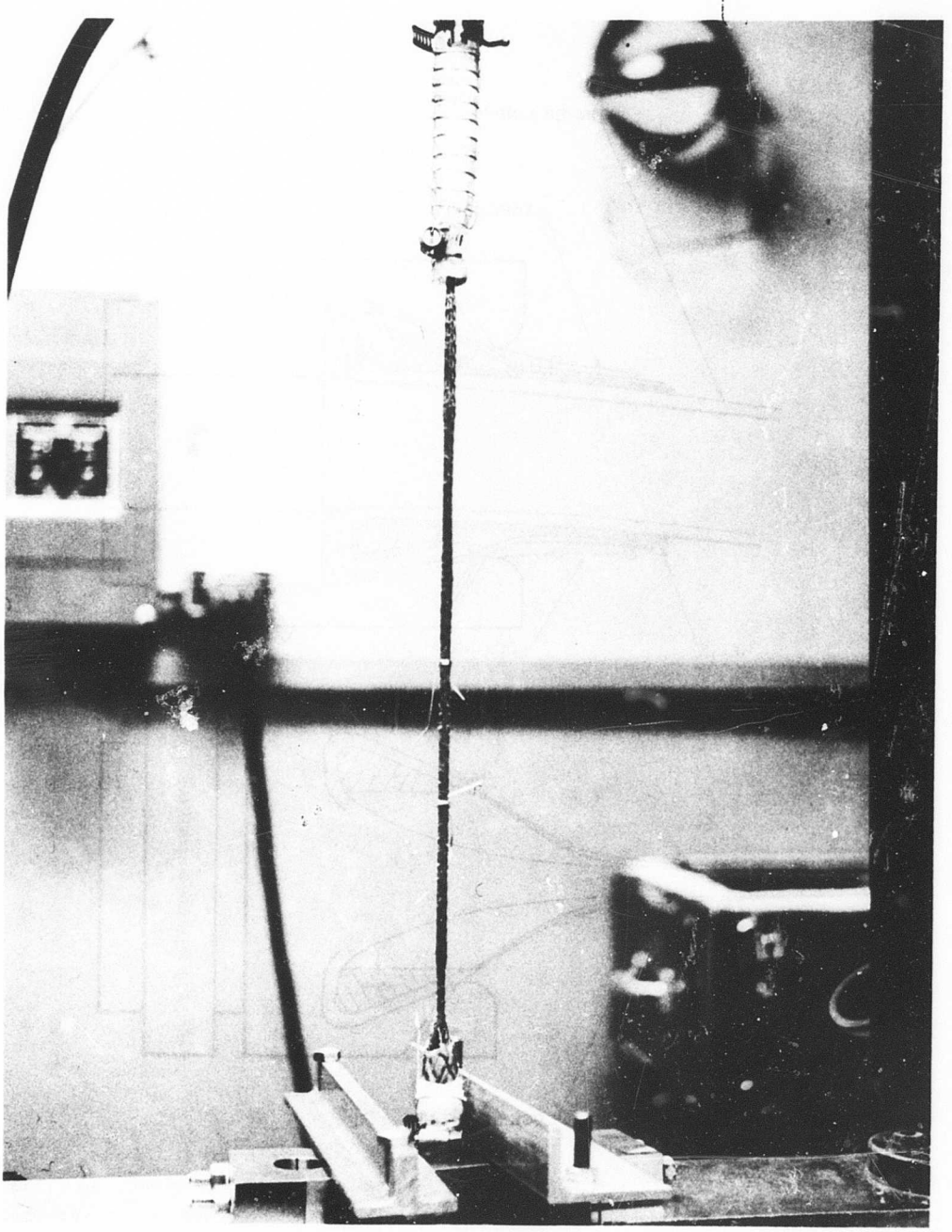

Figure 80. Testing of Self-Closing Line, Configuration CDE-3 (3 of 3).

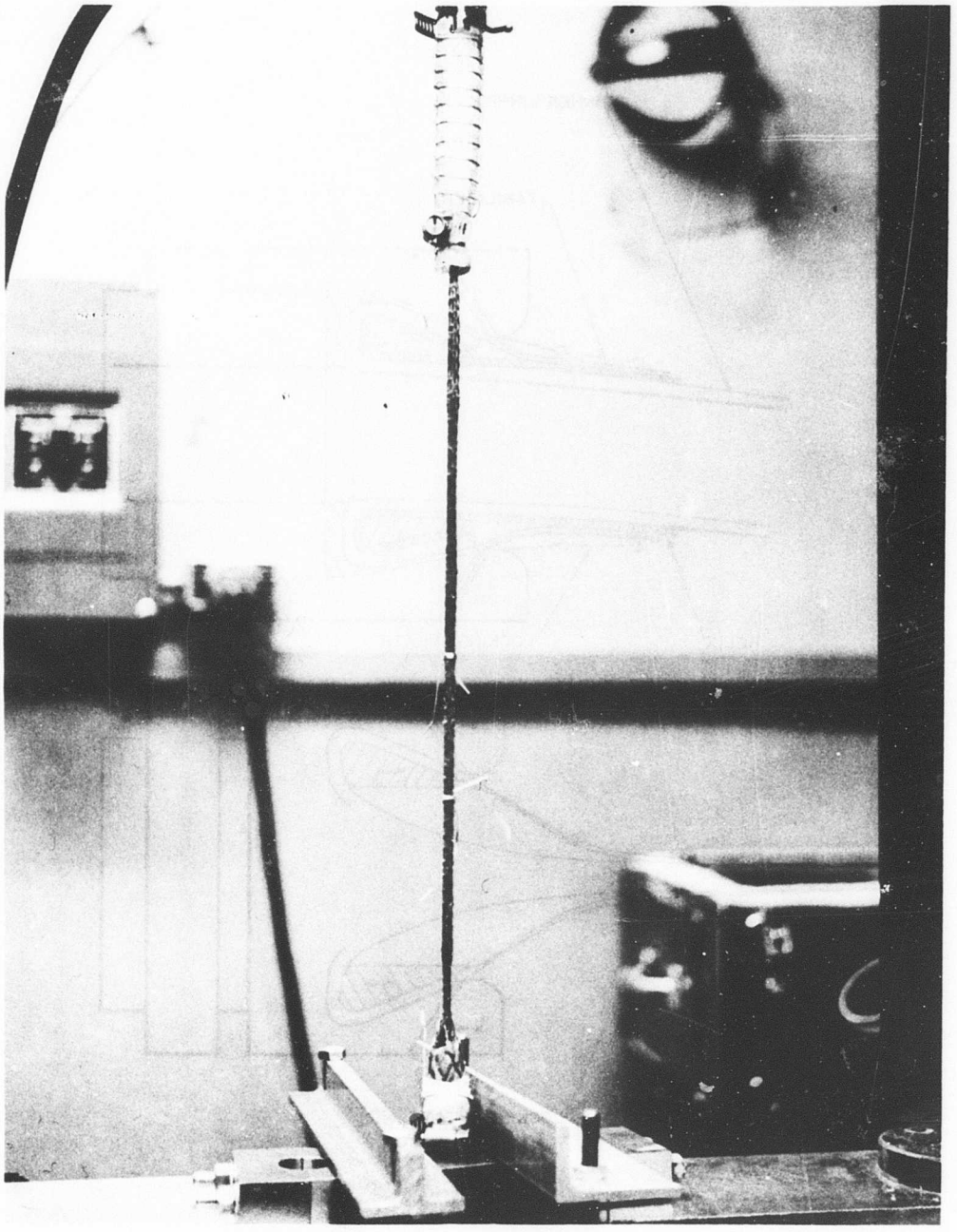

Figure 80. Testing of Self-Closing Line, Configuration CDE-3 (3 of 3).

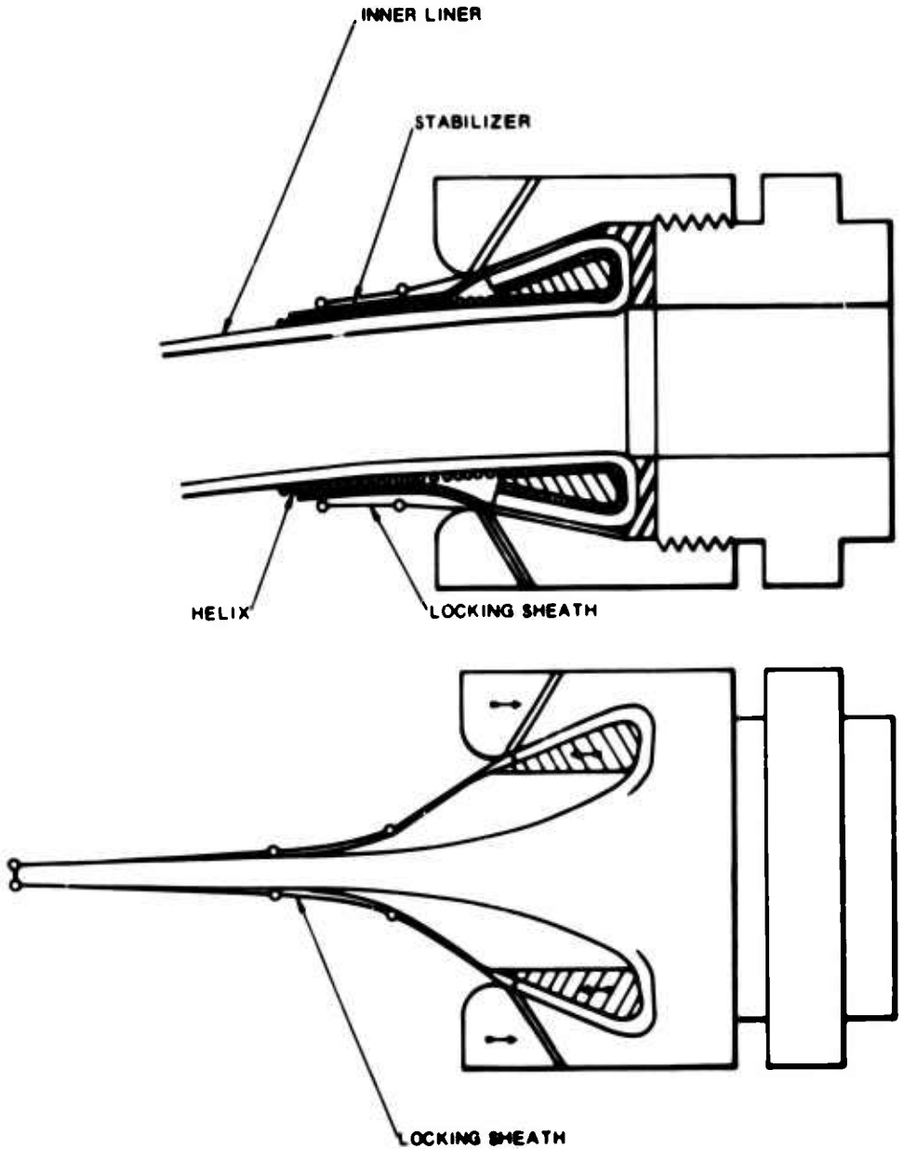

Figure 81. Externally Located End Fitting.

PART VI

SCHEMATIC DIAGRAMS OF FUEL SYSTEMS

Fuel systems safety features required in rotary-wing aircraft are presented in schematic form in this section. These diagrams are not meant to pertain to any individual aircraft but are general in nature. The basic designs illustrated are representative of various configurations found in existing operational aircraft. Detailed written descriptions of these safety features may be found within the text of the report. The schematics are shown in Figures 82, 83, and 84. (Pages 156, 157, and 158)

LEGEND FOR SCHEMATIC DIAGRAMS

1. Floor thickness adequate to protect tanks from ground protrusions.
2. Recessed tank filler with frangible breakaway attachment.
3. Self-sealing breakaway vent.
4. Self-sealing breakaway fuel tank interconnects.
5. Recessed sump drain with frangible outlet.
6. Frangible aft slanted quantity-indicator probe.
7. Boost pump with breakaway fitting (suction system preferred).
8. Breakaway self-sealing tank connections (redundant system preferred).
9. Extensible fuel lines.
10. As few fuel line fittings as possible.
11. Breakaway thorough-bulkhead fittings.
12. Fuel filter should be mounted within the fuel tank.
13. In-line valves should be shrouded and compartmentalized.
14. Adequate compartment flow diverters and drains.
15. Electrical compartment located away from fuel tanks.
16. Heater located away from fuel tanks.
17. Improved crash-resistant self-sealing fuel tank construction.
18. Mount tanks as far from engines as possible.
19. Provide adequate protective fire barriers.
20. Fuel tank should not be located beneath large weight mass.

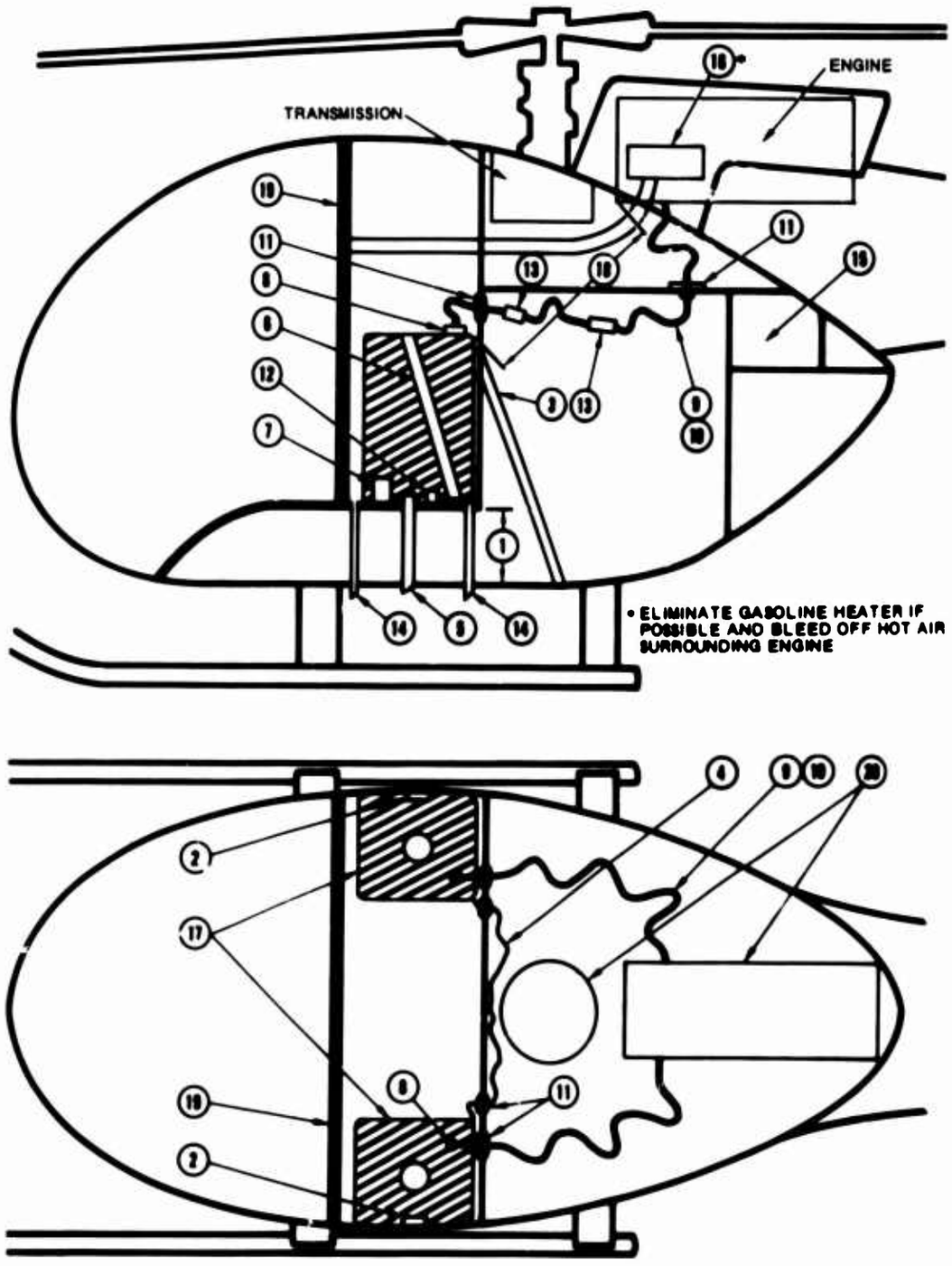

Figure 82. Aft High-Mount Fuel System Schematic.

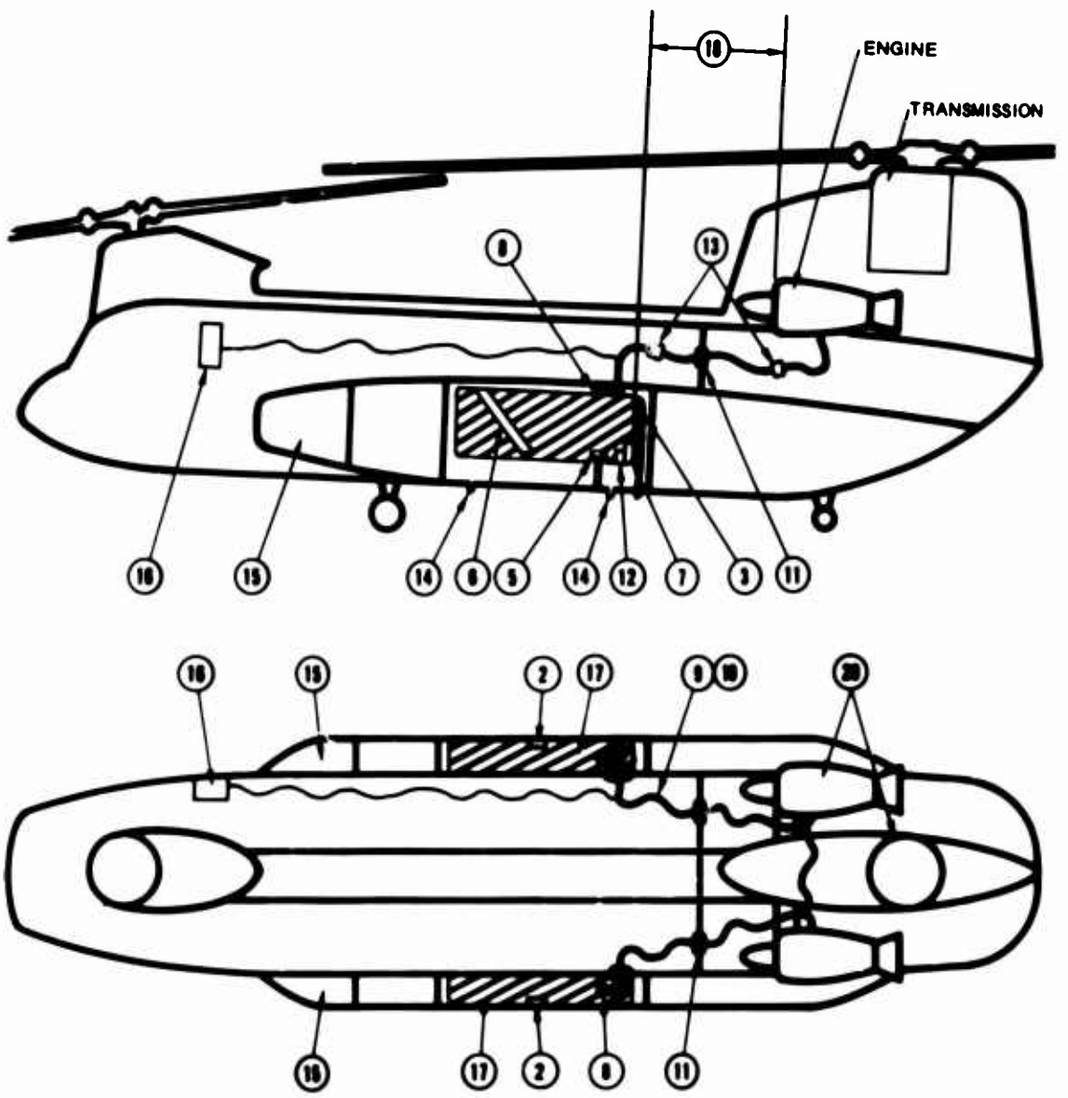

Figure 83. Low Side-Mount Fuel Tank Schematic.

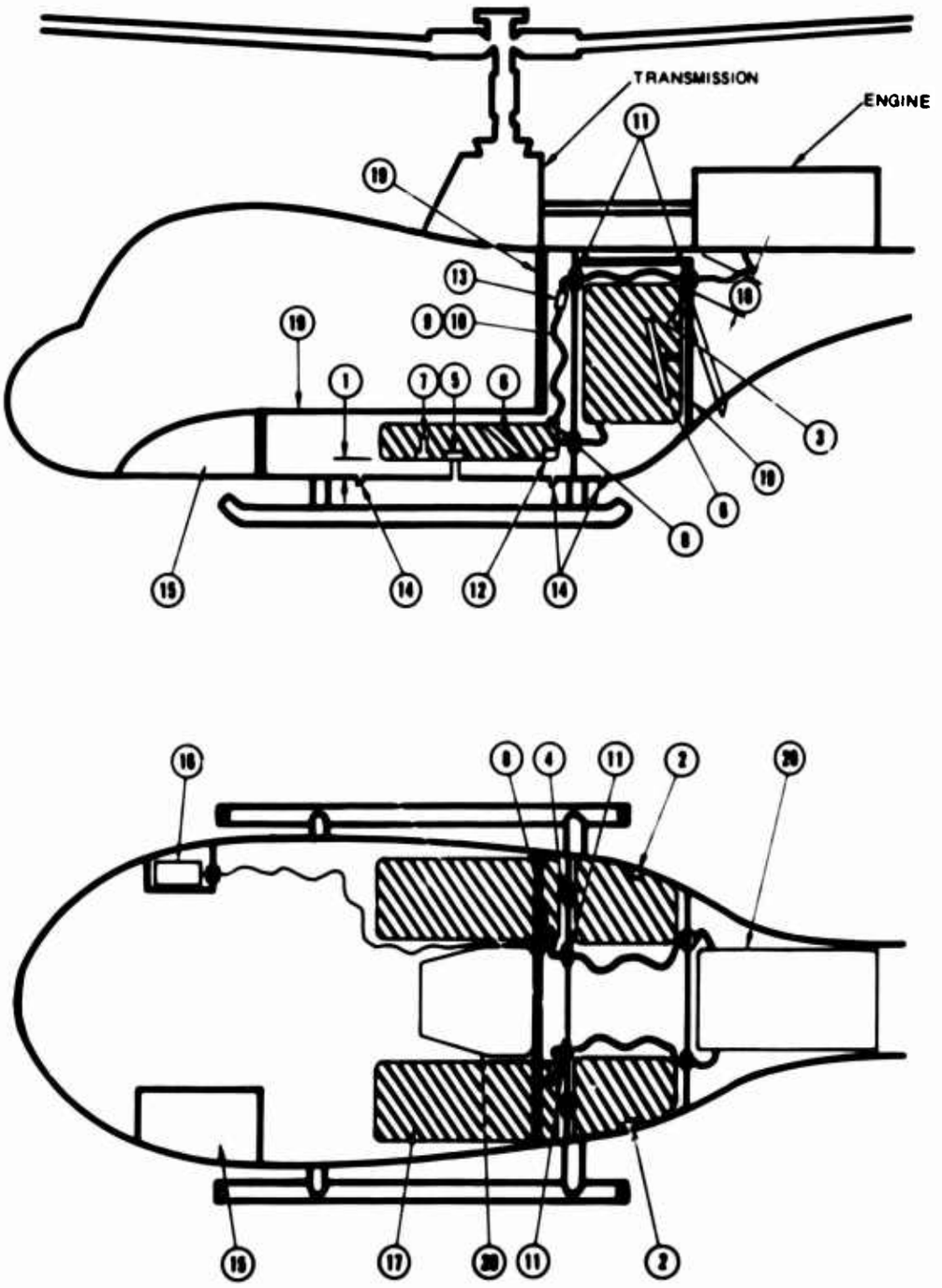

Figure 84. Combined Aft High and Floor Tanks Schematic.

PART VII

CONCLUSIONS

Data from the study of the specified aircraft (UH-1B, UH-1D, CH-47, and OH-6A) showed that the same weaknesses generally prevailed in all four fuel systems, even though a specific weakness may have been more or less pronounced in one than in others.

The cast aluminum components used throughout the fuel systems are subject to gross fuel loss and flash ignition when located outside the fuel tanks, and they present a considerable explosive hazard from ballistic impact when located inside the tank (Part II).

Fuel-transfer components are inadequately compartmentalized or shrouded, leaving the system extremely vulnerable to vapor explosion from fuel sprayed on ignition sources (Part IV). These ignition sources can even include the flash caused by a ballistic hit on a component, although the greatest hazard appears to be the complex array of fuel lines surrounding the engine.

The fuel tank location is an important factor in the general vulnerability of the fuel system. Tanks mounted too low in the airframe structure are susceptible to penetration from irregular ground objects and to broken structure.

Access ports and filler necks mounted rigidly to the aircraft structure lack the ability to break away from the structure; in a crash environment the tanks tear away from these highly stressed fitting areas and severe fuel loss ensues (Part II).

As with the filler and access ports, the fuel-transfer outlets are mounted rigidly to the structure with no provisions for separation during a crash; if a fuel-transfer or vent line is torn away, considerable fuel loss will result because no automatic shutoff valve is provided (Part II and Appendix III).

Specification MIL-V-27393A, which governs breakaway valve design, is obsolete and excessively limited in scope.

Fuel-level indicator probes, used in three of the aircraft, present a serious puncture hazard to fuel tanks because of their strength and rigidity.

Frangible component attachments and self-sealing breakaway fuel-line connections (Part IV) will greatly reduce fuel cell failures and subsequent fuel loss.

Fuel transfer lines generally consist of tubing that is unable to sustain the excessive deformations often occurring in a crash. Even flexible hose lacks the extensibility

to sustain gross structural deformations. Since no self-sealing breakaway fittings are provided, either fittings or lines will fail and fuel loss is imminent.

Rigid fuel line connections to bulkheads prevent line displacement and are another cause of fitting and line failures. Standard (AN) line fittings are generally incapable of transferring loads exceeding 50 percent of the maximum line load.

Highly extensible fuel-transfer lines, typified by the self-closing line (Part V) and properly located self-sealing breakaway fittings, will greatly alleviate the problem of fitting failure by preventing load transfer to the fittings.

PART VIII

RECOMMENDATIONS

Cast aluminum components should not be used inside the fuel tanks. Nonflashing substitutes such as plastics should be investigated for possible use in boost-pump housings, filler necks, and quantity indicator heads. Cast aluminum should also be excluded from use in external components because of its susceptibility to excessive ballistic damage (with consequent massive fuel loss) and its tendency to cause flash ignition of the fuel vapor ejected from the wound.

Fuel-transfer components, including lines, shutoff valves, and filters, should be isolated from ignition sources to the extent that, if ballistic damage is incurred, the fuel spray will be contained. The filter should be located within the fuel tank for this reason. Shrouding of individual components should be utilized wherever feasible. Though it would be desirable to have shrouding with a complete containment capability, it should be mandatory that devices capable of at least a moderate spray suppression be utilized in critical locations. High-temperature line shrouds should be developed to prevent spray in the hot areas surrounding the engine.

Fuel cells need not be located especially high in the aircraft but should be located where the possibility of snagging on ground protrusions during crash impact is minimal. The fuel cells should be fabricated from newly developed materials which possess much greater puncture and tear resistance than materials currently in use.

Fuel cells should be located as far away as possible from all ignition sources, such as the engine, heaters, and electrical compartments. The cells should be located where they will not be damaged by displaced cargo or heavy components in a crash impact and should never be mounted to the structure by high-strength fasteners. Frangible devices, capable of failing at a prescribed load well within the tolerable limits of the tank, should be mandatory for all tank-to-structure mounts such as filler necks, boost pumps, and fuel indicator probes.

Self-sealing breakaway valves should be mandatory for all tank outlets. Valves capable of complete fuel containment should be further developed. As an interim measure, the Wiggins-type valve should be modified for use in fuel-transfer outlets wherever possible. MIL-V-27393A, which limits the design of breakaway valves to one specific type, is considered obsolete because fuel is lost in the process of separation. This specification should be rewritten to allow valve manufacturers to take an imaginative approach toward a more efficient valve design.

The existing fuel indicator probes should be eliminated or modified to reduce their puncture hazard within the tank.

The replacement of rigid fuel-transfer lines by a slack-mounted flexible hose capable of gross displacement should be mandatory. The highly extensible, self-closing line should be developed to the point where it can be used in highly vulnerable areas.

Self-sealing breakaway fuel line connectors should be used wherever fuel lines and fittings will be subjected to excessive stress in crash conditions.

Breakaway bulkhead fitting adapters should be used to permit line reorientation wherever fuel lines pass through bulkheads, thereby reducing line and fitting stresses in a crash environment.

Standard AN line fittings, though considerably weaker than the hose, are acceptable in a crash environment, so long as proper care has been taken to permit satisfactory fuel line displacement. The nonstandard aluminum elbows should not be used in any part of the fuel-transfer system where there is even a remote possibility of fuel loss from overstressed fittings. For greater ballistic protection, nonflashing and self-sealing materials should be investigated as possible substitutes for the cast aluminum AN fittings.

Drainage holes and flow diverters should be strategically located throughout the airframe to channel and dispose of any spilled fuel. Protective fire curtains should be installed between the occupiable area and the fuel cell compartment as an additional safety measure.

BIBLIOGRAPHY

1. Ad Hoc Group on Aviation Fuel Safety, Aviation Fuel Safety, CRC Project Number CA-37-64 (Revised), Coordinating Research Council, New York, New York, December 1964.

2. Anspach, R., et. al., Gasoline Fire Studies, Technical Report T-759 (Confidential), Research and Development Division, New Mexico School of Mines, Socono, New Mexico, March 1951.

3. Buckson, W., Schlegel, W., and Smith, I.R., Design, Development, and Evaluation of a Crash Resistant Fuel System Installation, Technical Report, Contract FA-WA-4580, Federal Aviation Agency, Washington, D.C., August 1964.

4. Custard, G.H., Study of Aircraft Fuel Protection Systems (U), Technical Report 66-15 (Secret), U.S. Army Aviation Materiel Laboratories, Fort Eustis, Virginia, April 1966.

5. Magnesium Alloys and Products, Magnesium Division, Dow Chemical Company, Midland, Michigan, 1950.

6. Parriott, W.E., Vulnerability of Aircraft to Fragments, Research Memorandum RM-1279 (For Official Use Only), The Rand Corporation, Santa Monica, California, May 1954.

7. Robertson, Harry S., U.S. Army CH-47 "Chinook" Helicopter Accident, Fort Benning, Georgia, 10 July 1965, Technical Report AvSER 65-16, Aviation Safety Engineering and Research, Phoenix, Arizona, 1965.

8. Robertson, Harry S., and Turnbow, James W., Aircraft Fuel Tank Design Criteria, Technical Report 66-24, U.S. Army Aviation Materiel Laboratories, Fort Eustis, Virginia, March 1966.

APPENDIX I

AvSER METHOD OF EVALUATING AIRCRAFT CRASH VULNERABILITY

INTRODUCTION

AvSER has developed a crash-survival evaluation method based on the probable performance of an aircraft in a severe but survivable accident. While the term "survivable accident" implies a lack of precise definition because of its many variables, an approximation of the survivability threshold has been attained through the use of acceleration and strain data gathered from studies of controlled aircraft crashes. Comparisons of these data with those of other investigators have resulted in the establishment of a reasonably accurate evaluation method that is based on six factors governing crash survivability.

A reasonable numerical rating was established by assigning weighted values to the various factors. The percent of weight assigned to each was based on its relative hazard potential. The six factors along with their hazard potentials are as follows:

		Hazard Potential (%)	Optimum Number
1.	Crew retention system	17.92	130
2.	Troop retention system	17.23	125
3.	Postcrash fire potential	35.19	255
4.	Basic airframe crashworthiness	17.23	125
5.	Evacuation	8.29	60
6.	Injurious environment	4.14	30
	Totals	100.00	725

To make the job of rating easier, the hazard potential percentage was converted to an optimum numerical value, where a perfect score on all six factors would equal 725. For existing aircraft, inadequate restraint systems and postcrash fires have been equally responsible for injuries and fatalities in accidents, so they were weighted at approximately 35% each. A poor score on either of these important items could indicate a critical situation from a crash-survival point of view, depending on such variables as number of personnel carried, operating terrain, and rescue facilities.

Each of the six factors was in turn broken down into subfactors against which a hazard potential percentage was assigned and converted to an optimum numerical value. That portion of the optimum numerical value that each subfactor is worth is listed opposite the optimum value in a space provided under "Actual Value." Of the six factors, only the postcrash fire potential pertains to this study. The postcrash fire factor is broken down to include spillage control and ignition control.

POSTCRASH FIRE POTENTIAL

As previously indicated, the postcrash fire potential constitutes 35.19 percent of the total hazard potential. Of that value, spillage control is equivalent to 51 percent, and ignition control, 49 percent; spillage and ignition control are subdivided in Table XII.

Since this study was confined to fuel systems, only those postcrash fire items relative to the fuel system were evaluated. However, when comments regarding the hydraulic, oil, or electrical systems are pertinent, they are included. The next subsections present discussions of the areas evaluated and each evaluation parameter.

Flammable Fluid Containment

Location

The tank locations are evaluated with respect to the anticipated impact area, the occupiable area, the large weight masses, and the primary ignition sources.

Vulnerability

The vulnerability of the tanks is evaluated with respect to their rupture resistance when exposed to various aircraft structural failures, such as landing gear failure and vertical column deflections. Also included with structural displacements is the probability of fuel cell failure around the filler neck, the fuel line entry and exit area, the quantity indicators, and the tank tiedown devices.

Construction Technique

The tank construction technique is evaluated in two primary areas: (1) tank geometry, and (2) tank construction materials. Smooth contoured shapes are preferred over irregularly shaped and interconnecting cell systems. Certain types of construction materials have demonstrated better crash resistance than others. Materials having high puncture and tear resistance and high-elongation properties are rated best, while rigid tanks are considered poorest.

TABLE XII

SPILLAGE AND IGNITION CONTROL PERCENTAGE BREAKDOWNS

Spillage Control	Percent of Fire Potential Total		Ignition Control
Fuel Containment	24	12	Induction and Exhaust Flame Locations
Location		12	Location of Hot Metals and Shielding
Vulnerability		6	Engine Location and Tiedown Strength
Construction technique (tank geometry, material, and attachments)		5	Battery Location and Tiedown Strength
Oil Containment	8	5	Electrical Wire Routing
Location		3	Fuel Boost Systems
Vulnerability		2	Inverter Location and Tiedown Strength
Construction and tiedown adequacy		2	Generator Location and Tiedown Strength
Flammable Fluid Lines	12	1	Lights (beacon, search, and navigation)
Construction		1	Antenna Location
Routing			
Components			
Firewall	3.5		
Fuel Flow Interrupters	3.5		

The construction of the fuel lines is evaluated with reference to the hose material and couplings. Experience has shown that rigid lines fail before the flexible type;

thus, flexible lines are rated higher. In addition, it has been determined that the fewer couplings a system contains, the better. Ninety-degree couplings are less desirable than the straight type, and any coupling is inferior to an uninterrupted hose. Aluminum fittings usually fail before steel ones and are rated accordingly.

Routing

Low ratings are given to lines which pass through areas where damage to them is likely to occur. Extra-length hose in areas of anticipated structural deformation is desirable, and large holes through which the fuel lines pass are given higher ratings than small restrictive holes.

System Components

Components such as boost pumps, filters, and selector valves are evaluated from the standpoint of their fuel-spillage susceptibility, either by failing themselves or by causing a failure at the tank or the fuel line connections. Additionally, these components are considered with respect to the anticipated impact area, the occupiable area, and probable ignition sources.

Firewall

Firewalls are evaluated from the standpoint of how well they will function as a shield between crash-induced fluid spillage and the various engine ignition sources.

Fuel Flow Interrupters

Fuel flow interrupters are evaluated as to their effectiveness in interrupting the flow of spilled flammable fluids.

APPENDIX II

FUEL SYSTEM DIAGRAMS

This appendix contains illustrations of the fuel systems of the four aircraft studied in this program.

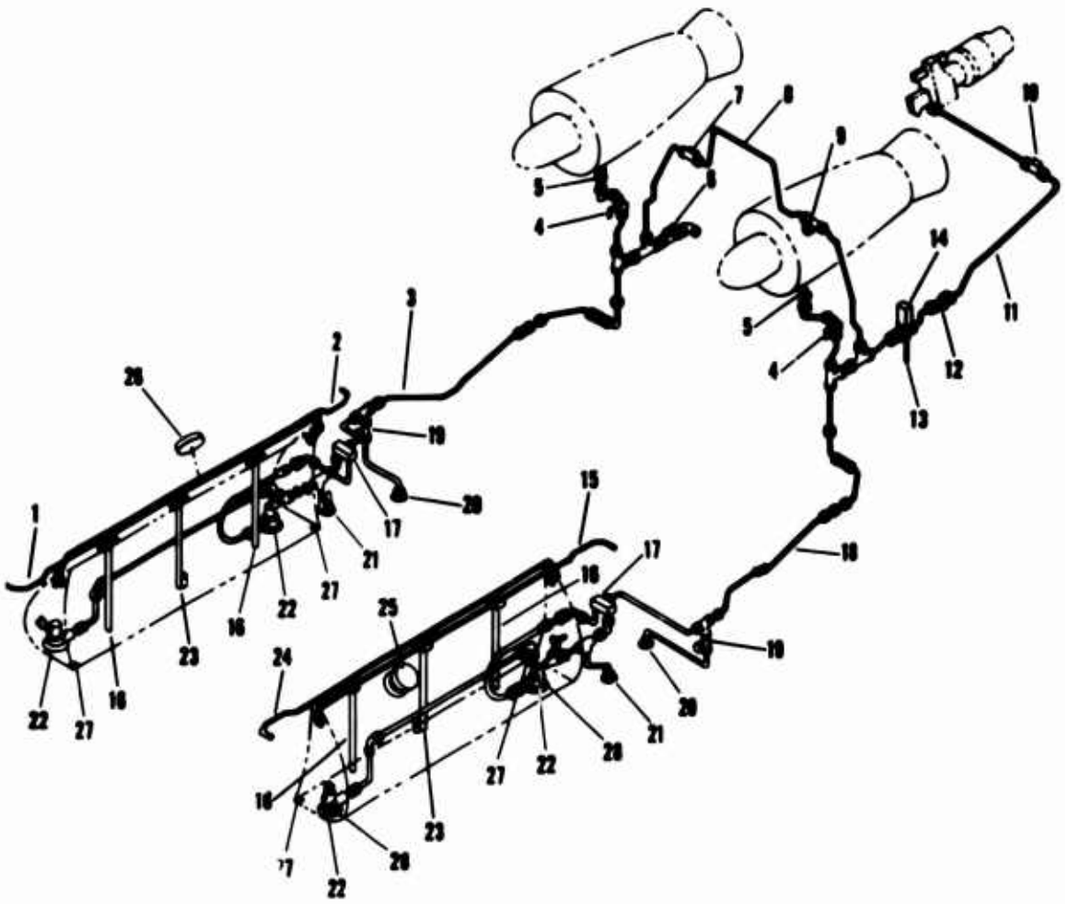

1. NO. 2 FUEL TANK VENT LINE
2. NO. 2 FUEL TANK VENT LINE
3. NO. 2 ENGINE FUEL LINE
4. GATE (SHUTOFF) VALVE
5. COUPLING
6. DEFUELING VALVE
7. GATE (CROSSFEED) VALVE
8. CROSSFEED LINE
9. HEATER FUEL LINE CONNECTION
10. APU FUEL SOLENOID VALVE
11. APU FUEL LINE
12. APU SHUTOFF VALVE
13. DRAIN LINE
14. APU FUEL BOOST PUMP
15. NO. 1 FUEL TANK VENT LINE
16. TANK UNIT
17. SELECTOR VALVE
18. NO. 1 ENGINE FUEL LINE
19. PRESSURE SWITCH
20. SYSTEM POPPET DRAIN VALVE
21. SYSTEM POPPET DRAIN VALVE
22. FUEL BOOSTER PUMP
23. TANK UNIT WITH THERMISTOR
24. NO. 1 FUEL TANK VENT LINE
25. LEFT-HAND TANK FILLER
26. RIGHT-HAND TANK FILLER
27. TANK POPPET DRAIN VALVE
28. FLOAT SWITCH (TYPICAL BOTH TANKS)

Figure 85. Fuel System, CH-47.

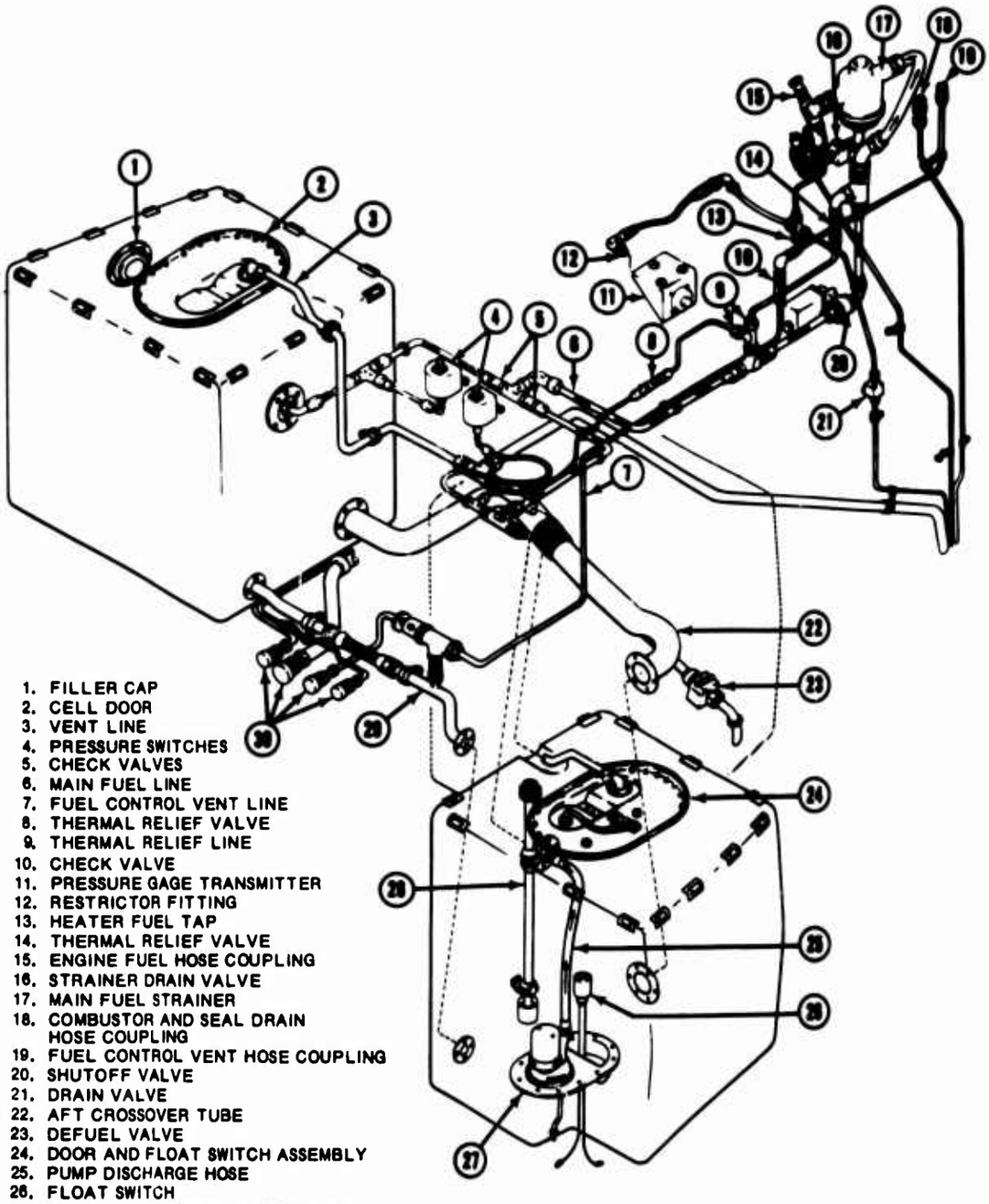

1. FILLER CAP
2. CELL DOOR
3. VENT LINE
4. PRESSURE SWITCHES
5. CHECK VALVES
6. MAIN FUEL LINE
7. FUEL CONTROL VENT LINE
8. THERMAL RELIEF VALVE
9. THERMAL RELIEF LINE
10. CHECK VALVE
11. PRESSURE GAGE TRANSMITTER
12. RESTRICTOR FITTING
13. HEATER FUEL TAP
14. THERMAL RELIEF VALVE
15. ENGINE FUEL HOSE COUPLING
16. STRAINER DRAIN VALVE
17. MAIN FUEL STRAINER
18. COMBUSTOR AND SEAL DRAIN HOSE COUPLING
19. FUEL CONTROL VENT HOSE COUPLING
20. SHUTOFF VALVE
21. DRAIN VALVE
22. AFT CROSSOVER TUBE
23. DEFUEL VALVE
24. DOOR AND FLOAT SWITCH ASSEMBLY
25. PUMP DISCHARGE HOSE
26. FLOAT SWITCH
27. SUMP AND BOOST PUMP ASSEMBLY
28. FUEL GAGE TANK UNIT
29. FORWARD CROSSOVER TUBE
30. AUXILIARY TANK COUPLINGS

Figure 86. Fuel System, UH-1B.

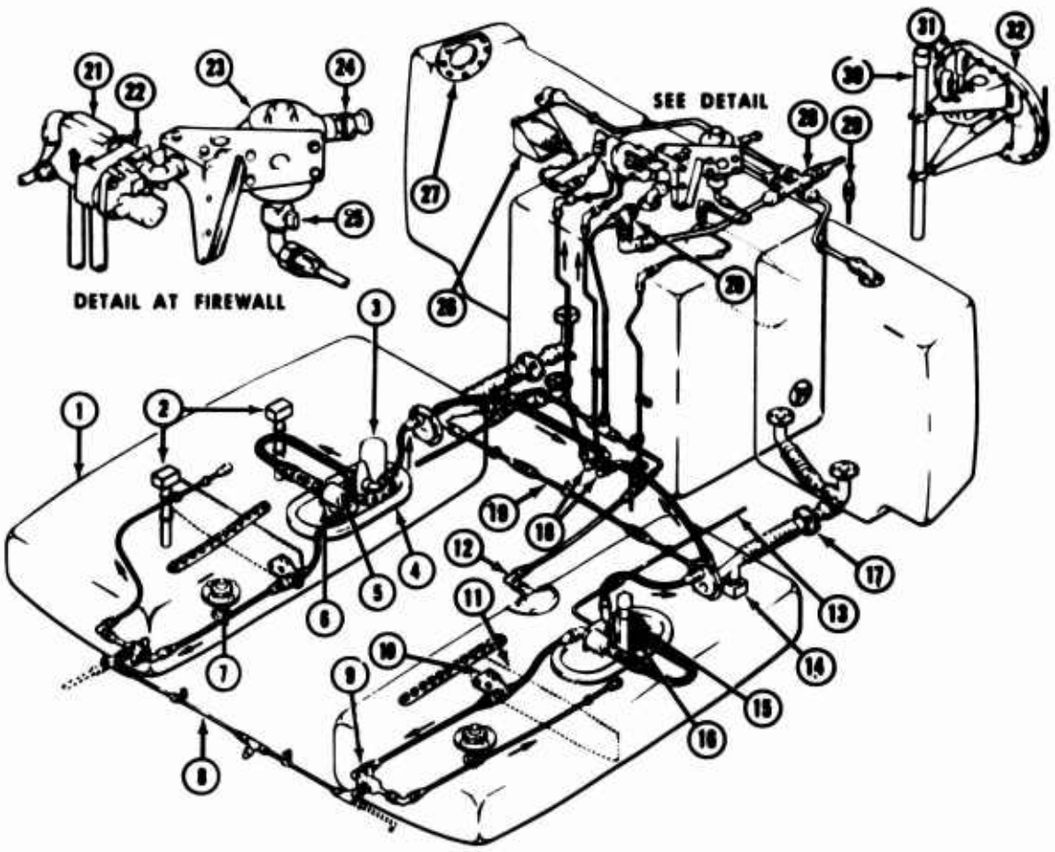

1. FORWARD CELL
2. FUEL QUANTITY TRANSMITTERS
3. ELECTRIC BOOST PUMP
4. SUMP ASSEMBLY
5. FLOW SWITCH WITH CHECK VALVE
6. SUMP DRAIN VALVE
7. DRAIN VALVE
8. CROSSFEED LINE
9. EJECTOR PUMP
10. FLAPPER VALVE
11. BAFFLE
12. VENT LINE
13. BLEED AIR LINE FROM ENGINE
14. DEFUEL VALVE
15. AIR-DRIVEN BOOST PUMP
16. FLOAT SWITCH
17. CROSSOVERS
18. FUEL LINES - TANKS TO VALVE MANIFOLD
19. CROSSFEED LINE
20. SIPHON BREAKER VALVE
21. CHECK VALVE MANIFOLD
22. FUEL SHUTOFF VALVE
23. MAIN FUEL STRAINER
24. COUPLING FOR ENGINE FUEL HOSE
25. STRAINER DRAIN VALVE
26. PRESSURE GAGE TRANSMITTER
27. FILLER CAP
28. VENT MANIFOLD
29. FUEL CONTROL VENT LINE
30. FUEL QUANTITY TRANSMITTER
31. FLOAT SWITCHES - AUXILIARY FUEL TRANSFER PUMP CONTROL
32. CENTER CELL ACCESS DOOR

Figure 87. Fuel System, UH-1D.

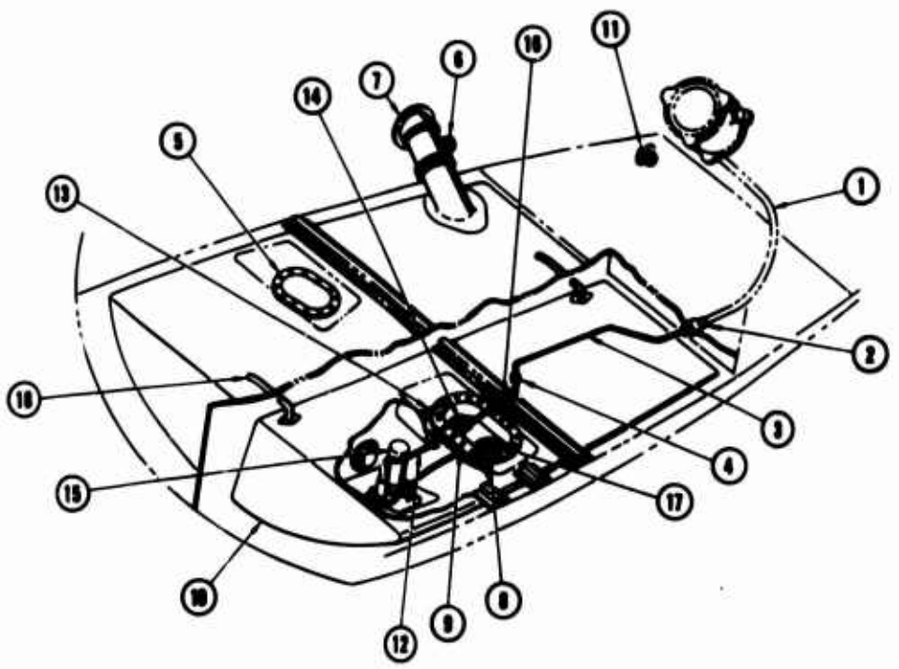

1. FUEL LINE (HOSE)
2. BULKHEAD COUPLING
3. FUEL LINE (TUBE)
4. CLAMP
5. COVER PLATE
6. PLUG
7. CLAMP
8. BRACKET
9. COVER FLATE
10. FUEL TANK
11. TELEPHONE JACK
12. FUEL LINE (HOSE)
13. BRACKET
14. FUEL SHUTOFF VALVE
15. BOOST PUMP
16. BRACKET
17. FUEL INDICATOR
18. VENT LINE

Figure 88. Fuel System, OH-6A.

APPENDIX III

HYDRAULIC FLUID EXPULSION FROM AN ORIFICE

The rate of flow, $Q_{(t)}$, from an orifice during crash impact may be calculated using the laws of fluid dynamics.

Static flow, Q, may be calculated from $Q = CA\sqrt{2gh}$

where:

C = Coefficient of discharge
A = Area of orifice
g = Acceleration due to gravity
h = Static head

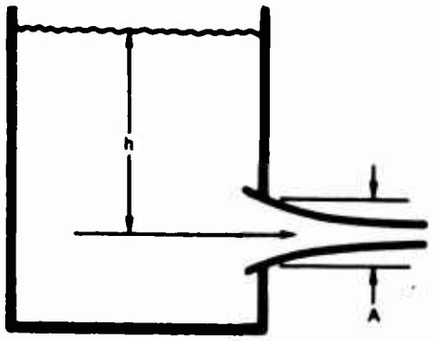

The coefficient of discharge varies with the shape of the orifice, but is always less than 1.00. Several coefficients, along with the appropriate orifices, are listed below.

C = 0.61  Sharp edge

C = 0.98 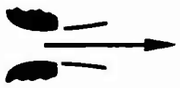 Rounder orifice

C = 0.80 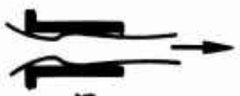 Short tube

C = 0.51  Borda tube

During an impact the effective head will be $H_{(t)}$, given by

$$H_{(t)} = h \times G_{(t)} = h \times \frac{a_{(t)}}{g} .$$

Therefore,

$$Q_{(t)} = CA\sqrt{2ghG_{(t)}}$$

$$= CA\sqrt{2gh\frac{a_{(t)}}{g}}$$

$$= CA\sqrt{2ha_{(t)}}$$

$$Q_{(t)} = 1.414\ CA\sqrt{h}\sqrt{a_{(t)}}$$

where

C = Nondimensional
A = Area of orifice (sq ft)
h = Static head (ft)
$a_{(t)}$ = Acceleration (ft/sec).

$Q_{(t)}$ has the units $ft^2\sqrt{ft\ (ft/sec^2)}$

= cubic feet per second.

For a given pulse,

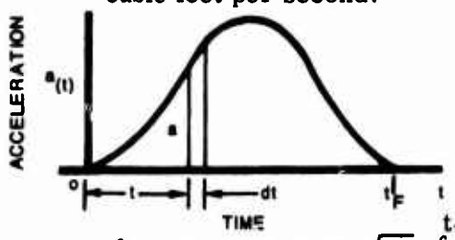

the total flow will be $Q_T = \int Q_{(t)}dt = 1.414\ CA\sqrt{h}\ \int_0^{t_F} a_{(t)}^{1/2}dt$ when C can be considered constant.

For a rectangular pulse

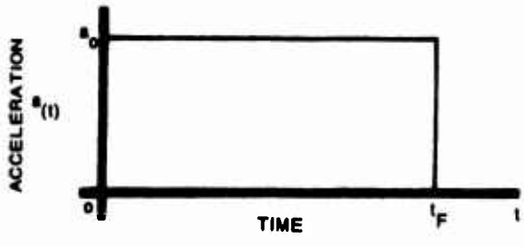

$$Q_T = 1.414\ CA\sqrt{ha_o t_F}$$

where

a_o = Peak acceleration
t_F = Pulse duration.

For a triangular pulse

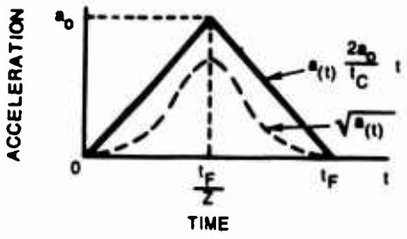

$$\int_o^{t_F} \sqrt{a_{(t)}}\,dt = 2 \int_o^{\frac{t_F}{2}} \left(\frac{2a_o}{t_F}\right)^{1/2} t^{1/2}\,dt$$

$$= 2\sqrt{2}\,\frac{\sqrt{a_o}}{\sqrt{t_F}} \int_o^{\frac{t_F}{2}} t^{1/2}\,dt$$

$$= 2\sqrt{2}\,\frac{\sqrt{a_o}}{\sqrt{t_F}}\,\frac{t}{3/2}^{3/2} \Bigg|_o^{t_F/2}$$

$$= \frac{4}{3}\sqrt{2}\,\frac{\sqrt{a_o}}{\sqrt{t_F}}\,\frac{\sqrt{t_F}}{\sqrt{2}}\,\frac{t_F}{2} = \frac{2}{3}\sqrt{a_o}\;t_F$$

Hence

$$Q_T = 1.414\,CA\sqrt{h}\,\frac{2}{3}\sqrt{a_o}\;t_F$$

$$Q_T = 0.943\,CA\sqrt{h_o}\;t_F$$

A sample calculation follows for an impact at a velocity of 40 feet per second and an acceleration level on impact of 100 G.

Assumptions:

Short tube orifice	C = 0.80
Static head	h = 2.00 feet

Triangular pulse:

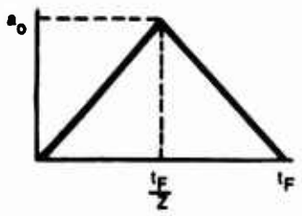

where

$\Delta V = 40$ ft/sec

$a_o = 100\ G \times g = 3220$ ft/sec^2

$t_F = 80/3220 = 0.0248$ sec.

$$Q_T = (0.943)(0.80)\frac{\pi D^2}{4}\sqrt{2 \times 3220} \times \frac{80}{3220}$$

$$Q_T = 0.592D^2 \times 1.98 = 1.18D^2$$

where

Q_T has the units of cubic feet and D is diameter of orifice in feet.

For other units:

$$Q_{T_{GAL}} = \frac{1.18D^2}{231} \times \frac{1728}{144} \qquad \text{(D in inches)}$$

$$Q_{T_{GAL}} = 0.0612D^2_{(IN.)}$$

To provide some comparison the static loss is calculated through the same orifice in 1 second.

$$Q_{STAT} = CA\sqrt{2gh}$$

$$= 0.80\ \frac{\pi D^2}{4} \times \frac{1728}{231 \times 144}\ \sqrt{2g}\ \sqrt{h}$$

where

h = 2 feet

D in inches

$$Q_{STAT} = 0.371D^2 .$$

Therefore,

$$\frac{Q_{STAT}}{Q_T} = \frac{0.371D^2}{0.0612D^2} = 6.07 .$$

This difference is graphically illustrated below.

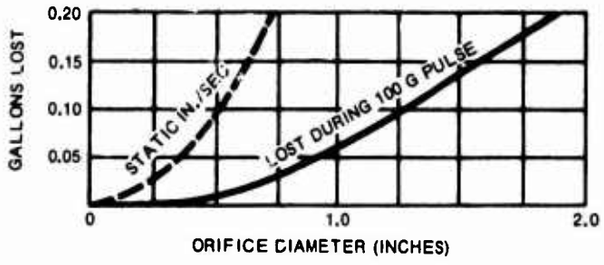

Although the total loss in 1 second under static conditions is greater than the loss occurring during impact, the velocity of the exiting fluid is greater during impact, as the following calculations show.

Velocity of fluid under static head

h = 2 feet

$V_{STAT} = \sqrt{2gh} = \sqrt{2(32)(2)} = 11.3$ feet per second.

Velocity of fluid at peak of crash pulse

100 G
h = 2 feet

$V_{Impact} = \sqrt{2gh_{(t)}}$

$V_{Impact} = \sqrt{(2)(32)(200)}$

$V_{Impact} = 113$ feet per second.

This difference in velocity leads to quite different spray patterns under static and impact conditions. The horizontal versus the vertical displacement of the exiting fluid may be calculated from the following relations:

$$X = VT$$

$$Y = gT^2 = g\left(\frac{X}{V}\right)^2$$

where

X = Horizontal displacement (ft)
Y = Vertical displacement (ft)
g = Acceleration due to gravity
V = Velocity (ft/sec).

The spray patterns thus calculated for these two velocities are shown below.

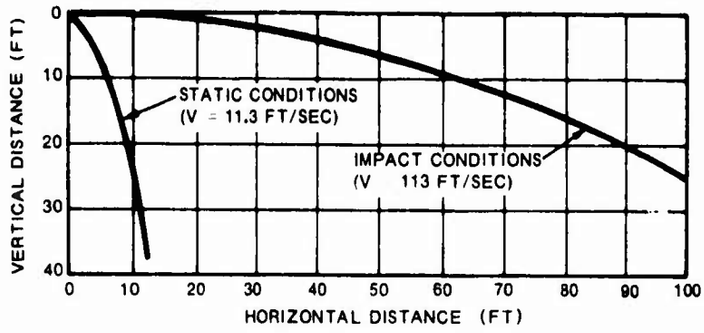

Horizontal Versus Vertical Displacement of Fluid Expelled From Orifice

APPENDIX IV

TENSILE AND SHEAR TESTS OF FUEL LINES AND FITTINGS

TEST OBJECTIVES

The objectives of this series of tests were to determine (1) the failure mode of fuel lines and fittings when subjected to tensile and shear loads, (2) the load at which failure occurs, and (3) maximum extension at failure.

TEST PROCEDURE

The test specimens were composed of various combinations of flexible hose, rigid aluminum tubing, and aluminum fittings, all of which are in common use in the fuel-transfer systems of the four aircraft studied. Three outer-diameter sizes of hose and tubing, along with the respective fittings, were tested; these sizes corresponded to 3/8-, 5/8-, and 1-inch tubing.

The flexible hose chosen for this test series was Aeroquip 601 hose, which is used extensively within the fuel tanks of the UH-1 helicopters. This hose consists of a seamless, synthetic inner tube reinforced with a partial braid of stainless steel wire. A full outer cover of stainless steel wire braid completes the configuration. The hose was used in conjunction with aluminum Aeroquip hose fitting 816 (straight) or 8891 (90-degree elbow). The hose and fittings were assembled by the manufacturer.

The rigid tubing tested was 5052-0 aluminum tubing with a wall thickness of 0.035 inch. This tubing was flared at the end for use with standard aluminum AN818 nuts and MS20819 sleeves.

The hose and tube assemblies were connected to various standard aluminum aircraft fittings. The fittings used in these tests were AN815 flared tube unions, AN832 flared tube bulkhead and universal unions, and AN833 flared tube bulkhead and universal 90-degree elbows. AN924 nuts were used with the bulkhead fittings. All connections were tightened to the torque values specified in Aeronautical Design Standard AND10064.

The various test configurations, along with the test series numbers, are listed in Table XIII. Figures 89 through 96 illustrate representative test arrangements and are referenced in Table XIII to the corresponding test number. All tests were conducted on an Instron Universal Testing Instrument, Model TT-C. The loading rate was 2 inches per minute. Sample elongation was obtained from a synchronously driven chart recorder that was also operated at a speed of 2 inches per minute.

FOR OFFICIAL USE ONLY

TABLE XIII

TEST CONFIGURATIONS OF LINES AND FITTINGS

Test Series Number	Hose or Tubing	Hose Fitting	Aircraft Fitting	Load Direction	Illustration Number
1-1	Hose	816	AN815	Tension	-
1-2	Hose	816	AN832*	Tension	Figure 90
1-3	Tubing	-	AN815	Tension	-
1-4	Tubing	-	AN832*	Tension	-
2-1	Hose	816	AN815	Shear	Figure 91
2-2	Hose	816	AN832*	Shear	
2-3	Tubing	-	AN815	Shear	Figure 92
3-1	Hose	816	AN833**	Tension	-
3-2	Hose	816	AN833*	Tension	Figure 93
3-3	Hose	8891	AN815	Tension	Figure 94
3-4	Hose	8891	AN832*	Tension	-
3-5	Tubing	-	AN833**	Tension	-
4-1	Hose	816	AN833**	Shear	-
4-2	Hose	816	AN833*	Shear	-
4-3	Hose	8891	AN815	Shear	-
4-4	Hose	8891	AN832*	Shear	Figure 95
4-5	Tubing	-	AN833**	Shear	-

* Simulates through-bulkhead connection (Figure 89).
** Simulates component connection (Figure 90).

Fitting Descriptions:

816 Hose - straight
8891 Hose - 90-degree elbow
AN815 - flared tube union
AN832 - flared tube bulkhead and universal union
AN833 - flared tube bulkhead and universal 90-degree elbow

FOR OFFICIAL USE ONLY

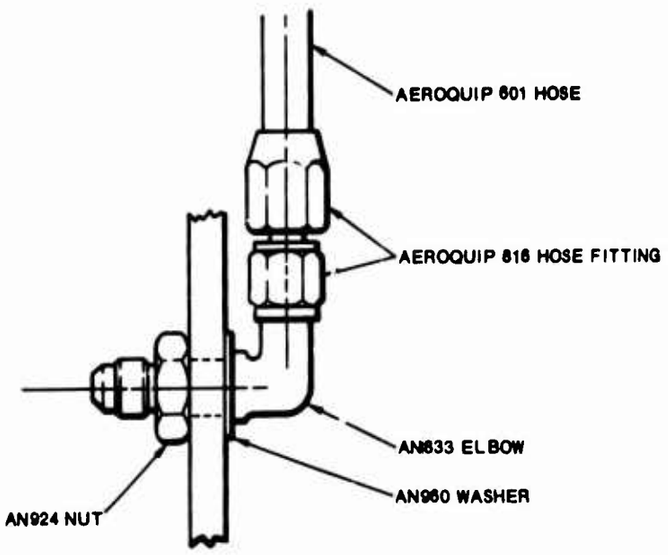

Figure 89. Typical Through-Bulkhead Connection

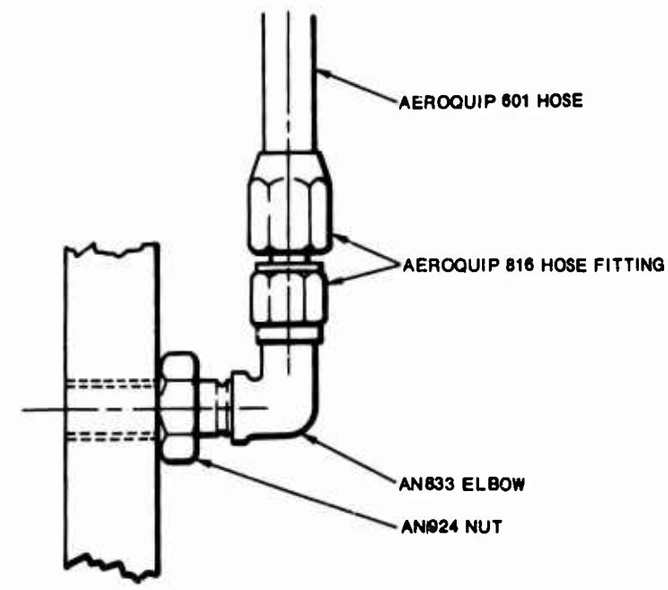

Figure 90. Typical Component Connection.

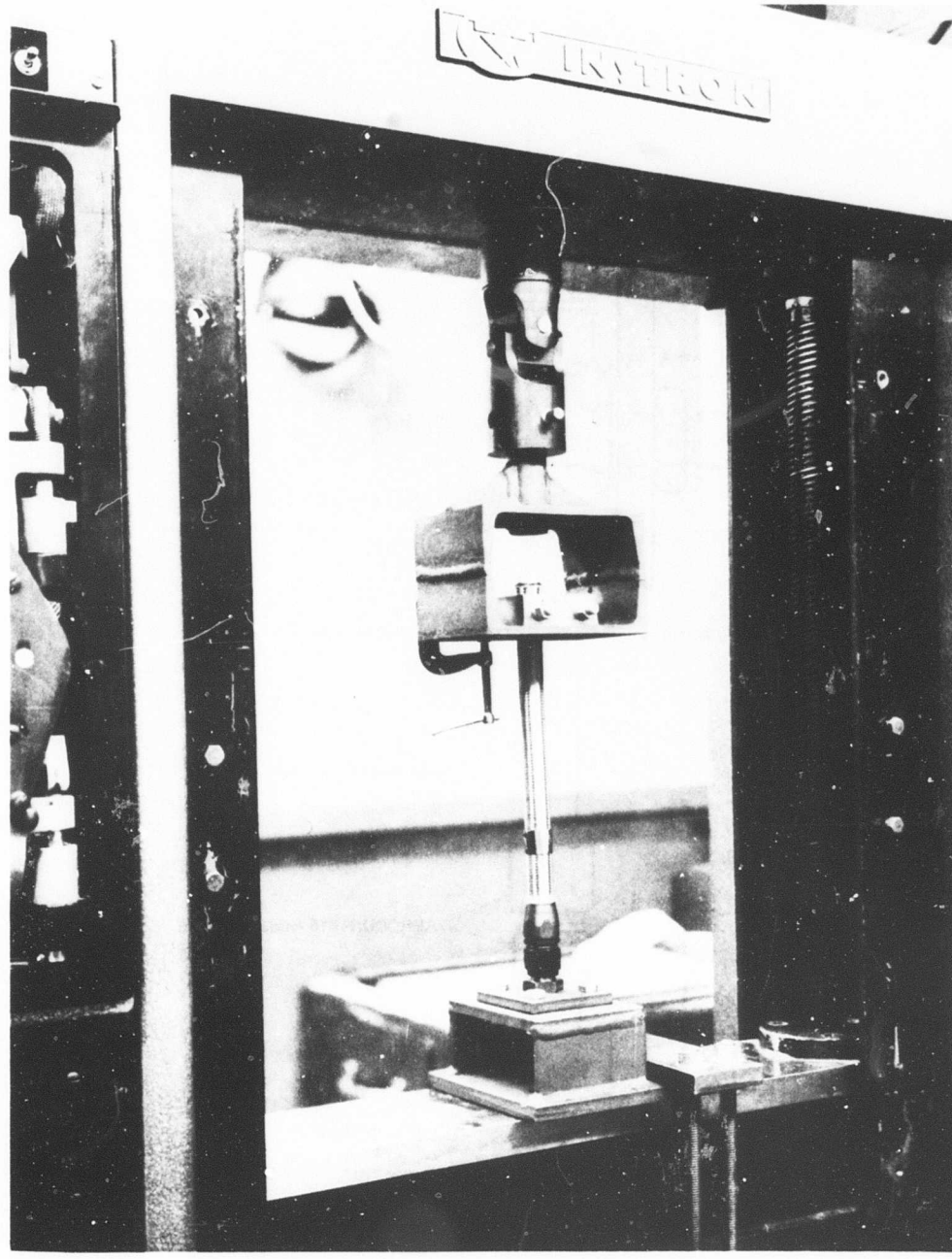

Figure 91. Test Series 1-2.

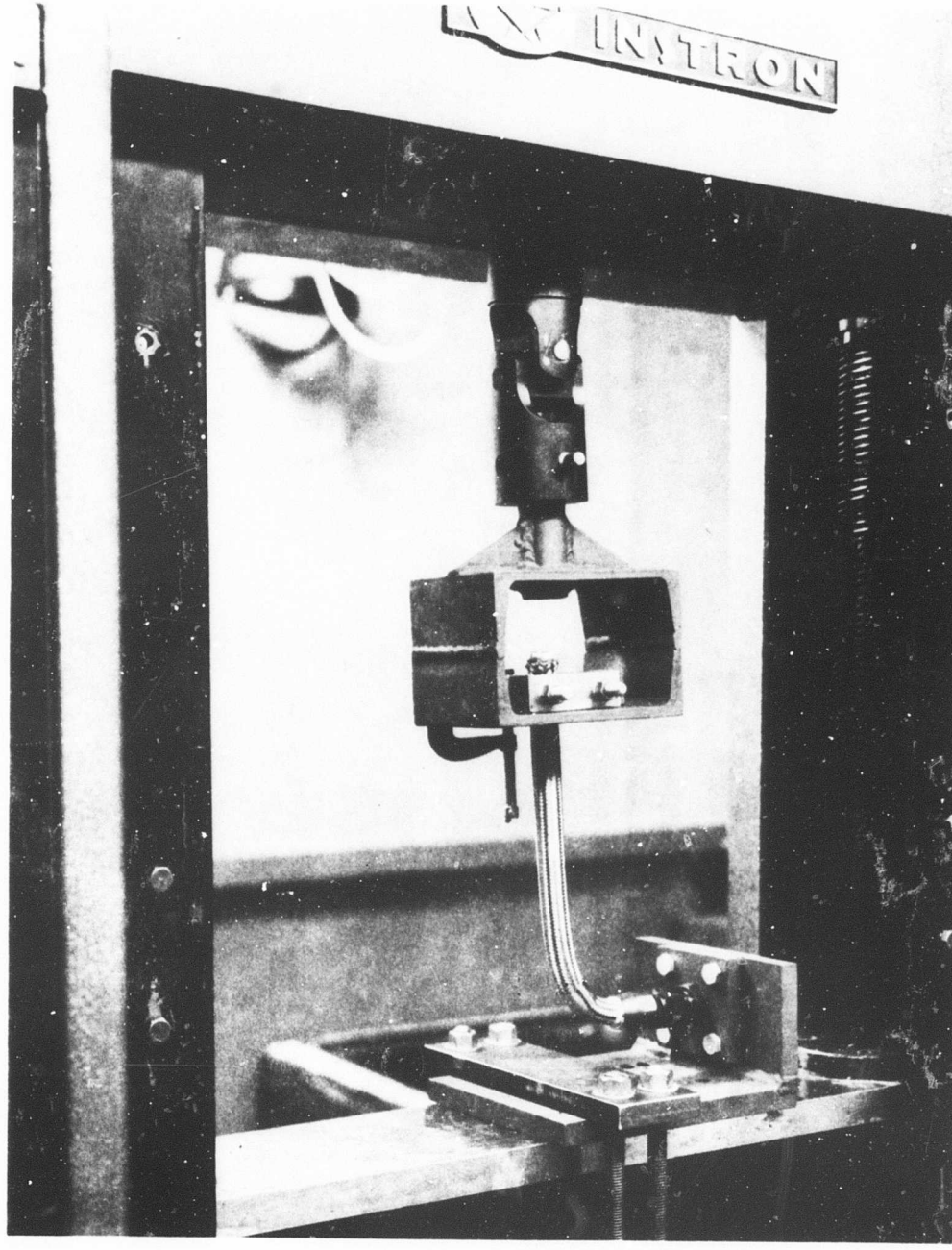

Figure 92. Test Series 2-1.

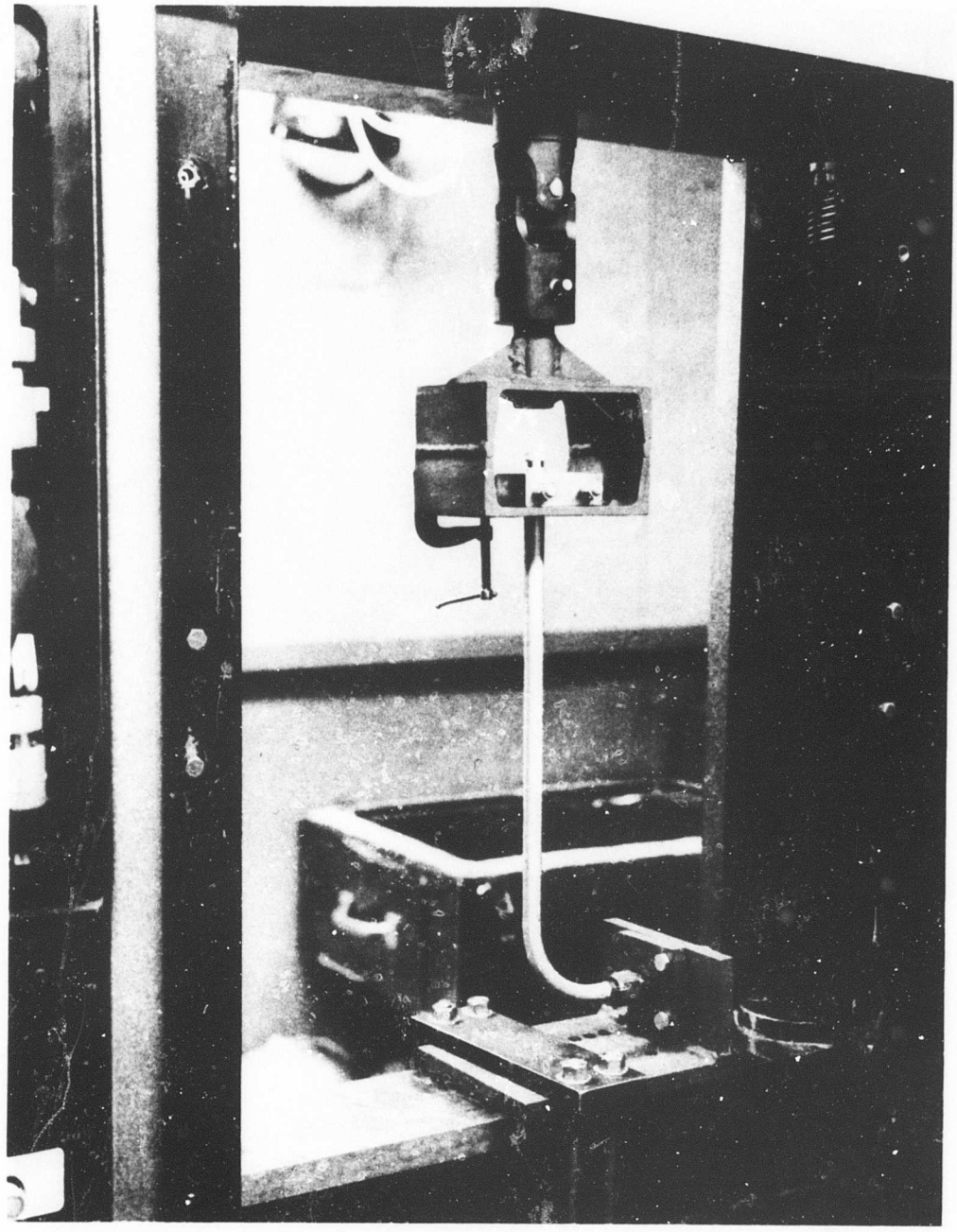

Figure 93. Test Series 2-3.

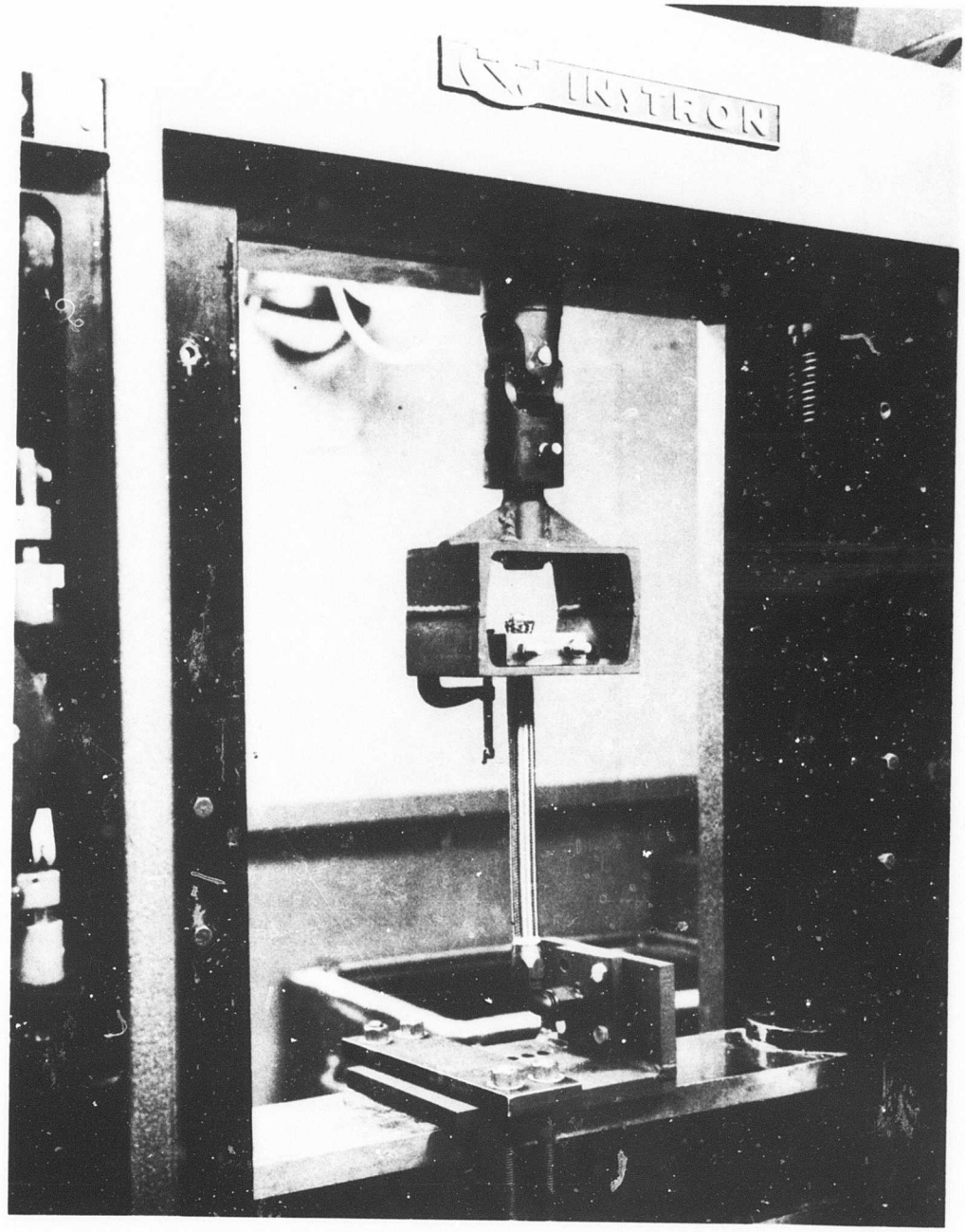

Figure 94. Test Series 3-2.

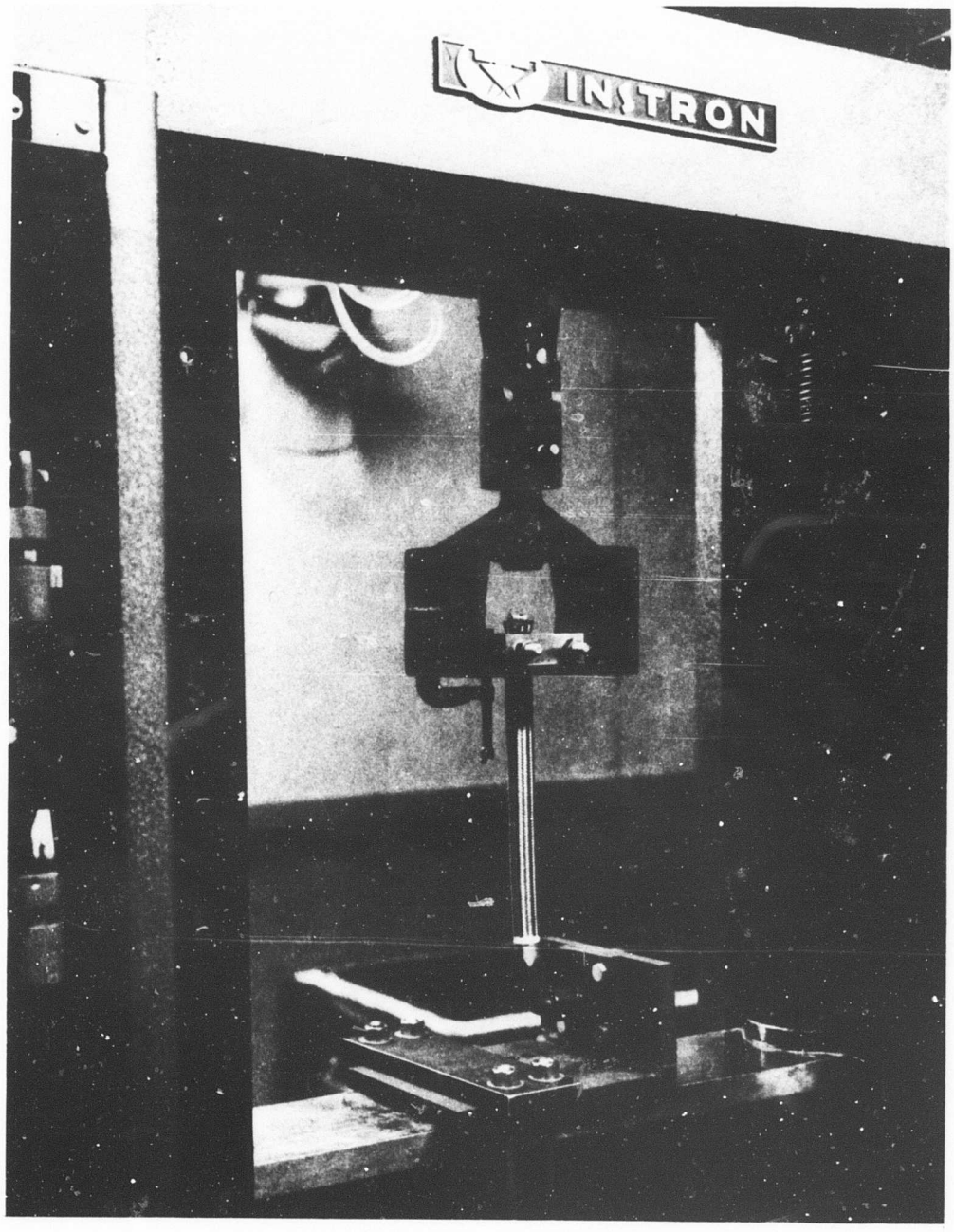

Figure 95. Test Series 3-3.

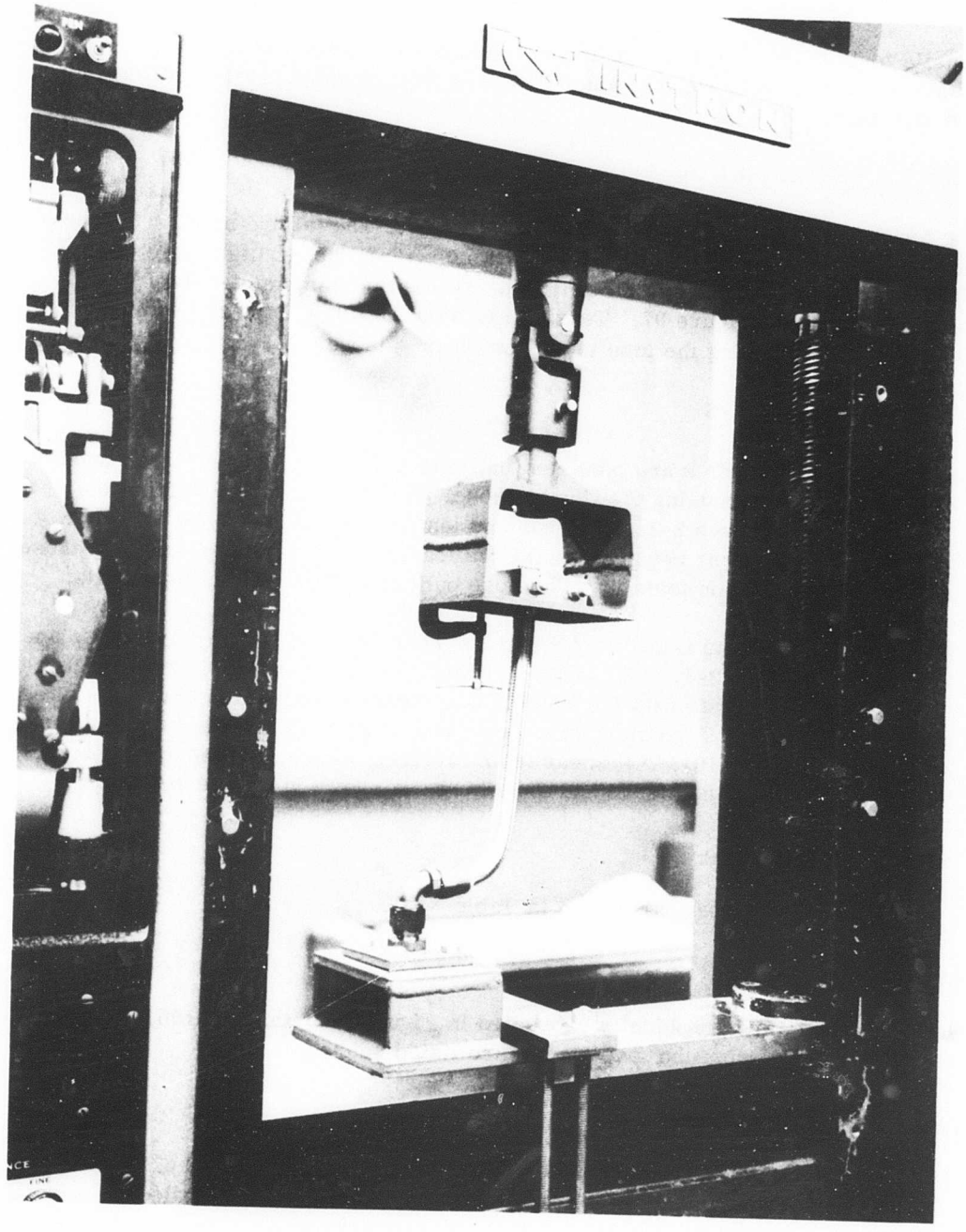

Figure 96. Test Series 4-4.

The number of tests conducted with each configuration and size are listed in Table XIV.

Tensile tests to determine the ultimate strength and elongation of the Aeroquip hose when tested alone were conducted on a 60,000-pound capacity Baldwin Universal Test Machine.

TENSILE TEST RESULTS

The tensile test results are tabulated in Table XV. The failure mode in all these tests was hose or tube pullout from the fittings with no apparent damage to the hose, tube, or fittings themselves. The flexible hose pulled completely out of the hose fitting, as shown in Figure 97. Tension loads on the tubing straightened the tube-end flare, thus allowing the tube to pull out of the sleeve.

SHEAR TEST RESULTS

Results of the shear tests are tabulated in Table XVI. Fitting failures occured in all but one of the tests using the flexible hose. A 1-inch hose pulled from the fitting during test series 2-1. This hose pullout was undoubtedly due to a poor hose-fitting installation, because the failure load was considerably less than those observed for the tension tests in which hose pullout was the only failure mode.

The only aircraft fitting failures (AN fittings) occurred with the 3/8-inch hose and fittings in test series 2-1, 2-2, and 4-1. This type of failure is shown in Figure 98. The remaining tests with the flexible hose resulted in manufacturer-installed hose-fitting failures. Typical failures occurring during these tests are shown in Figures 99, 100, and 101. All shear tests involving the rigid aluminum tubing resulted in failure of the sleeve and the tubing, as shown in Figure 102.

HOSE TENSILE TESTS

The results of these tests are given in Table XVII.

CONCLUSIONS

The test results are graphically presented in Figures 103 through 106. Conclusions that can be drawn from the test results are listed below.

Tension Tests

1. There is no significant difference between the failure load of hose or tubing in the 5/8- and 1-inch size. The 3/8-inch tubing failed at

TABLE XIV

NUMBER OF LINE AND FITTING TESTS CONDUCTED IN EACH CATEGORY

Test Series Number	Number of Tests*		
	3/8-in. OD	5/8-in. OD	1-in. OD
1-1	2	3	2
1-2	2	3	0
1-3	2	3	2
1-4	2	3	0
2-1	2	3	2
2-2	2	3	0
2-3	2	3	2
3-1	2	3	2
3-2	2	3	0
3-3	2	3	2
3-4	2	3	0
3-5	2	3	2
4-1	2	3	0
4-2	2	3	0
4-3	2	3	2
4-4	2	3	0
4-5	2	2	2

* Total number of tests:

3/8-in. OD	-	34
5/8-in. OD	-	50
1-in. OD	-	18
		102

FOR OFFICIAL USE ONLY

TABLE XV

TENSILE TEST RESULTS, LINES AND FITTINGS

Test Series Number	Failure Load (lb)			Average Elongation to Failure (%)			Failure Mode
	3/8-In. OD	5/8-In. OD	1-In. OD	3/8-In. OD	5/8-In. OD	1-In. OD	
1-1	830	1690	2660				Hose pullout (all sizes)
	730	1650	2300	47	53	45	
		1665					
1-2	665	1800					Hose pullout (all sizes)
	890	1695	-	54	57	-	
		1745					
1-3	500	1585	2475				Tube pullout (all sizes)
	575	1635	2270	1	6	5	
		1595					
1-4	520	1645					Tube pullout (all sizes)
	615	1540	-	1	6	-	
		1580					
3-1	730	1685	2825				Hose pullout (all sizes)
	770	1730	2370	47	56	48	
		1635					
3-2	755	1880					Hose pullout (all sizes)
	645	1650	-	55	54	-	
		1800					
3-3	725	1610	2200				Hose pullout (all sizes)
	665	1305	1360	45	48	46	
		1625					
3-4	740	1590					Hose pullout (all sizes)
	675	1510	-	58	59	-	
		1615					
3-5	565	1950	2250				Tube pullout (all sizes)
	575	1600	2450	1	8	5	

FOR OFFICIAL USE ONLY

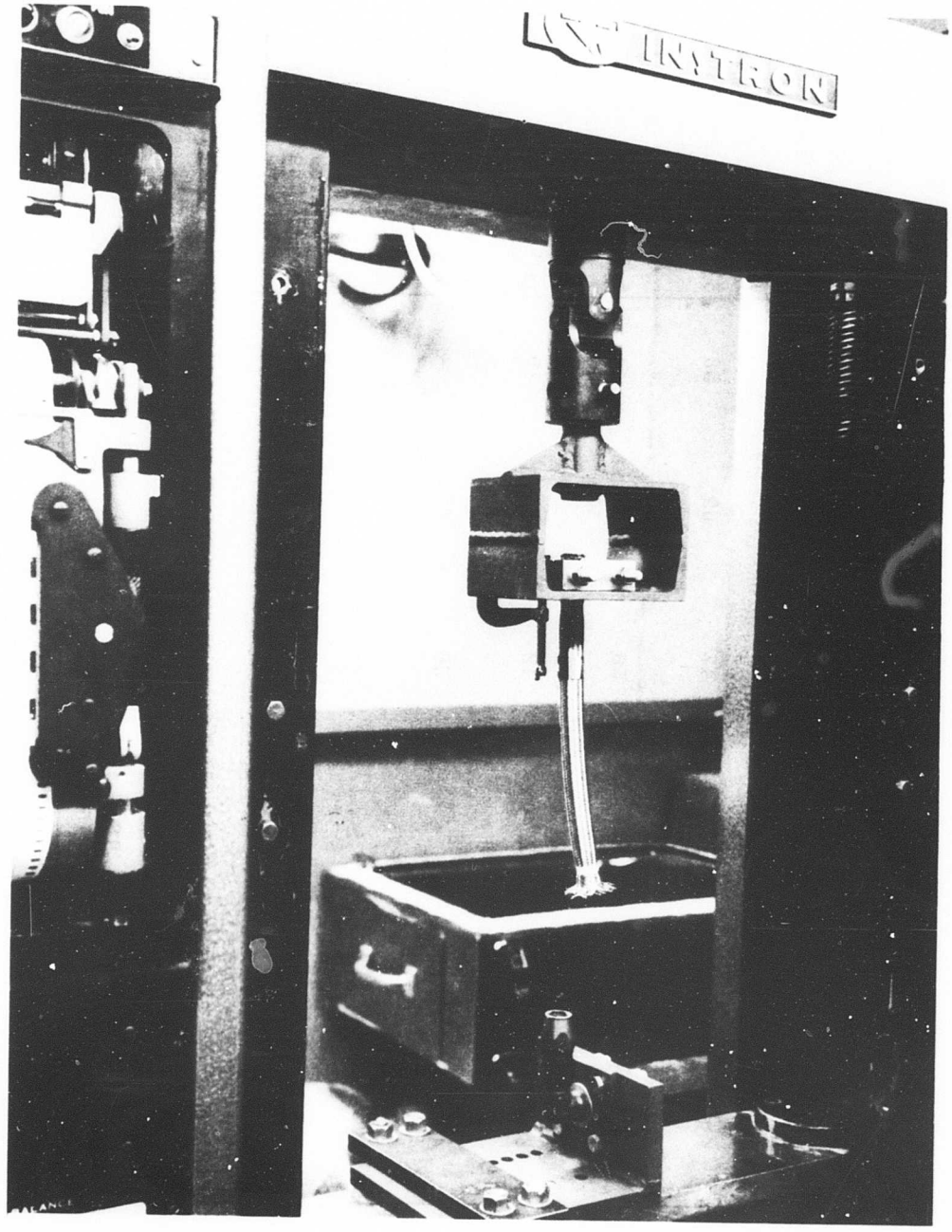

Figure 97. Flexible Hose Pulled From Fitting Under Tension Load (Test Series 3-2).

FOR OFFICIAL USE ONLY

TABLE XVI

SHEAR TEST RESULTS, LINE AND FITTINGS

Test Series Number	Failure Load (lb)			Average Elongation to Failure (%)			Failure Mode
	3/8-In. OD	5/8-In. OD	1-In. OD	3/8-In. OD	5/8-In. OD	1-In. OD	
2-1	-	835	1330*				3/8 in. - AN fitting failure
	460	980	1770	47	69	53	5/8 in. - Hose-fitting failure
		810					
2-2	560	805					3/8 in. - AN fitting failure
	560	885	-	56	62	-	5/8 in. - Hose-fitting failure
		900					
2-3	770	1335	2175				Tube and sleeve failure
	690	1280	2040	12	15	19	(all sizes)
		1040					
4-1	445	930					3/8 in. - AN fitting failure
	445	1150	-	56	62	-	5/8 in. - Hose-fitting failure
		1125					
4-2	555	875					Hose-fitting failure
	555	915	-	69	62	-	
		920					
4-3	155	475	1240				Hose-fitting failure
	160	525	1060	50	55	54	(all sizes)
		540					
4-4	160	460					Hose-fitting failure
	210	535	-	65	56	-	(all sizes)
		480					
4-5	810	1245	1855				Tube and sleeve failure
	750	1220	2150	13	15	19	(all sizes)

* Hose pullout.

FOR OFFICIAL USE ONLY

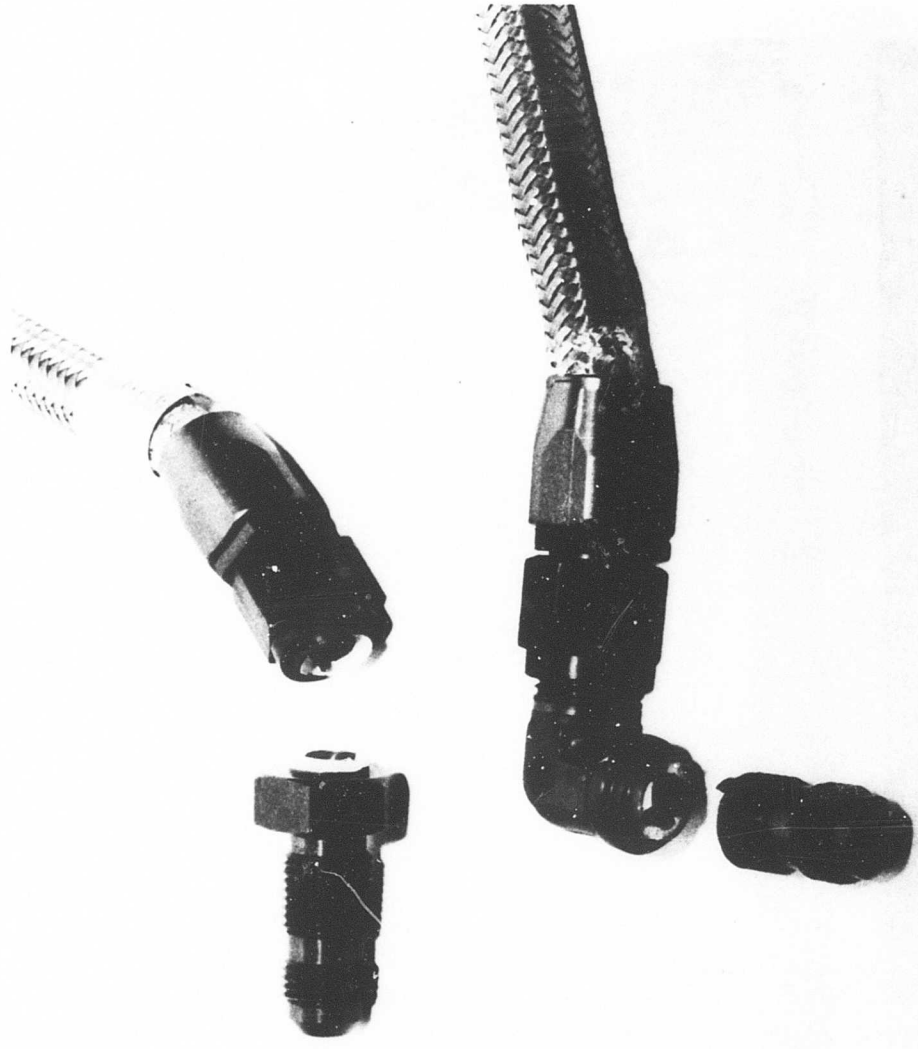

Figure 98. AN Fitting Failures, Test Series 2-2 (Top) and Test Series 4-1 (Bottom).

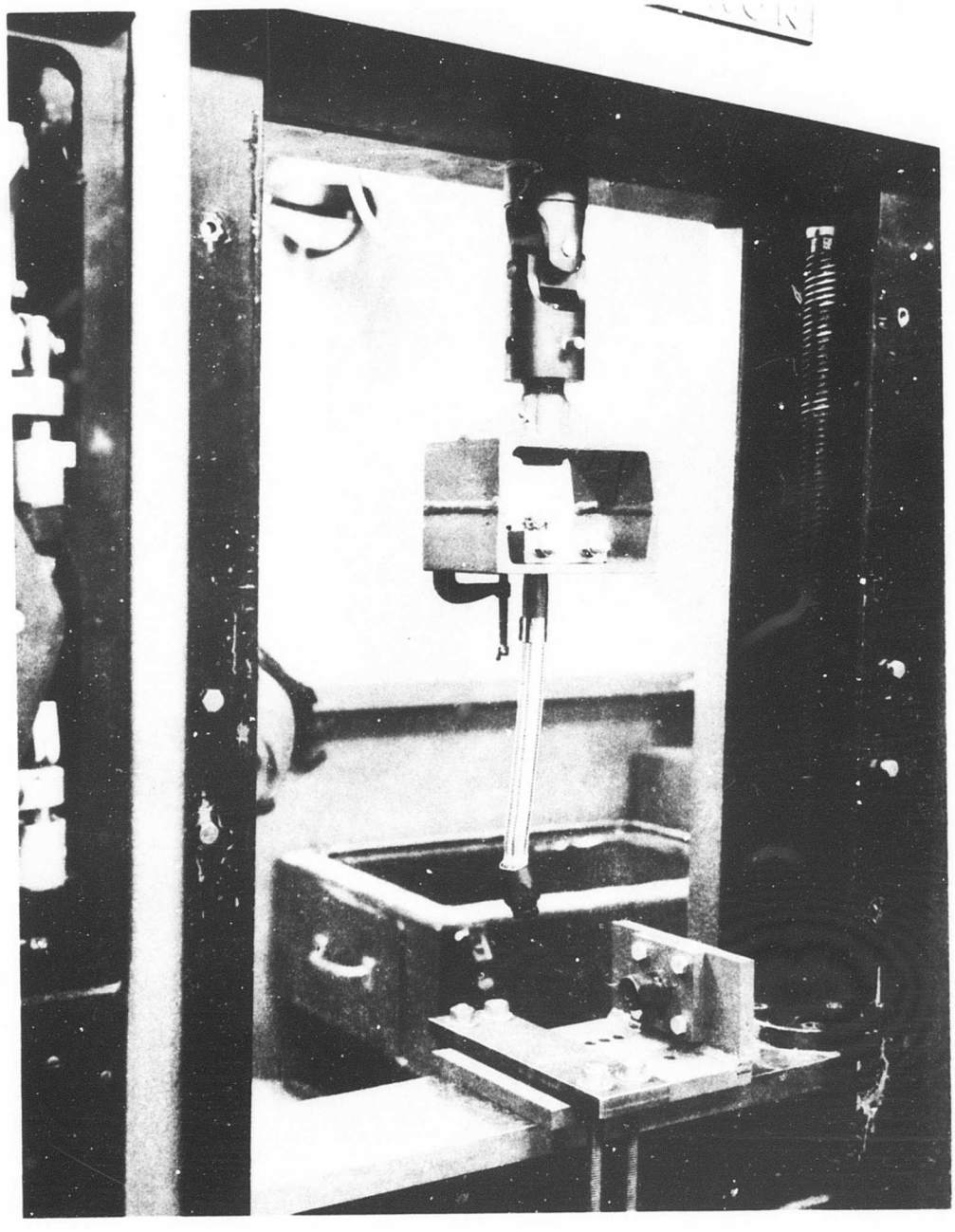

Figure 99. Hose-Fitting Failure Under Shear Load (Test Series 2-1).

Figure 100. Hose-Fitting Failure (Test Series 4-1).

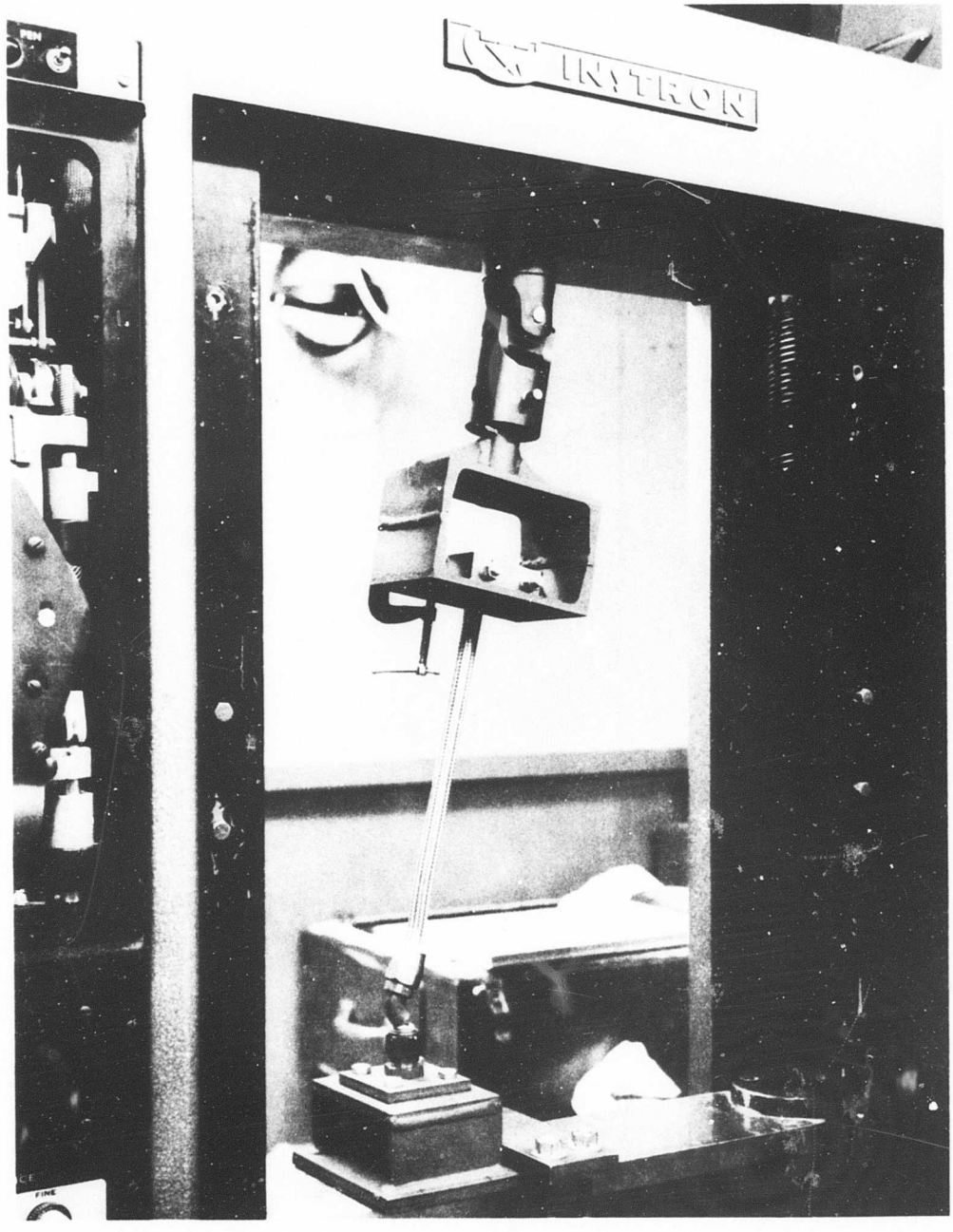

Figure 101. Hose-Fitting Failure Under Shear Load (Test Series 4-4).

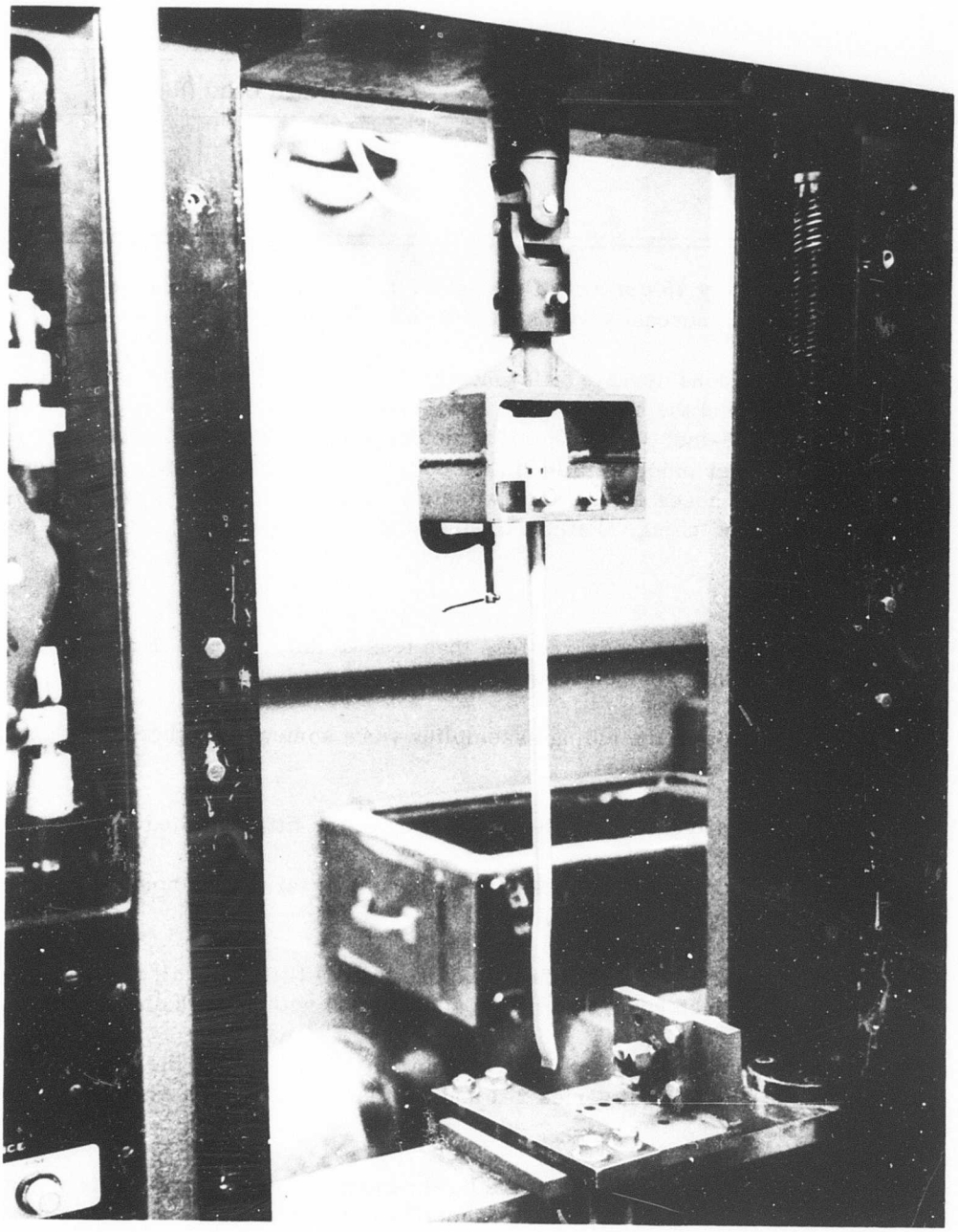

Figure 102. Tubing Failure Under Shear Load (Test Series 2-3).

TABLE XVII

TENSILE TEST RESULTS, AEROQUIP 601 HOSE

Hose Size (in.)	Failure Load (lb)
3/8	1525
5/8	2860

approximately 75 percent of the hose failure load. As might be expected, failure load increases with specimen size (Figures 103 through 105).

2. There is a considerable difference between the elongation-to-failure of the tubing and the hose (Figure 106). This difference is most pronounced with the 3/8-inch size. The 3/8-inch hose extends approximately 50 times farther prior to failure than does the same size tubing, while the larger size hoses extend approximately nine times farther than the comparable size tubing. Failure modes of the hose and tubing are the same.

Shear Tests

1. The shear failure loads are less than tensile failure loads in all cases except for the 3/8-inch tubing (Figures 103 through 105).

2. Failure loads of the tubing assemblies were somewhat higher than those of the hose assemblies.

3. The tubing and sleeves failed before any of the fittings failed.

4. The Aeroquip elbows (test series 4-3 and 4-4) failed at a much lower load than any other fittings.

5. The straight hose fittings failed before the AN fittings in all tests of the 5/8- and 1-inch hose, and in one series (4-2) with the 3/8-inch hose.

6. There was no significant difference in the failure load of the 3/8-inch AN straight unions (test series 2-1 and 2-2) and the 3/8-inch AN elbows (test series 4-1).

7. The elongation-to-failure of the hose assemblies was approximately four times as great as the tubing assemblies in the 3/8- and 5/8-inch sizes and approximately three times as great for the 1-inch size.

TABLE XVII

TENSILE TEST RESULTS, AEROQUIP 601 HOSE

Hose Size (in.)	Failure Load (lb)
3/8	1525
5/8	2860

approximately 75 percent of the hose failure load. As might be expected, failure load increases with specimen size (Figures 103 through 106).

2. There is a considerable difference between the elongation-to-failure of the tubing and the hose (Figure 106). This difference is most pronounced with the 3/8-inch size. The 3/8-inch hose extends approximately 50 times farther prior to failure than does the same size tubing, while the larger size hoses extend approximately nine times farther than the comparable size tubing. Failure modes of the hose and tubing are the same.

Shear Tests

1. The shear failure loads are less than tensile failure loads in all cases except for the 3/8-inch tubing (Figures 103 through 105).

2. Failure loads of the tubing assemblies were somewhat higher than those of the hose assemblies.

3. The tubing and sleeves failed before any of the fittings failed.

4. The Aeroquip elbows (test series 4-3 and 4-4) failed at a much lower load than any other fittings.

5. The straight hose fittings failed before the AN fittings in all tests of the 5/8- and 1-inch hose, and in one series (4-2) with the 3/8-inch hose.

6. There was no significant difference in the failure load of the 3/8-inch AN straight unions (test series 2-1 and 2-2) and the 3/8-inch AN elbows (test series 4-1).

7. The elongation-to-failure of the hose assemblies was approximately four times as great as the tubing assemblies in the 3/8- and 5/8-inch sizes and approximately three times as great for the 1-inch size.

In comparing the data in Figures 103 and 104 with those in Table XVII, it can be seen that both tension and shear failures occurred at approximately half of the load necessary to fail the hose itself.

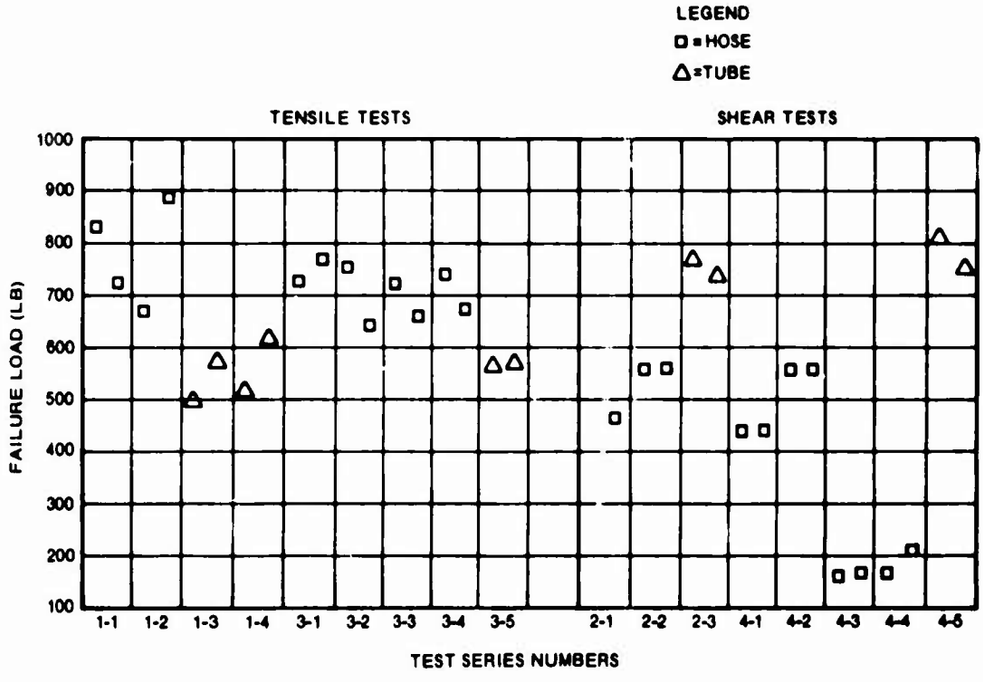

Figure 103. Hose, Tube, and Fitting Tests, 3/8 Inch.

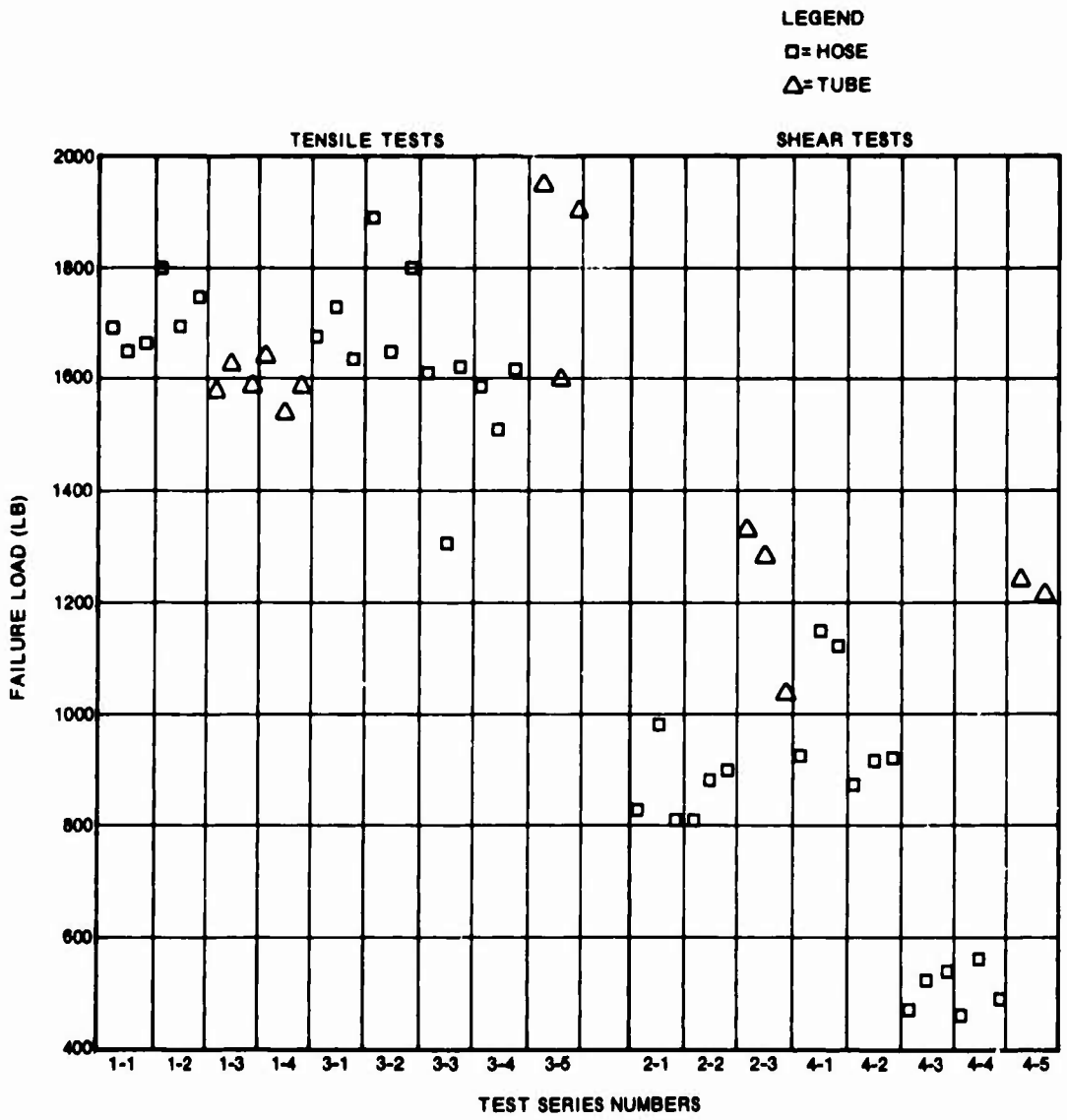

Figure 104. Hose, Tube, and Fitting Tests, 5/8 Inch.

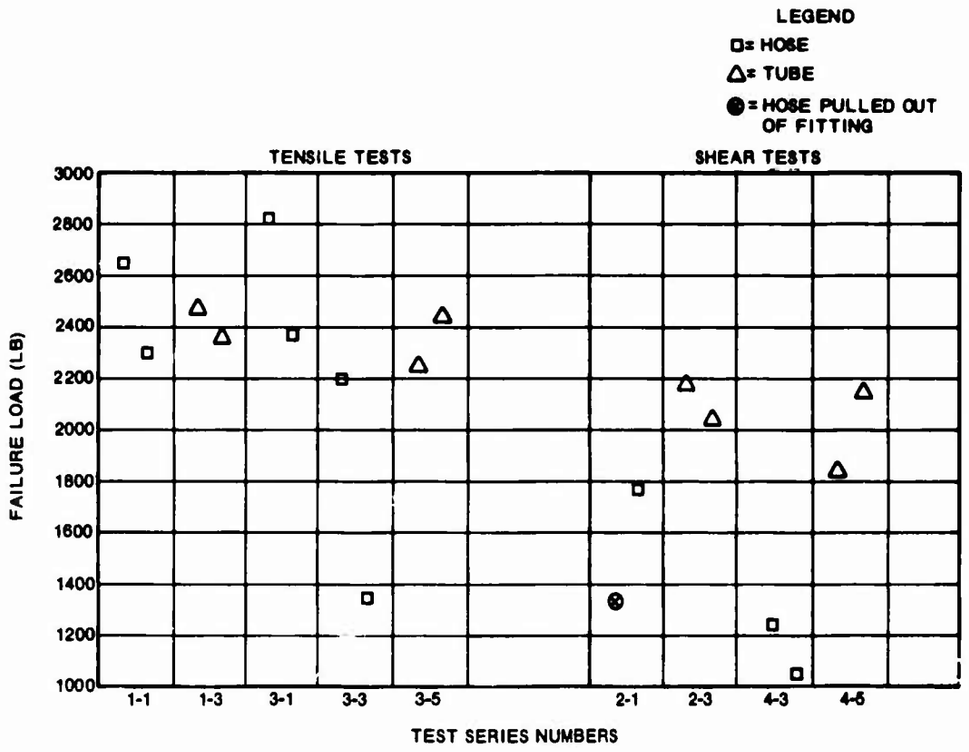

Figure 105. Hose, Tube, and Fitting Tests, 1 Inch.

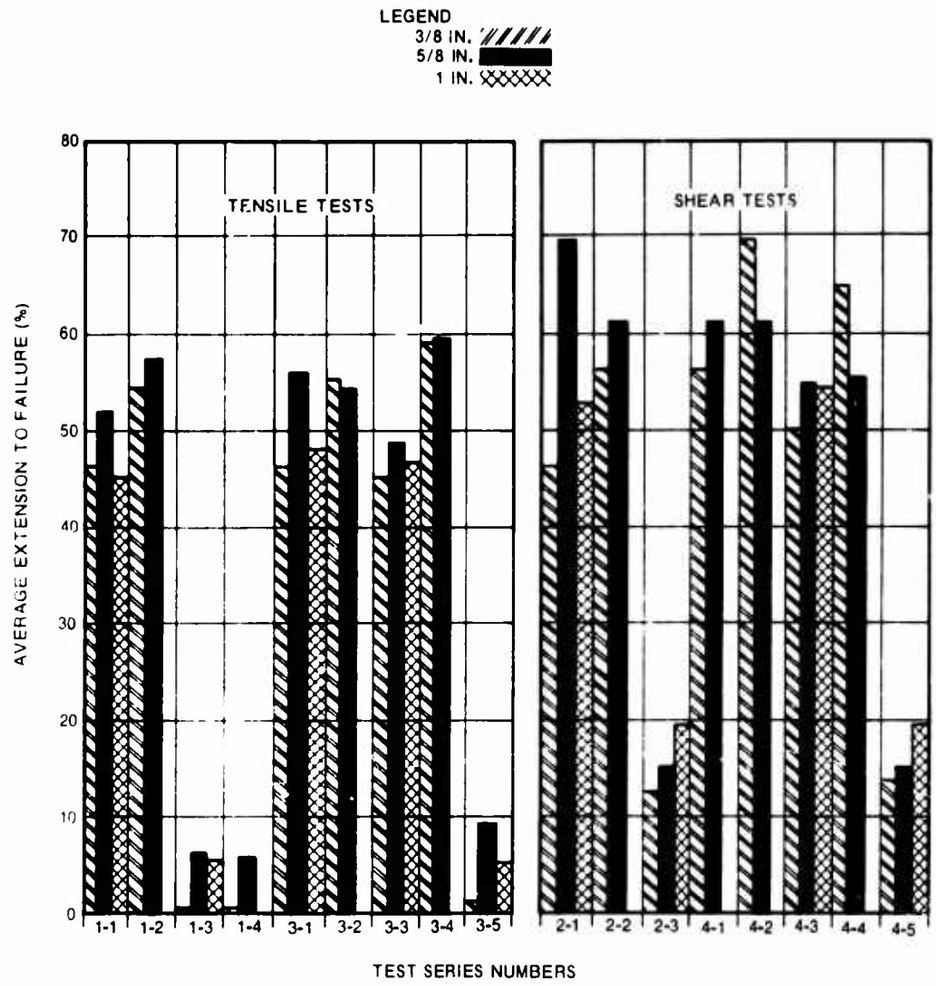

Figure 106. Extension to Failure, Hose, Tube, and Fitting Tests.

APPENDIX V

DYNAMIC TESTING OF FUEL SYSTEM COMPONENTS

This appendix includes a description of the apparatus used and the data obtained during the dynamic testing of the fuel system components.

TEST APPARATUS

Drop Tower

To subject the test components to acceleration environments, the use of a drop tower (Figure 107) was selected because: (1) the system can be used to impart velocity changes and accelerations closely approximating actual crash environments; (2) the repeatability of velocity and acceleration environments is good; and (3) it is an economical method of conducting a large number of tests. The maximum drop height for the universal jig (Figure 108) was 53 feet. Maximum impact values obtained using this apparatus were: (1) velocity - 58 feet per second; (2) acceleration - 156 G; and (3) pulse duration - 0.23 second. A 12-inch-deep knife blade was attached to the bottom of the drop jig to guide the jig during impact into the gravel bed. This blade was also used to increase the pulse duration slightly and decrease the onset rate. The blade was used throughout the test program.

The force was applied to the test specimen by use of a suspended weight guided within the universal drop-test jig. As the system was subjected to the acceleration applied to the jig, the suspended weight continued downward at the original velocity and a load was applied to the test specimen. The mass of the suspended weight was adjustable to ensure that sufficient energy would be available to cause specimen failure at any desired drop height.

Impact Media

The impact area, which consisted of a pit filled with pea gravel, was leveled prior to each drop to ensure the repeatability of the acceleration-curve pulse shape.

Camera Coverage

Each drop was photographed utilizing a high-speed camera (1500 frames per second). Timing marks (60 cycles per second) were superimposed on all film during test coverage.

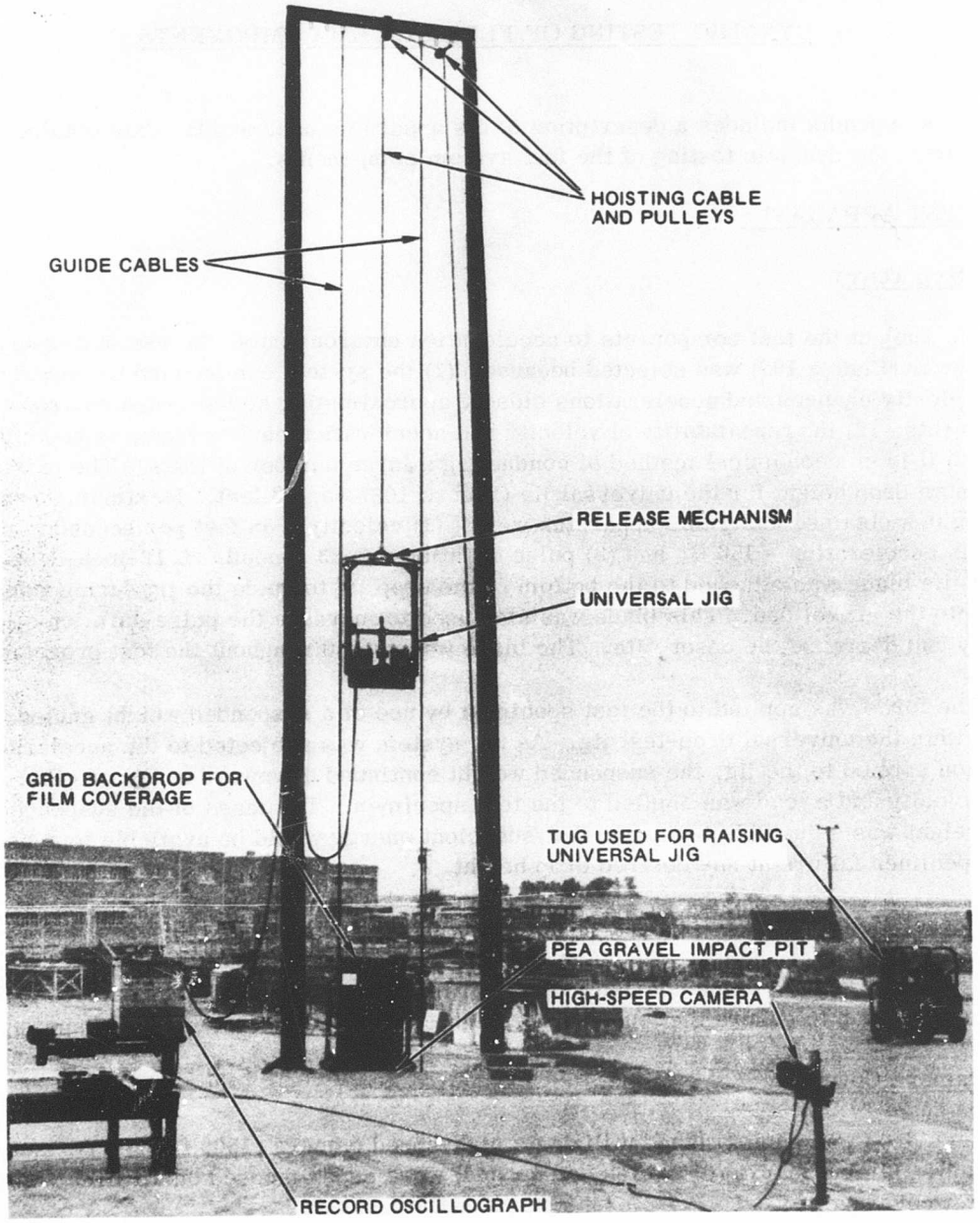

Figure 107. Drop Tower.

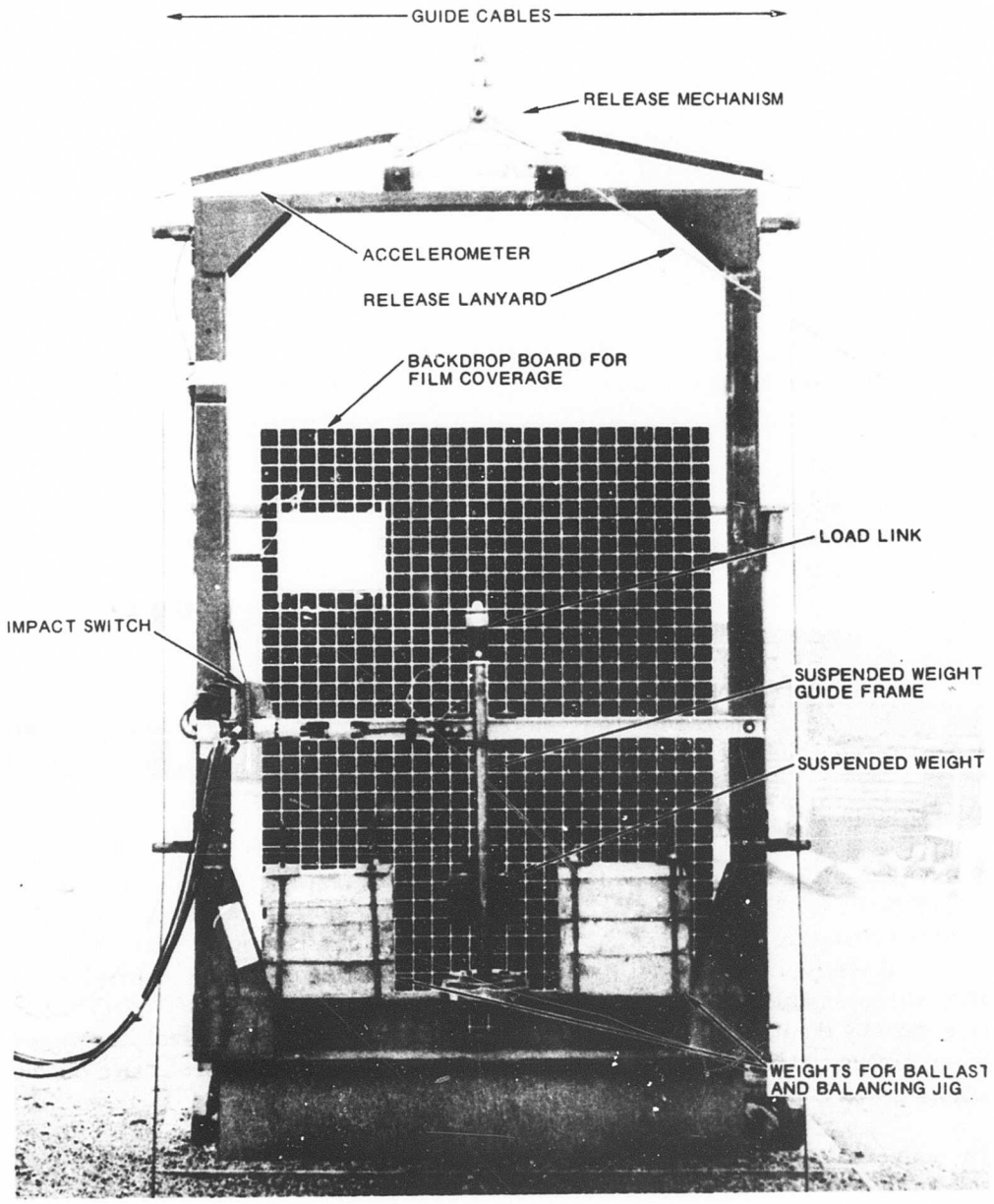

Figure 108. Universal Jig.

Instrumentation Coverage

A Control Equipment Corporation Number 5-124 oscillograph was used as the primary recording instrument.

Acceleration

A Statham Corporation Model A5-100, 100 G nominal-range accelerometer was mounted on the upper corner of the universal jig to record the acceleration to which the jig was subjected.

Load

A calibrated load link, having a zero-to-10,000-pound range, was used to connect the suspended weight to the system being tested. The duration and magnitude of the applied force during each test sequence were thus recorded.

Timing

A correlation between the oscillograph-recorded load and the high-speed camera record was obtained through the use of correlation lights for which the triggering current was recorded on the oscillograph.

Miscellaneous Recordings

Any unusual phenomena observed in the severance of the frangible portion of the test system were recorded. The penetration of the universal jig into the gravel was also recorded.

Test Systems

The universal jig was designed to hold four types of test specimens of various configurations. These four systems are: System I - a fuel line-to-fuel tank connection consisting of a breakaway fitting, a portion of a tank wall, and a hose; System II - a fuel line-to-fuel line connection consisting of a self-sealing breakaway fitting installed in a fuel line; System III - a fuel tank mounted to an aircraft structure by the use of a frangible attachment; and System IV - a fuel line attached to an aircraft structure at a bulkhead by the use of a frangible,protective bulkhead adapter.

The universal jig was weighed and balanced after each system was installed to ensure the repeatability of the acceleration pulse and the direction of force.

REVIEW OF DYNAMIC TESTING

System I

This system consisted of a fuel line connected to a fuel tank by a self-sealing breakaway fitting. The fitting assembly was a modified quick-disconnect coupling per MIL-C-7413A. The hose used was 1-1/4-inch-diameter Aeroquip Corporation Type 601 with standard Aeroquip fittings. The tank material specimen consisted of three plies of ARM-018 fuel cell material with local doublers as required. These components are shown in Figures 50, 51, and 52. Several configurations were tested; these were selected to represent the complete range of load applications that could be present in an actual crash.

The primary test objectives were to: (1) determine the feasibility of the design approach and discover possible mechanical problems not readily apparent during the design or in static testing, and (2) determine any variation in the system load-sustaining capability using several loading modes and various impact velocities.

The System I configurations are shown in Figures 109 through 115, and the data applicable to each test are presented in Tables XVIII through XXII and in Figure 116.

System I Test Conclusions

The breakaway fitting approach is feasible for increasing the degree of fuel containment during crash impacts. The breakaway connections functioned properly, except in the most severe loading modes. Results of the dynamic testing of System I revealed no unusual mechanical problems. After repeated tests, the sealing function of the fittings failed in the more severe tests. Although minor degradation was observed, the ARM-018 material and the bonded attachment to the fitting were unaffected.

Figure 116 shows the variations in the loads required to cause separation (breakaway) versus impact velocity for five loading configurations. A critical velocity of about 45 to 50 feet per second occurs for configurations 1 and 2, at which the load required to effect breakaway rapidly drops off with increasing impact velocity. This effect is apparently associated with the failure modes of the frangible collar in the valve body. As expected, the pure shear loading (Curve 4) produced the highest required breakaway load. With tension, the breakaway load generally lowers with increasing velocity impact. Conversely, in shear, the breakaway load increases with increasing impact velocity.

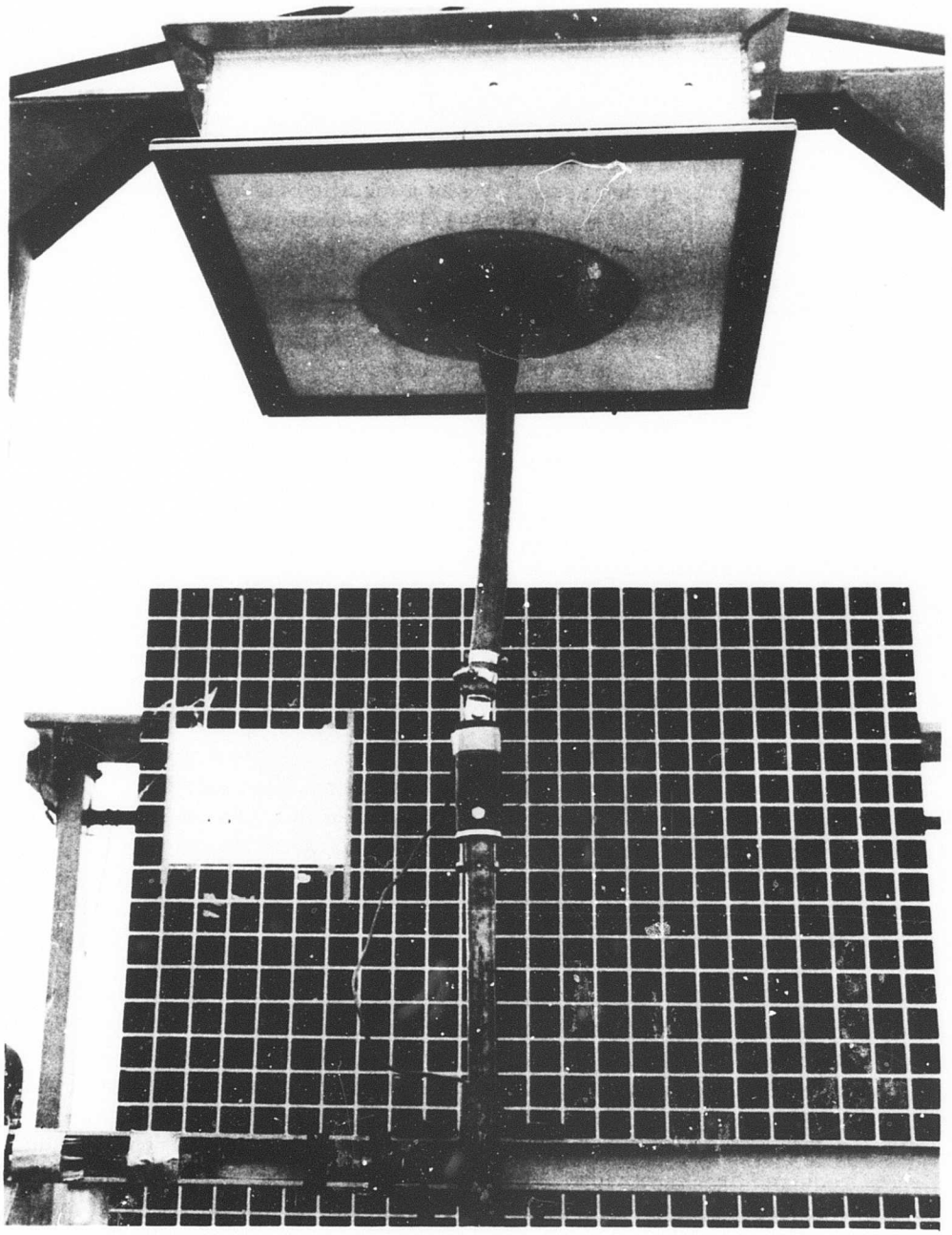

Figure 109. Fitting-to-Cell Direct Tension Load.

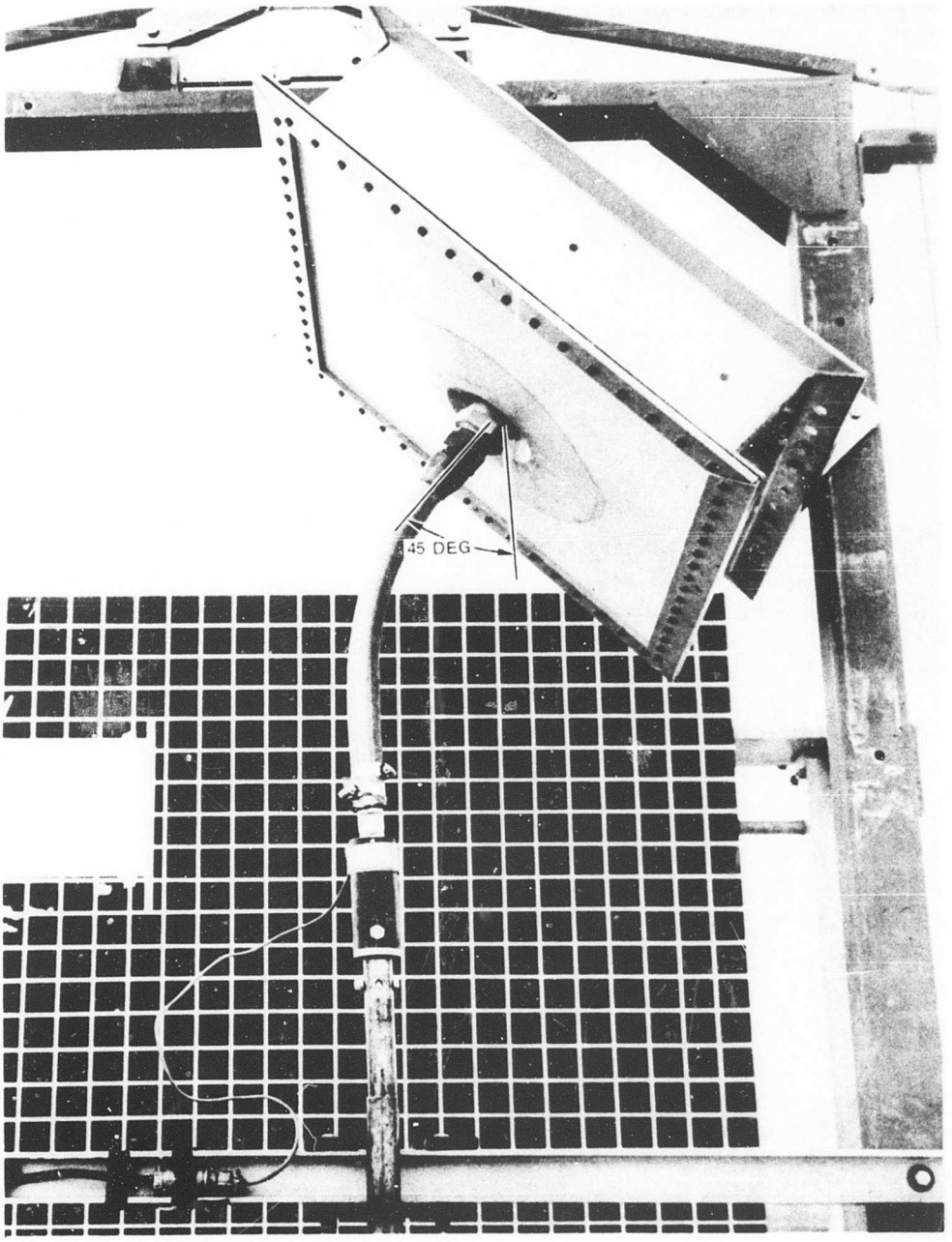

Figure 110. Fitting-to-Cell Combined Tension and Shear Load.

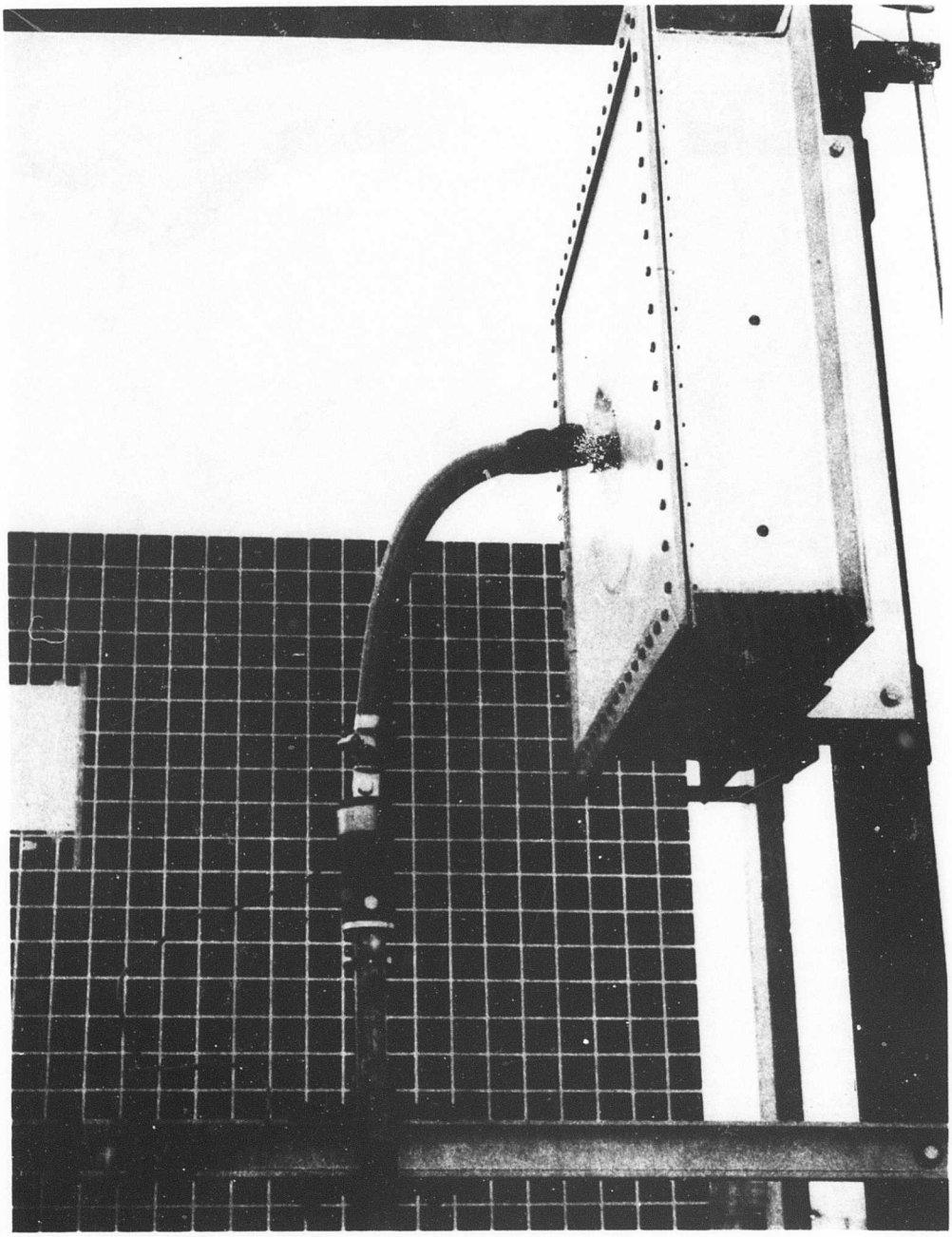

Figure 111. Fitting-to-Cell Shear Load.

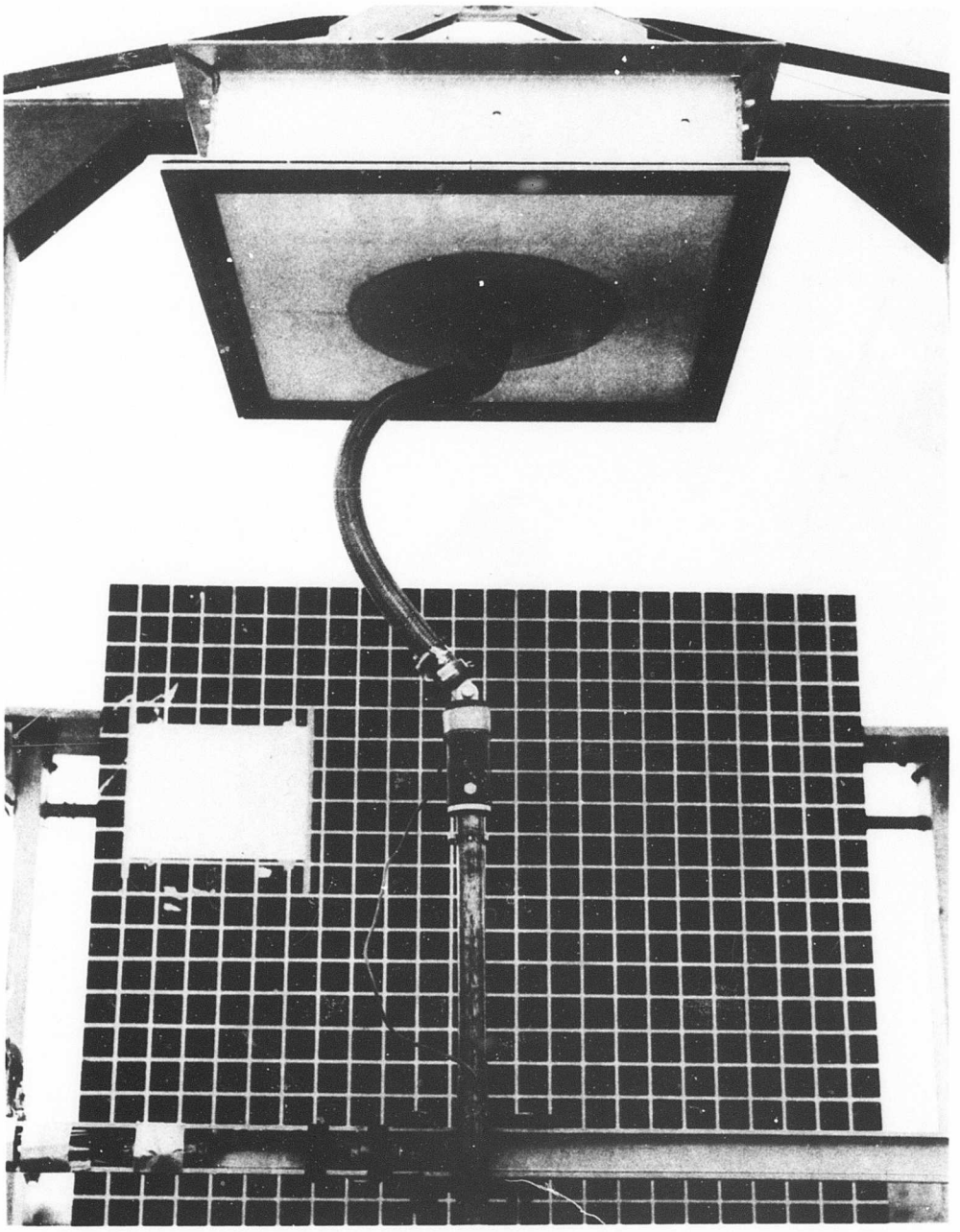

Figure 112. Fitting-to-Cell 90-Degree Elbow, Combined Tension and Shear.

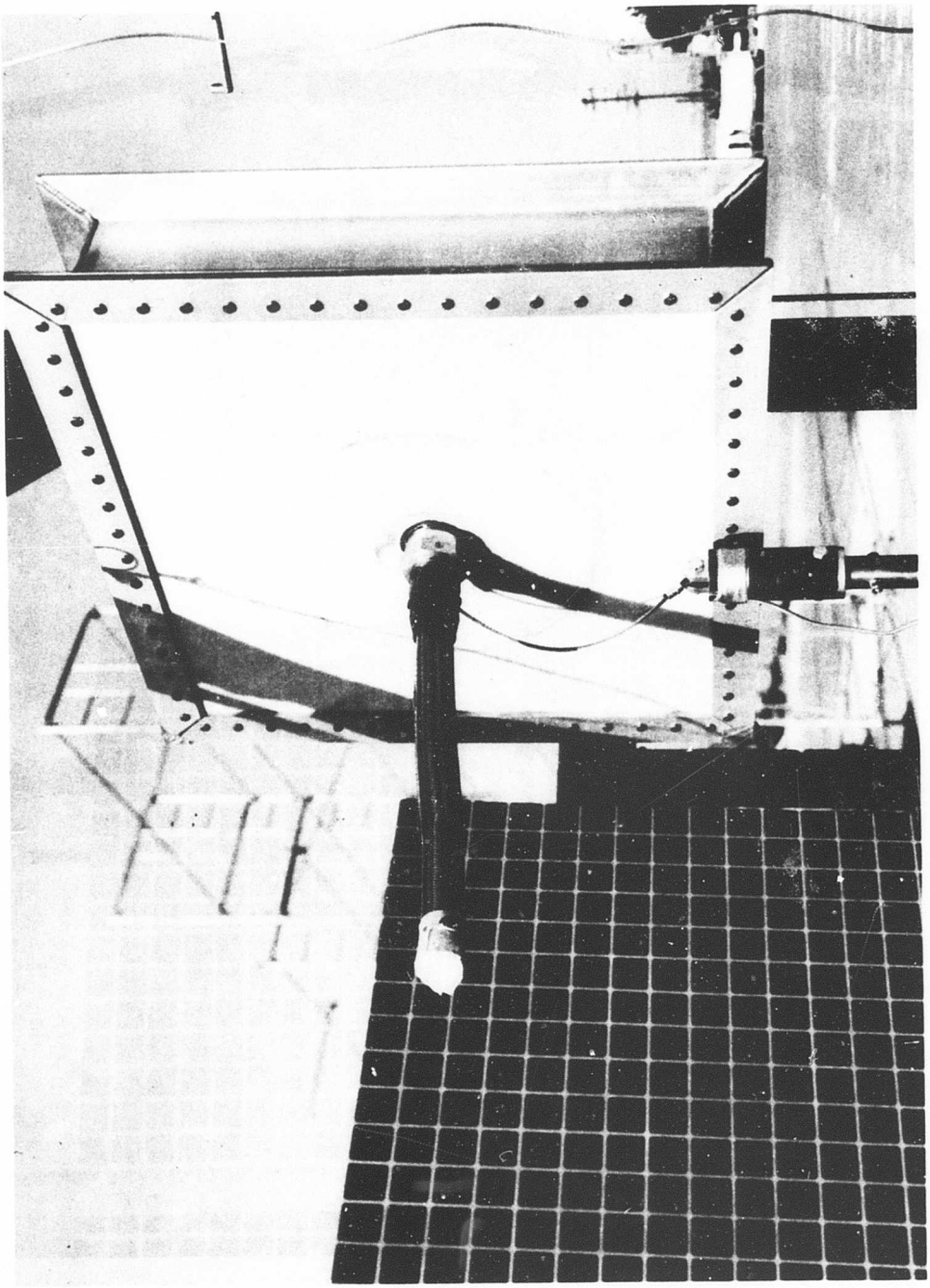

Figure 113. Fitting-to-Cell Bulkhead Impingement, Shear Load.

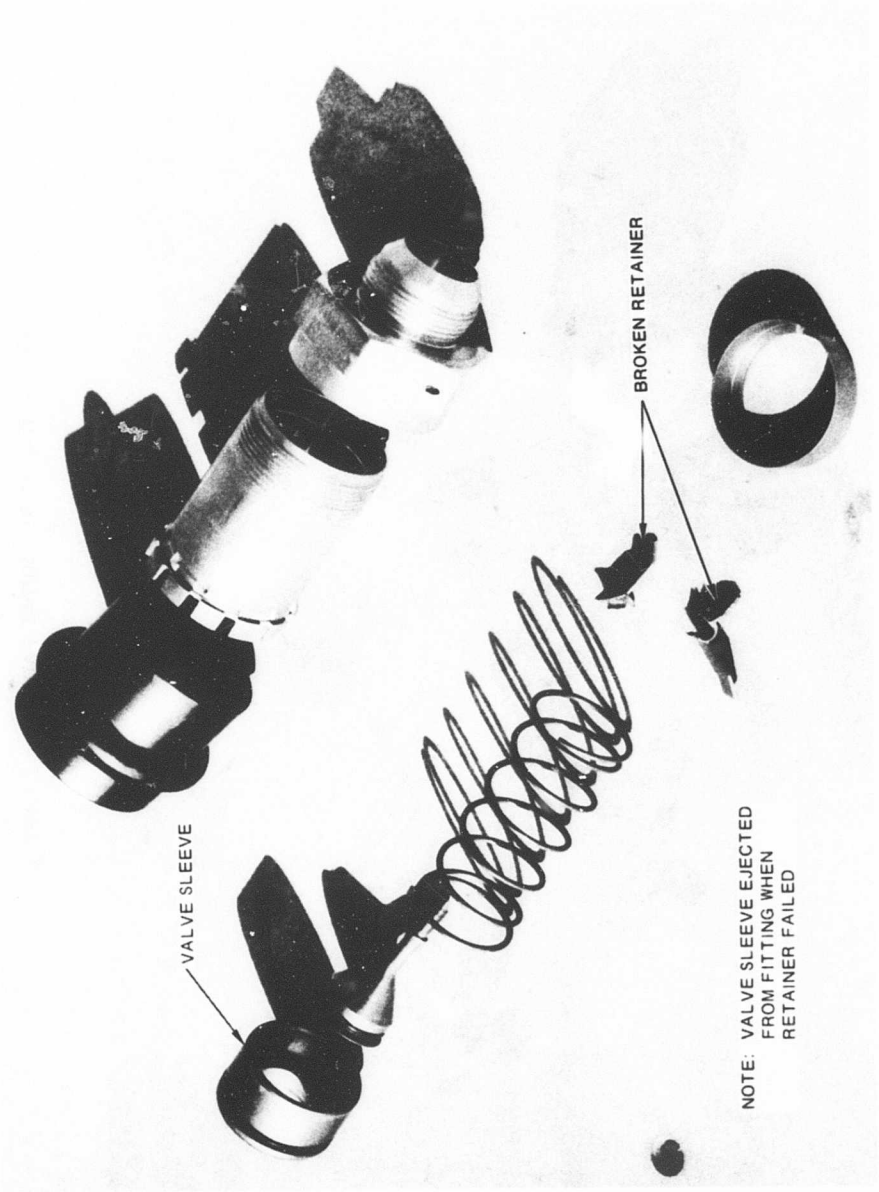

Figure 114. Valve Failure in Coupling Socket.

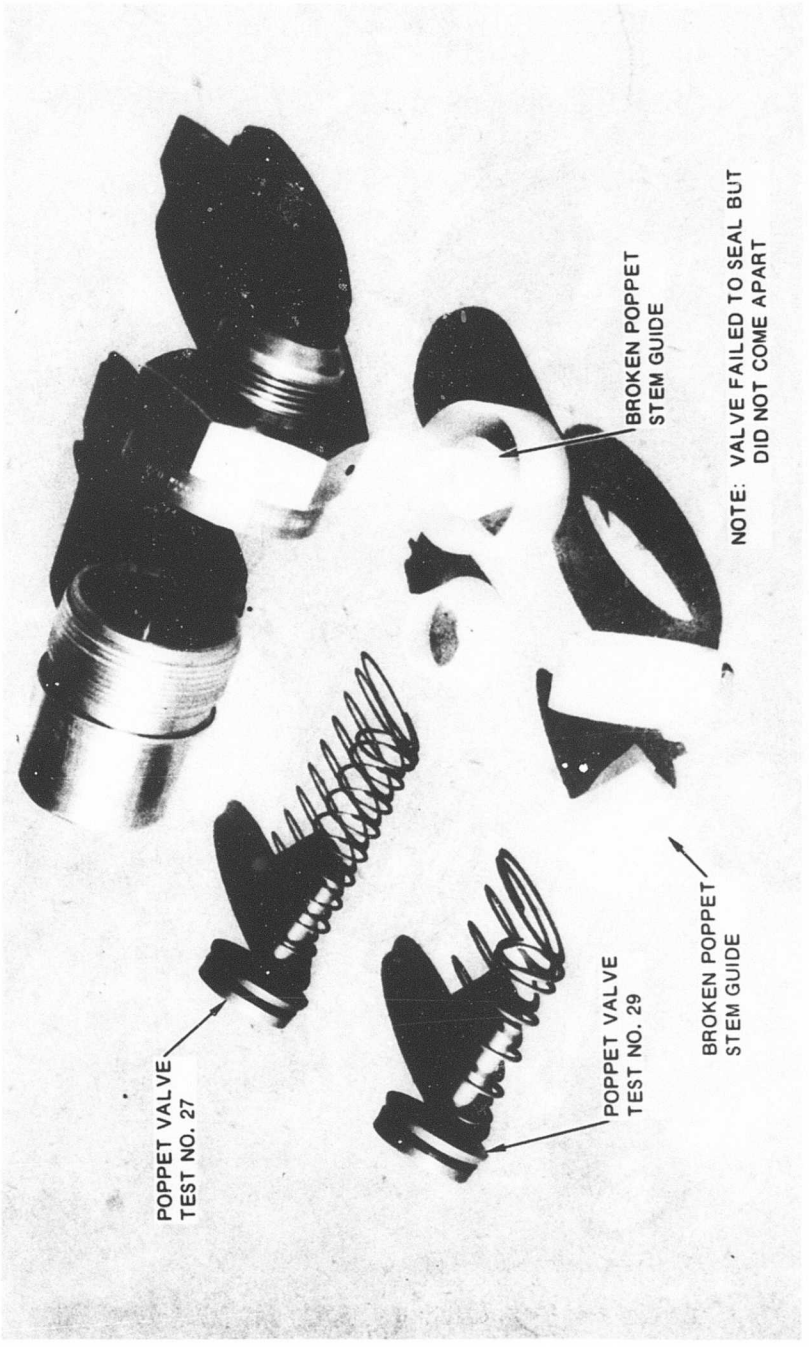

Figure 115. Valve Failure in Coupling Nipple.

TABLE XVIII

SYSTEM I TENSILE TEST DATA

Test No.*	Drop Hgt (ft)	Impact Vel (ft/sec)	G's on Frame	Load Wt (lb)	Max Load on Specimen (lb)	Pulse Duration (sec x 10^{-3})	Penetration Distance (in.)**
1	6	20	33	32	650	35	12.5
2	53	58	135	32	240	30	15.5
3	53	58	135	32	75	30	16.0
4***	6	20	40	32	600	25	12.5
5***	53	58	156	32	80	30	14.0
6	14	30	51	32	840	30	14.0
7	24	40	75	32	1160	30	13.5
8	38	51	123	32	225	30	13.5
9	30	45	89	32	1200	30	14.0

* See Figure 109.

** Penetration of jig into impact bed.

*** Rerun, no photo.

Note: Separation occurred in all tests.

TABLE XIX

SYSTEM I COMBINED TENSION AND SHEAR TEST DATA

Test No.*	Drop Hgt (ft)	Impact Vel (ft/sec)	G's on Frame	Load Wt (lb)	Max Load on Specimen (lb)	Pulse Duration (sec x 10^{-3})	Penetration Distance (in.)**
10	6	20	26	32	540	30	11
11	30	45	113	32	210	20	13
12	24	40	87	32	540	25	12
13	53	58	125	32	240	20	13

*See Figure 110.

** Penetration of jig into impact bed.

Note: Separation occurred in all tests.

TABLE XX

SYSTEM I SHEAR TEST DATA

Test No.*	Drop Hgt (ft)	Impact Vel (ft/sec)	G's on Frame	Load Wt (lb)	Max Load on Specimen (lb)	Pulse Duration (sec x 10^{-3})	Penetration Distance (in.)**
14	6	20	23	32	225	30	13.0
15	6	20	30	32	700	25	13.0
16	24	40	107	32	840	20	13.5
17	53	58	142	32	1140	20	12.0

*See Figure 111.

** Penetration of jig into impact bed.

Note: Separation occurred in all tests.

TABLE XX

SYSTEM I COMBINED TENSION AND SHEAR TEST DATA

Test No.*	Drop Hgt (ft)	Impact Vel (ft/sec)	G's on Frame	Load Wt (lb)	Max Load on Specimen (lb)	Pulse Duration ($sec \times 10^{-3}$)	Penetration Distance (in.)**
23	6	20	25	32	390	25	12.0
24	24	40	102	32	140	20	13.0
25	53	58	145	32	70	25	14.0

*See Figure 112.

** Penetration of jig into impact bed.

Note: Separation occurred in all tests.

FOR OFFICIAL USE ONLY

TABLE XXII

FORCE APPLIED TO FITTING, SYSTEM I*

Test No.**	Drop Hgt (ft)	Impact Vel (ft/sec)	G's on Frame	Load Wt (lb)	Max Load on Specimen (lb)	Pulse Duration (sec x 10^{-3})	Penetration Distance (in.)***	Remarks
26	6	20	29	32	860	20	14	Slight out-of-round deformation.
27	53	58	145	32	1714	20	14	Moderate out-of-round deformation of socket. Valve stem guide in nipple failed and valve did not seal.
28	24	40	84	32	1400	25	14	No deformation.
29	53	58	142	32	1605	20	17	Valve retainer in socket failed, allowing ejection of valve parts from socket. Valve stem guide in nipple failed and valve did not seal.

* Force applied directly to fitting in a direction parallel to tank wall to simulate loads on fitting caused by tank lateral displacement.

** See Figures 113 and 114.

Note: Separation occurred in all tests.

*** Penetration of jig into impact bed.

FOR OFFICIAL USE ONLY

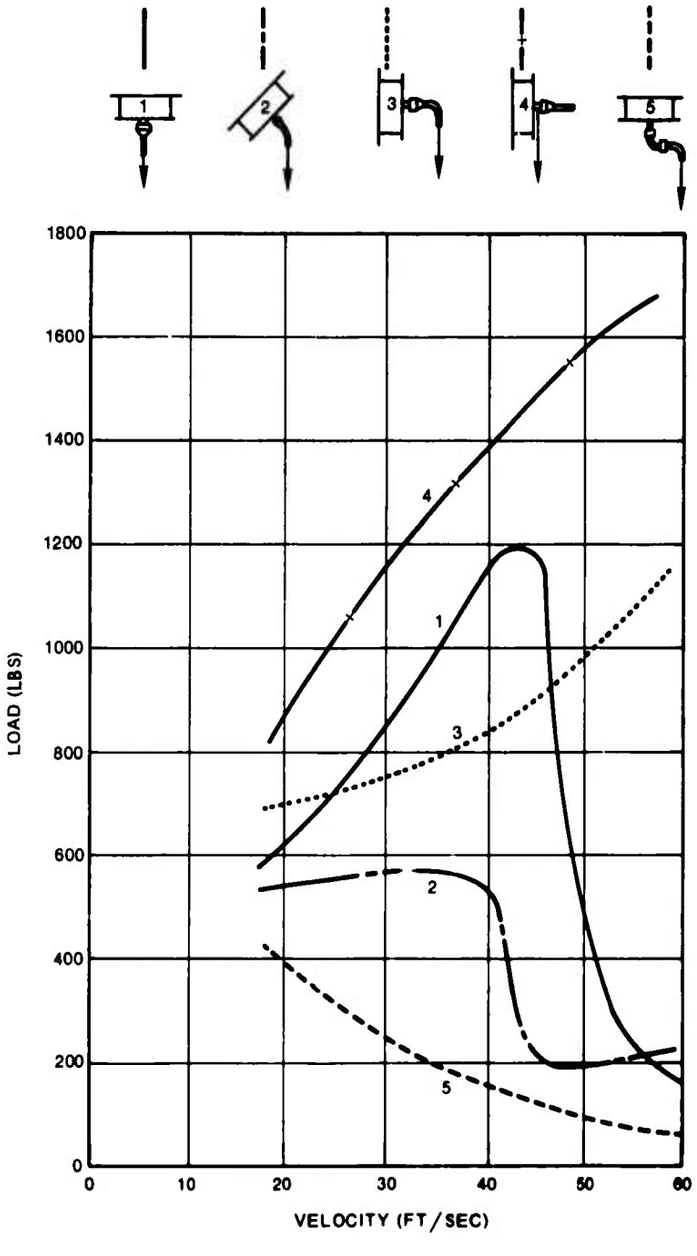

Figure 116. Relationship of Specimen Velocity at Impact to Breakaway Load.

System II

This system consisted of a fuel line connected to a fuel line by a self-sealing breakaway fitting. The fitting assembly (Figures 62 and 63) used was a modified quick-disconnect coupling (per MIL-C-7413A). The hose used was 1-1/4-inch-diameter Aeroquip Corporation Type 601 with standard Aeroquip fittings.

The primary test objectives were to: (1) determine the feasibility of the design approach and discover possible mechanical problems not readily apparent during the design or in static testing, and (2) determine the variation of the load-sustaining and disconnect capability using both a tension loading and a combined tension and shear loading, and by varying the impact velocity.

Two loading configurations were selected, both involving tension (or axial) loads. This is the most probable loading mode for a fuel line during an actual crash pulse. The number of drops were kept to a minimum because the self-sealing valve used was identical to the one tested in the line-to-tank tests.

The System II configurations are shown in Figures 117 and 118; the data applicable to each test are presented in Tables XXIII and XXIV.

System II Test Conclusions

This approach is considered feasible. The breakaway fitting functioned properly and fuel lines sealed against leakage in all tests. The load-bearing capability of the connection in the configurations tested appeared to be constant within the range of impact velocities used.

System III

The frangible attachment adapter used in this test series consisted of two aluminum discs fastened together with plastic inserts. One-half of the adapter was bolted to a 3-ply specimen of ARM-018 fuel cell material. The other half of the adapter was bolted to a fixture. The cell material was mounted in the universal jig and the load was applied to the fixture.

The test objectives were to (1) determine the feasibility of the design approach and discover possible mechanical problems not readily apparent during the design or in static testing, and (2) determine any variation in the system load-sustaining capability using several loading modes and various impact velocities.

The loading of any individual tank-to-structure attachment in a crash can be either tension, shear, torsion, or a combination of any or all of these. The tests were

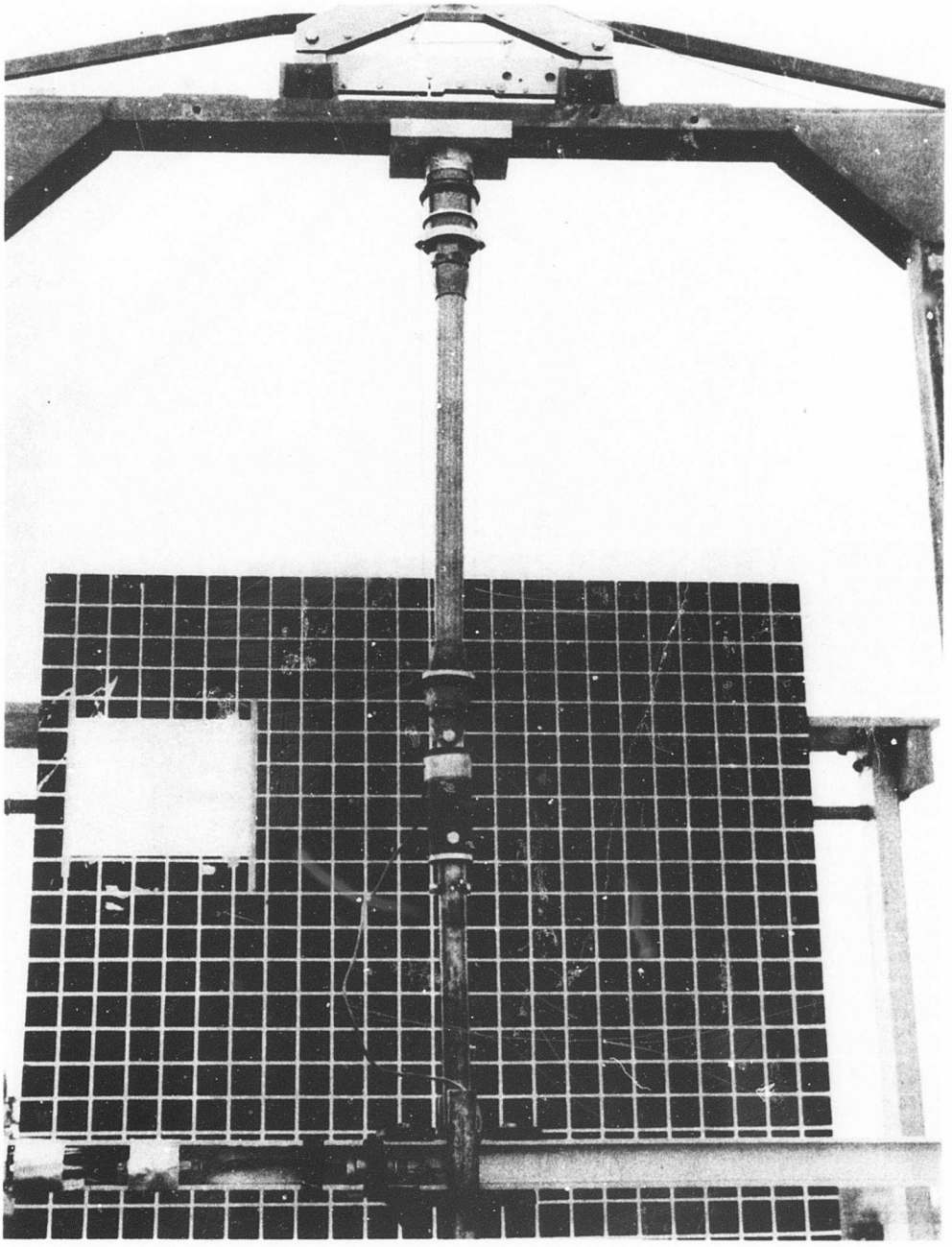

Figure 117. Line Disconnect, Direct Tension Load.

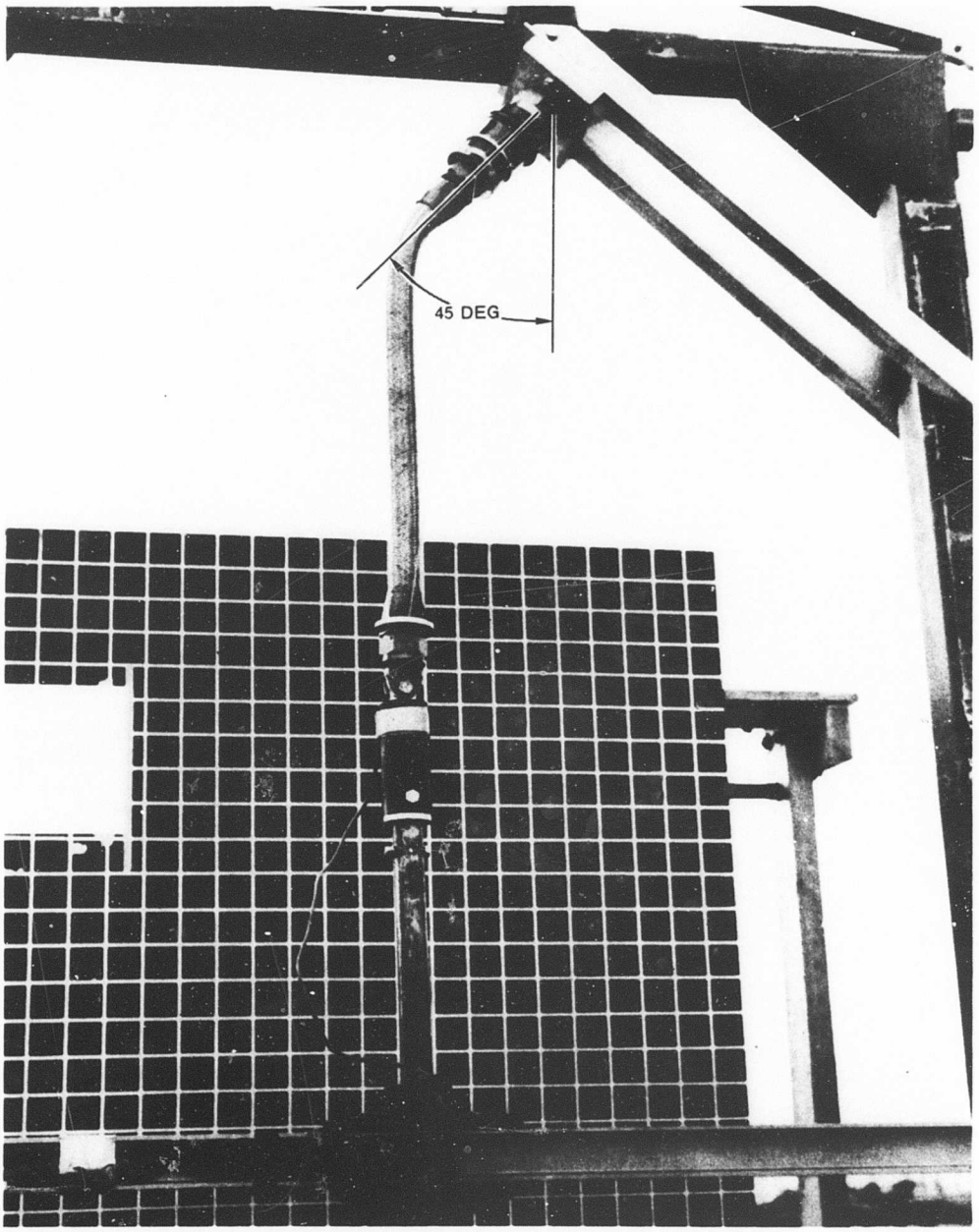

Figure 118. Line Disconnect, Combined Tension and Shear Load.

FOR OFFICIAL USE ONLY

TABLE XXIII

SYSTEM II TENSILE TEST DATA

Test No.*	Drop Hgt (ft)	Impact Vel (ft/sec)	G's on Frame	Load Wt (lb)	Max Load on Specimen (lb)	Pulse Duration (sec x 10^{-3})	Penetration Distance (in.)**	Remarks
18	53	58	125	32	570	20	14	
19	53	58	120	0	0	20	14	No weight. Fitting and hose only. No disconnect.

*See Figure 117.

Note: Separation occurred in test 18.

** Penetration of jig into impact bed.

FOR OFFICIAL USE ONLY

TABLE XXIV

SYSTEM II COMBINED TENSION AND SHEAR TEST DATA

Test No.*	Drop Hgt (ft)	Impact Vel (ft/sec)	G's on Frame	Load Wt (lb)	Max Load on Specimen (lb)	Pulse Duration (sec x 10^{-3})	Penetration Distance (in.)**
20	6	20	29	32	710	25	12
21	24	40	93	32	710	15	13
22	53	58	140	32	795	20	16

* See Figure 118.

** Penetration of jig into impact bed.

Note: Separation occurred in all tests.

conducted in five modes to simulate logical combination of the basic loading modes. The System III configurations are shown in Figures 119 through 123 and related test data in Tables XXV through XXIX and in Figure 124.

System III Test Conclusions

This approach is considered feasible. The frangible rings separated under high-velocity impact rates, and no degradation of the ARM-018 fuel cell material specimens was evident. There were no unusual mechanical problems. Figure 124 shows curves relating to the variation of load-bearing capability to impact velocity rates. Note the general increase in load-bearing capability as the impact velocity increases, a factor particularly noticeable when the major component of force is tension.

System IV

For a complete description of the frangible protective bulkhead adapter (Figures 54 and 55), see Part IV. The hose used was 5/8-inch-diameter Aeroquip Corporation Type 601 with Aeroquip standard hose ends (3/8-inch size was used for tests 86 and 87). AN832-10D bulkhead unions and AN833-10D bulkhead elbows were used.

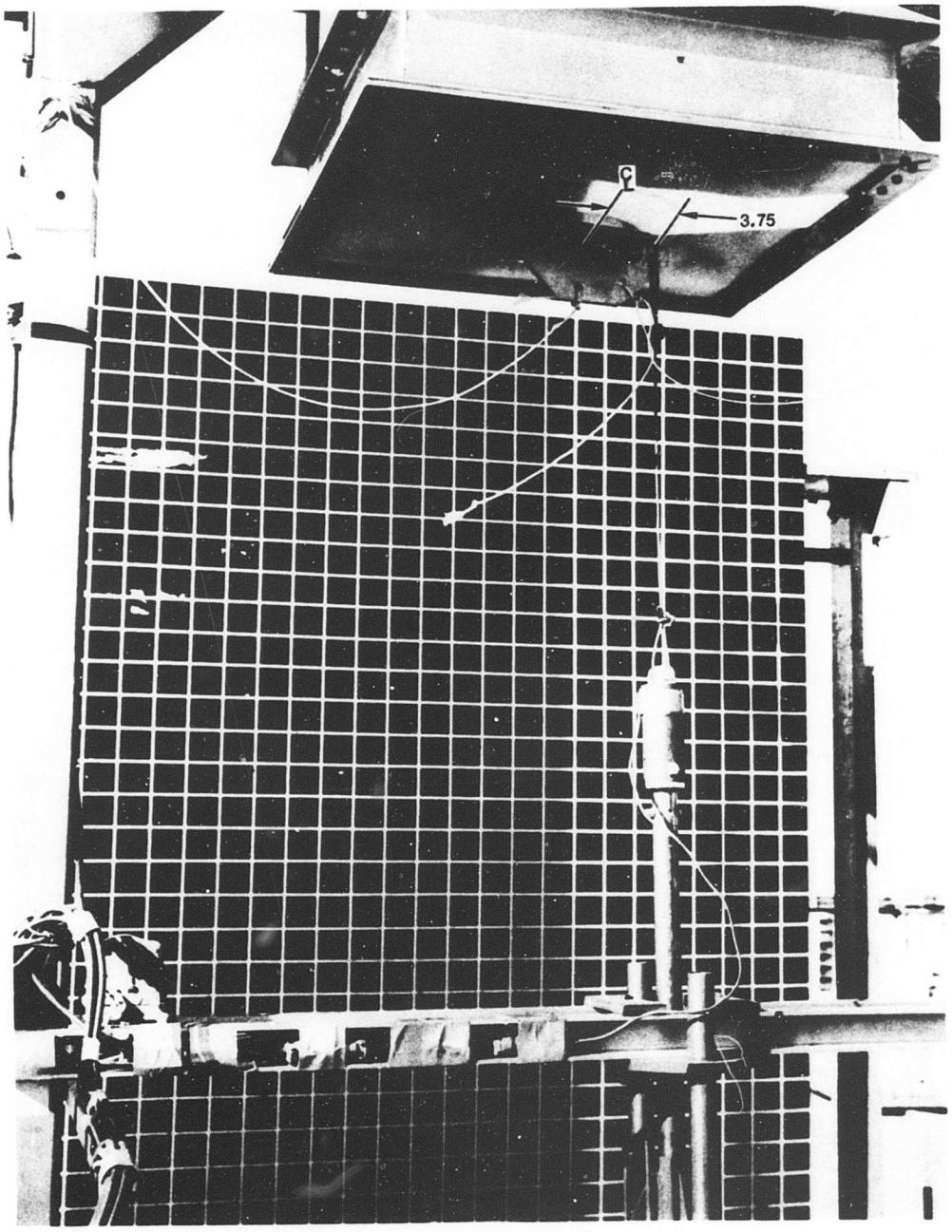

Figure 119. Frangible Cell Attachment, Peel Load.

Figure 120. Frangible Cell Attachment, Tension Load.

Figure 121. Frangible Cell Attachment, Combined Tension and Shear Load.

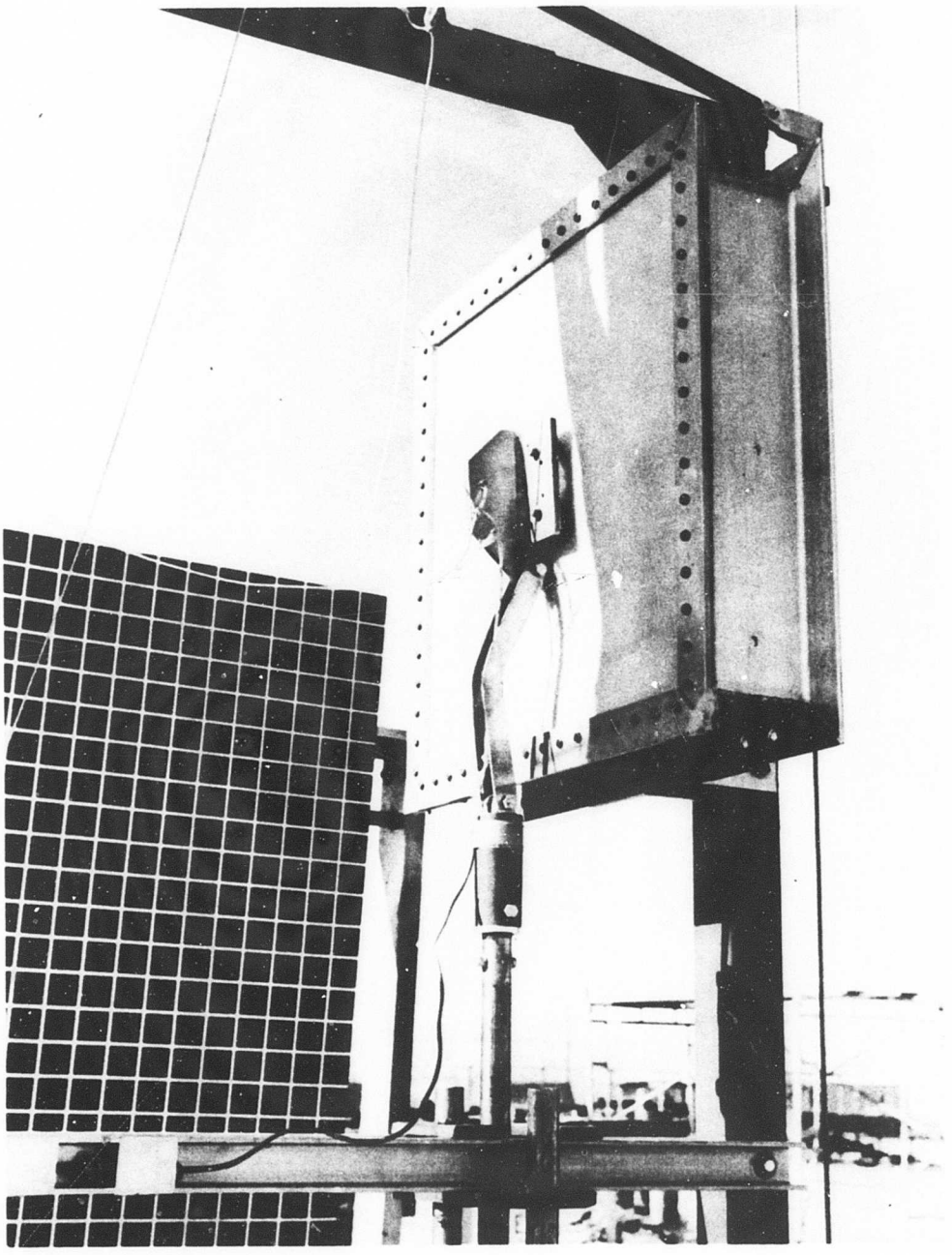

Figure 122. Frangible Cell Attachment, Shear Load.

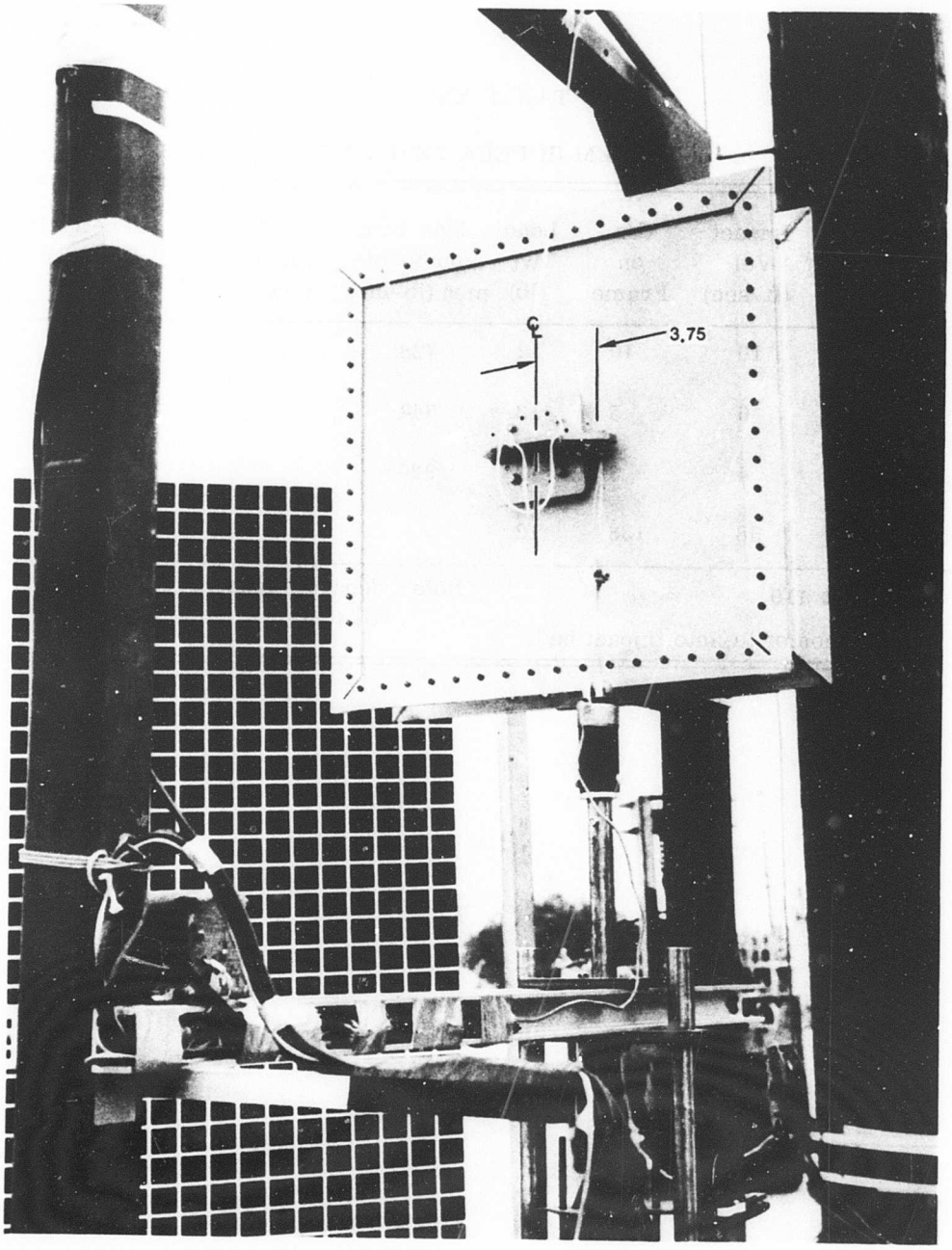

Figure 123. Frangible Cell Attachment, Torsion Load.

TABLE XXV

SYSTEM III PEEL TEST DATA

Test No.*	Drop Hgt (ft)	Impact Vel (ft/sec)	G's on Frame	Load Wt (lb)	Max Load on Specimen (lb-in.)	Pulse Duration (sec x 10^{-3})	Penetration Distance (in.)**
46	1-1/2	10	10	12	728	40	11.0
47	1/2	6	5	12	844	25	10.0
43	1/4	4	3	12	924	50	10.0
49	53	58	138	12		20	16.5

* See Figure 119.

** Penetration of jig into impact bed.

Note: Separation occurred in all tests.

TABLE XXVI

SYSTEM III TENSION TEST DATA

Test No.*	Drop Hgt (ft)	Impact Vel (ft/sec)	G's on Frame	Load Wt (lb)	Max Load on Specimen (lb)	Pulse Duration (sec x 10^{-3})	Penetration Distance (in.)**
50	1	8	11	12	525	30	11.0
51	1/2	6	6	12	260	30	10.0
52	3/4	7	8	12	345	25	10.0
53	53	58	143	12	840	20	17.0
54	30	45	94	12	1080	30	16.0

*See Figure 120.

**Penetration of jig into impact bed.

Note: Separation did not occur in test 51.

TABLE XXVII

SYSTEM III COMBINED TENSION AND SHEAR TEST DATA

Test No. *	Drop Hgt (ft)	Impact Vel (ft/sec)	G's on Frame	Load Wt (lb)	Max Load on Specimen (lb)	Pulse Duration (sec x 10^{-3})	Penetration Distance (in.)**
72	2	11	16	24	535	30	11.0
73	1	8		24			12.0
74	1/2	6	6	24	330	30	10.0
75	3/4	7	7	24	270	40	10.0
76	53	58	142	24	525	20	14.0

* See Figure 121.

** Penetration of jig into impact bed.

Note: Separation did not occur in test 74.

TABLE XXVIII

SYSTEM III SHEAR TEST DATA

Test No.*	Drop Hgt (ft)	Impact Vel (ft/sec)	G's on Frame	Load Wt (lb)	Max Load on Specimen (lb)	Pulse Duration (sec x 10^{-3})	Penetration Distance (in.)**
30	14	30	43	52	990	30	14.5
31	53	58	112	52	1020	20	15.5
32	53	58	120	52	1140	20	15.5
55	1/2	6	4	12	50	40	10.0
56	1	8	10	12	150	25	10.0
57	2	11	14	12	225	30	11.0
58	3	15	28	12	300	20	11.0
59	1	8	11	52	675	25	10.0
60	2	11	24	52	945	20	10.0

*See Figure 122.

** Penetration of jig into impact bed.

Note: Separation did not occur in tests 55 through 59.

TABLE XXIX

SYSTEM III TORSION TEST DATA

Test No.*	Drop Hgt (ft)	Impact Vel (ft/sec)	G's on Frame	Load Wt (lb)	Max Load on Specimen (lb-in.)	Pulse Duration (sec x 10^{-3})	Penetration Distence (in.)**
33	14	30	-	12	-	-	-
34	6	20	37	12	1762	20	12.5
35	4	16	31	12	1837	20	12.5
36	2	11	14	12	1294	30	11.5
37	1	8	11	12	731	-	11.5
38	1	8	11	12	787	-	11.5
39	1-1/2	10	13	12	1012	-	12.0
40	2	11	18	12	1012	-	10.0
41	2-1/2	13	20	12	1237	-	11.5
42	3	15	24	12	1125	20	11.5
43	3-1/3	16	35	12	1406	15	11.5
44	30	45	120	12	2531	20	14.0
45	53	58	137	12	2568	20	15.0

* See Figure 123.

** Penetration of jig into impact bed.

Note: Separation did not occur in tests 37 through 42.

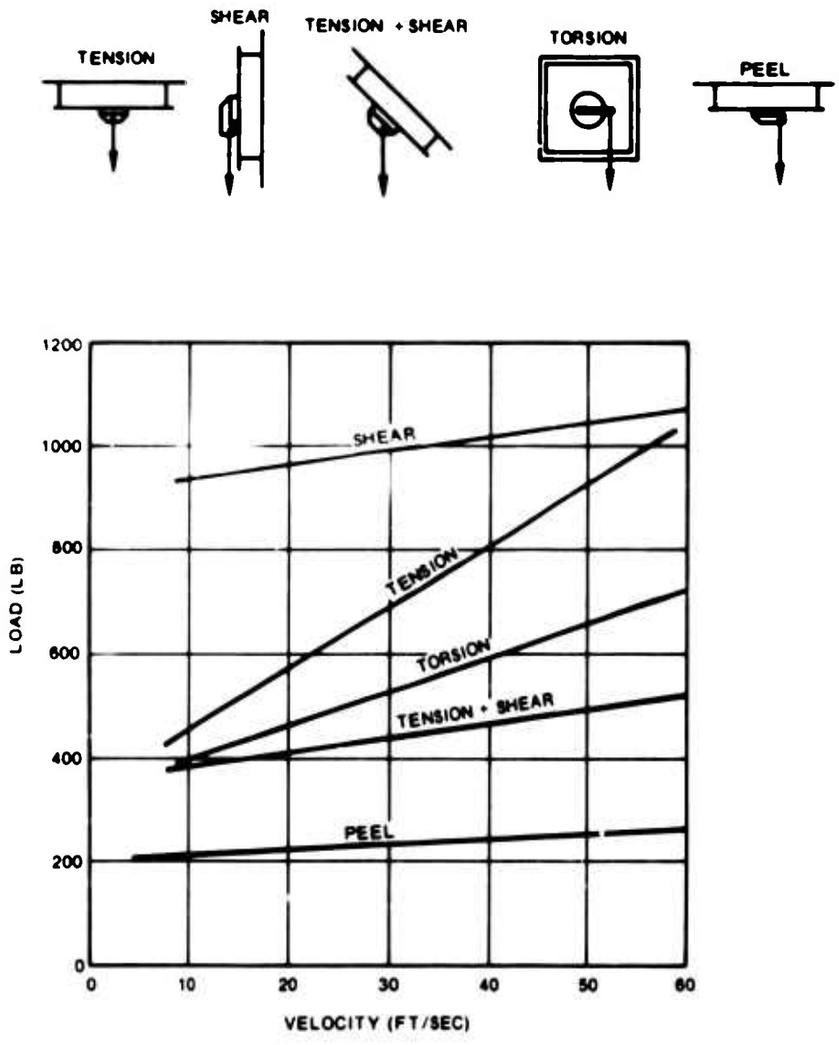

Figure 124. Relationship of Specimen Velocity at Impact to Breakaway Load, Tank-to-Structure Attachment.

The test objectives were to: (1) determine the feasibility of the design approach and discover possible mechanical problems not readily apparent during design or in static testing; (2) determine if the load required to separate the frangible section varies as impact velocity varies; and (3) determine the amount of protection the torus offers the fuel line as the line is pulled through the bulkhead opening.

The load was applied in tension at various impact velocity rates to determine the failure load of the frangible section. Various typical line configurations were tested at a given velocity. The configurations were tested first using the bulkhead fitting to support and protect the line. Then the test was repeated with the same line configuration passing through a bare opening in the bulkhead material.

Two drops were made with the line firmly attached to the bulkhead. This is a common method used to support fuel lines at a point where they pass through a bulkhead. The test setups are shown in Figure 125 and the results in Figure 126. Supporting test data are presented in Table XXX. Tests 68 through 71 were conducted to determine if the failure of the torus would occur prior to fuel line failure.

System IV Test Conclusions

This approach is considered feasible. The bulkhead fitting does support the line under normal flight loads and releases under loading conditions associated with a crash pulse. There is some degree of protection afforded the fuel line by the torus when the line is being pulled through the opening.

As shown in Figure 127, the load-bearing capability of the frangible section increases slightly as impact velocity increases. The degree of protection that the torus portion provided the fuel line when the line was being rapidly pulled through the bulkhead opening is summarized in the following paragraphs.

Three configurations were compared by pulling the line through the opening with a bulkhead fitting installed. The test was then repeated with no bulkhead fitting (tests 77, 78, 79, 80, 83, and 84). The first configuration (tests 77 and 78) would not pass through the opening under the rapid loading conditions imposed. The mode of system failure differed in the two tests. The hose fitting failed in pure tension in the first test, with the torus preventing any scarring or cutting of the hose or fitting. In the second test the force was concentrated at a point where the bare bulkhead impinged against the hose, and a shear-type failure occurred.

The second configuration (tests 79 and 80) satisfactorily demonstrated that some amount of protection is offered. In the first test (with a bulkhead fitting installed), the hose and fittings passed through the opening with no visible damage. A line failure

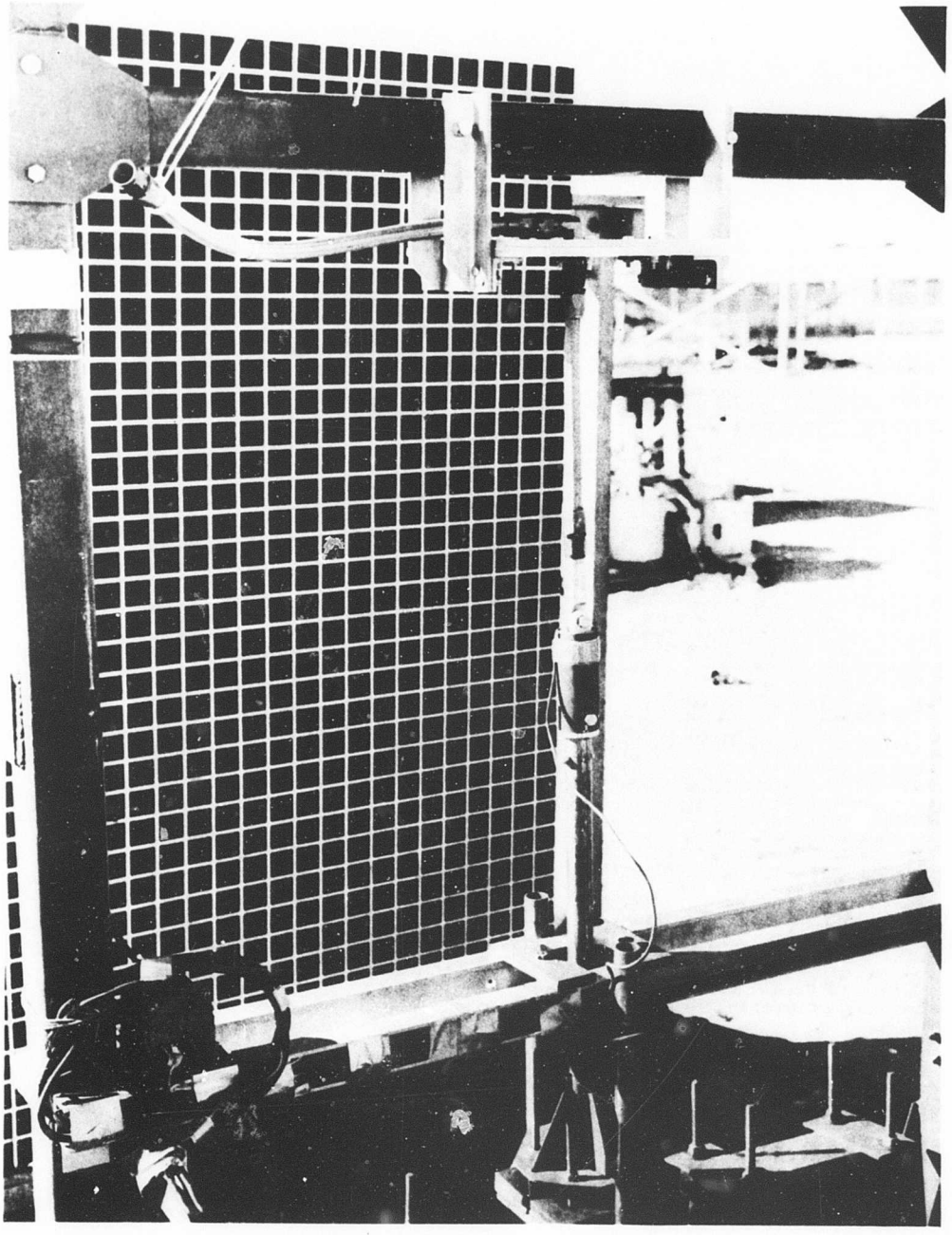

Figure 125. Test Setup, Frangible Protective Bulkhead Adapter (1 of 14).

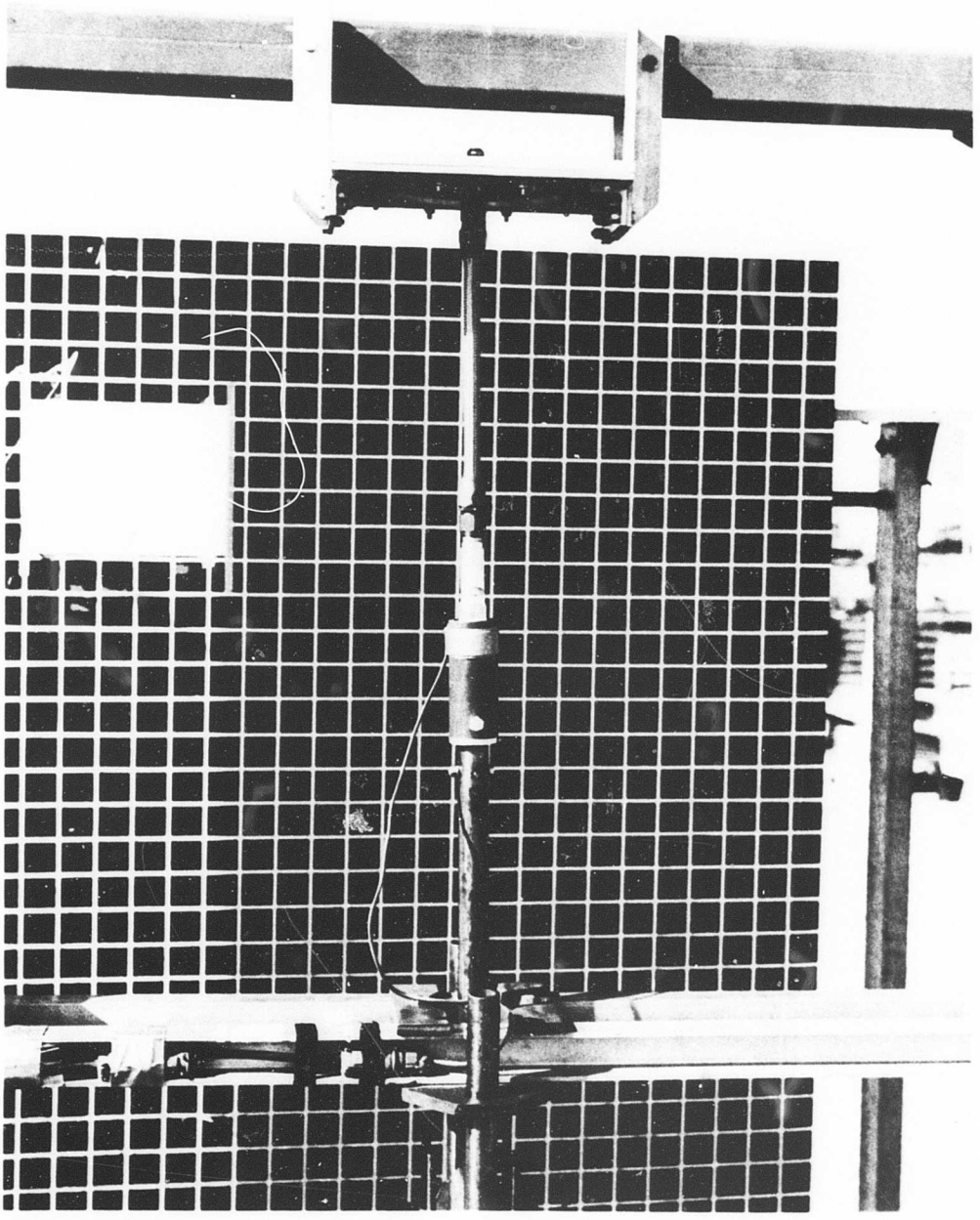

Figure 125. Test Setup, Frangible Protective Bulkhead Adapter (2 of 14).

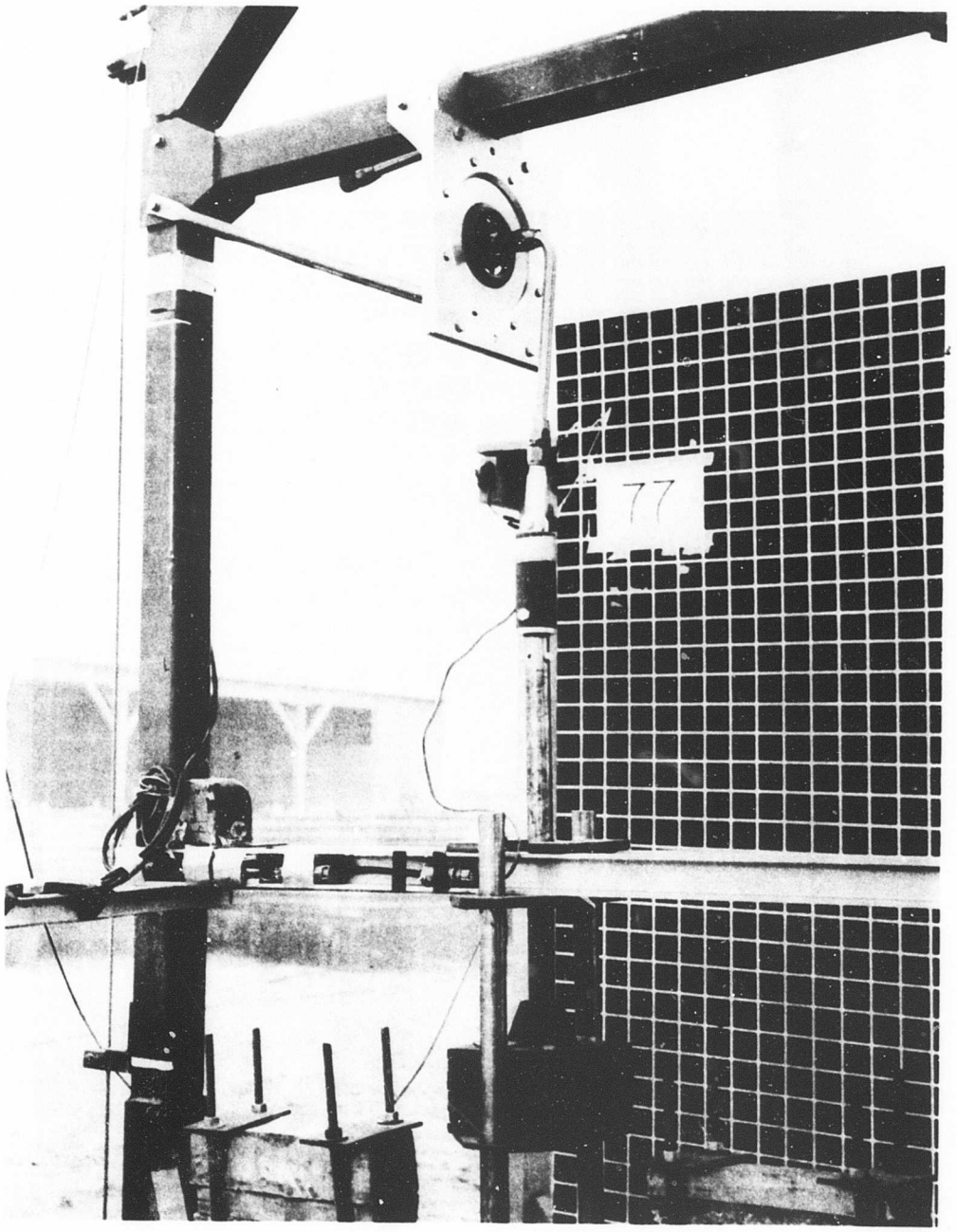

Figure 125. Test Setup, Frangible Protective Bulkhead Adapter (3 of 14).

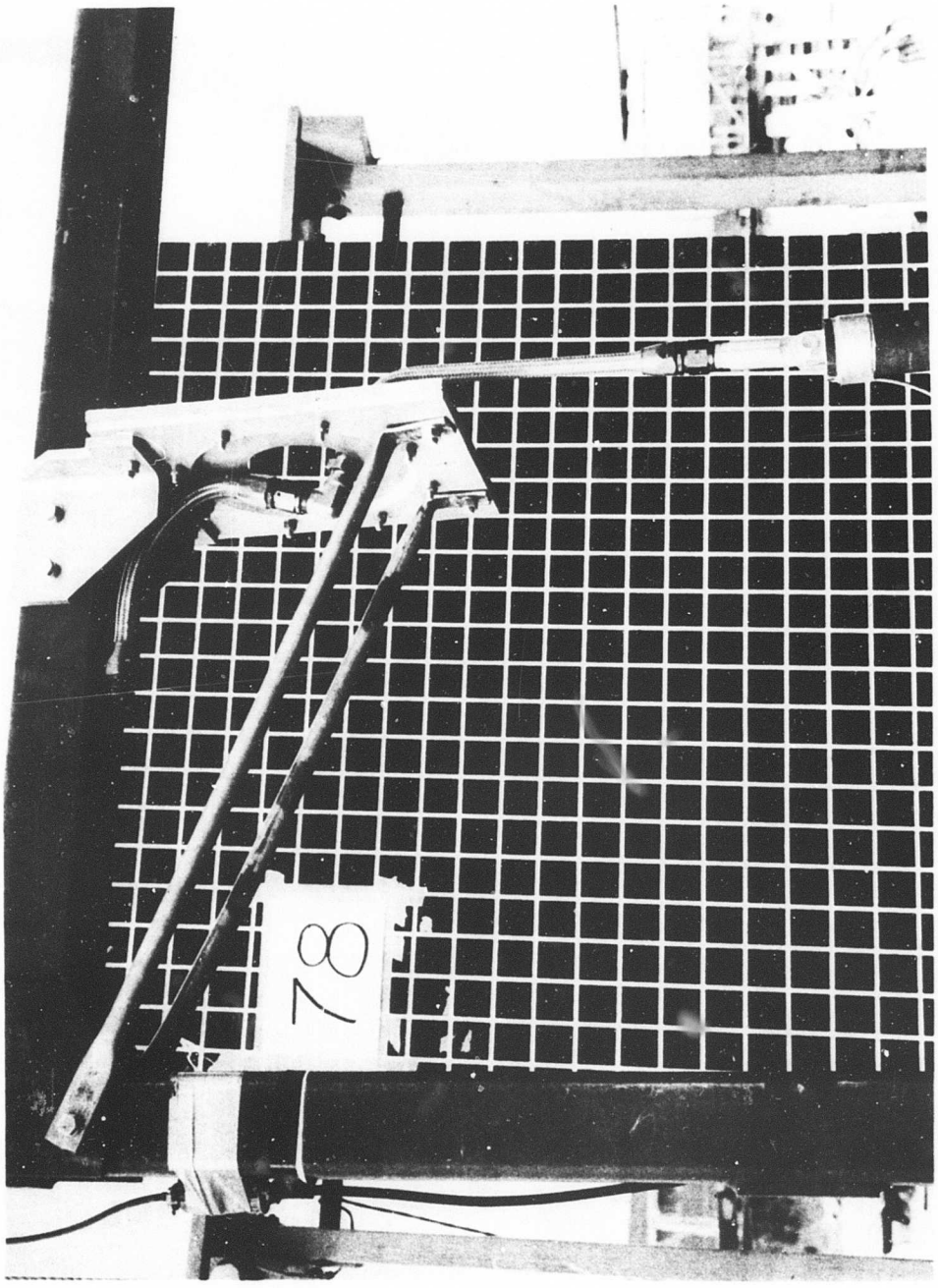

Figure 125. Test Setup, Frangible Protective Bulkhead Adapter (4 of 14).

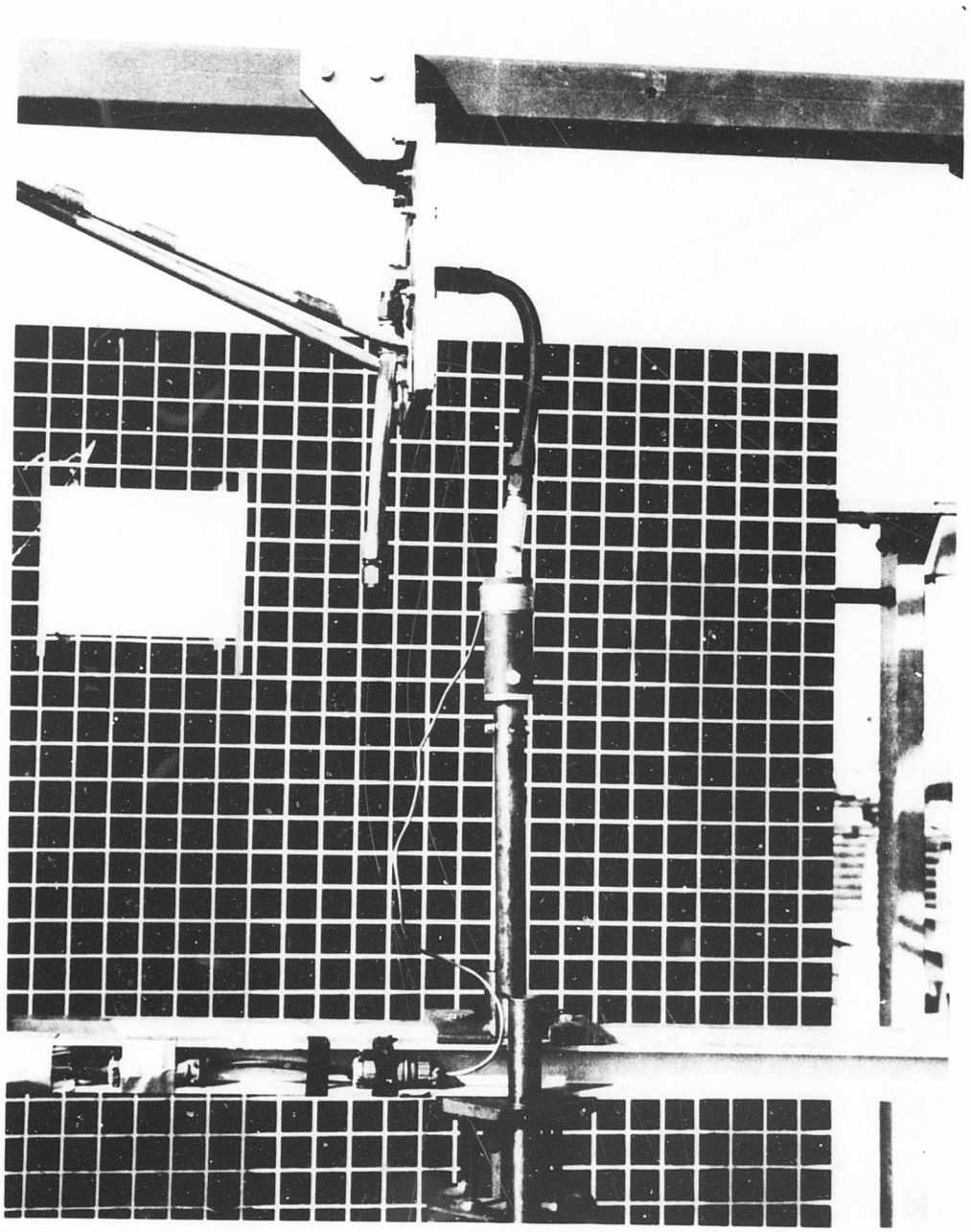

Figure 125. Test Setup, Frangible Protective Bulkhead Adapter (5 of 14).

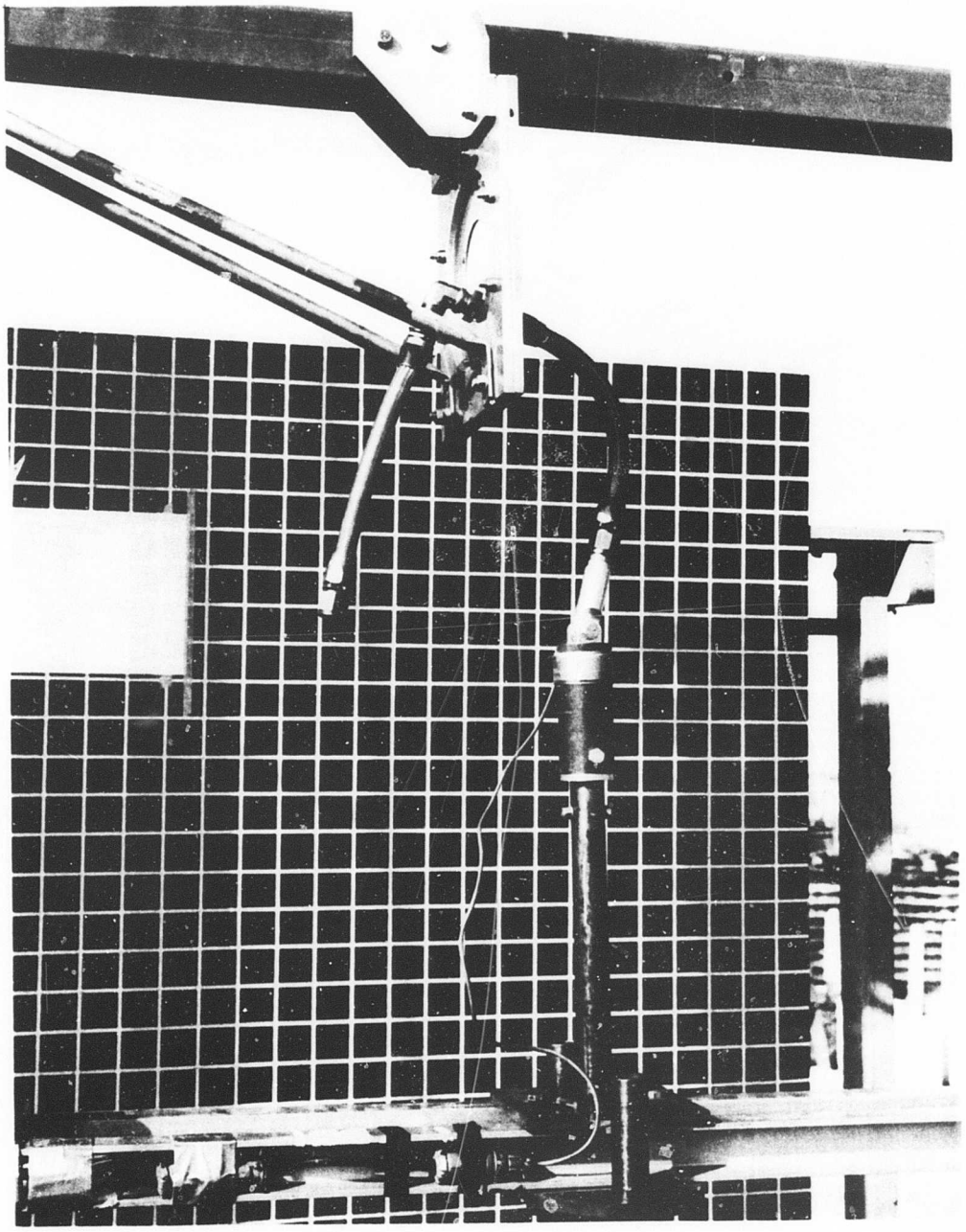

Figure 125. Test Setup, Frangible Protective Bulkhead Adapter (6 of 14).

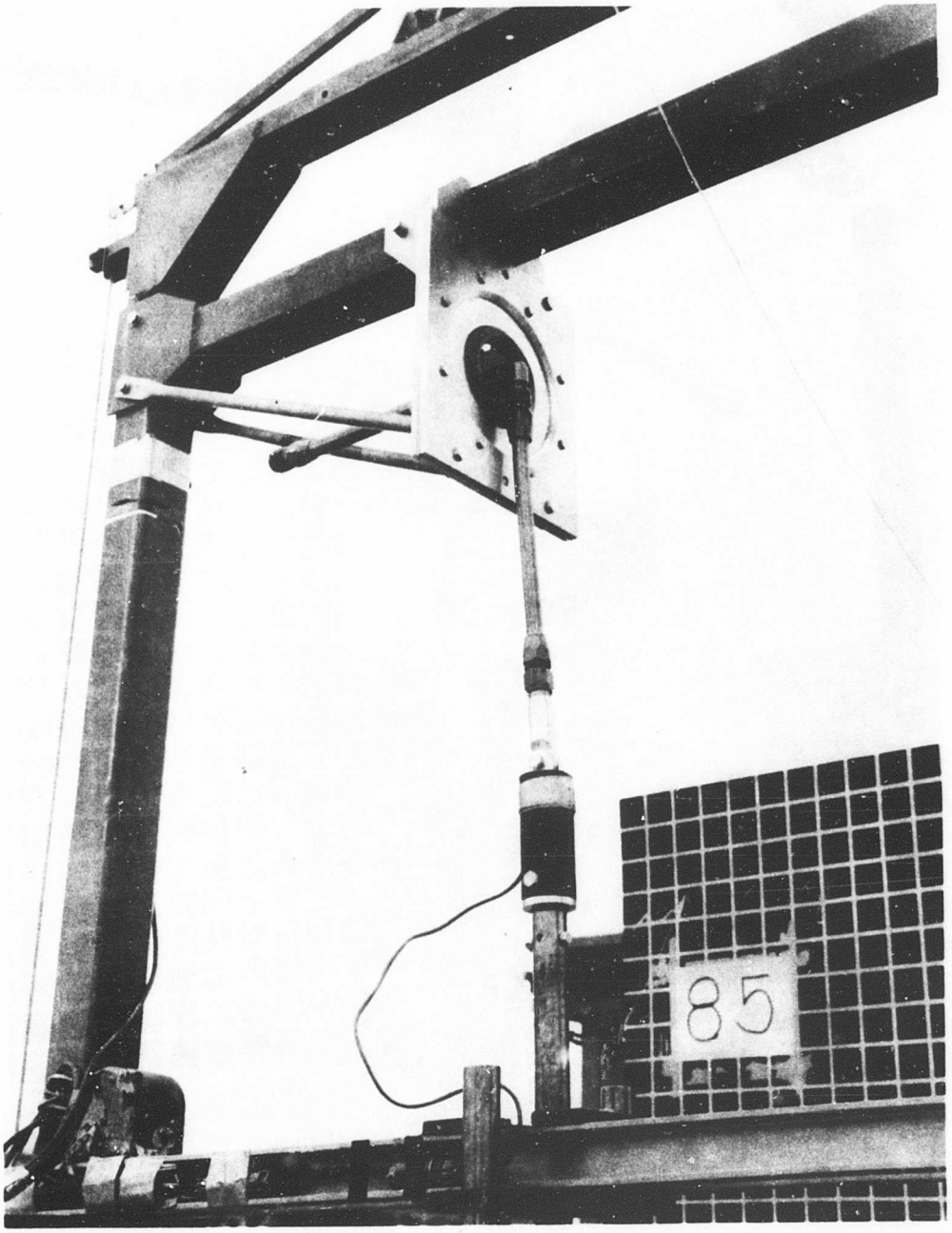

Figure 125. Test Setup, Frangible Protective Bulkhead Adapter (7 of 14).

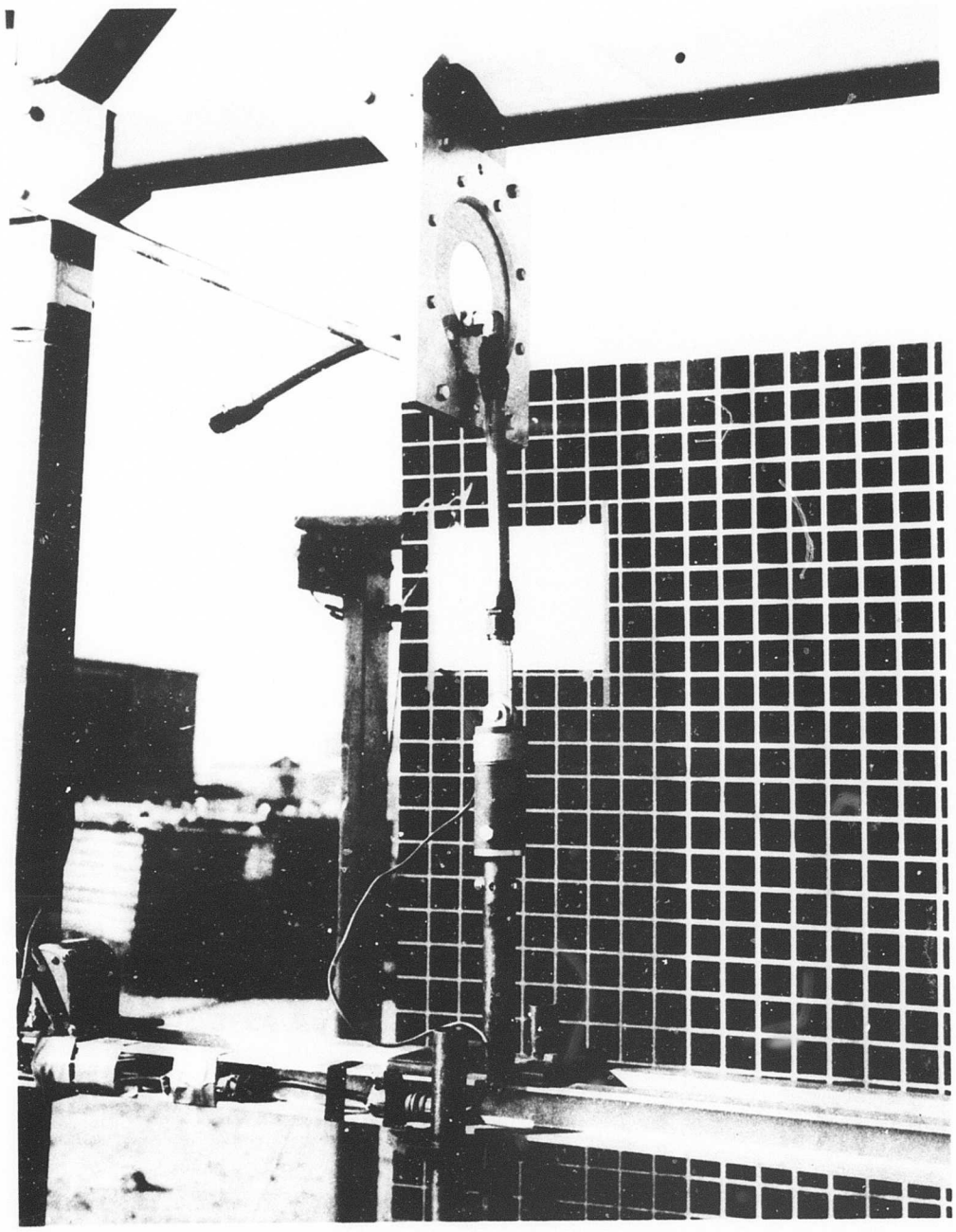

Figure 125. Test Setup, Frangible Protective Bulkhead Adapter (8 of 14).

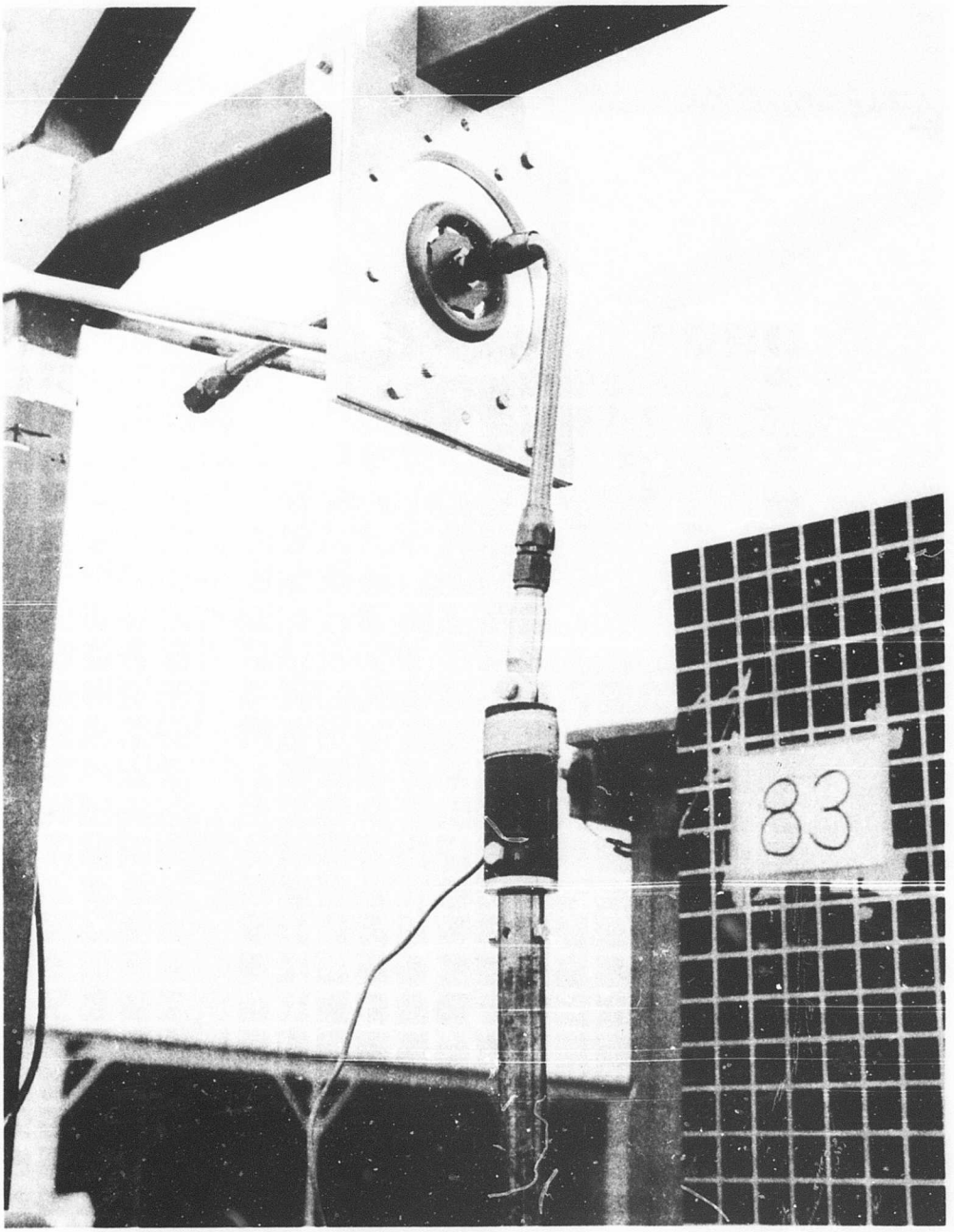

Figure 125. Test Setup, Frangible Protective Bulkhead Adapter (9 of 14).

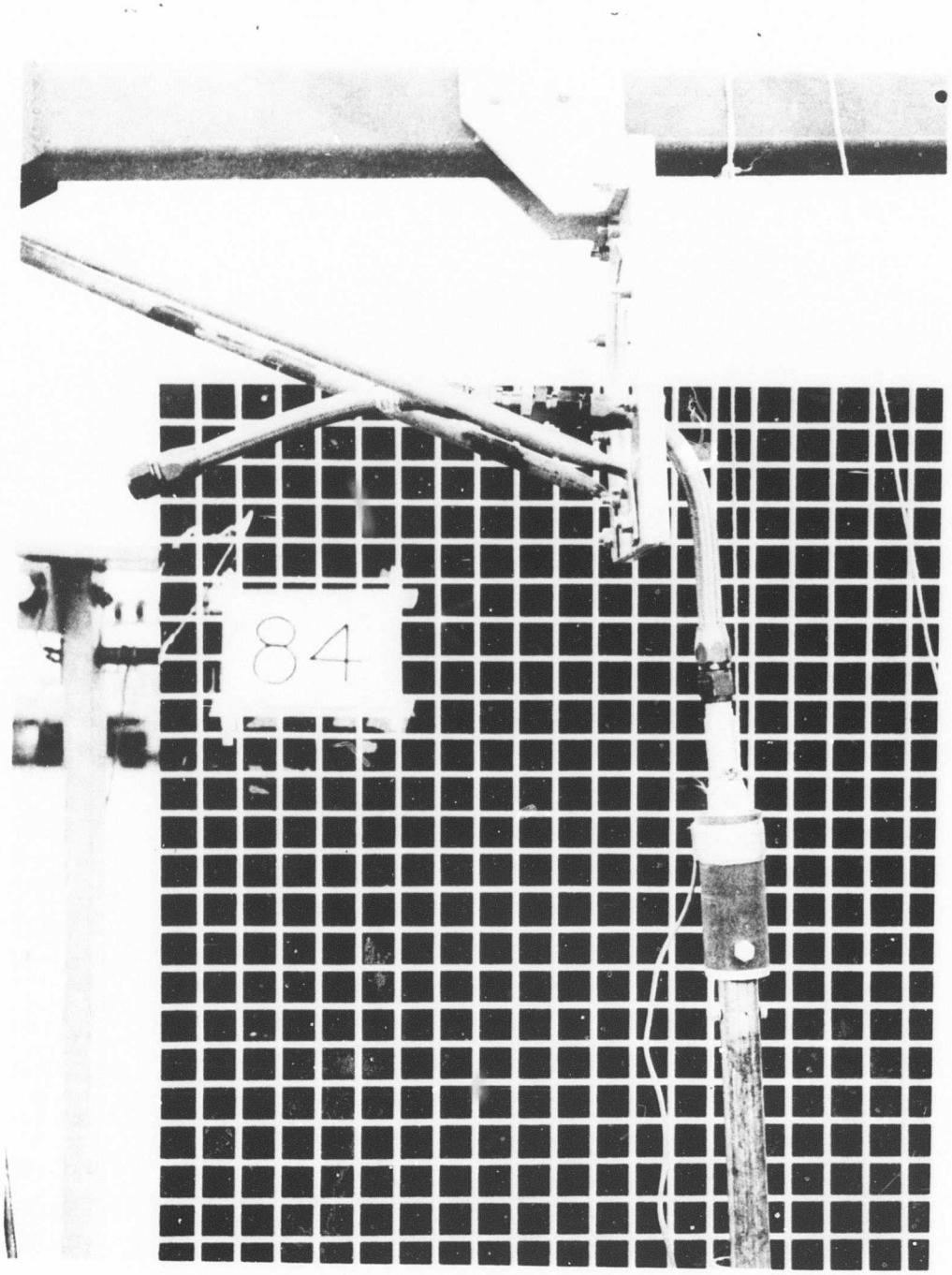

Figure 125. Test Setup, Frangible Protective Bulkhead Adapter (10 of 14).

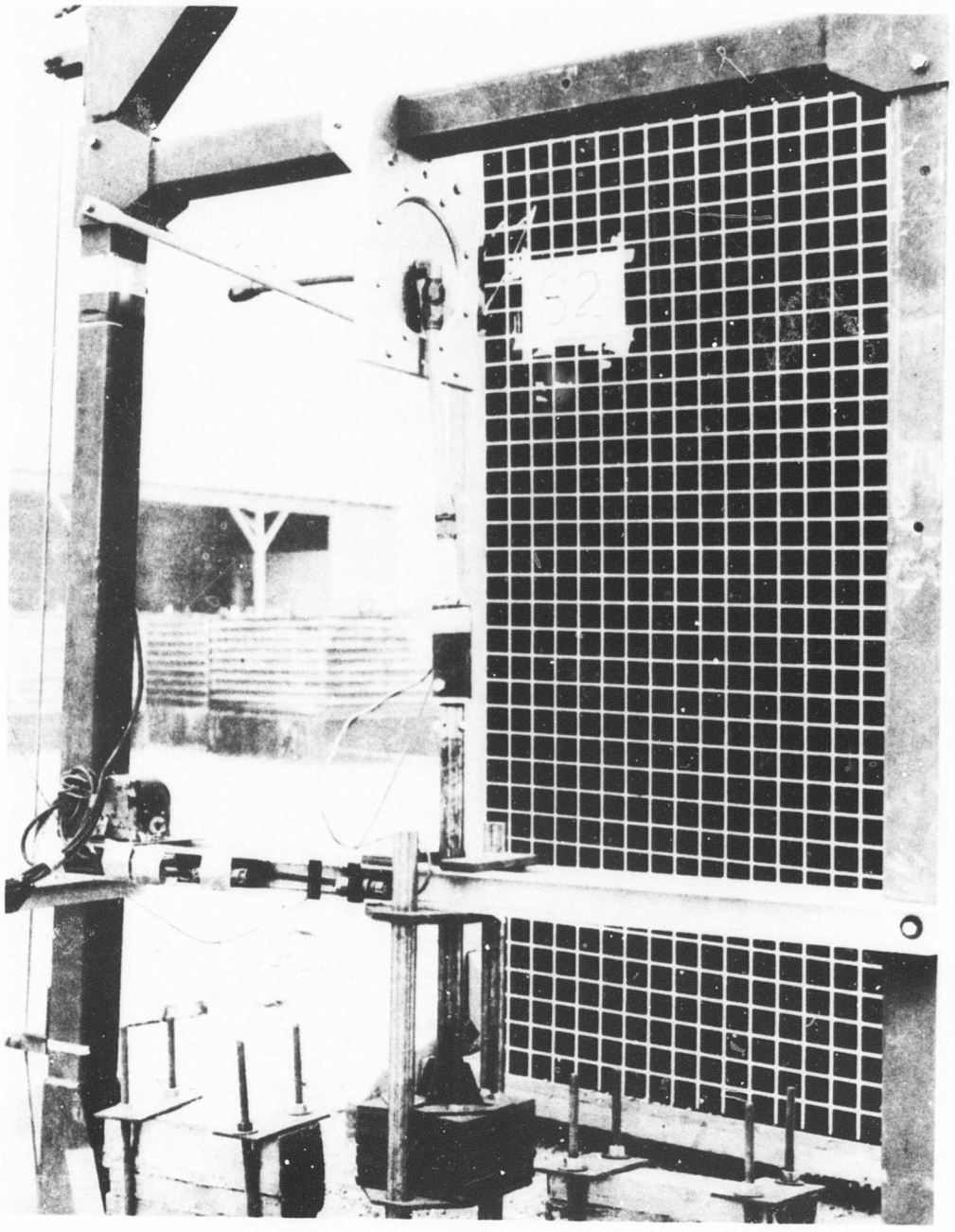

Figure 125. Test Setup, Frangible Protective Bulkhead Adapter (11 of 14).

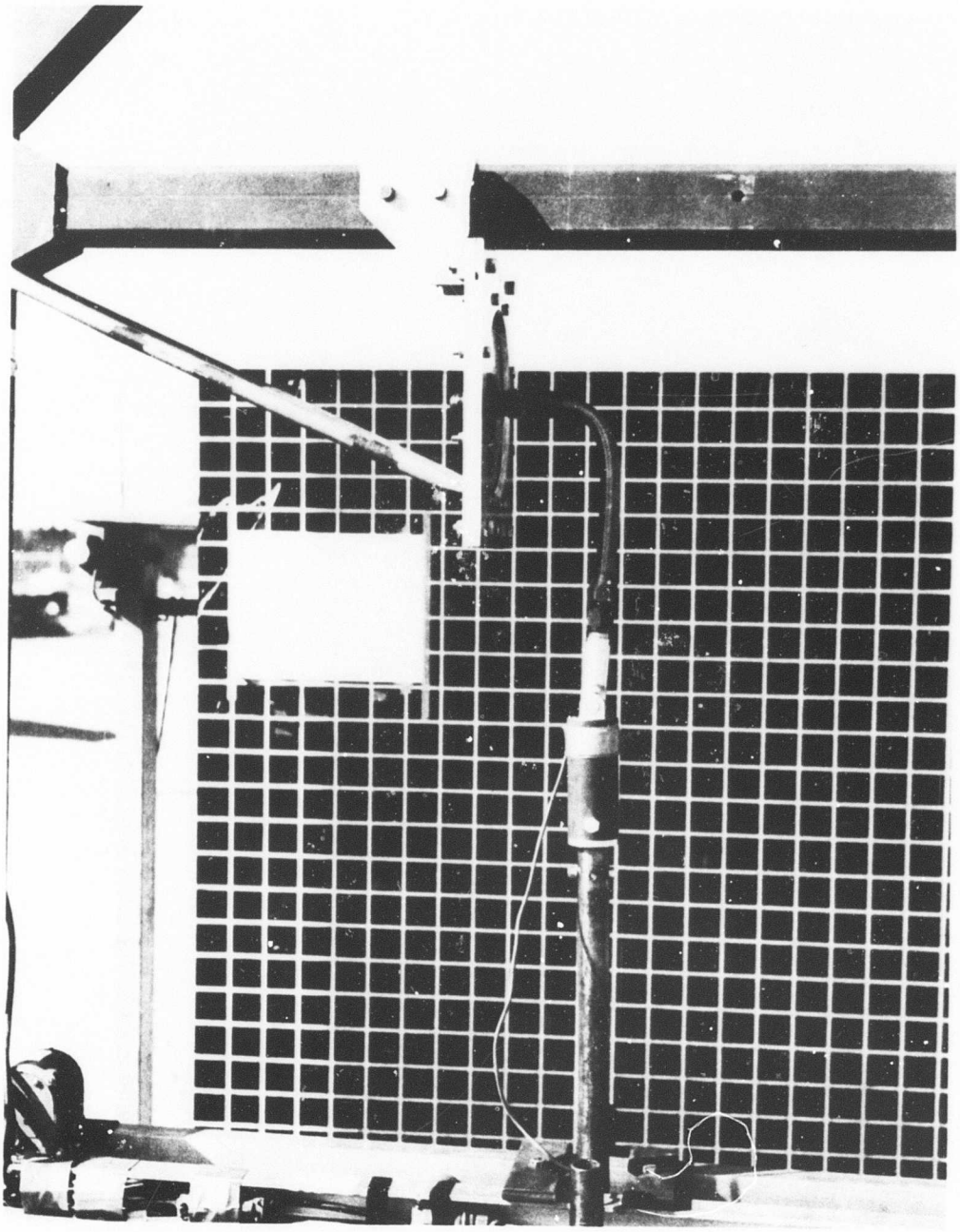

Figure 125. Test Setup, Frangible Protective Bulkhead Adapter (12 of 14).

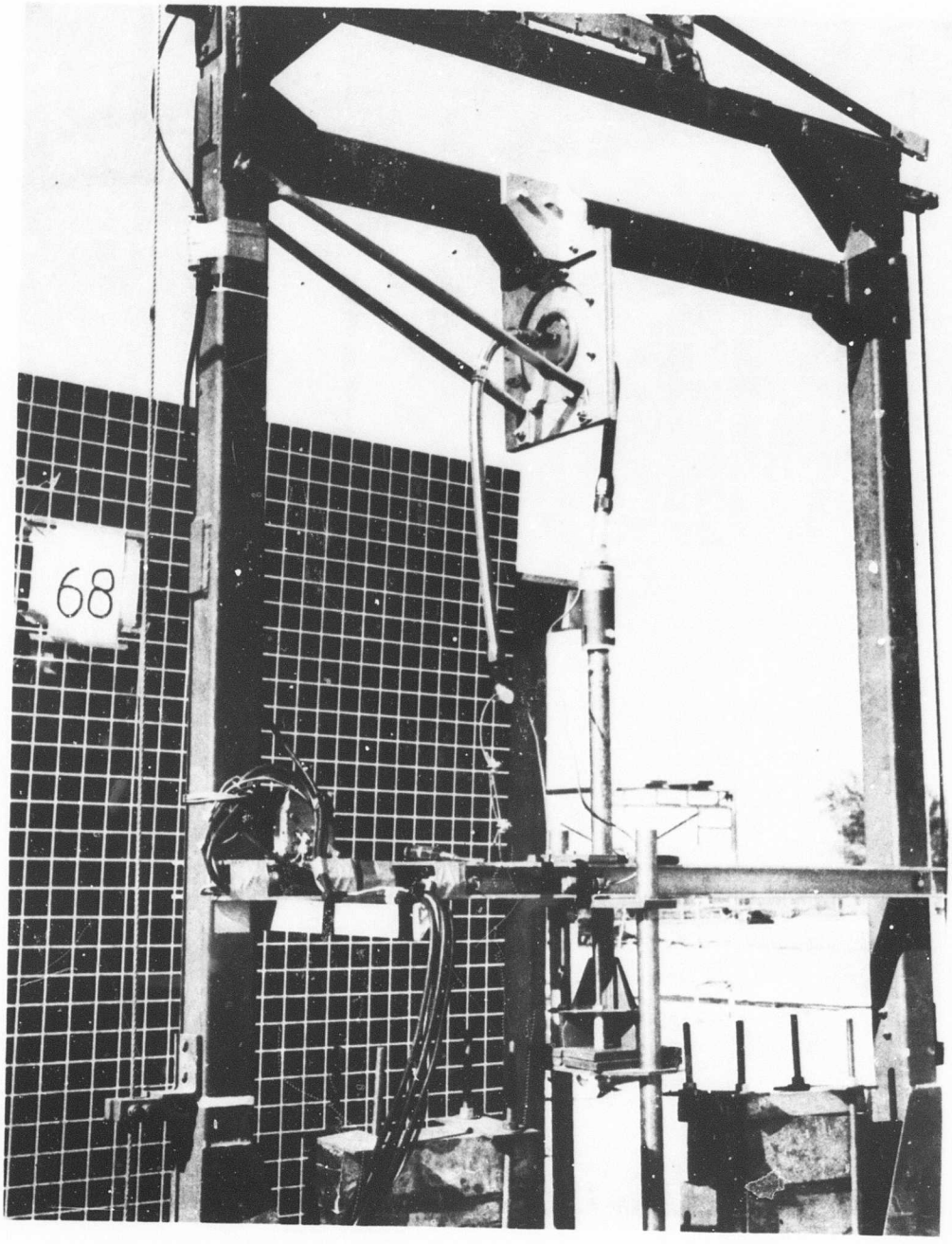

Figure 125. Test Setup, Frangible Protective Bulkhead Adapter (13 of 14).

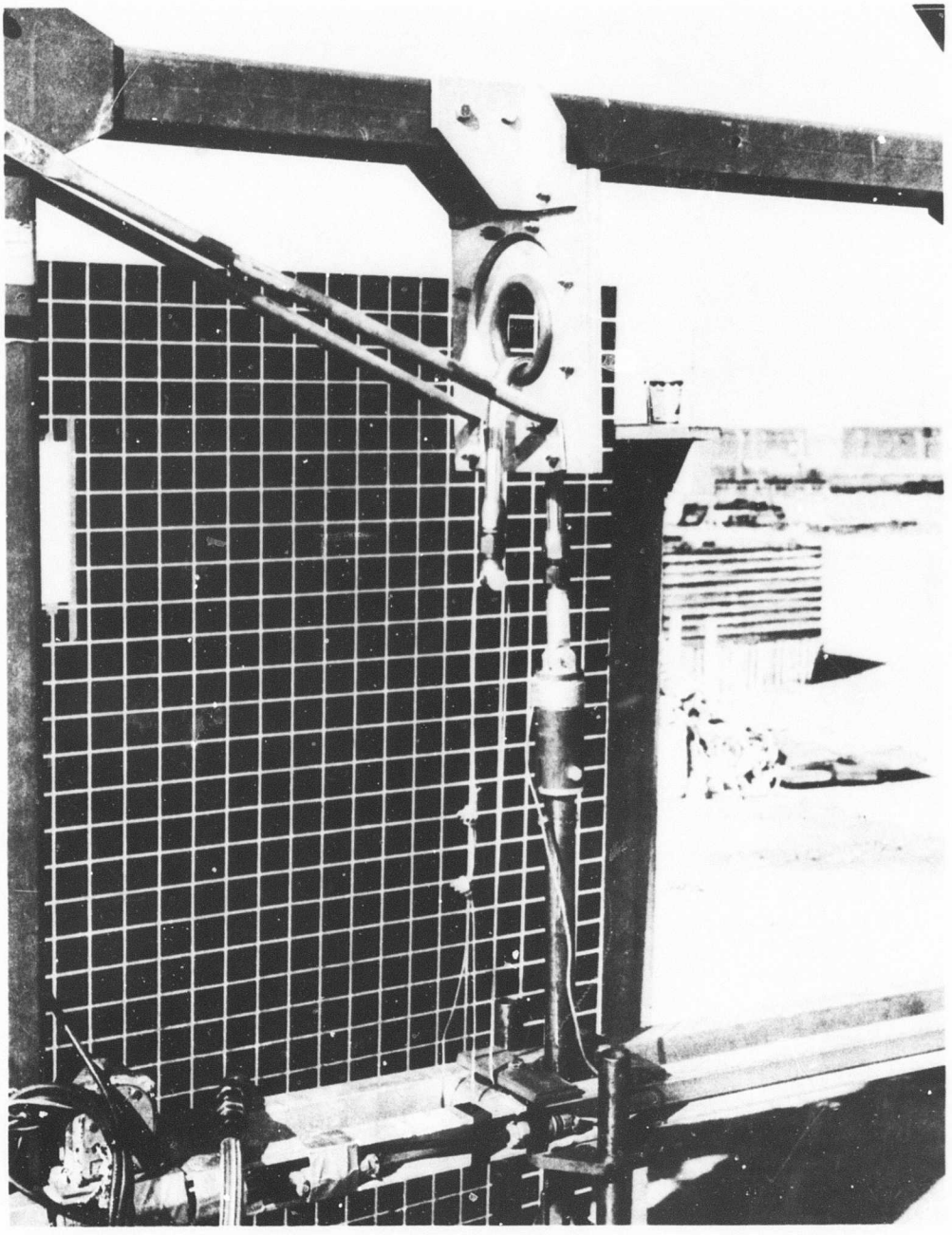

Figure 125. Test Setup, Frangible Protective Bulkhead Adapter (14 of 14).

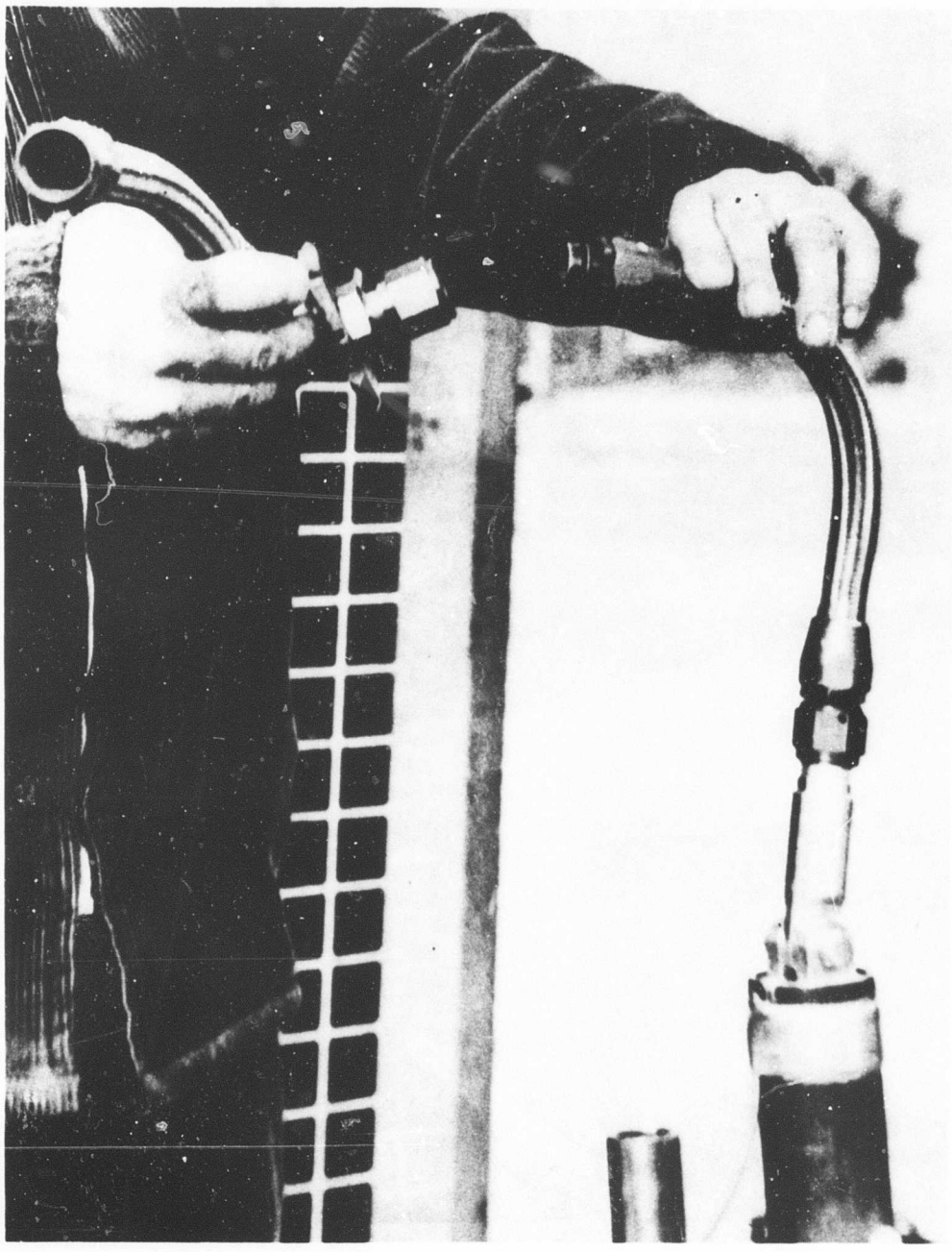

Figure 126. Test Results, Frangible Protective Bulkhead Adapter (1 of 10).

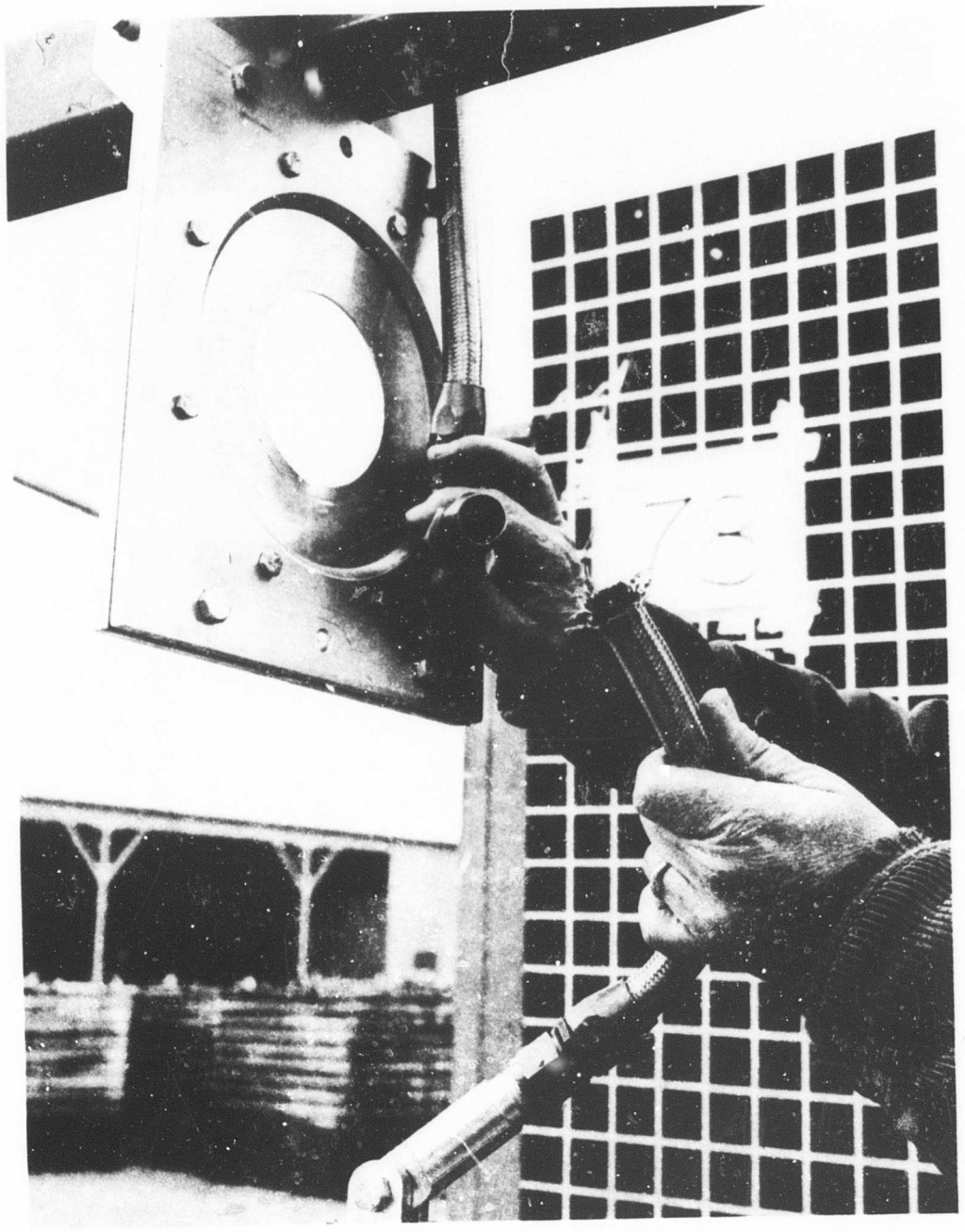

Figure 126. Test Results, Frangible Protective Bulkhead Adapter (2 of 10).

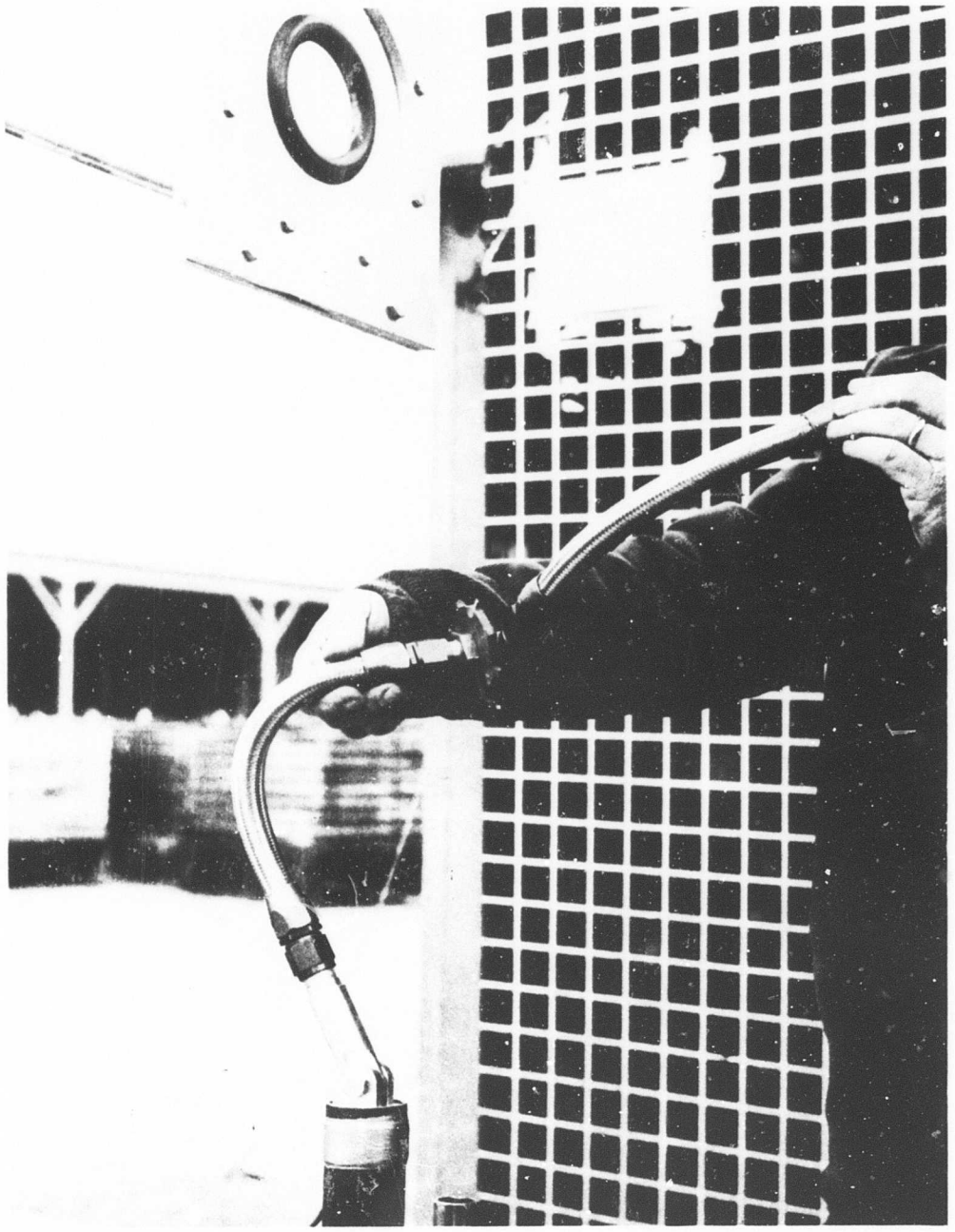

Figure 126. Test Results, Frangible Protective Bulkhead Adapter (3 of 10).

Figure 126. Test Results, Frangible Protective Bulkhead Adapter (4 of 10).

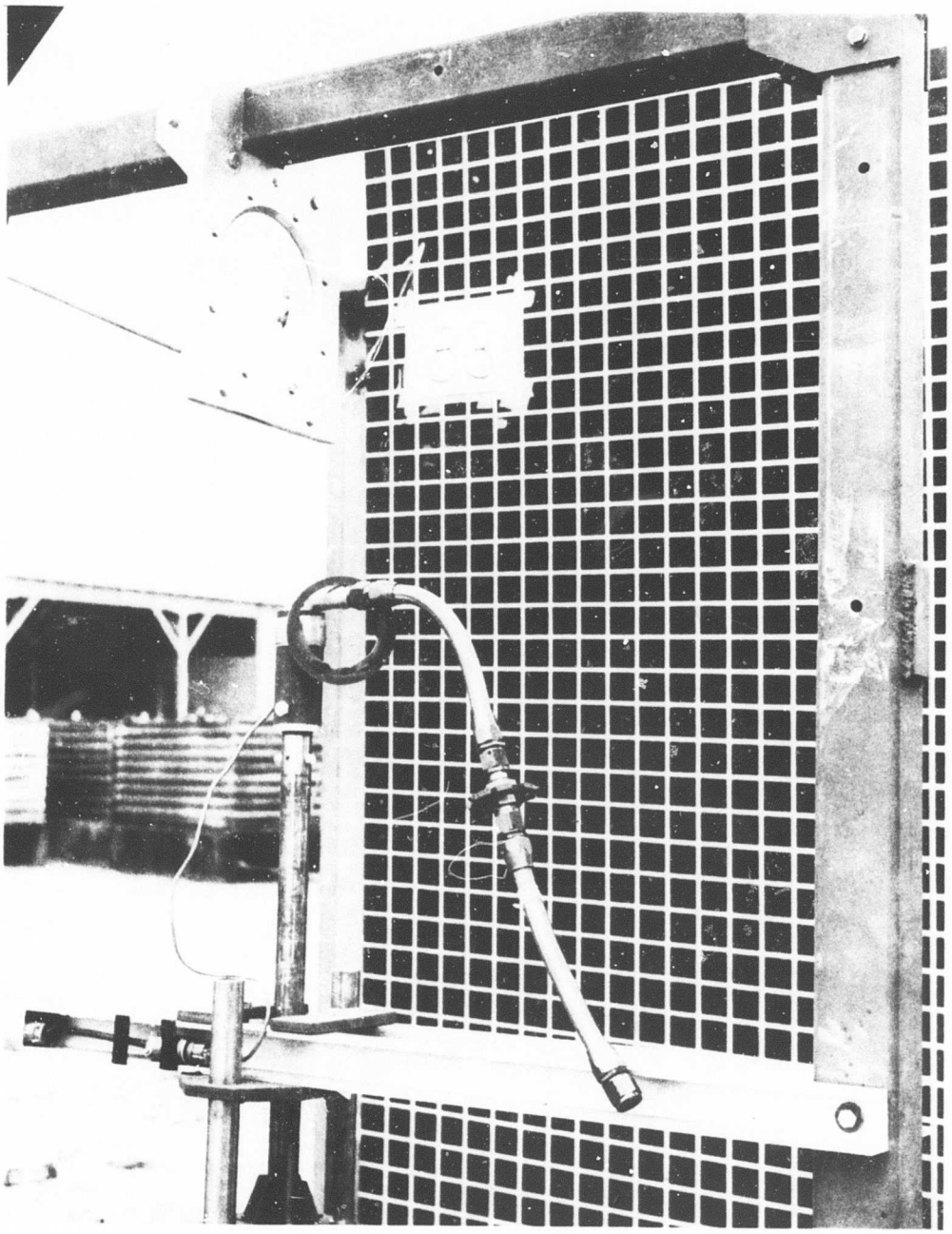

Figure 126. Test Results, Frangible Protective Bulkhead Adapter (5 of 10).

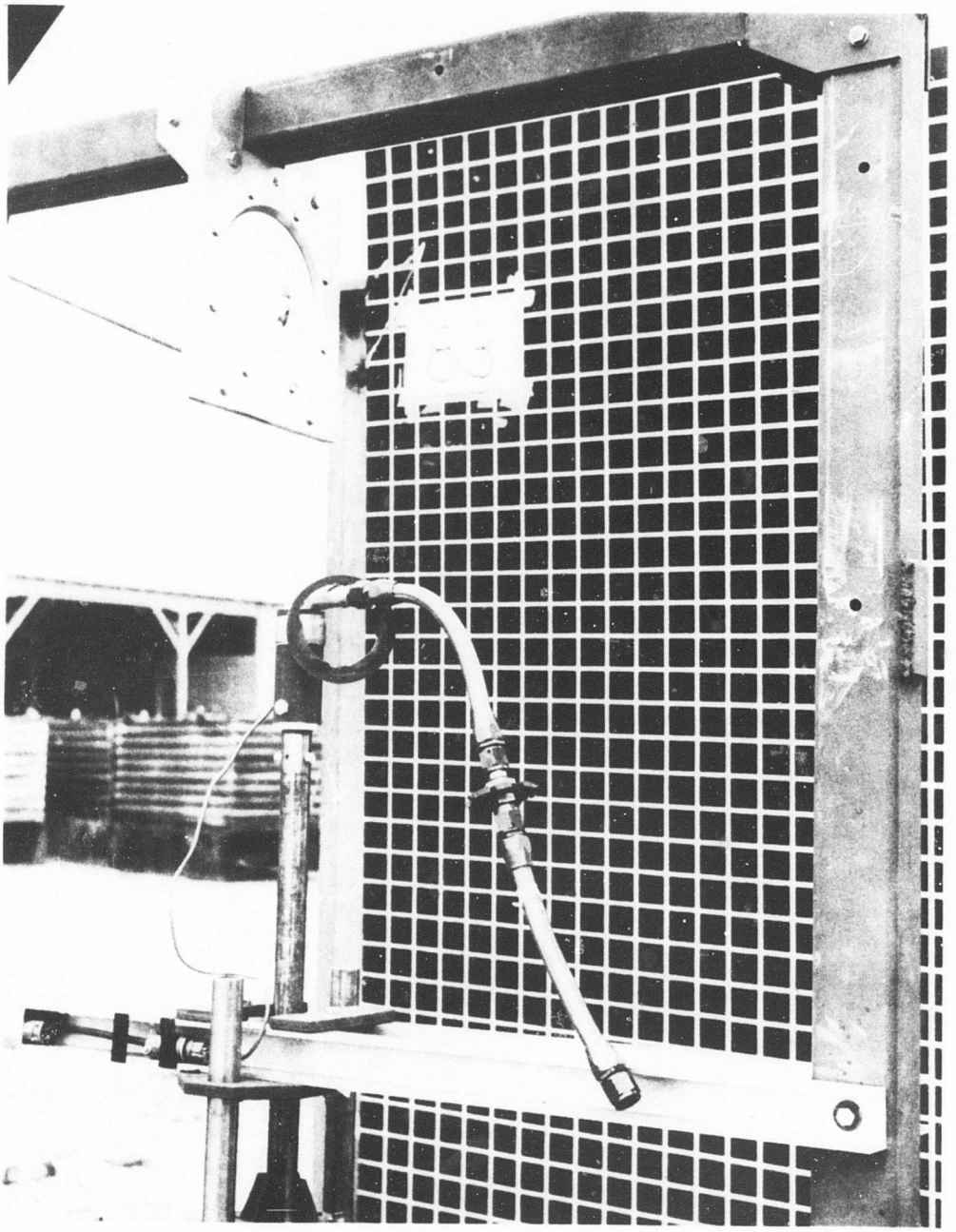

Figure 126. Test Results, Frangible Protective Bulkhead Adapter (5 of 10).

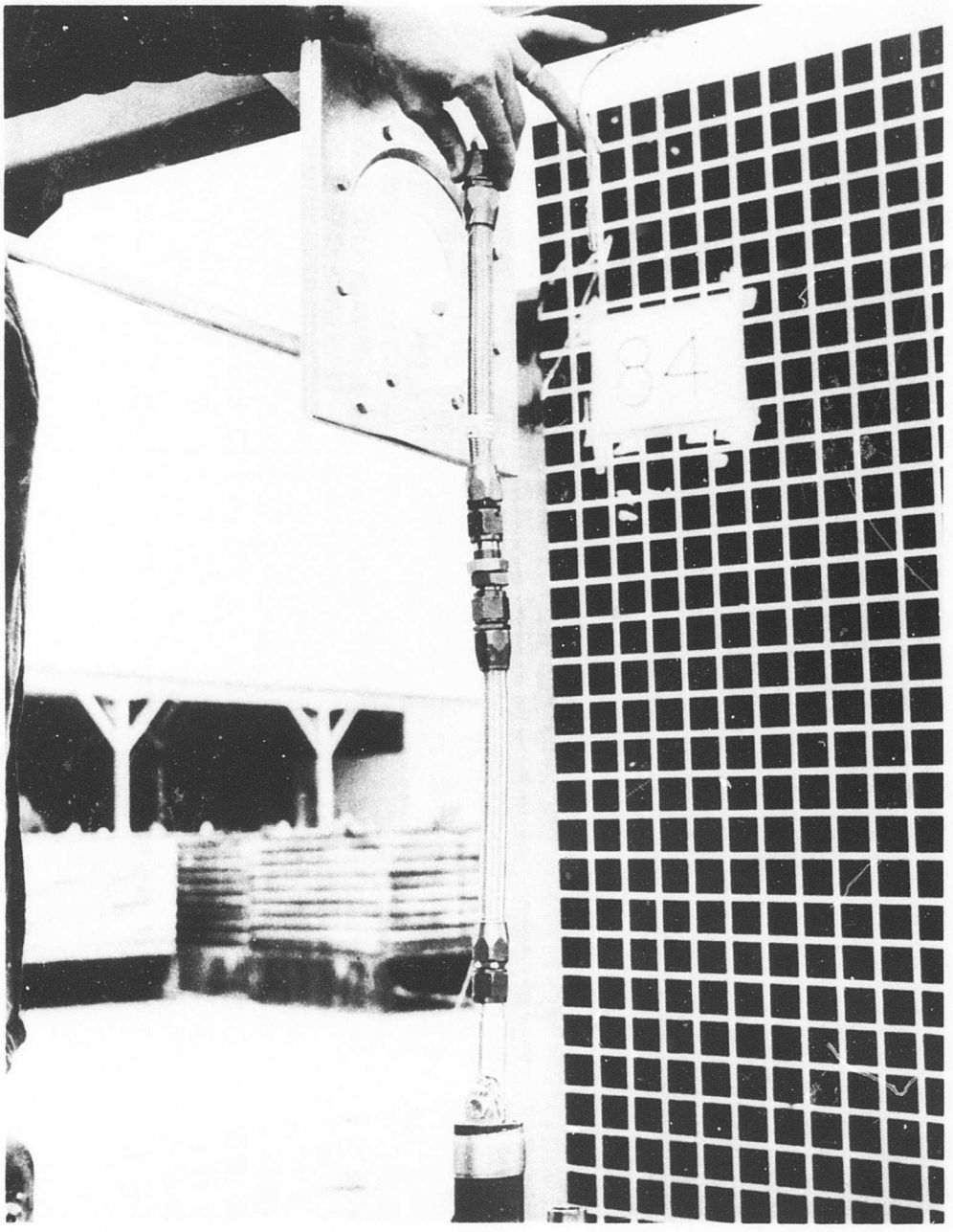

Figure 126. Test Results, Frangible Protective Bulkhead Adapter (6 of 10).

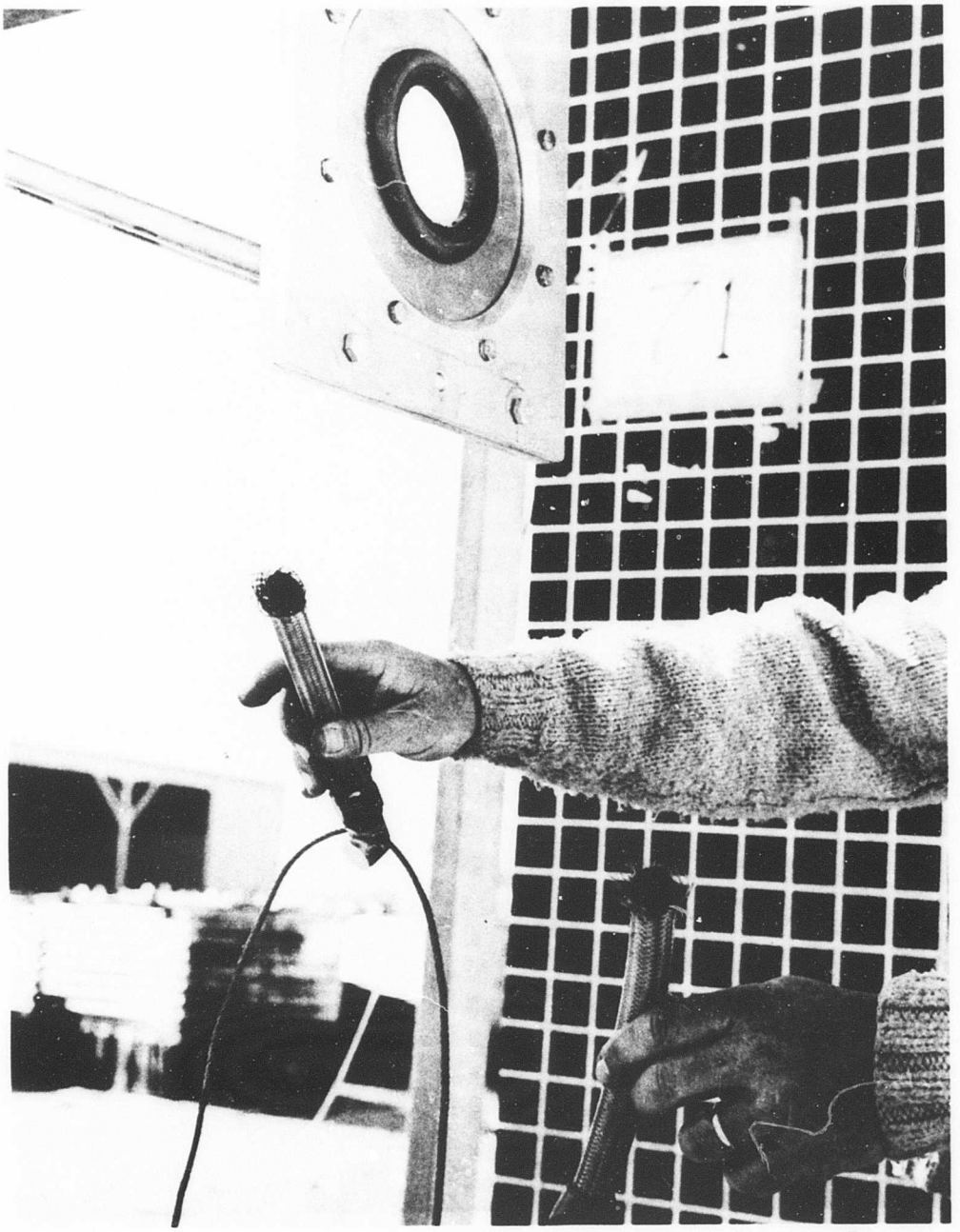

Figure 126. Test Results, Frangible Protective Bulkhead Adapter (7 of 10).

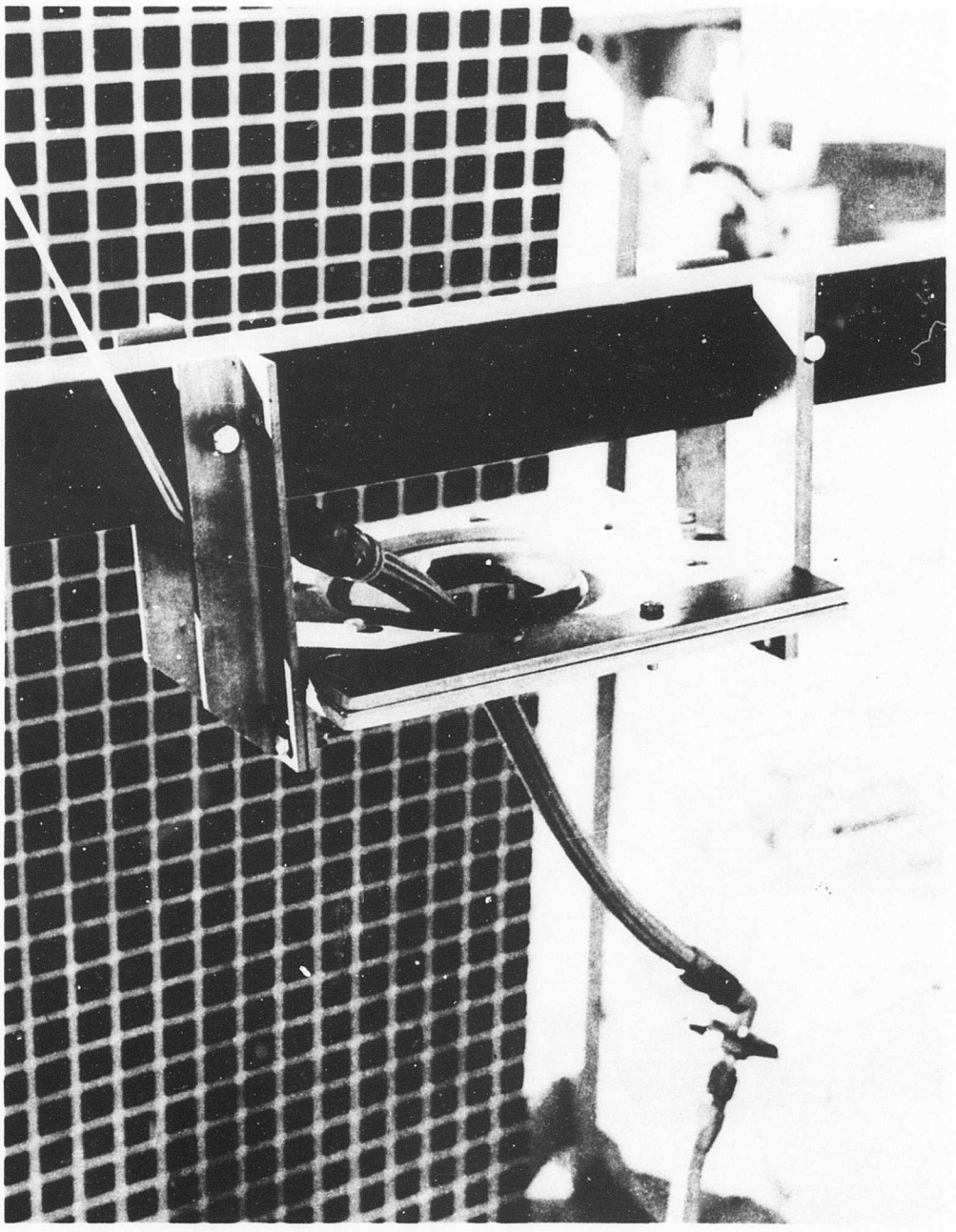

Figure 126. Test Results, Frangible Protective Bulkhead Adapter (8 of 10).

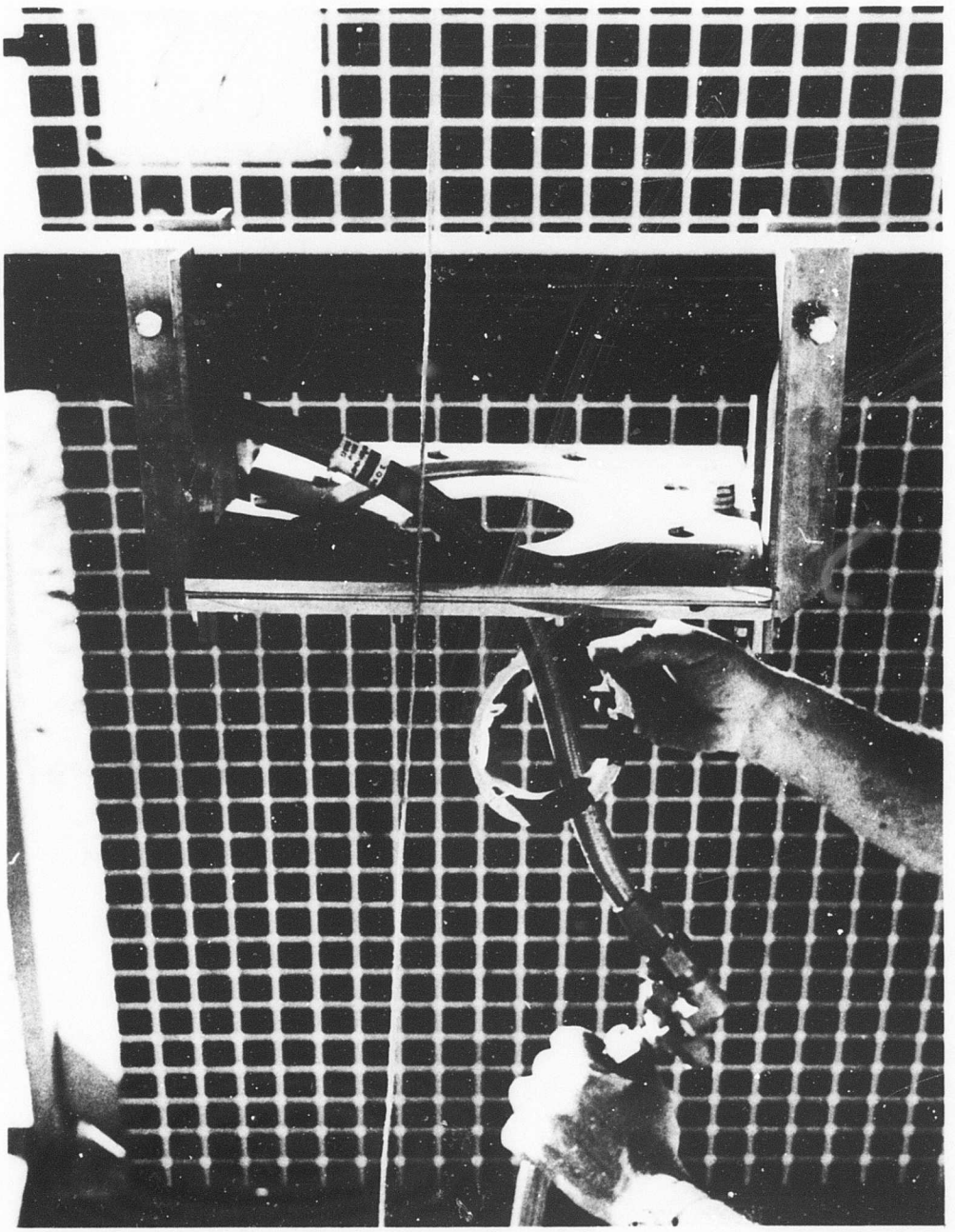

Figure 126. Test Results, Frangible Protective Bulkhead Adapter (9 of 10).

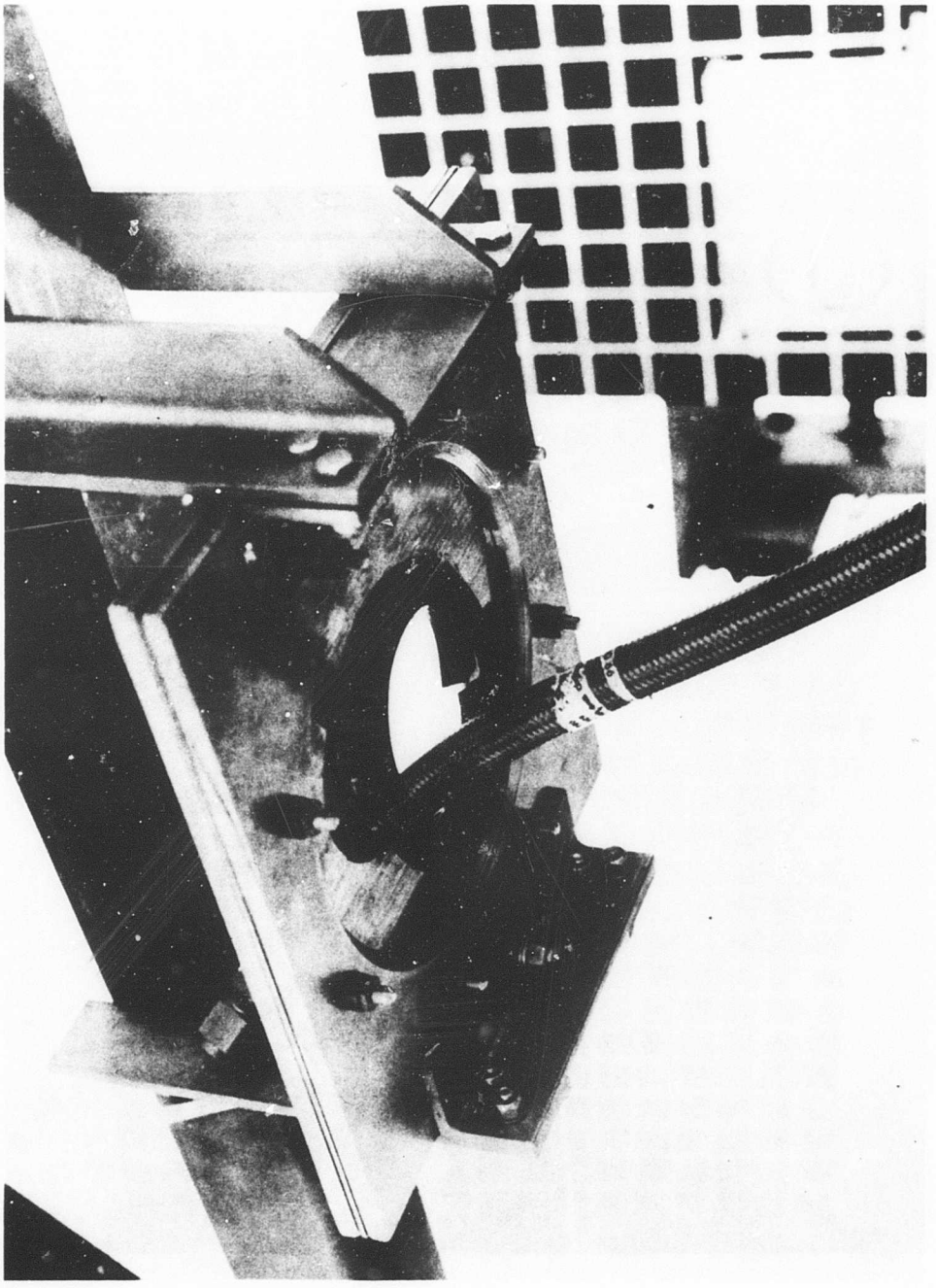

Figure 126. Test Results, Frangible Protective Bulkhead Adapter (10 of 10).

TABLE XXX

SYSTEM IV TENSION TEST DATA

Test No.*	Drop Hgt (ft)	Impact Vel (ft/sec)	G's on Frame	Load Wt (lb)	Max Load on Specimen (lb)	Pulse Duration (sec x 10^{-3})	Penetration Distance (in.)**	Remarks***
61	1 2	6	6	24	210	30	9.0	-
62	1	8	10	24	375	20	9.0	-
63	2	11	18	24	510	20	11.5	1
64	2	11	16	24	495	20	12.0	1
65	30	45	110	24	675	20	14.0	4
66	53	58	143	24	885	20	16.0	4
67	14	30	53	24	640	25	16.0	4
68	14	30	66	24	690	25	14.5	5
69	53	58	130	24	1650	20	16.0	5
70	2	11	-	24	-	-	10.0	6
71	53	58	135	24	1500	20	18.5	3
77	14	30	44	54	1085	30	16.0	2
78	14	30	64	54	1265	20	16.0	8
79	14	30	64	54	255	25	16.0	1
80	14	30	75	54	1900	20	16.0	9
81	14	30	77	54	1120	20	16.0	9
82	14	30	73	54	2005	20	16.0	9
83	14	30	74	54	1580	20	16.0	4
84	14	30	78	54	930	20	16.0	7

TABLE XXX (CONT)

Test No.*	Drop Hgt (ft)	Impact Vel (ft/sec)	G's on Frame	Load Wt (lb)	Max Load on Specimen (lb)	Pulse Duration (sec x 10^{-3})	Penetration Distance (in.)**	Remarks***
85	14	30	76	54	1400	20	16.0	1
86	14	30	83	54	1025	20	16.0	1
87	14	30	71	54	257	20	16.0	1
88	14	30	71	54	1765	10	16.0	1
89	14	30	68	54	780	20	16.0	1
90	14	30	75	54	1050	25	16.0	4
91	53	58	144	54	570	20	12.0	1

* See Figures 125 and 126.

** Penetration of jig into impact bed.

*** Code
1 Torus intact, hose assembly intact.
2 Torus intact, hose fitting failed.
3 Torus intact, hose failed.
4 Torus damaged, hose assembly intact.
5 Torus damaged, not enough travel in test setup to extend hose assembly to the point of hose or fitting failure.
6 Torus intact, not enough travel in test setup to extend hose assembly to the point of hose or fitting failure.
7 Hose assembly intact.
8 Hose fitting failed.
9 Hose failed.

Note: Separation did not occur in tests 61 and 62.

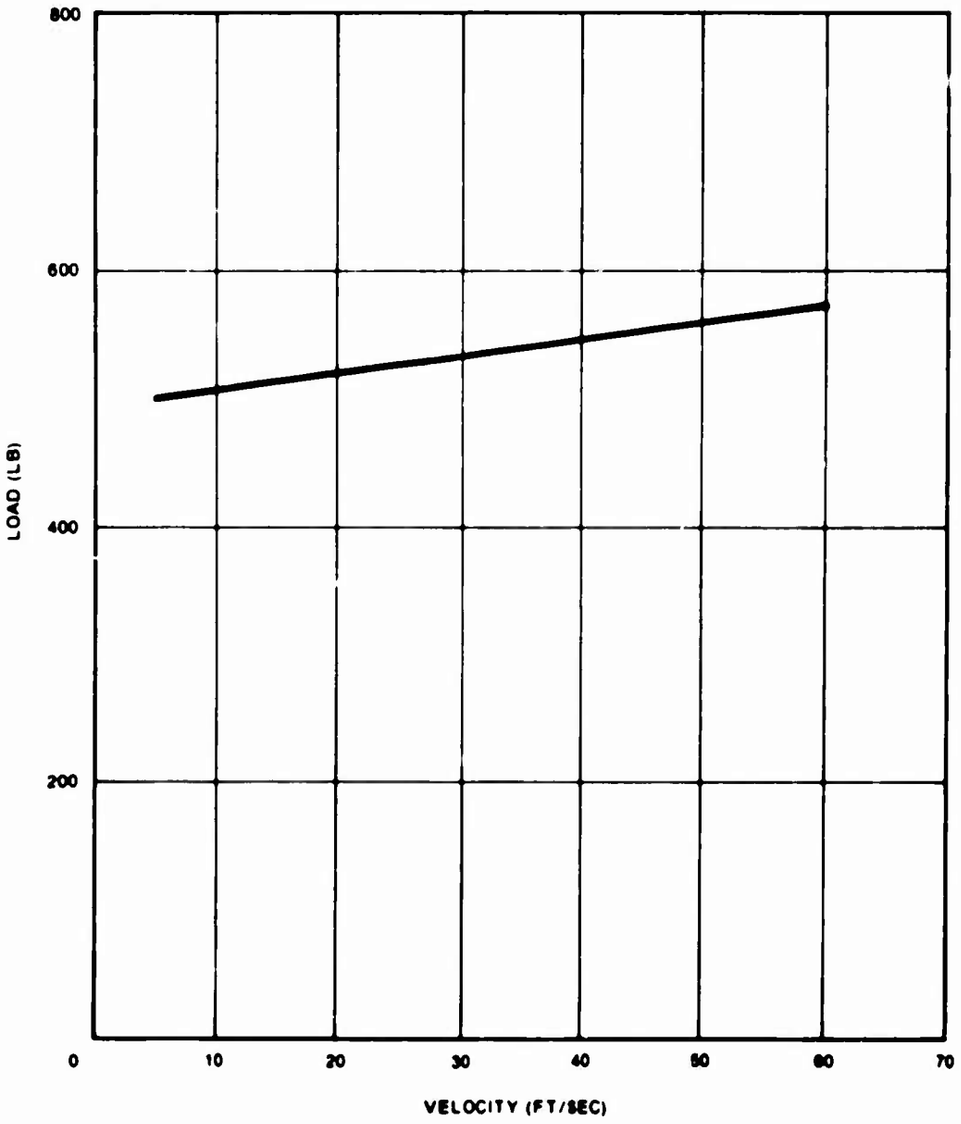

Figure 127. Load-Bearing Capability of Frangible Bulkhead Section

occurred in the second test when the fittings impinged against the bare bulkhead opening. This failure appeared to be a combination of shear and tension.

The third configuration (tests 83 and 84) passed through the opening in both tests without line failure. In the first test (with a bulkhead fitting installed), the hose and fittings passed through the opening with no visible damage. Abrasions and cuts were evident in the second test at the points where the bare bulkhead impinged against the fuel line. No failure occurred in either test. The results of tests 68 through 71 showed that the fuel line failed at a 1500-pound tensile load; the torus remained intact.

The torus appeared to be sensitive to side-impact loads, that is, impact loads applied perpendicular to the plane of the bulkhead. Throughout the test program when loads were applied in this manner, the torus would fail in modes varying from cracking to total destruction. These failures indicate the need for an improved torus, either through design or material change.

APPENDIX VI

FUEL SYSTEM OF SIKORSKY CH-53 HELICOPTER

The fuel system of the Sikorsky CH-53 helicopter is shown schematically in Figure 128. No electrical power is required for any component that supplies fuel to the engine. Each engine has a separate supply tank and system, although crossfeeding is possible. The fuel is supplied to the engine by suction, which reduces the fire hazard due to leakage or combat damage. The system basically consists of the following items:

1. A tank outlet strainer with a number 10 mesh screen.
2. A no-leak check valve to prevent loss of system prime. Pressure-relief provisions compensate for fuel thermal expansion.
3. The fuel line size from the tank to the fuel control valve is sufficient in diameter to accommodate twice the maximum single-engine fuel flow requirements.
4. A manually operated fuel control valve for emergency engine shutdowns or tank isolation.
5. The engine feed line between the fuel control valve and the engine-mounted, engine-driven boost pump is of sufficient diameter to accommodate the maximum engine power fuel flow requirements. The line includes a firewall fitting that aids in rapid engine removal and that prevents loss of system pressure when a fuel line is disconnected.
6. The engine-mounted, engine-driven fuel boost pump is the Nash multiphase centrivac type. It increases the altitude capability of the aircraft by about 5000 feet. Incorporated internally in the boost pump is a bypass system that allows fuel to be delivered to the engine by the engine pump in case of boost pump failure.
7. The fuel inlet line between the boost pump and inlet side of the engine pump contains a pressure-sensing switch to actuate a warning light indicating a loss of pressure as a result of boost pump failure or a closed fuel control valve. Approximate fuel pressures in the engine operating range are: supply tank to boost pump, -4 inches Hg.; boost pump outlet, 40 pounds per square inch; engine pump outlet, 600 pounds per square inch.
8. A crossfeed line between the fuel control valves is provided which permits the following:

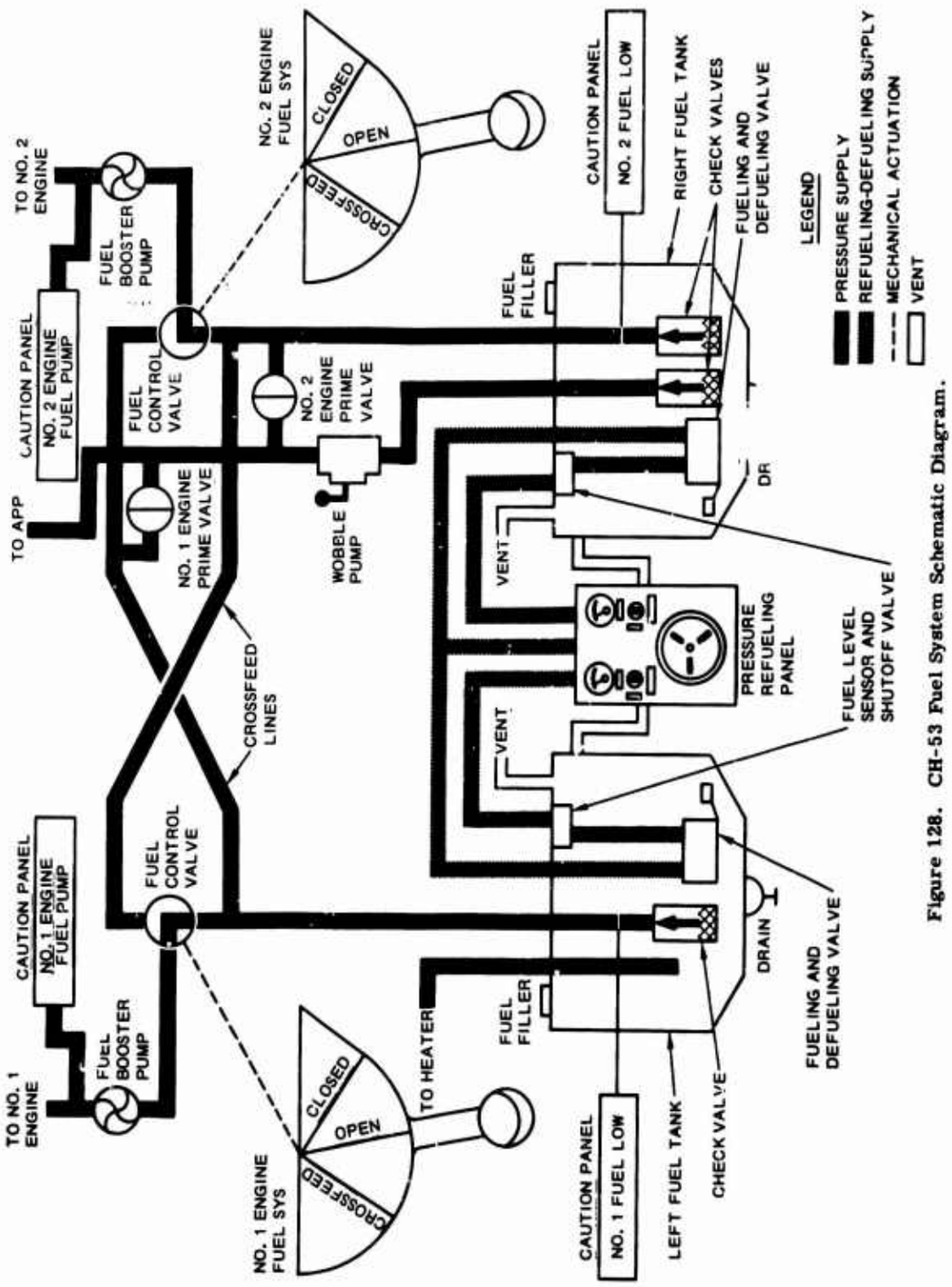

Figure 128. CH-53 Fuel System Schematic Diagram.

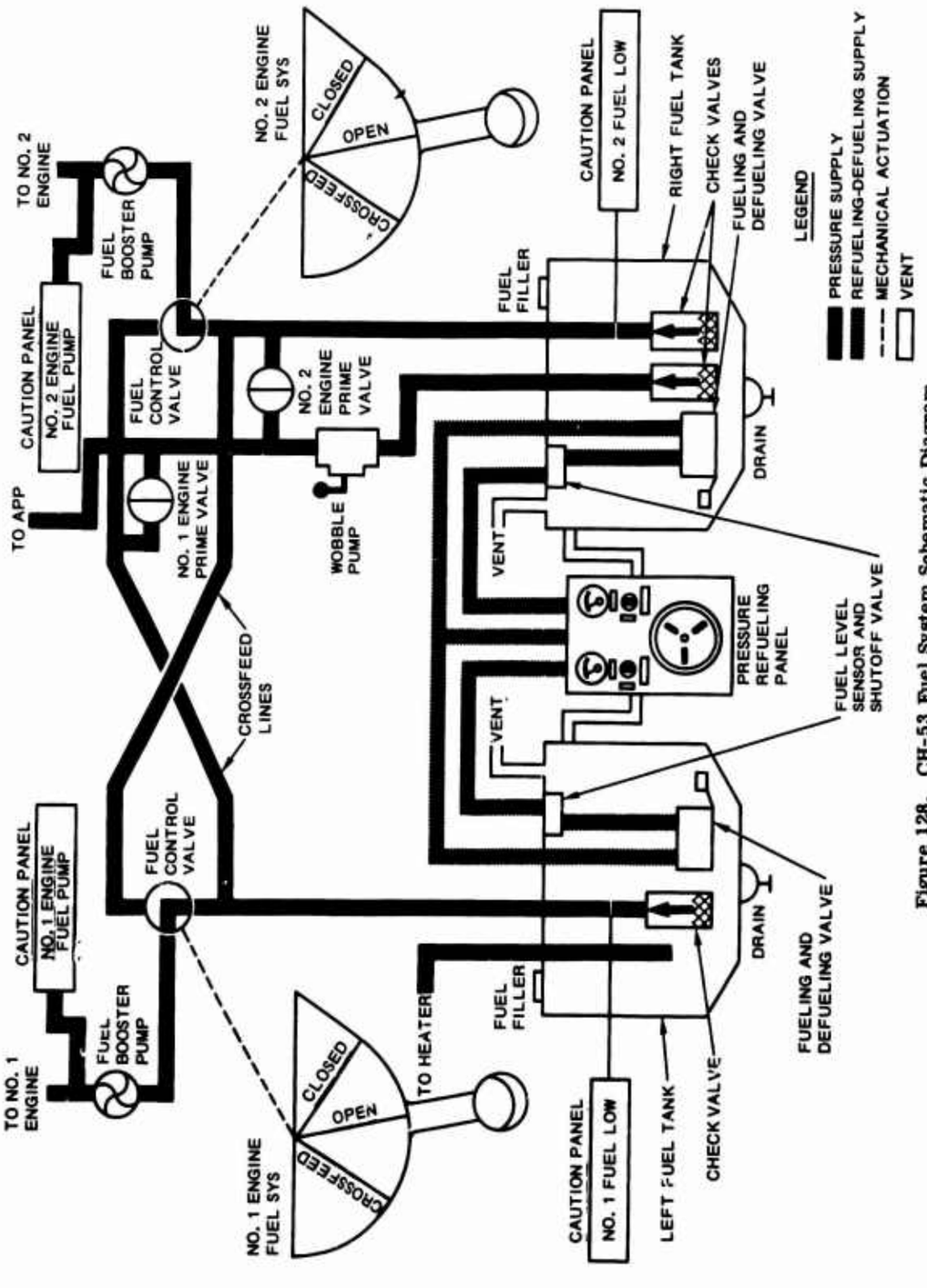

Figure 128. CH-53 Fuel System Schematic Diagram.

a. Individual fuel supply from one tank to its engine with both systems isolated
b. Fuel feed from one tank to both engines
c. Fuel supply from both tanks to one engine alone.

SUPPLEMENTARY

INFORMATION

AD-818330L

SAVFE-SOS (2 Jan 70) 1st Ind Mrs. Horn/cl/555-1720-3002
SUBJECT: Request for Public Release of Technical Document

Headquarters, US Army Aviation Materiel Laboratories, Fort Eustis, VA 23604 27 January 1970

TO: Administrator, Defense Documentation Center, ATTN: DDC-TSR-2, Cameron Station, Alexandria, VA 22314

1. USAAVLABS Technical Report 67-33 has been reviewed. The protective marking: FOR OFFICIAL USE ONLY, and the present release statement should be deleted as production contracts have been awarded to install crashworthy fuel systems in Army aircraft.

2. A new release statement should be applied as follows:

This document is subject to special export controls, and each transmittal to foreign governments or foreign nationals may be made only with prior approval of US Army Aviation Materiel Laboratories, Fort Eustis, VA 23604.

FOR THE COMMANDER:

ROCCO J. COLAFRANCESCO
MAJ, TC
Chief, Support Office

AD 818330L